DEVELOPMENT OF A DYNAMIC STILL FOR MEASURING LOW PRESSURE VAPOUR-LIQUID-LIQUID EQUILIBRIA

(Systems of Partial Liquid Miscibility)

Mkhokheli Ndlovu

B.Eng. (Hons)

National University of Science and Technology, Zimbabwe

Submitted in fulfillment of the Academic Requirements for the Award of a Master of Science Degree in Engineering at the School of Chemical Engineering, University of KwaZulu-Natal

Durban

2005

"Kubazali bami"

(To my Mom and Dad)

Abstract

The dynamic still originally designed by Raal (Raal and Muhlbauer [1998]) has been transformed into a valuable still that can now be used for measuring both low pressure vapour-liquid equilibria (VLE) for systems that are completely miscible and vapour-liquid-liquid equilibria (VLLE) for systems that are partially miscible. The resultant equilibrium data are important in the design and analysis of distillation and allied separation process equipment, with VLLE data, in particular, being useful in the design of heterogeneous azeotropic distillation columns.

The original Raal still was based on the designs of Heertjies [1960] and Yerazunis [1964], who successfully used a packed equilibrium chamber where the liquid and vapour phases are forced downward co-currently to achieve rapid and dynamic equilibrium (Joseph et al [2001]). Direct analysis of the vapour composition prior to condensation through a new heated valving system with superheated sample conveyance to a gas chromatograph, a modification incorporated into the Raal still, ensured that accurate and reproducible equilibrium data were obtained. This new arrangement dispenses with the impossible task of getting the actual vapour composition that would result were the vapours allowed to condense and form two liquid phases. The initial testing of the still which established the operating procedures was conducted on two previously measured systems - the first which was homogeneous and the second heterogeneous. For the homogeneous system the new vapour sampling system was tested by comparing the measured composition to that of a condensed sample sent manually to the GC using a gas-tight syringe. In order to completely describe the VLLE for the systems studied, the liquid-liquid equilibrium (LLE) data for these systems were also measured. The LLE measurements were conducted in a newly-developed small jacketed glass cell with temperatures maintained constant by circulating water from a bath maintained at the desired temperatures. The main focus of this project was thus the development of an apparatus and procedures for measuring low pressure vapour-liquid-liquid equilibria. The project also went on to measuring and modeling VLE, VLLE and LLE data for selected binary and ternary systems. Both the Gamma-Phi and the Phi-Phi methods of VLE analysis were carried out on the measured data. The NRTL, Wilson, TK-Wilson and UNIQUAC activity coefficient models were used in the Gamma- Phi method together with the Virial equation of state for vapour phase non-idealities. In the Phi-Phi method, The Peng and Robinson Equation of State (EOS), the Soave Redlich-Kwong EOS and the Stryjek and Vera modified Peng and Robinson EOS were all used, first with the classical mixing rules and then with the theoretically correct Wong and Sandler [1992] mixing rules. Ternary LLE binodal curves were correlated to the Hlavaty correlation, the beta function and the log gamma function while the corresponding tie-lines were fitted to the NRTL model.

Preface

The work contained herein was performed at the University of KwaZulu-Natal from July 2004 to October 2005 and was supervised by Professor J. D Raal, Professor D. Ramjugernath and Dr D. Ikhu-Omoregbe.

This dissertation is submitted as a full requirement for the award of a Master of Science Degree in Chemical Engineering. All the work presented in this thesis is original, unless otherwise stated. It has not (in whole or part) been previously published in any tertiary institution as part of a degree.

M Ndlovu

Acknowledgements

Dreams too seldom come true. This dissertation is one such dream and was made possible through the help from several people. I would thus take this opportunity to express my indebtedness to those men and women who not only contributed in making my research a success but helped in the production of this dissertation.

Profound gratitude goes to my supervisors; Professor D Ramjugernath, Professor J.D Raal and Doctor. D Ikhu-Omoregbe for their guidance and outstanding support during the months I spent as a research student. It is because of their expert knowledge that this work has been a success. Special thanks go to Professor J.D Raal and Professor D Ramjugernath, who read each and every word in this report and offered invaluable contributions for improvement - errors that remain are mine. Despite all the pressures from their busy schedules, they would always find time to help me. I will never tire of recalling their wholehearted devotion to the service of education in this country.

My thanks are also due to the NRF Thuthuka programme for financial assistance. I am gratefully indebted to Professor D Ramjugernath who too provided me with financial support.
The Workshop personnel did a sterling job during the setting up of the equipment used in this work. Many thanks go especially to Mr. Les Henwood and Mr Colin Mandri, not mentioning Mr. Ayanda Khanyile who was not only helpful in organizing chemicals and laboratory equipment for me, but was also a good friend of mine.
On a personal note, I would like to thank my family members for their encouragement and moral support during the seemingly endless days that I have been working on this project.

Finally, I would like to thank my colleagues in the Chemical Engineering Department for friendship and helpful criticism, in particular L. Lerotholi, D. Mwasiswebe, P. Reddy, J. Knock, E. Wilson, S.L. Clifford, I. Habyalimana, A. Hwengwere, and M. Motchelaho. I say to them "Guys we laughed our way out but never missed the point, the moments we cherished will always be remembered".
Above all, I thank the Almighty Lord God through whom everything has been possible.

M. Ndlovu

Contents

* The names MBE and 2-methyl -3 buten-2 ol are synonymous and will be used interchangeably thoughout this thesis. Similarly for Cresol and m-Cresol (refering to m-Cresol) and Tolunitrile and o-Tolunitrile (referring to o-Tolunitrile).

List of Figures

Chapter 2

Chapter 3

Chapter 4

Chapter 5

Chapter 6

Chapter 7

Chapter 8

Appendix 1

Appendix 2

List of Tables

Chapter 3

Chapter 5

Chapter 6

Chapter 7

Chapter 8

Appendix 4

Nomenclature

English Letters

A	Constant in the Antoine or Wagner vapour pressure equations
a	Intermolecular attraction force parameter in the Peng and Robinson EOS, Soave Redlich-Kwong EOS and in the Peng and Robinson Stryjek and Vera EOS
a'	parameter in the Tsonopoulos [1974] correlation
B	Constant in the Antoine or Wagner vapour pressure equations
B^o	Parameter in the Pitzer-Curl [1957] correlation
B^l	Parameter in the Pitzer-Curl [1957] correlation
B_{ii}	Second virial coefficient of pure component I [cm^3/mol]
B_{ij}	Second virial coefficient for the species I – species j interaction [cm^3/mol]
b	Molecular size parameter in in the Peng and Robinson EOS, Soave Redlich-Kwong EOS and in the Peng and *Robinson* Stryjek and Vera EOS
C	Constant in the Antoine or Wagner vapour pressure equations
c	Numerical Constant in Equation 3-151
D	Constant in the Wagner vapour pressure equation and also Summation term in the Wong and Sandler [1992] mixing rule (equation 3-144)
f	Fugacity [Kpa]
$\hat{f}$	Fugacity in solution [Kpa]
G	Molar Gibbs Energy [J/mol]
G_{12}	Parameter in the NRTL equation
G_{21}	Parameter in the NRTL equation
$\overline{G}$	Partial molar Gibbs energy [J/mol]
$g_{ij} - g_{ii}$	Parameter representing energy interactions between species in the NRTL equation
k	mixing rule parameter
li	Parameter in the UNIQUAC model (Equation 3 – 114)
n	Number of moles
P	Pressure (Kpa)
P'	Parachor
Q	Quadratic sum of second Virial coefficients

R	Universal gas constant [J/mol K]
R_d	Mean radius of gyration [$\dot{A}$]
r_i	Pure- component parameter in the UNIQUAC model
T	Temperature [°C or K]
V	Molar or specific volume [cm^3/mol]
x	liquid phase mole fraction
y	vapour phase mole fraction
Z	Compressibility factor

Greek Letters

α	Scaling factor in Peng and Robinson equation of State (EOS), in Soave Redlich-Kwong EOS and in the Stryjek and Vera modified Peng and Robinson EOS
α_{12}	Parameter in the NRTL model representing the solution non-randomness
δ	Denotes a residual (e.g. δP)
δ_{ij}	Term relating the second virial coefficients
ε	Tolerance in iterations also Constant temperature term and Constant Pressure term in the Van Ness Direct Test
Φ	Ratio of fugacity coefficients with the Poynting correction factor (Equation 3-48)
Φ_i	Segment fraction in the UNIQUAC model
ϕ	Fugacity coefficient
$\hat{\phi}$	Fugacity coefficient in solution
γ	Activity coefficient
η	Solvation parameter
κ	Characteristic coefficient in Peng and Robinson equation of State (EOS), in Soave Redlich-Kwong EOS and in the Stryjek and Vera modified Peng and Robinson EOS
Λ_{ij}	Parameter in Wilson equation
$\lambda_{ij} - \lambda_{ii}$	Parameter representing molar interactions between species in the Wilson and UNIQUAC model
μ	Dipole moment [Debye] and Chemical potential

θ	Area fraction in the UNIQUAC model
τ_{ij}	Parameter in the NRTL model
ω	Acentric factor

Subscripts

1	Denotes component 1
2	Denotes component 2
n	Denotes critical property
Ant	Denotes Antoine equation
Wagner	Denotes Wagner equation
m	Denotes mixture property

Superscripts

E	Denotes excess property
Exp	Denotes experimental value
Cal	Denotes calculated value
id	Denotes ideal solution
l	Denotes saturated liquid
Sat	Denote saturation
∞	Denotes the infinite pressure value
V	Denotes vapour

1

Chapter One

Introduction

It is well known that distillation and allied industrial separation processes such as absorption and solvent extraction for the recovery of products, byproducts and unreacted raw materials bring into contact multicomponent phases (usually vapour and/or liquid phases) that are not in equilibrium. The rate of transfer of a species from one phase to the other is directly related to the departure of the system from equilibrium; hence the analysis of these rate processes requires knowledge of the equilibrium states of the system (Smith et al [1975]). This makes the measurement of phase equilibria for systems involved in such processes essential for the detailed design of the process equipment that is used. This equilibrium information is also vital in optimizing existing similar processes.

One of the distillation types, heterogeneous azeotropic distillation, is an extensively used technique for separating binary azeotropic mixtures into their pure components. The *modus operandi* works by adding a third component, called the entrainer, which causes liquid liquid phase separation and thus an efficient mode for moving across distillation boundaries caused by the azeotrope in the mixture (Gomis et al [2000]). The development of such a process requires isobaric vapour-liquid-liquid equilibrium (VLLE) data. However, few VLLE data are available in the open literature. For example Norman [1945] pointed out the huge unavailability of VLLE data and more than 50 years later Gomis [2000] made a similar observation. Thus the major focal point of this project was the development of an apparatus and procedures for measuring low pressure vapour-liquid-liquid equilibria to be used in the design of sub-atmospheric pressure

separation equipment. The project also went on to measuring and modeling VLE, VLLE and LLE for selected binary and ternary systems.

The apparatus that was used in the project (discussed in more detail in Chapter 4), is a modification of the Raal still (Raal and Muhlbauer [1998]) for homogeneous systems. The Raal and Muhlbauer [1998] still was based on the designs of Heertjies [1960] and Yerazunis [1964], who successfully used a packed equilibrium chamber where the liquid and vapour phases are forced downward co-currently to achieve rapid and dynamic equilibrium (Joseph et al [2001]). The still has the following important properties; the Cottrell tube is not depended on as a means of establishing equilibrium since the equilibrium chamber increases the transfer of mass between the vapour and liquid phases, thus allowing for rapid attainment of equilibrium. The still also has direct analysis of the vapour composition through a new heated valving system with superheated sample conveyance to a gas chromatograph. This eliminates the difficulties encountered in analyzing the two phase condensate in systems of limited liquid miscibility. The capacities of the condensate receiver and the boiling chamber were small enough to make it possible for magnetic stirring to completely emulsify the two-phase liquid mixture obtained in systems of partial miscibility. This has the advantage that temperature and any possible concentration gradients that may affect reproducibility of the sample concentrations are eliminated and the returning condensate is thoroughly mixed with the rest of the liquid and thus prevents flashing (Raal and Muhlbauer [1998]).

In order to completely describe the VLLE for the systems studied, the liquid-liquid equilibrium (LLE) data for these systems were also measured. The LLE measurements were conducted in a newly-developed small jacketed glass cell (also described in more detail in Chapter 4) with temperatures maintained constant by circulating water from a bath maintained at the desired temperatures. A two phase liquid mixture placed initially in the cell was mixed and allowed to settle so as to attain equilibrium, after which samples of the two liquids were taken for analysis by gas chromatography from two different sampling points.

After setting up the equipment, the next phase of the project was to test the apparatus to ensure that desired operation would be achieved and hence come up with the equipment operating procedures. Firstly, VLE data were measured for a completely miscible system at constant pressure. The cyclohexane (1) + ethanol (2) system was chosen for this purpose and the measurements were carried out at 40 kPa. The results were rated by thermodynamic consistency

tests and also compared to literature sources (Joseph et al. [2001]). Any discrepancies in the measured data necessitated changes in the measuring procedure until the results agreed with the literature data. This system was also used to test the new heated vapour sampling mechanism; the measured composition was compared to that of a condensed sample sent manually to the GC using a gas-tight syringe.

In the second test, VLLE data were measured for a partially miscible system; water (1) + 2-methyl 3- buten-2-ol (2) at 97.2 kPa. The results were also subjected to the same treatment as that for the homogeneous system. In both cases, excellent agreement was obtained with literature data which lead to a high degree of confidence in the equipment and operating procedures. New, previously unavailable, LLE, VLE and VLLE data were then measured for the following systems:

- m-Cresol (1) + Naphthalene (2) at 120°C , 110°C and 55 kPa
- m-Cresol (1) + Water (2) and 55 kPa
- Water (1) + o-Tolunitrile (2) at 55 kPa
- m-Cresol (1) + Water (2) + Naphthalene (3) LLE at 80°C and 90°C

The vapour pressures of all the components studied were measured first. The resultant vapour pressure data were then regressed to obtain parameters for the Antoine equation and the Wagner equation (Reid et al [1988]). Measured VLE were modeled using both the Gamma – Phi and the Equation of State methods while VLLE data were modeled using only the Gamma –Phi method. In the combined method (Gamma – Phi method), the NRTL (Renon and Prausnitz [1968]), Wilson [1964], TK-Wilson (Tsuboka and Katayama [1975]) and UNIQUAC (Abrams and Prausnitz [1975]) equations were used to correlate the liquid phase activity coefficients. The vapour phase non-idealities were accounted for by using fugacity coefficients from the virial equation of state with the virial coefficients obtained from the Pitzer and Curl [1957] correlation.

Three equations of state (EOS), the Soave [1972] Redlich-Kwong EOS, the Peng and Robinson [1976] EOS and the Stryjek and Vera [1986] modified Peng and Robinson EOS were used in the direct method (Equation of State method). Classical mixing rules were used for all the equations of state together with the theoretically attractive Wong and Sandler [1992] density independent mixing rules.

For the ternary LLE measurements, the binodal curves were correlated to the Hlavaty [1972] equation, the β- function (Shultz et al [1973]) and the log-γ function (Letcher et al. [1989]). The corresponding tie line data were correlated to the NRTL model.

The last phase of the project was to test the measured VLE/VLLE data for thermodynamic consistency. Three tests were carried out on all the isotherms and isobars measured in the project. These are the Point Test of Van Ness [1973], The Area Test of Redlich and Kister [1948] and the Direct Test of Van Ness [1995]. The measured data generally passed all these tests.

1.1 Background to the research problem

The measurement of vapour-liquid-liquid equilibrium (VLLE) data in the School of Chemical Engineering at the University of KwaZulu-Natal dates back to 1992 (then University of Natal) when Raal and Brouckaert [1992] measured VLLE data for the partially miscible system; water(1) + 2-methyl-3 buten-2-ol (2) using a homogeneous equilibrium still of unusual design which had been adapted for heterogeneous systems. Since then, no such work has been carried out. This work, the second in the department on VLLE measurement, is part of a greater study by SASOL, (a South African chemicals and energy concern, producing petrol and diesel from coal and natural gas using the Fischer-Tropsch process), for the design of a distillation column for separating a partially miscible multicomponent mixture produced in one of their processes. Equilibrium data for the systems of interest were unavailable in the previous literature and thus the need to provide these important data prompted this research work.

1.2 Objective of the study

The objective of this project was:

- To develop a dynamic still together with equipment operating procedures for measuring low pressure vapour-liquid-liquid equilibria.

This involved:

(a) Setting up and testing the apparatus.
(b) Measuring equilibrium data for new systems and,
(c) Analysing the measured data so that they can be used in design calculations.

1.3 Thesis outline

After this introductory chapter is a detailed literature review of the equipment that has been used previously to measure VLLE for systems of partial liquid miscibility. The review is followed, in chapter three, by a review of the thermodynamic equations and principles for low pressure VLE, VLLE and LLE. Chapters four and five present, respectively, the equipment that was used in this work and the equipment operating procedures. The measured results together with their analysis, for the systems that were used to test the equipment used in the project, are presented in chapter six. Chapter seven presents the analysis of the results for the new systems measured in this work and chapters eight and nine wrap up the report, with chapter eight being a discussion of the results and chapter nine giving the conclusion and recommendations.

2

Chapter Two

Experimental Techniques for Low Pressure VLE/VLLE

Experimental determination of vapour-liquid-liquid equilibria (VLLE) involves the separation of the two liquid phases from the upper vapour phase at steady state and the subsequent determination of the compositions of the three equilibrium phases. Unlike in vapour-liquid equilibrium (VLE) where the literature on experimental techniques to measure the data is voluminous (Malanowski [1982a]), Gomis [2000] reports that by year 2000 there was no standard commercial instrument available to sample out the three phases in equilibrium. Researchers have therefore been using modifications of conventional instruments used in the determination of VLE.

This chapter thus outlines how the methods for the determination of VLE have been adapted for measuring VLLE for systems which show limited miscibility in the liquid phase. The main reason why these methods fail, particularly those of the circulation type, is that the vapour after condensation and cooling usually separates into two layers and this has two serious implications. The first is that the condensate cannot be returned to the boiling flask with the liquid phases in the correct ratios and the second is that accurate determination of the resultant liquid composition is not possible. Other difficulties encountered will be outlined as the methods are discussed.

The methods for the direct measurement of VLE are classified according to Hala et al. [1967] into the following groups:

1. Distillation Methods
2. Dynamic Methods (Circulation)
3. Static Methods
4. Flow Methods
5. Dew and Bubble Point Methods

According to Raal and Muhlbauer [1998] and Hala et al. [1967] the development of newer and efficient methods for the measurement of VLE has led to the dew and bubble point methods losing favour. The discussion on these methods will thus be limited to a single apparatus that has been used in VLE measurements for systems showing limited miscibility in the liquid phase. The reader interested in further details about the subject is referred to excellent reviews by Malanowski [1982b] and Hala et al. [1967]

The other methods are now discussed in detail giving their advantages and disadvantages and citing examples from the literature. Particular emphasis will be on the dynamic and static methods. Apart from it not being the intention of this chapter, it will certainly not be possible to present all the methods that have been published in the open literature. Only a selection illustrating the development of techniques for VLLE will thus be given and the reader is therefore referred to reviews by Hala et al. [1967], Abbott [1986], Malanowski [1982 a & b] and more recently by Raal and Muhlbauer [1998]. The latter have also presented methods for measuring infinite dilution activity coefficients, Raal [2000].

2.0 The Distillation method

The distillation method is the oldest method for measuring VLE/VLLE. During operation, a relatively small amount of liquid is distilled off in a boiling flask which contains a large liquid charge. The method was proposed by Carveth [1899] and his apparatus is shown in Figure 2-1 below (extracted from Joseph [2001]).

The experiment starts by adding a liquid charge, approximately 400cm^3 into the boiling flask A. The solution is heated and the boiling point is recorded. This is done initially with glass tube B placed so that no liquid can enter through D and that no condensed vapour can fall from the condenser tube into F. Once the boiling point of the first component has been found the other component is added in small known amounts after which the tube B is lowered until E and D are below the level of the solution in the boiling flask. The flask is then heated until the readings of both thermometers give the same temperature, which is the boiling point of the solution.

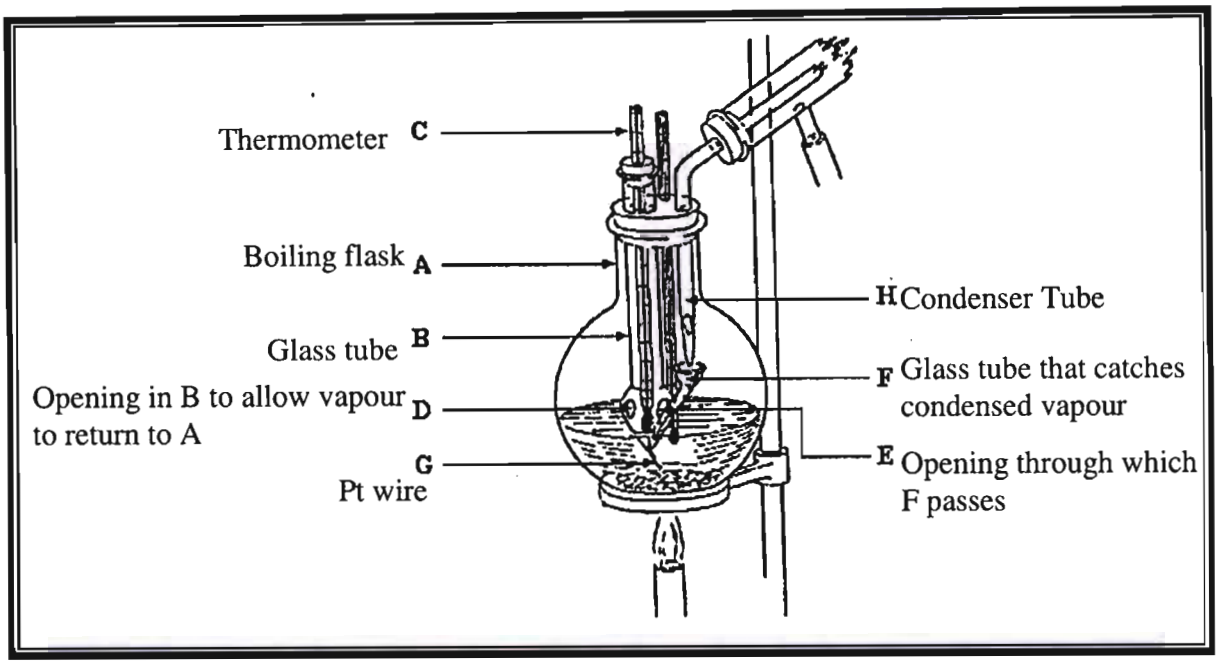

Figure 2 - 1: The Experimental Apparatus of Carveth

The tube B is afterwards raised and turned to catch the condensate which enters at the base of the tube B. The liquid will eventually overflow into A resulting in the temperature of the bulb being constant. The temperature of the bulb and that of the boiling flask, A, are recorded and then the bulb is totally immersed in the boiling solution where both thermometers should give the same reading.

This method was later modified by Rosanoff et al. [1914] and was shown by Young [1922] to give good results. It, however, assumes that the liquid and vapour obtained by boiling a liquid are in equilibrium, the adequate proof of which has not been provided. Theoretical considerations show that only those molecules in the liquid 'surface' are in true thermodynamic equilibrium with the vapour phase. It has an advantage, however, of simplicity and according to Hala et al. [1967], it was important in that it laid the foundation for the development and improvement of experimental techniques for phase equilibria. Another of its major drawbacks affecting the attainment of true equilibrium is that the vapour condenses on the cold sides of the flask during the experiment resulting in rectification. As such this method is very seldom used nowadays (Hala et al. [1967], Gomis et al. [2000]). It will therefore not be discussed any further. Its later modifications, described below could even handle systems with limited miscibility in the liquid

phase. One of the first apparatus using the distillation principle for the measurement of vapour liquid equilibrium for systems of limited miscibility in the liquid phase was proposed by Hands and Norman [1945].

The Dynamic method.

This method, also called the circulation method, can be classified into two categories depending on which phase is circulating (Hala et al [1967]):

2.1 Circulation of the vapour phase only
2.2 Circulation of both the liquid and vapour phases

Circulating methods have an advantage over the other methods in that they are simple, precise and the amount of test chemicals required per run is small. In all the circulation stills, which can be operated under isobaric or isothermal conditions, the following features are common. A liquid mixture is charged into a distilling flask and brought to a boil. The evolved vapours are condensed (except in methods where there is direct circulation of the vapour phase) into a receiver from where the condensate returns to the distilling flask and mixes with the boiling liquid. The thermodynamic properties (temperature, pressure, liquid and vapour compositions) are recorded once steady state conditions have been reached (Joseph et al. [2001]).

2.1 Circulation of the vapour phase only (The Othmer type)

Othmer [1928] published the first valuable still from earlier ideas of Sameshima [1918], on which principle many published apparatus are based (Malanowski [1982a]). In his still, shown in Figure 2-2, the vapour generated by boiling the liquid is led to a condenser from where the condensate returns to the boiling flask via a condensate trap. The still is also provided with liquid and vapour sampling points.

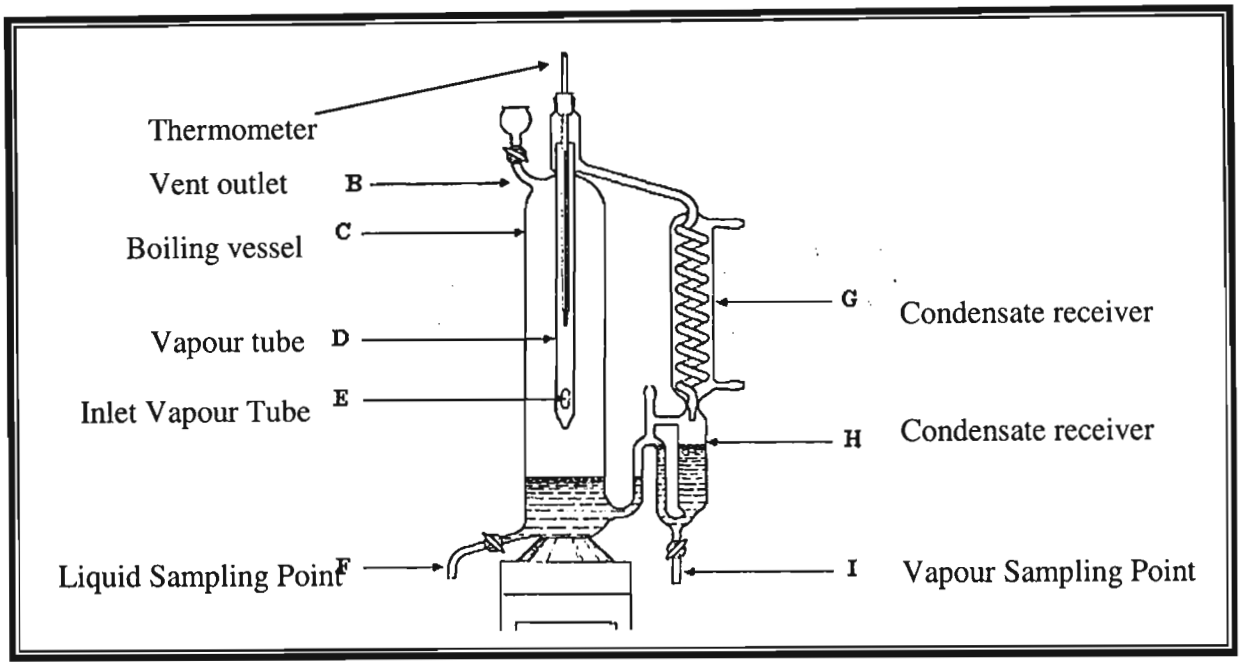

Figure 2 - 2: The apparatus of Othmer

The apparatus of Othmer had the advantage of being simple and can be operated with minimum attention. Its main drawbacks however are:

- There is partial condensation of the vapour on the walls of the flask which results in fractionation.
- It is not possible to determine the equilibrium temperature accurately (For accurate temperature determination, the measuring device should be in contact with both the equilibrium phases).
- It is not possible to get uniform compositions in both the condensate trap and the flask as there is no mixing provided.

The design of Othmer [1928] was modified further in other papers (Othmer [1943] and Othmer [1948]). However, even in its latest form the apparatus suffered the defect that the equilibrium liquid sample was withdrawn from the bulk liquid in the still and therefore does not represent the liquid composition that is in true equilibrium with the vapour sample.

Othmer's apparatus could also not handle systems which are partially miscible since, as has already been said; the vapour after condensation and cooling separates into two layers and the

condensate cannot be returned to the boiling flask with the liquid phases in the correct ratios. This results in the vapour phase becoming rich in the more volatile component.

2.1.1 Modifications for systems of partial liquid miscibility

The following are modifications of the Othmer still for systems which show limited miscibility in the liquid phase.

2.1.1.1 The experimental apparatus of Stockhardt and Hull (1931)

One of the first equilibrium stills designed to measure VLE for systems with limited miscibility was proposed by Stockhardt and Hull [1931] (see Figure 2-3). The central feature of the apparatus is the flexible connection between the flask and the condenser. The condenser could be tilted so that the condensate either refluxed totally or was wholly collected in the receiver.

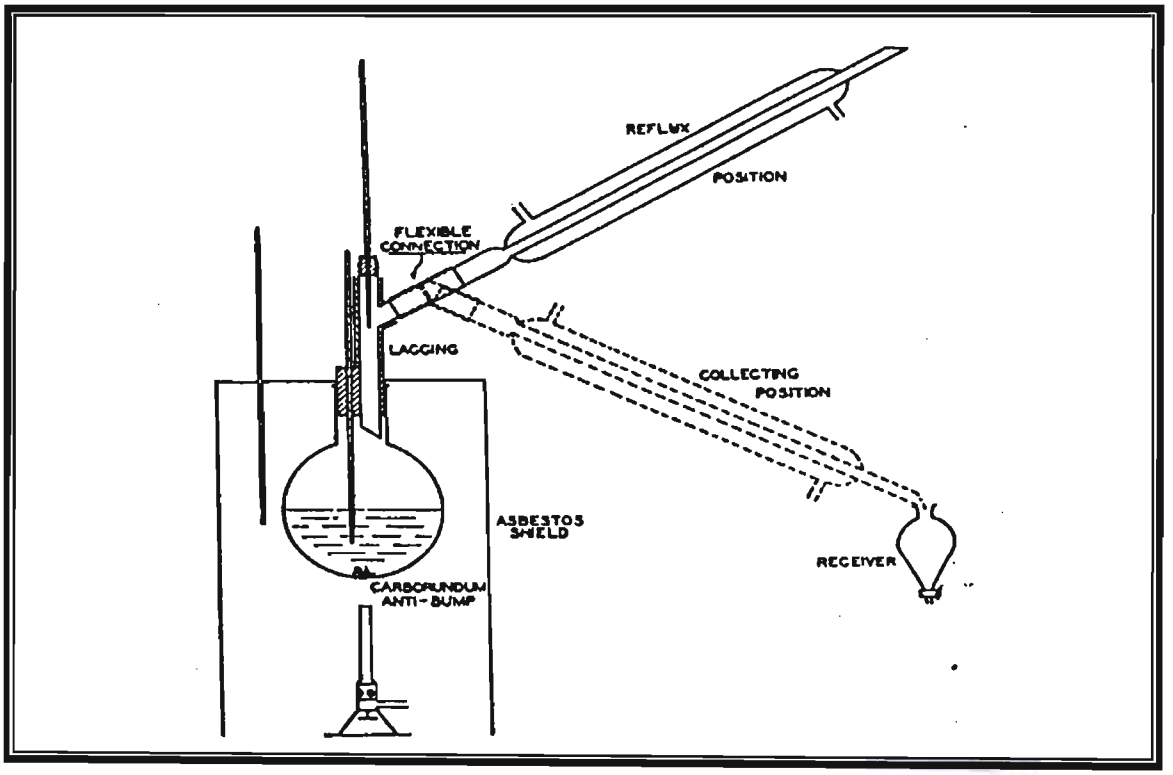

Figure 2 - 3: The Apparatus of Stockhardt and Hull

During operation, the flask is charged with approximately 1000 grams of liquid mixture and then boiled gently under total reflux for about 30 to 45 minutes. During this period the external

temperature was adjusted to within 0.5 °C of the temperature of the liquid (by controlled venting of the combustion gases from the Bunsen burner) in order to prevent wall superheating and condensation. At the end of this period, the slope of the condenser was changed and several successive samples collected in separating funnels for gravimetric analysis. Liquid and vapour temperatures and the barometer reading were taken at the time of collection. According to Smith and Bonner [1949], the Stockhardt and Hull apparatus is simple to set up and operate. It however, tends to produce vapours too rich in the more volatile component and it thus suffers from similar problems as the Othmer still. Fractionation is caused by the scrubbing action of reflux which passes down the neck of the apparatus prior to sampling. Another disadvantage according to Hala [1958] is that it can only be used for systems that are homogeneous at the boiling point. It is however capable of producing good results as confirmed by Smith and Bonner [1949].

2.1.1.2 The experimental apparatus of Baker et al (1939)

In an attempt to eliminate problems associated with earlier designs, Baker et al [1939] proposed a still which could prevent condensed vapours from going back to the boiling pot. The apparatus (see Figure 2-4) was a modification of that of Trimble and Potts [1935].

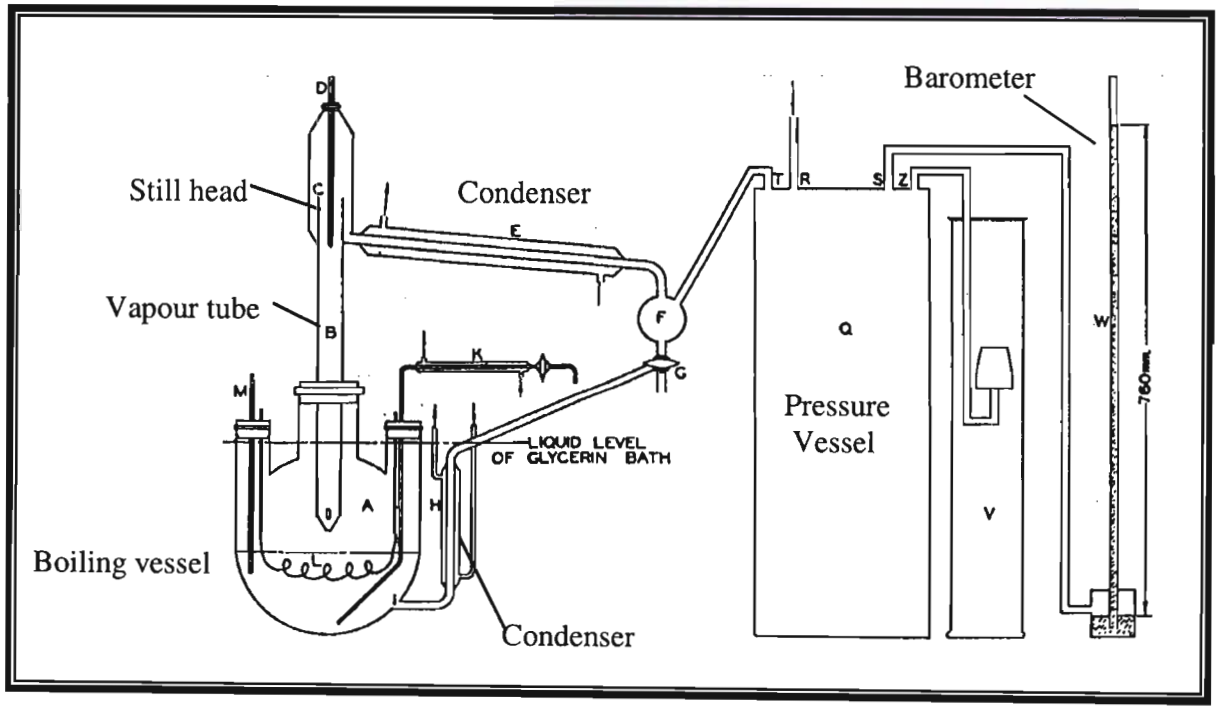

Figure 2 - 4: The experimental apparatus of Baker et al

The sample to be analysed is put into a two litre still, A, which is heated and is agitated by an electric stirrer. The vapour from the still rises to the condenser through B and the still head C removes as distillate any vapours condensed in the upper portion, thus preventing the return of the reflux to the surface of the still liquor. Except when liquid and vapour samples are being withdrawn for analysis, the condensate in F goes through the three-way cock, G, and the air cooled condenser, H, and is returned to the still A. The containers Q and V are for pressure stabilisation and control during the experiment.

As in the apparatus of Stockhardt and Hull, it is not possible to determine the true equilibrium temperature with this apparatus because the thermometer is not in contact with the two phases in equilibrium. Again, the large volume of liquid needed in the still makes the method less attractive. The method cannot handle systems that are heterogeneous at the boiling point as the mixing is not adequate for complete emulsification of the large volume of the heterogeneous mixture in the still (Hala et al [1967]).

2.1.1.3 The experimental apparatus of Smith and Bonner (1949)

The design of Baker et al. [1939], described above, was modified by Smith and Bonner [1949]. Their apparatus is shown below, Figure 2-5. The solution to be measured (about 700 ml) is placed in the magnetically stirred flask and brought to boil with the internal heater, H. The vapour leaving through the main conduit, P, condenses in the cooler (not shown) and returns through the three way cock and small cooler, CH1, to the boiling vessel.
After attainment of steady state (about 60 min) the three-way valve, K, is turned so that the condensate flows through the auxiliary cooler, CH2, directly into a sampling bottle.

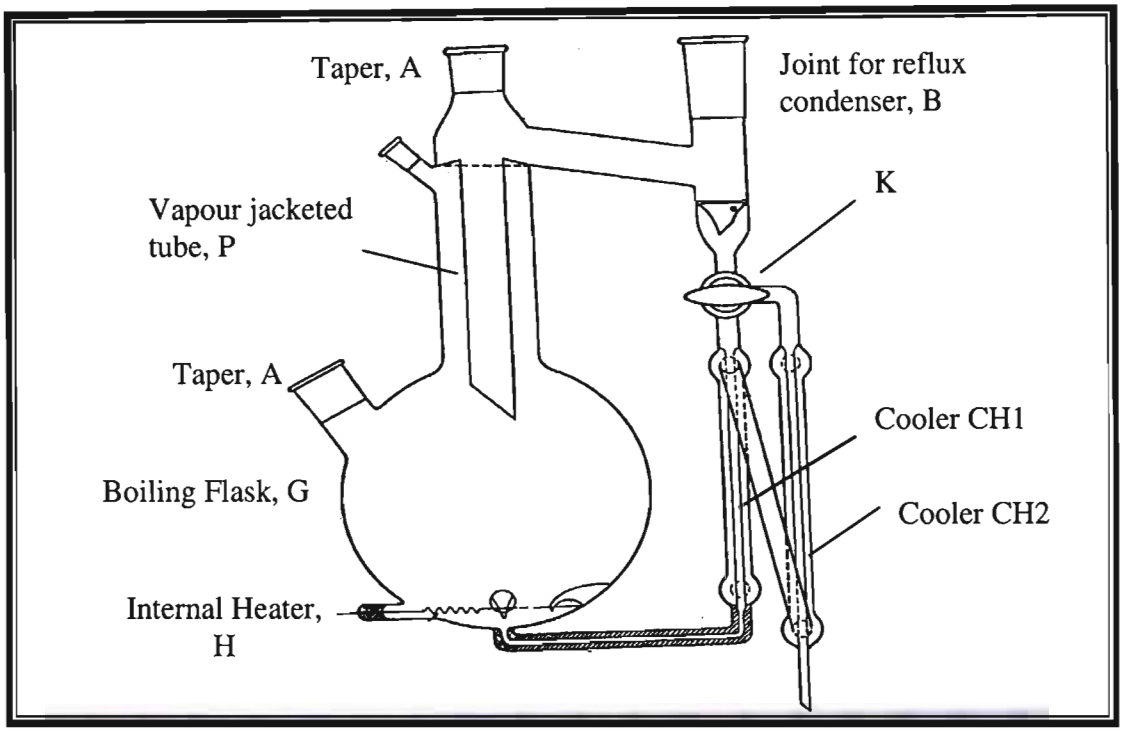

Figure 2 - 5: The Experimental apparatus of Smith and Bonner

It is claimed that the absence of a condensate trap ensures that the two-phase condensate formed in systems with partial liquid miscibility is sent to the reboiler with the two liquid phases in the correct ratios. However, magnetic stirring is inadequate for the large chemical volume (700ml) added to the flask. For this reason, the still is unsuitable for heterogeneous systems as without adequate stirring the vapour formed becomes rich in the more volatile component. For this reason Kollar [1952] proposes the use of mechanical mixing. As with the Othmer [1928] still the measurement of the equilibrium temperature (not shown) is not acceptable. Another drawback of this apparatus, also similar to that of Othmer, is that of partial condensation of the rising vapours on the cold parts of the boiling flask.

2.2 Circulation of both the liquid and vapour phases (The Gillespie type)

Gillespie [1946] published a still which was based on an earlier version by Lee [1931] who pioneered the work of circulation of both the liquid and vapour phases with the aid of a Cottrell pump (Cottrell [1919]). According to Coulson et al. [1948], his still, which had a separator for the liquid and vapour streams and provision for the removal of both the liquid and vapour samples without interrupting the operation of the still, was found to be greatly superior to the designs of

the earlier workers with vapour condensate circulation (Othmer [1943]) and even those modified with the additional Cottrell pump (Scatchard et al. [1938]).

The apparatus of Gillespie is shown in Figure 2-6. Boiling is produced in the equilibrium chamber and the Cottrell pump squirts a mixture of vapour and liquid into the disengagement chamber where the temperature is monitored. The condensed vapour returns to the boiling chamber via a sample trap and premixes with the liquid from the equilibrium chamber before entering the boiling flask.

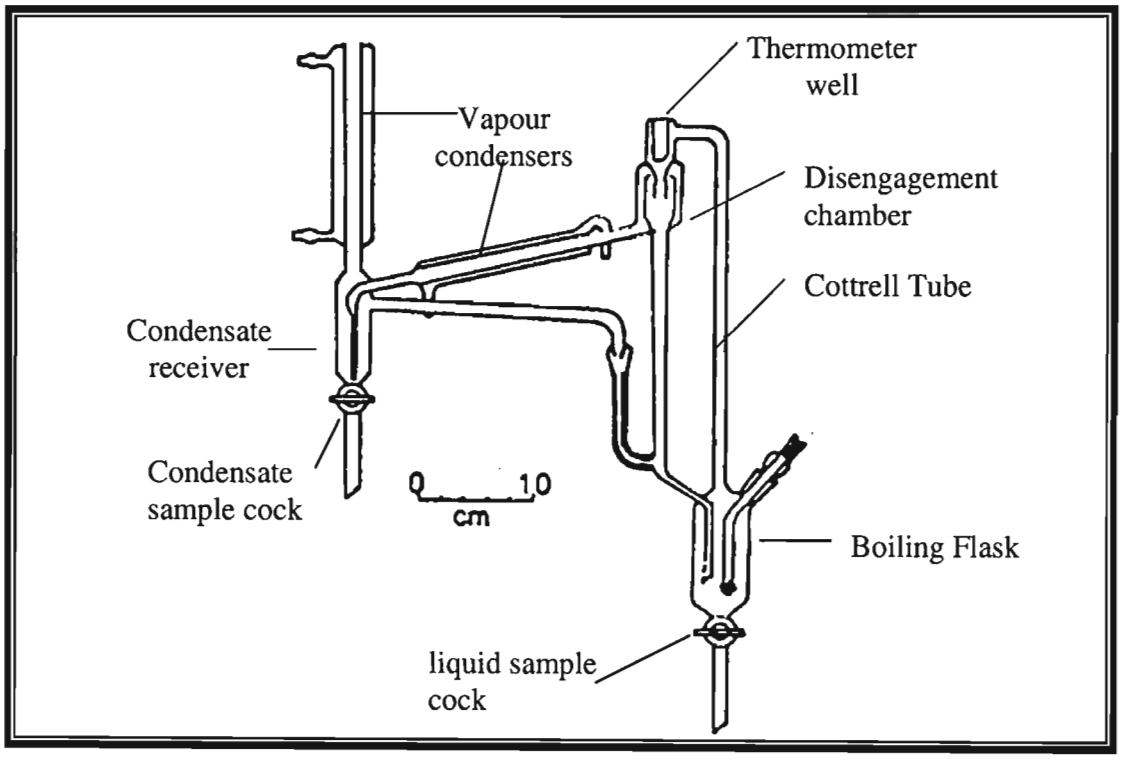

Figure 2 - 6: The original apparatus of Gillespie

In the above apparatus, the liquid sample is again withdrawn from the still reboiler - a situation which has persisted in all the earlier apparatus.

2.2.1 Modifications for systems of partial liquid miscibility

Presented below are modifications of the Gillespie still for systems which show limited miscibility in the liquid phase.

2.2.1.1 The experimental apparatus of Thornton (1951)

The Thornton still was one of the first stills employing the principle of the Cottrell pump in the circulation of both the liquid and vapour phases for systems of limited miscibility. The special feature of this unit is its vacuum insulated receiver for collecting condensate located directly in the vapour space. The apparatus is shown below, see Figure 2-7.

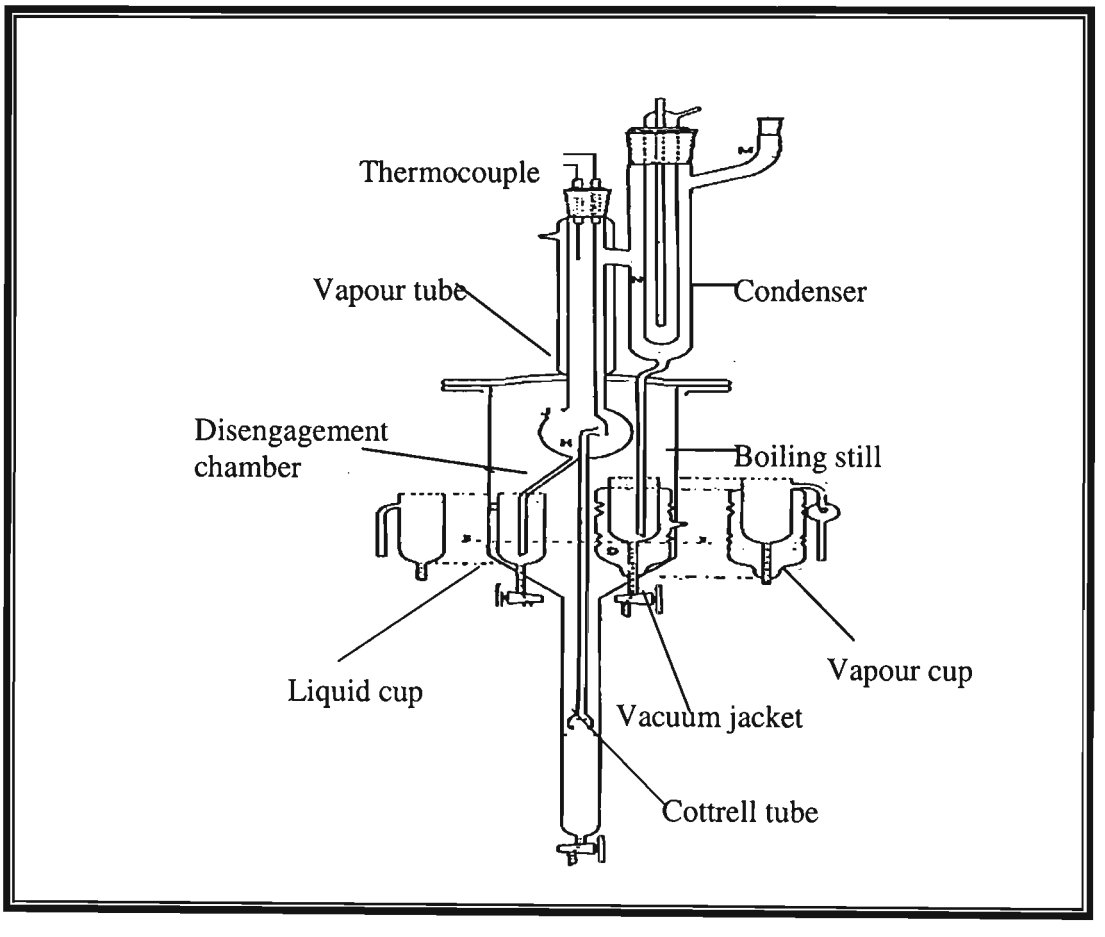

Figure 2 - 7: The Thornton still

The condensate returns to the boiling chamber as soon as it is formed, thus preventing separation into two phases. A similar instrument was proposed by Fenske et al. [1947].

During operation, 400ml of the liquid mixture is charged into the still which is electrically heated. The vapour bubbles formed rise up the Cottrell tube, entraining liquid droplets as they go, and finally discharge in the vapour-liquid disengagement chamber. The liquid phase runs into the appropriate cup and the vapour ascends through a tube to the condenser and returns to the vapour

cup by a different route to that taken by the ascending vapour. The returning condensate is preheated on its way down and is thus always maintained at a temperature higher than the boiling point and hence remains homogeneous.

After equilibration (about 2-3 hours) the still is switched off and liquid and vapour samples withdrawn for analysis (two-phase liquid mixtures occurring upon withdrawal are made homogeneous through the addition of a third component miscible with the mixture constituents before analysis). One of the major drawbacks of the Thornton still is that, like the Gillespie still, it depends on the principle of the Cottrell pump for the attainment of equilibrium. According to Raal and Muhlbauer [1998], a Cottrell tube itself is not a satisfactory device for rapid attainment of equilibrium. The opportunity for mass transfer between the liquid and vapour phases in the Cottrell tube is limited due to the short contact times and small interfacial areas. They propose the use of a spirally curved Cottrell tube to help improve the contact between the liquid and vapor phases. The operation of the still may also be disturbed by the sampling process, which is another drawback of the apparatus.

2.2.1.2 The experimental Apparatus of Ellis and Garbett (1960)

Ellis and Garbett [1960] proposed a still similar in principle to the recirculating stills for homogeneous systems of earlier workers but using vibratory stirrers for the liquid and condensate. The apparatus, shown below, could thus handle systems which are heterogeneous.

The still consists essentially of a liquid chamber, A, provided with a main heater wound onto a porcelain glass tube inserted into the bayonet, B, a 20 mm diameter vapour space containing a saucer – shaped baffle C, which eliminates entrainment by deflecting the liquid spray from condenser D and condensate chamber, E, and a line back from this to the liquid chamber. During operation, the still is charged with 200 ml. of the heterogeneous liquid of desired composition which is boiled and completely emulsified by the stirrer, details of which are also shown in Figure 2-8.

Because of its pumping action in emulsifying the two liquid phases, the stirrer replaces the Cottrell pump used in stills for miscible liquids. The arrangement thus permits accurate boiling point measurement. The equilibrium vapour condenses into a two-phase liquid which collects in the condensate chamber, E. The condensate stirrer is powered by the same vibrator unit as the main stirrer. The still is allowed to circulate steadily for 2.5 to 3 hours after which the boiling point is read and the heaters, but not stirrers turned off – so as to avoid separation into two liquid

phases and the subsequent difficulties in the composition analysis. Samples of the liquid and condensate are then withdrawn for analysis.

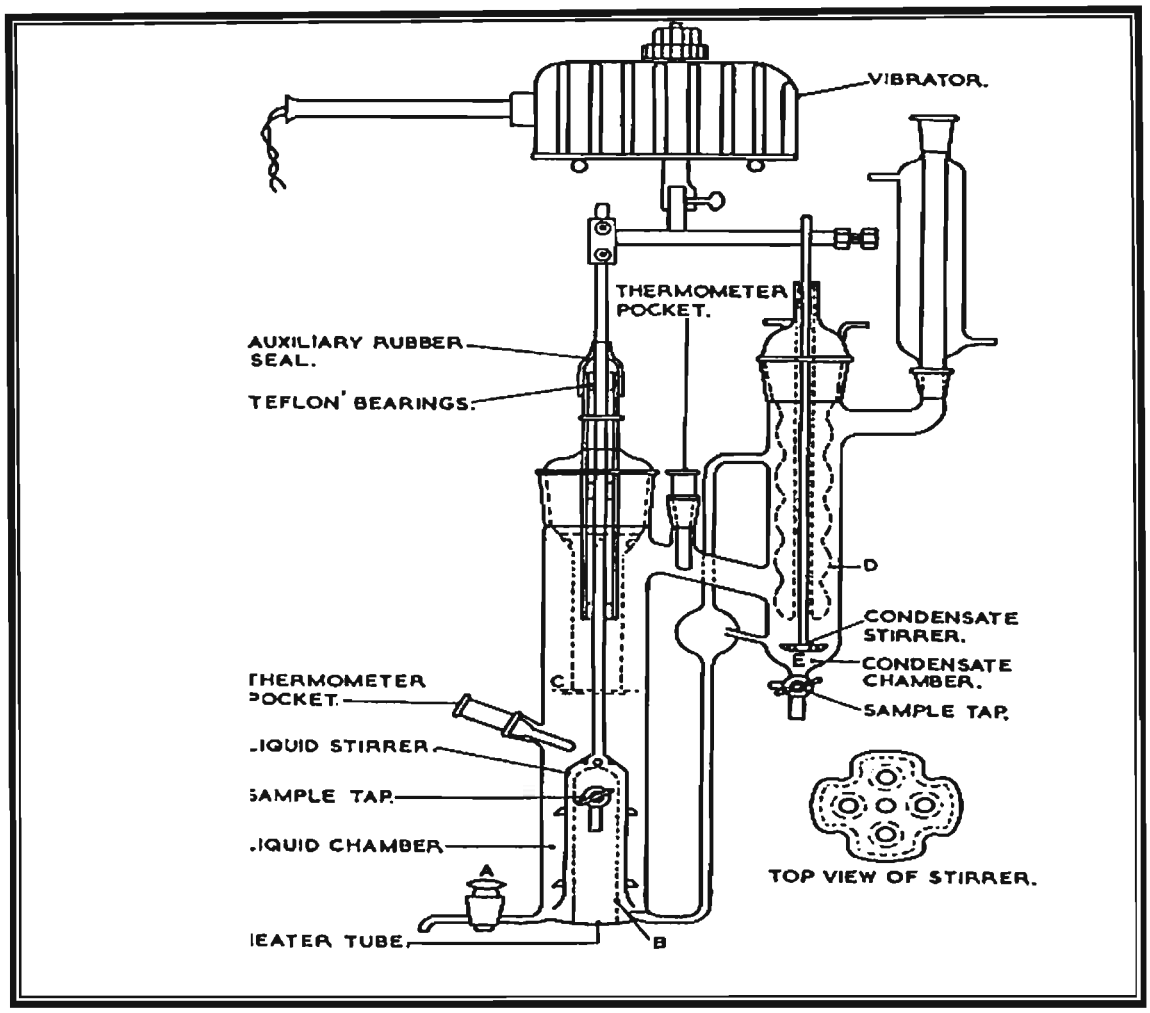

Figure 2 - 8: The Experimental apparatus of Ellis and Garbett.

One disadvantage of the method is the complexity of the apparatus. It also has long periods to reach equilibrium and like the earlier method of Thornton [1951] which relied on the principle of the Cottrell pump for the attainment of equilibrium, it relies only on the principle of the stirring action for achieving equilibrium.

2.2.1.3 The experimental apparatus of Zandijcke and Verhoeye (1974)

Zandijcke and Verhoeye [1974] incorporated the principle of the Swietoslawski [1945] ebulliometer for heterogeneous liquid systems in their design which was able to provide vapour-

liquid equilibrium measurements for systems that are heterogeneous. Their still, shown in Figure 2-9, is divided into two parts A and B which are heated separately.

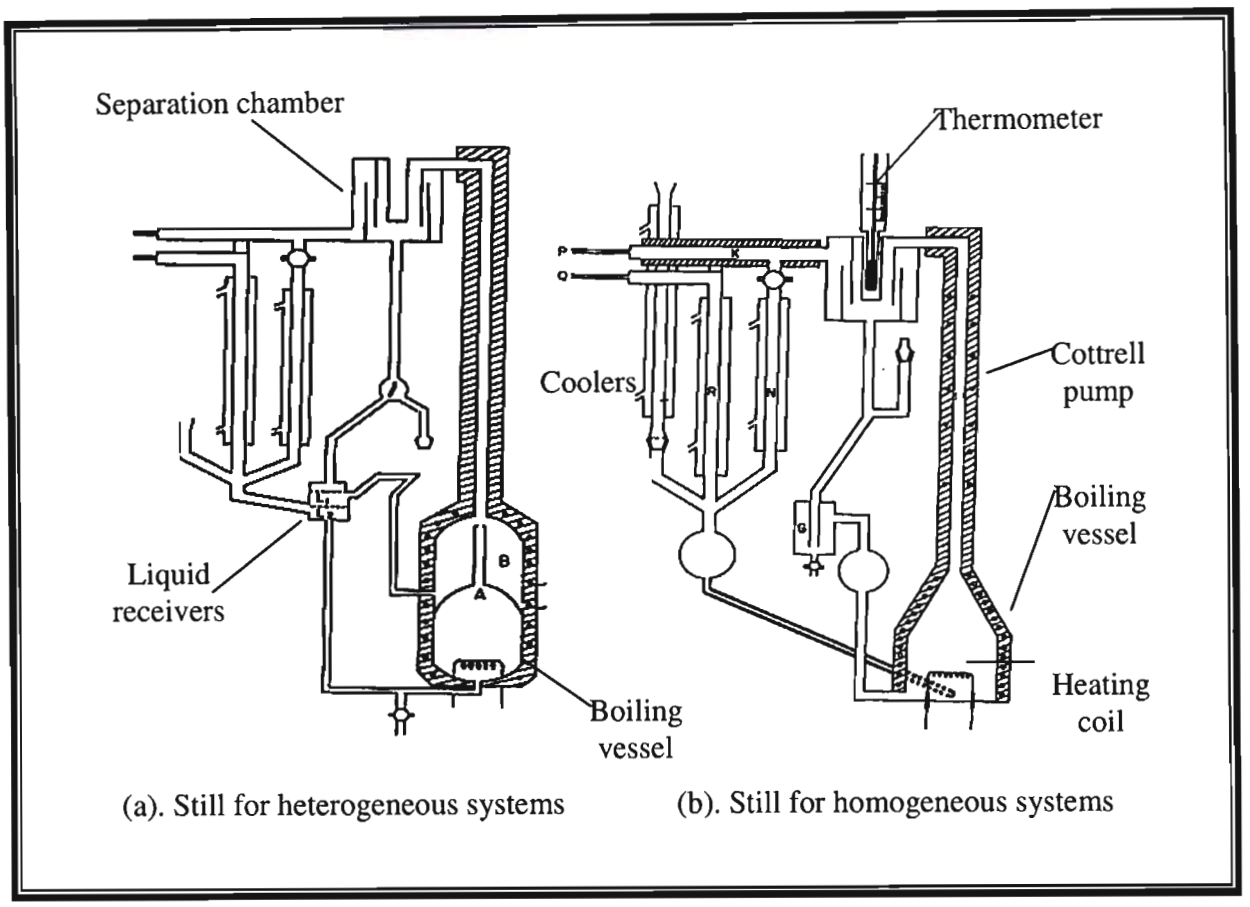

Figure 2 - 9: The Experimental Apparatus of Van Zandijke and Verhoye (1974)

The lower part contains the phase with the highest heat of evaporation. For this a separator is placed in the liquid path, which is sufficient to permit separation of both liquid phases to a sufficient degree. In the Cottrell pump, three phases come to equilibrium and they spout together onto the thermometer well, thus permitting accurate measurement of the boiling point. After separation the liquid phase flows back to the boiling vessel.

The vapour from the separation chamber (see diagram b) goes through a tube, K, partially to the cooler, N, and partially along P to the vapour sampling valve of a chromatography apparatus; through the valve, along Q to the cooler R. The condensate is brought back down into the boiling vessel along Y. An important feature of the apparatus is that the vapour is not condensed and in this way, the difficulties of the separation into the two layers of the condensate are avoided. The

liquid phase is not sampled in this apparatus. Instead liquid-liquid equilibrium data at the boiling point are measured with a different still (not shown) (Zandijcke and Verhoeye [1974]).

The advantage of the Van Zandijcke and Verhoeye still is that mechanical mixing of the two liquids is unnecessary and the two liquids and vapour phases are able to rise together in the Cottrell pump. However, they also assume that a Cottrell pump is adequate for the attainment of equilibrium. According to Iwakabe [2001] who tested the apparatus, the observed fluctuation of the temperature inside the equilibrium chamber was relatively large and the accuracy of the observed data was somewhat poor in terms of thermodynamic consistency. This inaccuracy is caused by the incomplete separation of the light and heavy liquids at the upper and lower chambers inside the still, thus the amount of the lighter liquid in the lower chamber fluctuates with time. Gomis et al. [2000] attribute the temperature fluctuations to inadequate mixing in the liquid phase and discontinuity in the flow of the phases. He proposed a modified Gillespie type still with an ultrasonic homogenizer that stirs the suspended liquid in the flask and later patented his method.

2.2.1.4 The experimental apparatus of Koichi Iwakabe (2001)

Koichi Iwakabe (Iwakabe [2001]) recently modified the still proposed by Van Zandijcke et al [1974]. The still can measure both VLE and VLLE for heterogeneous systems and is shown in Figure 2-10 below. It consists of a boiling flask A, a Cottrell pump B, an equilibrium chamber C with a thermometer well I, and a vapour liquid mixing chamber F. A conical shaped cup G is placed above the electric heater, M, in the boiling flask to allow the heavier liquid and vapour to rise up together in the Cottrell pump, and a conduit H, is attached at the top of the boiling flask to send the lighter liquid and vapour to the Cottrell pump. To obtain LLE for the two liquids flowing from the equilibrium chamber, C, a small cell with the volume of 2 ml is placed in the liquid collector, D. The liquid samples in the small cell are drawn through the sampling port, K, with a syringe.

During operation, about 200ml of the liquid mixture is loaded into the boiling flask and heated by an electric heater. The vapour and liquid rise in the Cottrell tube, get separated in the equilibrium chamber and the liquid collects in D with the vapour proceeding to the condenser E. At steady state (attained within 60 minutes), the equilibrium temperature is recorded and the condensed vapour and liquid samples are withdrawn for analysis by gas chromatography. If the condensed vapours are immiscible, a suitable solvent is added to make the sample homogeneous. For the

LLE measurement, the liquids in the small cell J are allowed to settle for around 2 hours during which period the compositions of the upper and lower sections in the cell are checked by GC analysis.

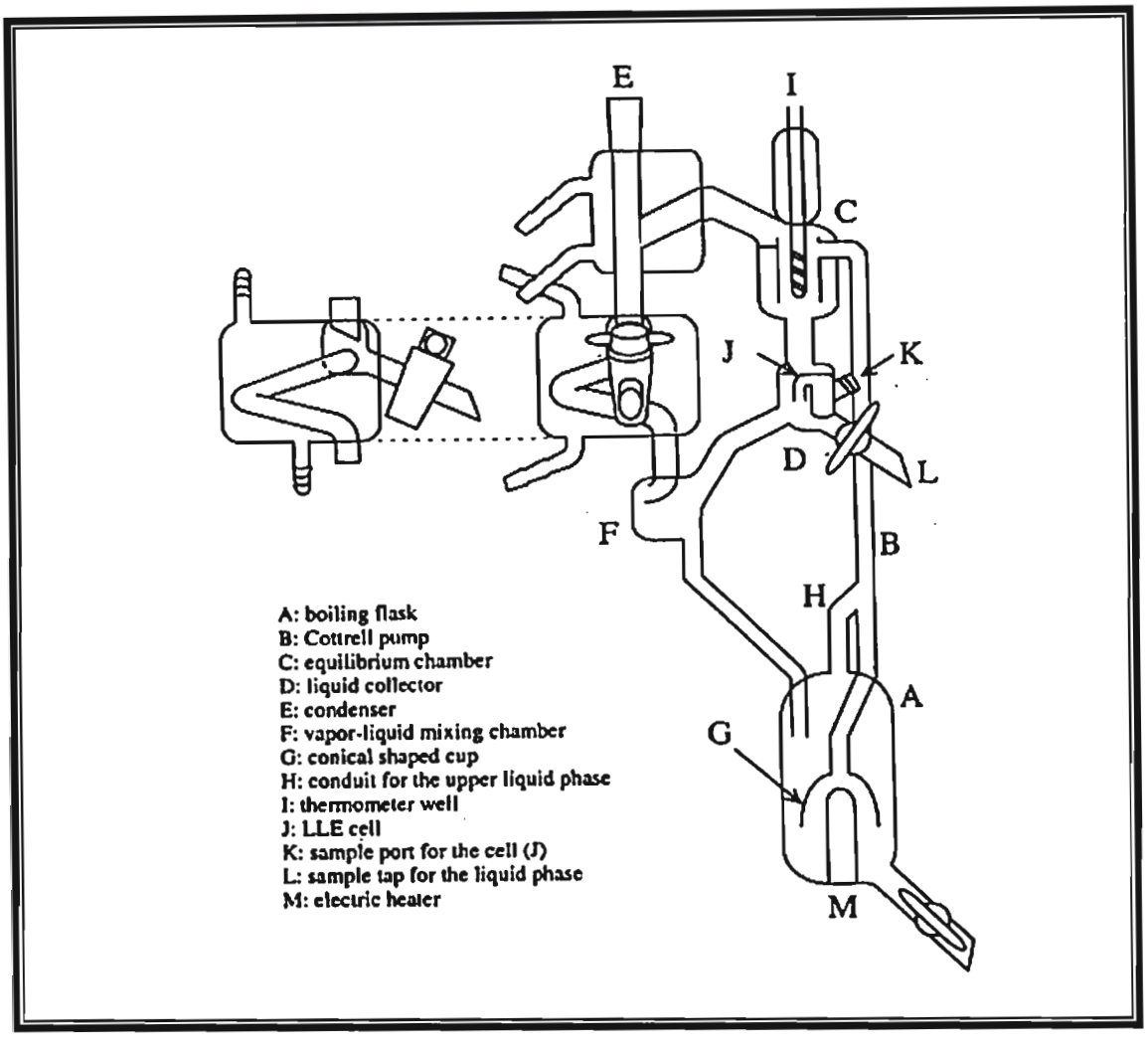

Figure 2 - 10: The Apparatus of Koichi Iwakabe

The Iwakabe [2001] still has the advantage over the Van Zandijcke still in that it is simple to operate. It also produces data with a high degree of thermodynamic consistency. It however, has the same weakness of the earlier apparatus of relying solely on the Cottrell pump for the attainment of equilibrium. Another drawback is the method of vapour composition analysis. It is difficult to get the exact compositions when the vapours are allowed to condense. In this study the direct analysis of the vapour composition prior to condensation is advocated.

2.2.1.5 The experimental apparatus used in this work

The apparatus that was used in this project, discussed in more detail in Chapter 4, is a modification of the Raal and Muhlbauer [1998] still. The Raal and Muhlbauer [1998] still was based on the designs of Heertjies [1960] and Yerazunis [1964], who successfully used a packed equilibrium chamber where the liquid and vapour phases are forced downward co-currently to achieve rapid and dynamic equilibrium. The Raal and Muhlbauer [1998] still was used and further modified by Joseph et al. [2001] who reported data of high thermodynamic consistency.
It is believed that all the errors in the previous designs have been eliminated. The special features to note are:

- The Cottrell tube is not depended on as a means of establishing equilibrium since the equilibrium chamber increases the transfer of mass between the vapour and liquid phases, thus allowing for rapid attainment of equilibrium.
- The direct analysis of the vapour composition by gas chromatography eliminates the difficulties encountered in analyzing the two-phase condensate that is formed a few degrees below the boiling point.
- The small volumes of the condensate receiver and the boiling chamber make it possible for magnetic stirring to completely emulsify the two-phase liquid mixture obtained in systems of partial miscibility.
- Efficient magnetic stirring in both the condensate receiver and the boiling chamber eliminates temperature and any possible concentration gradients that may affect reproducibility of the sample concentrations. Stirring in the boiler also ensures that the returning condensate is thoroughly mixed with the rest of the liquid and thus prevents flashing.

2.3 The Static method

In this method, a liquid mixture is charged into an evacuated equilibrium cell which is placed in a thermostat. The contents of the cell are then agitated mechanically until equilibrium is established between the liquid and its vapour, whereupon samples are removed from one or both phases for analysis. This method presents great difficulties when sampling the vapour phase. At low

pressures, the amount of vapour required for analysis is of the same order as the total amount of the vapour phase in the equilibrium cell (Hala et al. [1958]), so that removal of a sample upsets the equilibrium. As such the vapour phase is not sampled in most static cells (Raal and Muhlbauer [1998]). Inoue et al. [1975] solved the problem of vapour phase sampling but according to Abbot [1986], their ideas were not popular with the majority of experimentalists who only measured the liquid composition. The vapour composition was then computed from the measured pressure and liquid composition values. This technique has the disadvantage that it removes the possibility of thermodynamic consistency testing (Raal and Muhlbauer [1998]).

Another difficulty associated with this method is the need to completely degas the system, which is a time-consuming process. The degassing cannot be ignored as its omission will result in inaccurate measured pressures.

Gibbs and Van Ness [1972] proposed a static cell, shown in Figure 2-11, where the degassed liquids are transferred into a magnetically stirred cell placed in a thermostated bath using piston injectors. The liquids are degassed by refluxing, cooling, and evacuation in a special flask.

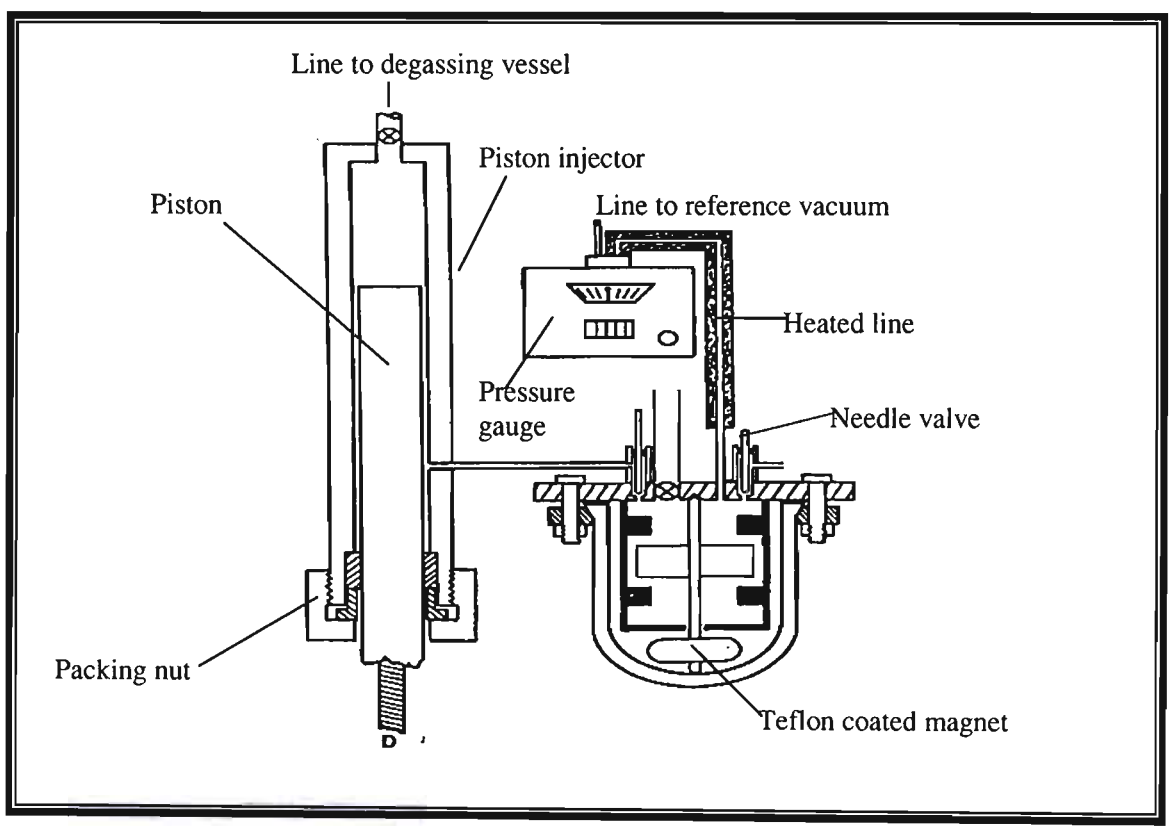

Figure 2 - 11: The Apparatus of Gibbs and Van Ness

The operation starts by metering one of the pure liquids into the equilibrium cell of approximately 100 cm^3 capacity. The vapour pressure is measured when equilibrium is reached after which a small amount of the second component is added to the cell from a separate but similar injector. The total pressure apparatus of Gibbs and Van Ness [1972] was modified by Dielsi et al. [1978] and was used by Loehe et al. [1983] for partially miscible systems.

The following is a description of two other methods that have been applied to systems showing limited miscibility in the liquid phase.

2.3.1 Modifications for systems of limited miscibility in the liquid phase

2.3.1.1 The experimental apparatus of M J Lee et al (2002)

Lee et al. [2002] proposed a static VLLE cell in which both the liquid and vapour phases are circulated to promote equilibrium. The centre of their apparatus, shown in Figure 2-12, is the visual equilibrium cell that is immersed in a transparent thermostatic bath. The gas phase was directly analysed using a gas chromatograph with a thermal conductivity detector.

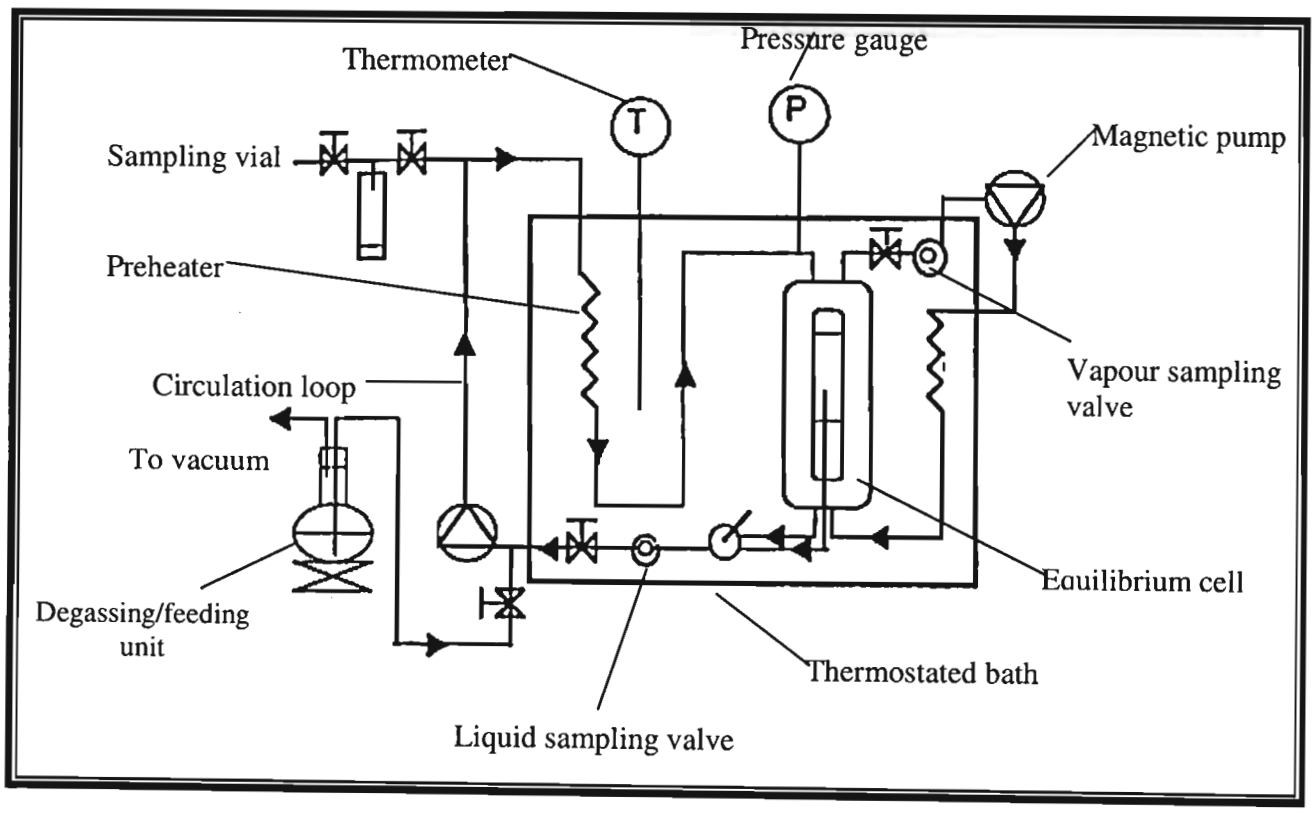

Figure 2 - 12: The Experimental apparatus of Lee et al

The operation starts by degassing the solution using the procedure of Lee and Hu [1995] and then loading the appropriate amounts into the equilibrium cell in which the levels of the vapour-liquid-liquid interfaces are adjusted properly such that the upper liquid can be circulated. Circulation of both phases commences and at equilibrium the pressure is recorded and samples of the three phases sent to the GC's for analysis. The advantage of the apparatus of Lee et al. is that, like the apparatus of Van Zandijke and Verhoeye [1972], the vapour phase composition is determined directly before condensation. This eliminates the difficulties encountered in obtaining the composition when phase separation occurs upon condensation. Apart from the long degassing times, a drawback of the apparatus is that at low temperatures, circulation of the liquid phases becomes difficult as the liquid mixtures become viscous. Their apparatus however, gave good results that agreed with earlier data by Cho et al. [1984] and Pai and Chen [1999]. The same equipment was also used by Lee et al. [2003] and gave thermodynamically consistent results.

2.3.1.2 The experimental apparatus of Bobbo et al (2003)

The experimental apparatus of Bobbo et al (2003) is shown in Figure 2-13. The glass cell with a volume of about 30 cm^3 is immersed in a thermostated bath of about 2.5 litres capacity. The temperature of the setup is maintained by means of a PID controlled system governing a heater immersed in the bath. Pressure is measured by a differential pressure gauge and the bulk composition is gravimetrically measured.

During operation, a liquid mixture of known composition is injected after degassing into the glass cell. Liquid phase splitting is visually observable from the appearance of the cloud point. The equilibrium temperature is taken as the average value between the appearance and disappearance of the second liquid phase with the lowering and raising of the bath temperature. The amount of the vapour phase is disregarded and it is assumed that with the low pressures and small vapour volumes, the omission will introduce no significant error in taking the charge composition as the equilibrium liquid composition.

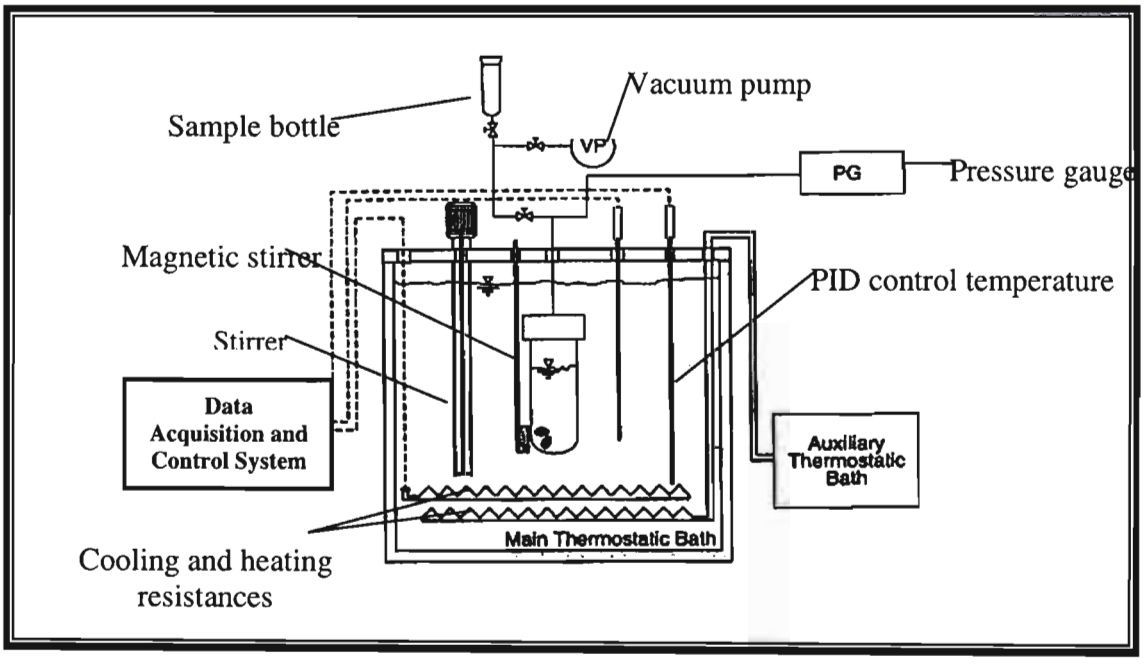

Figure 2 - 13: The Apparatus of Bobbo et al

2.4 Flow methods

According to Hala et al. [1958] the flow methods were specifically designed to handle systems of limited miscibility in the liquid phase. In these methods, the equilibrium chamber is fed with a steady stream of constant composition which can be either liquid or vapour phase or a combination of the two. Two examples of flow vapour-liquid equilibrium apparatuses are given below.

2.4.1 The Colburn flow still (1943)

Colburn [1943] proposed one of the first flow stills with a feed consisting of vapour of a given composition. The feed is prepared by mixing vapours of the individual pure components which are vaporized in separate boiling vessels. The composition of the vapour feed is controlled by varying the amount of energy added to the boiling vessels. The Colburn still is shown in Figure 2-14 below.

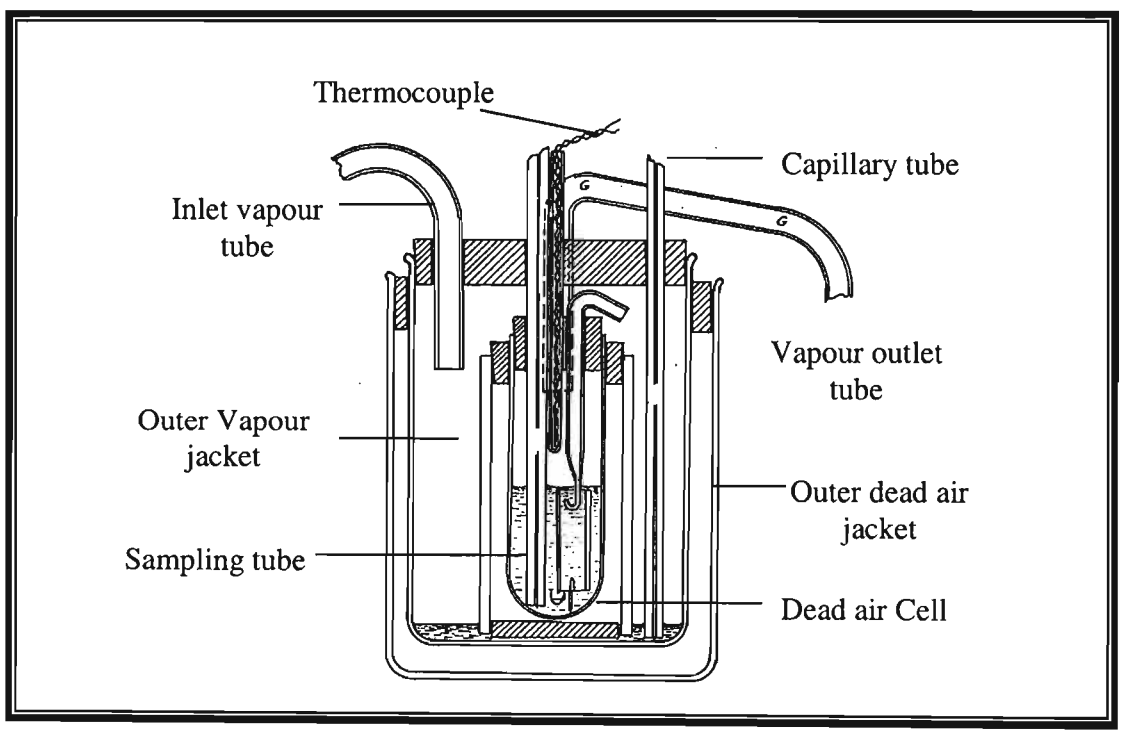

Figure 2 - 14: The Colburn flow still

In starting the measurements, liquid with a composition approximately equal to that for equilibrium with the vapour is first introduced to the equilibrium chamber through the sampling capillary K, the vapour is then introduced where it first heats the liquid and partially condenses before steady state is attained (indicated by constant temperature indicating no vapourisation or condensation). The vapour leaves through G and is totally condensed. At equilibrium a liquid sample is withdrawn through the capillary K and a condensate sample is taken from the cooler. An important point to note with the Colburn method is that when treating systems of partial liquid miscibility, the composition of the vapour feed is chosen so that the equilibrium liquid forms only one phase at equilibrium. The method has the advantage of being relatively simple and according to Hala et al., the method gives consistent data. The Colburn still was further modified by Mertes and Colburn [1947] who proposed a still with several equilibrium chambers.

2.4.2 The Flow still of Newsham et al. (1973)

The flow still of Newsham et al (1973) differs from that of Colburn in that the feed to the boiling chamber is a liquid mixture. It is a modification of a still initially proposed by Vilim et al. [1954], see Figure 2-15 below. The apparatus differs from that of Vilim et al. in that it avoids recirculation of the condensed vapour, which results in reasonably precise results in a short time (15minutes).

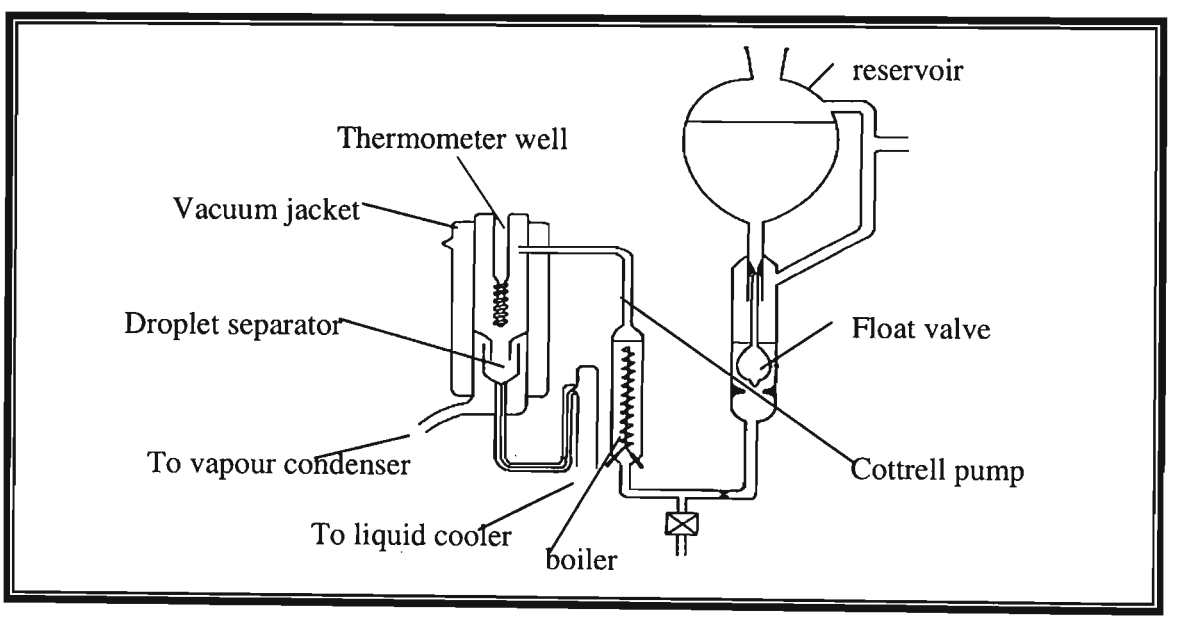

Figure 2 - 15: The equilibrium chamber of the Newsham et al. (1973) still

2.5 Dew and Bubble Point methods

The principle of operation of these methods is first presented and then a single apparatus which has been applied to systems of limited miscibility in the liquid phase is discussed.

2.5.1 The principle of the method.

The principle of the method can be seen from Figure 2-16, which shows the equilibrium P-x-y curve together with the P-V profile. With the instruments described previously for the determination of the equilibrium curves, pairs of points on horizontal lines MN were determined giving the compositions of the two phases that are in equilibrium.

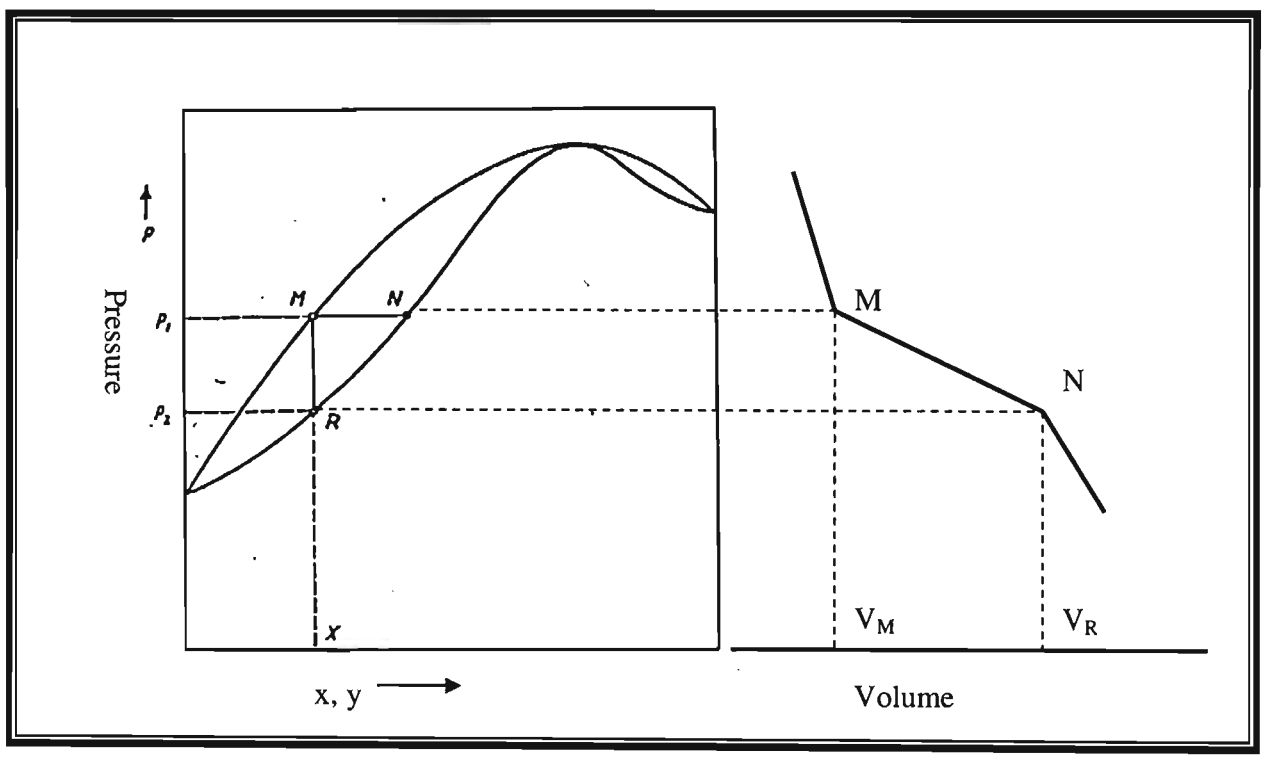

Figure 2 - 16: Principle of the Dew and Bubble Point method

The equilibrium curves for the liquid and vapour phases were obtained by joining a number of such points. As can be seen from the above diagram it is also possible to obtain the same curves by determining pairs of points lying on vertical lines MR. These lines describe the behaviour of mixtures of constant composition at variable pressure and constant temperature. For example if a liquid of composition x at pressures higher than P1 is compressed to P1, an infinitesimal amount of vapour is formed which is in equilibrium with the liquid. This point is known as the bubble point. When the pressure is further lowered, the liquid diminishes and the vapour increases until the pressure P2 is reached when the last drop of liquid vanishes. At this point, the dew point, an infinitesimal amount of liquid is in equilibrium with the vapour of the same composition as the original liquid.

As already stated, with the development of newer methods for measuring phase equilibrium, the dew and bubble point methods have lost favour (Raal and Muhlbauer [1998]). Although the dew and bubble point methods are particularly suited for binary mixtures only, the circulation methods have gained favour mainly due to their higher accuracy and the rapidity with which the data is obtained. However, these methods have particularly been applied for the determination of high pressure VLE although they can be employed for low pressure applications (Hala et al. [1967]). For a more detailed discussion of these methods the reader is referred to Malanowski [1982b].

2.5.2 Modifications for systems of partial miscibility

A single method for the determination of phase equilibrium for systems of limited miscibility in the liquid phase wraps up this review. This is the method that was proposed by Hirata et al [1970].

2.5.2.1 The experimental apparatus of Hirata et al (1970)

The apparatus of Hirata et al (see Figure 2-17) consists of two electrically heated boiling flasks for the pure components, two vapour tubes, two three way cocks, one mixing tube, ten thermometer pockets for dew point measurements, a flow type ebulliometer of 15ml. capacity, four condensers and two receivers for measurement of flow rate.
First, the boiling flasks are filled with pure liquid and then electric power is supplied to the heaters. The three way valves are turned so that the vapours flow into the mixing tube. The

superheated vapour mixture, indicated by point M in the enthalpy concentration diagram (Figure 2-17b) is obtained throughout the mixing tube. In a temperature heat loss diagram the temperature bends at the dew point as the specific heat is much less than the latent heat. The dew point is thus determined by plotting the temperature at each thermometer pocket and each position number. The bubble points are measured in a flow type ebulliometer (not shown).

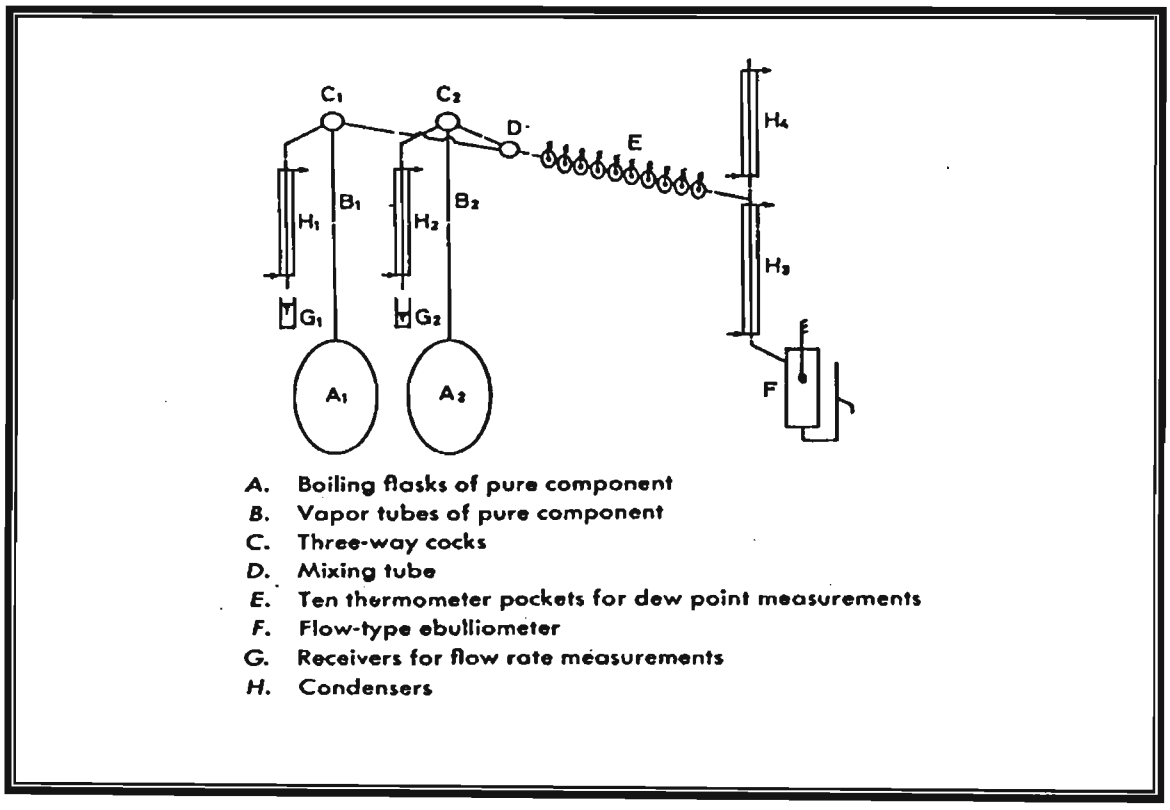

Figure 2 - 17: The apparatus of Hirata et al.

In measuring the composition, the three way valves are turned so that the pure vapours are condensed separately. The amounts are then weighed and the composition determined by the flow ratio. To get other points, the composition is altered by changing the heat ratio between the boiling flasks.

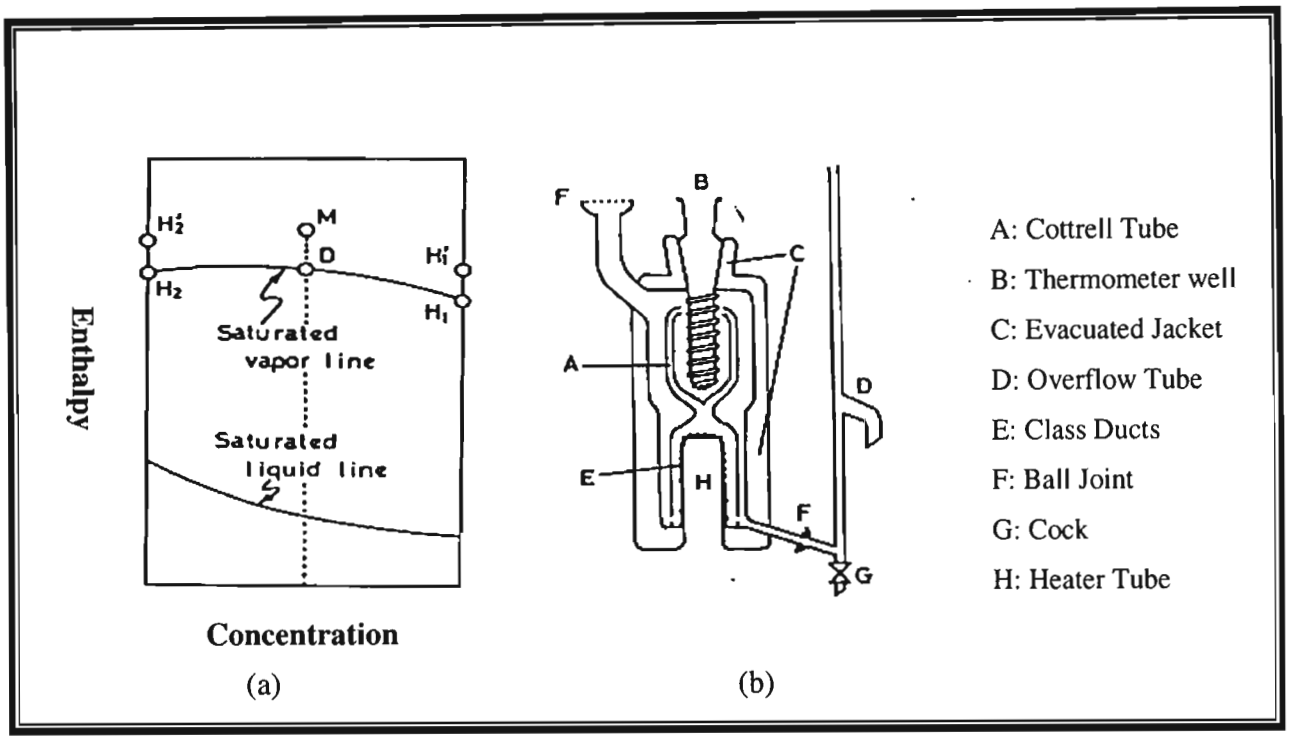

Figure 17:(a) Enthalpy Concentration diagram (b) Equilibrium chamber of the apparatus of Hirata et al. (1970)

2.6 Concluding remarks

Different methods for the measurement of VLE and VLLE have been presented and these generally fall into five categories; the Distillation methods, Dynamic methods, Static methods, Flow methods and Dew and Bubble Point methods. Unlike in the measurement of VLE, where the literature on the equipment is voluminous, few methods are available for VLLE and consequently researchers have been using modifications of conventional VLE methods for the determination of VLLE. This chapter outlined how the methods for the determination of VLE have been adapted for measuring VLLE for systems which show limited miscibility in the liquid phase. A discussion on advantages and disadvantages of a selection of the methods from literature illustrated the techniques that have been developed over the years for measuring VLLE.

Chapter Three

Thermodynamic Principles

3.1 Introduction

Most industrial separation processes, similar to those discussed at the beginning of Chapter 1 viz. distillation, absorption, solvent extraction and leaching, treat multi-component phases. However, experimental VLE and VLLE data are often though not invariably measured for binary systems (furthermore if such data are available for the desired components they are usually not at the required operating conditions of temperature and pressure and often are not of good quality). This is so because for more than two components, the cost and experimental work required for a reasonably complete system description "rapidly mushrooms to impractical proportions" (Raal and Muhlbauer [1998]). For example, the measurement of a 10-component system in 10 mole % steps at only atmospheric pressure would last approximately 37 years (Gmehling [2003]). Prausnitz et al. [1967] say it is unreasonable to expect that experimental VLE will be ever available for a significant fraction of the incredibly large number of liquid and vapour mixtures which occurs in technological processes.

It is therefore necessary to be able to compute multi-component properties from binary data. A sound thermodynamic basis has therefore been developed for such computations and it is the aim

of this chapter to give the fundamental equations on which such calculations are based, thus making it possible to reliably extrapolate and interpolate with respect to temperature, pressure and composition the minimum amount of available data to other unknown conditions. Maximum information and understanding of a particular system can thus be obtained.

This review looks into the theoretical aspects of both low pressure vapour-liquid equilibrium and vapour-liquid-liquid equilibrium. It starts by giving the criteria for equilibrium together with definitions of fugacity, fugacity coefficient, activity and activity coefficient. It then goes on to the methods for the evaluation of fugacity and activity coefficients and data reduction, i.e. regression and correlation of experimental data. The Gamma-Phi formulation of VLE together with the associated activity coefficient models and the direct (Phi-Phi) method with the corresponding equations of state (EOS) are also reviewed. The chapter ends with a discussion on thermodynamic consistency testing which comes after an appraisal of the reduction methods for liquid-liquid equilibria (LLE) and vapour-liquid-liquid equilibria. For the reader interested in greater coverage of the subject, the following excellent texts are suggested: Raal and Muhlbauer [1998], Walas [1985], Smith and Van Ness [1996], Malanowski and Anderko [1992], and Prausnitz et al. [1986].

3.2 The chemical potential defined

In a somewhat lengthy but simple procedure, a combination of the First and Second Laws of thermodynamics yields for a closed system, after invoking the definition of the Gibbs free energy (G = H – TS):

$$d(nG) = (nV)dP - (nS)dT \tag{3-1}$$

It follows from multivariable calculus that:

$$\left[\frac{\partial(nG)}{\partial P}\right]_{T,n} = nV \qquad \text{and} \qquad \left[\frac{\partial(nG)}{\partial T}\right]_{P,n} = -nS \tag{3-2}$$

In an open system, the Gibbs free energy is in addition to the temperature and pressure, also a function of the mole numbers of the system constituents, thus:

$$nG = g(P, T, n_1, n_2 \ldots\ldots\ldots n_i) \tag{3-3}$$

A total differential gives:

$$d(nG)=\left[\frac{\partial(nG)}{\partial P}\right]_{T,n} dP+\left[\frac{\partial(nG)}{\partial T}\right]_{P,n} dT+\sum_{\text{all i}}\left[\frac{\partial(nG)}{\partial n_i}\right]_{P,T,n_j} dn_i \qquad (3\text{-}4)$$

and after substituting for the partial derivatives with respect to T and P from Equation (3-2) above, we get:

$$d(nG)=(nV)dP-(nS)dT+\sum_{\text{all i}}\left[\frac{\partial(nG)}{\partial n_i}\right]_{P,T,n_j} dn_i \qquad (3-5)$$

In the above equations the subscript j indicates that all the mole numbers except n_i are held constant. By using the identity:

$$\mu_i \equiv \left[\frac{\partial(nG)}{\partial n_i}\right]_{T,P,n_j} \qquad (3\text{-}6)$$

Equation (3-5) is transformed to:

$$d(nG)=(nV)dP-(nS)dT+\sum_{\text{All i}}\mu_i dn_i \qquad (3\text{-}7)$$

Equation (3-7) is called the *Fundamental property relation* and is of extraordinary importance in phase equilibria (Smith et al [1975]). Equation (3-6) defines a thermodynamic property, the chemical potential of species i in solution. An analogous derivation based instead on the Helmholtz free energy and the internal energy would give different forms of Equation (3-7) and thus yield two other defining equations for the chemical potential similar to Equation (3-6). The criterion of equilibrium is based on the chemical potential just defined and is discussed in the following section.

3.3 The criterion for phase equilibrium

Equilibrium is a static condition in which the macroscopic properties of a system do not change with time (Smith et al. [1975]). Following the pioneering work of J. W. Gibbs, a vapour phase, α, and a liquid phase, β, are in thermodynamic equilibrium when the temperature and pressure of

each phase equals that of the other and when the chemical potential of each molecular species ,i , present is the same in both phases*. Mathematically this condition is:

$$\mu_i^{\alpha} = \mu_i^{\beta} \tag{3-8}$$

The above equation equally applies for each component in more than two phases, thus for π phases and N chemical species we have:

$$\mu_i^{\alpha} = \mu_i^{\beta} = \ldots\ldots\ldots \mu_i^{\pi} \qquad (i = 1, 2 \ldots\ldots N) \tag{3-9}$$

3.4 Fugacity and fugacity coefficient

According to Prausnitz et al. [1967], the chemical potential introduced above (Equation (3-8)) is "an awkward mathematical quantity devoid of any immediate sense of physical reality". This is so because the chemical potential cannot be related to measurable quantities such as T and P and thus cannot be easily calculated from $P\ V\ T$ Data. It was G. N. Lewis who introduced a quantity called fugacity, symbol f with units of pressure defined by the equations:

$$dG = RTd \ln f \qquad \text{(constant T)} \tag{3-10a}$$

$$\lim_{P \to 0} \left(\frac{f}{P} \right) = 1 \tag{3-10b}$$

For a component i in solution, the fugacity is defined by an equation similar to Equation (3-10):

$$d\overline{G}_i = RTd \ln \hat{f}_i \qquad \text{(constant T)} \tag{3-11a}$$

and completed by the equation:

* The Proof of this criterion is available in any standard text of Thermodynamics for example Smith et al [1975] and will not be given here.

$$\lim_{P\to 0}\left(\frac{\hat{f}_i}{x_i P}\right)=1 \qquad (3\text{-}11b)$$

The chemical potential is identical to the partial molar Gibbs free energy, thus:

$$\mu_i \equiv \overline{G_i} \qquad (3\text{-}12)$$

The foregoing identity transforms Equation (3-11) to:

$$d\mu_i = RTd\ln\hat{f}_i \qquad \text{(constant T)} \qquad (3\text{-}13)$$

Integration gives:

$$\mu_i = RT\ln\hat{f}_i + \theta_i(T) \qquad (3\text{-}13)$$

where θ_i is a constant that depends on temperature only. Since all phases are at the same temperature, substitution of the preceding equation for the μ_i's in Equation (3-9) leads to an alternative criterion for equilibrium:

$$\hat{f}_i^{\alpha} = \hat{f}_i^{\beta} = \ldots\ldots\ldots \hat{f}_i^{\pi} \qquad (i=1,2\ldots\ldots N) \qquad (3\text{-}14)$$

In words this criterion for phase equilibrium requires that for multiple phases at the same T and P to be in equilibrium, the fugacity of each component must be the same in all phases.

The dimensionless coefficient (f/P) in equation (3-10b) is called the *fugacity coefficient*, i.e.:

$$\phi = \left(\frac{f}{P}\right) \qquad (3\text{-}15)$$

For a component i in solution,

$$\hat{\phi}_i = \left(\frac{\hat{f}_i}{y_i P}\right) \quad \text{and} \quad \hat{\phi}_i = \left(\frac{\hat{f}_i}{x_i P}\right) \qquad (3\text{-}16)$$

for the vapor and liquid phases respectively.

3.4.1 Evaluation of fugacities

The fugacity of a pure liquid at a pressure above the saturation pressure (pressure at boiling point) is evaluated in a two-step procedure. First, at saturation the liquid phase fugacity equals the vapour fugacity:

$$f_i^L = f_i^{sat} = \phi_i^{sat} P_i^{sat} \tag{3-17}$$

The change in liquid fugacity with increase of pressure above P_i^{sat} is then determined in the second step. At constant T we have from Equation (3-1) and Equation (3-10):

$$dG_i = V_i dP - S_i dT = RT d\ln f_i \tag{3-18}$$

or

$$d\ln f_i = \frac{V_i^L}{RT} dP \tag{3-19}$$

Integration from P_i^{sat} to P gives the fugacity as:

$$f_i^L = f_i^{sat} \exp\left[\frac{1}{RT}\int_{P_i^{sat}}^{P} V_i^L dP\right] \tag{3-20}$$

The exponential term in Equation (3-20) is known as the *Poynting Correction* and is small at low pressures but increases with pressure. V^L_i represents the liquid molar volume and at temperatures well below the critical point. The liquid molar volume is a weak function of pressure. Its dependence on P can thus be acceptably neglected allowing the direct integration of Equation (3-20) to:

$$f_i^L = \phi_i^{sat} P_i^{sat} \exp\left[\frac{V_i^L\left(P - P_i^{sat}\right)}{RT}\right] \tag{3-21}$$

with f_i^{sat} being eliminated in favour of P_i^{sat} from the definition of the fugacity coefficient (Equation (3-15)).

The liquid molar volume of component i, V^L_i in the above equation is evaluated from the Rackett [1970] equation:

$$V_i^L = V_{ci} Z_{ci}^{(1-T_r)^{0.2857}} \tag{3-22}$$

The critical molar volume, V_{ci} and compressibility factor, Z_{ci} are given in Reid et al [1988] for a large number of components and the reduced temperature T_r is calculated from *T/Tc*. The only remaining unknown in Equation (3-21) for the evaluation of liquid fugacities is ϕ_i^{sat} and its evaluation from an EOS, in particular the Virial EOS, is dealt with in the following section.

3.4.2 Calculating the fugacity from the Virial equation of state (Sound theoretical basis)

When the Virial equation is assumed to adequately describe the vapour phase, an assumption valid at low pressures, useful expressions can be obtained for the fugacity coefficients of the pure vapour (ϕ_i^{sat}) and of component i in a gas mixture (ϕ_i^{v}). Equations (3-26a) and (3-26b) below are based on the truncated, pressure explicit form of the Virial equation:

$$Z = 1 + \frac{BP}{RT} \tag{3-23}$$

The quantity *Z* is known as the compressibility factor and equals *PV/RT*. For an ideal gas the compressibility factor is unity. *B* is the second virial coefficient and is a function of temperature only for pure components. In a mixture B is a function also of composition and is calculated from the following equation based on statistical mechanics:

$$B_{mixture} = \sum_{\text{All i}} \sum_{\text{All j}} y_i y_j B_{ij} \tag{3-24}$$

where B_{ij} represents both the pure components and mixture second virial coefficients. $B_{ij} = B_{ji}$ and is called the cross coefficient. It typifies the molecular interaction between molecule i and molecule j. The assumption that the Virial equation adequately describes the vapour phase leads to the following equation for the vapour phase fugacity coefficient of a pure liquid:

$$\phi^V = \exp\left(\frac{BP}{RT}\right) \tag{3-25}$$

For gas mixtures, the corresponding equations for components 1 and 2 in a binary mixture are:

$$\hat{\phi}_1^V = \exp\left(\frac{P\left(B_{11} + y_2^2\delta_{12}\right)}{RT}\right) \quad (3\text{-}26a)$$

$$\hat{\phi}_2^V = \exp\left(\frac{P\left(B_{22} + y_1^2\delta_{12}\right)}{RT}\right) \quad (3\text{-}26b)$$

B_{11} and B_{22} are the pure component Virial coefficients and δ_{12} is given by:

$$\delta_{12} = 2B_{12} - B_{11} - B_{22} \quad (3\text{-}27)$$

Various compilations give second Virial components for pure components, for example those of Cholinski et al. [1986] and Dymond and Smith [1980]. However, as already stated at the beginning of this chapter, finding experimental data for species of interest is often impossible. Satisfactory correlations for the determination of the second Virial coefficients have thus been developed and some of the most popular ones are discussed below.

3.4.2.1 The Pitzer Curl correlation

Pitzer and Curl [1957] proposed a relation in which the second Virial coefficient, B, is a function of reduced temperature , T_r (where $T_r = T/T_c$) :

$$\frac{BP_c}{RT_c} = B^o + \omega B^1 \quad (3\text{-}28)$$

where the parameters B^o and B^1 are given by

$$B^o = 0.083 - \frac{0.422}{T_r^{1.6}} \quad (3\text{-}29a)$$

$$B^o = 0.139 - \frac{0.172}{T_r^{1.6}} \quad (3\text{-}29b)$$

The term ω in Equation (3-28) is the accentric factor and is a pure component constant which gives a measure of the nonsphericity or accentricity of a molecule. It can be calculated from its definition given by (Reid et al. [1988]):

$$\omega = -\log P_r^{sat}\left(\text{at } T_r = 0.7\right) - 1.000 \quad (3\text{-}30)$$

where P^{sat}_r is the reduced vapour pressure calculated using $P^{sat}_r = P^{sat}/P_c$

When applied to mixtures, Equation (3-28) takes the form:

$$B_{ij} = \frac{RT_{cij}}{P_{cij}}\left(B^{o} + \omega_{ij}B^{1}\right) \tag{3-31}$$

The cross coefficient parameters are calculated from the following rules proposed by Prausnitz et al. [1986]:

$$\omega_{ij} = \frac{\omega_i + \omega_j}{2} \tag{3-32a}$$

$$T_{cij} = \sqrt{\left(T_{ci}T_{cj}\right)}\left(1-\kappa_{ij}\right) \tag{3-32b}$$

$$P_{cij} = \frac{Z_{cij}RT_{cij}}{V_{cij}} \tag{3-32c}$$

where

$$Z_{cij} = \frac{Z_{ci} + Z_{cj}}{2} \tag{3-33a}$$

and

$$V_{cij} = \left(\frac{V_{ci}^{1/3} + V_{cj}^{1/3}}{2}\right)^{3} \tag{3-33b}$$

κ_{ij} in Equation (3-22b) is a binary interaction parameter.

3.4.2.2 The Tsonopoulos correlation

The Tsonopoulos [1974] correlation is an extended Pitzer and Curl [1957] correlation and can be used for calculating Virial coefficients for both polar and non-polar compounds. For non-polar gases the equation takes the form:

$$\frac{BP_c}{RT_c} = f^{(o)}(T_r) + \omega f^{(1)}(T_r) \tag{3-34}$$

where:

$$f^{(o)}(T_r) = 0.1445 - \frac{0.330}{T_r} - \frac{0.1385}{T_r^2} - \frac{0.0121}{T_r^3} - \frac{0.000607}{T_r^8} \tag{3-35}$$

and

$$f^{(1)}(T_r) = 0.0637 + \frac{0.331}{T_r^2} - \frac{0.423}{T_r^3} - \frac{0.008}{T_r^8} \tag{3-36}$$

When applied to polar compounds, those characterized by a nonzero dipole moment, the above equation for non-polar compounds has an additional term which incorporates the polar effects:

$$\frac{BP_c}{RT_c} = f^{(o)}(T_r) + \omega f^{(1)}(T_r) + f^{(2)}(T_r) \tag{3-37}$$

where

$$f^{(2)}(T_r) = \frac{a}{T_r^6} \tag{3-38}$$

In polar compounds (e.g. carboxylic acids, phenols and alcohols) where hydrogen bonding and hence dimerization occurs, the temperature dependence of the polar term in Equation (3-37) is modified to cater for the increase in complexity and becomes:

$$f^{(2)}(T_r) = \frac{a}{T_r^6} - \frac{b}{T_r^8} \tag{3-39}$$

The parameters *a* and *b* in the above equations are dependent on the dipole moments and are thus specific to each compound. They are found through regression of available experimental data of B for similar compounds. Tsonopoulos [1974] tabulated a number of these parameters for eight different alcohols including phenol and water, all of which have a tendency to dimerize in solution.

When applied to mixtures, the same mixing rules for T_{cij} and ω_{ij} are used as in the Pitzer Curl [1957] correlation but for P_{cij} Tsonopolous [1974] proposed the equation:

$$P_{cij} = \frac{4T_{cij}\left(P_{ci}V_{ci}/T_{ci} + P_{cj}V_{cj}/T_{cj}\right)}{\left(V_{ci}^{1/3} + V_{ci}^{1/3}\right)^3} \tag{3-40}$$

When analyzing polar/non-polar systems it is assumed that B_{ij} has no polar term and a_{ij} and b_{ij} are set equal to zero. With polar/polar systems, B_{ij} is determined using $a_{ij} = 0.5(a_i + a_j)$ and $b_{ij} = 0.5(b_i + b_j)$.

3.4.2.3 The Hayden and O'Connell correlation

The method of Hayden and O' Connel [1975] is based on the assumption that the various kinds of intermolecular forces contribute to the Virial coefficient in distinct ways (Frendenslund et al. [1977]). The total virial coefficient is taken to be a sum of several contributions:

$$B_{total} = B_{free} + B_{metastable} + B_{bound} + B_{chem} \tag{3-41}$$

where B_{free} represents the molecular volumes, $B_{metastable} + B_{bound}$ results from the potential energy from more or less strongly-bound pairs of molecules and B_{chem} results from associating substances. The calculation procedure is complex and will not be detailed here. It is however available in Appendix A of Prausnitz et al [1980].

In order to use the method of Hayden and O 'Connell [1975] several basic parameters for each component must be known. These are the critical parameters (T_c, P_c, Z_c), the radius of gyration R_D, the dipole moment μ as well as the solvation and association parameter η. For most compounds the critical parameters are available in literature for example in Reid et al. [1988], Frendeslund et al. [1977] and the Dortmund Data Bank (DDB). With no experimental values the Lydersen group contribution method outlined in Reid et al. [1988] can be used. Dipole moments are available in McClellan [1974] and can also be determined by the method of Smyth [1955].

The mean radius of gyration R_D may be obtained from the parachor P' by the following equation (Hayden and O'Connell [1975]):

$$R_D = -0.2764 + 0.2697\sqrt{P' - 48.95} \tag{3-42}$$

where values of the parachor may be obtained from a group contribution method outlined in Reid et al. [1986]). According to Fredenslund et al. [1977] the solvation and association parameters are the most difficult to estimate because they must be determined empirically. They tabulated values of these parameters for some components. Prausnitz et al. [1980] also give tables for these parameters. When unavailable Fredenslund et al. [1977] suggest that for pure substances (hydrocarbons, halogenated alkanes, ethers and sulphides) the association parameters should be set equal to zero. Hayden and O'Connell suggest that for interaction between components in a mixture the solvation parameters η_{ij} should be set equal to zero unless the components of the mixture are in the same group of substances or a special solvation could be justified and empirically determined.

3.5 Activity and activity coefficient

Activity, given the symbol a, at a given temperature is defined as the ratio of the fugacity of a component to its fugacity in some defined standard-state:

$$a_i = \frac{\hat{f}_i}{f_i^o} \tag{3-43}$$

For an ideal solution the activity equals the mole fraction, i.e. $a_i = x_i$. The departure from ideal solution behaviour is accounted for by the activity coefficient, γ, defined as the ratio of the activity to the mole fraction:

$$\gamma_i = \frac{a_i}{x_i} = \frac{\hat{f}_i}{x f_i^o} \tag{3-44}$$

Thus for an ideal solution the activity coefficient is unity. The activity coefficient as given by Equation (3-44) is completely defined if the standard-state fugacity is specified. When specifying the standard state, f_i^o is usually taken as the fugacity of component i at the same temperature as that of the mixture but at some fixed composition and some specified pressure.

This work is on condensable (subcritical) components and the fugacity at standard-state can be conveniently taken as the pure-component fugacity at the same conditions of the mixture, i.e. at the mixture temperature and pressure (Prausnitz et al. [1967]).

Ideal solution behaviour can be represented by the Lewis/Randall rule defined as:

$$f_i^{id} = x_i f_i^L \tag{3-45}$$

It shows that the fugacity of a species in an ideal solution is proportional to its mole fraction. As x_i approaches unity, the fugacity of a real solution becomes equal to the fugacity of the pure liquid at the solution temperature and pressure. For dilute solutions an alternative ideal solution behaviour is defined in terms of Henry's law:

$$f_i^{id} = x_i H_i \tag{3-46}$$

where H_i is the *Henry's Law's constant.*

3.6 Vapour-liquid equilibria (VLE)

According to Equation (3-14) the condition for equilibrium between a liquid, L, and a vapour, V, at the same temperature and pressure is:

$$f_i^L = f_i^V \tag{3-14}$$

Invoking the definition of the fugacity coefficient for a component i in solution:

$$\hat{\phi}_i = \left(\frac{\hat{f}_i}{y_i P} \right) \tag{3-16}$$

and the definition of the activity coefficient of a component i in solution:

$$\gamma_i = \frac{a_i}{x_i} = \frac{\hat{f}_i}{x_i f_i^o} \tag{3-44}$$

transforms Equation (3-14) to:

$$y_i \hat{\phi}_i P = x_i \gamma_i f_i^l \tag{3-47}$$

f_i^o in Equation (3-44) has been replaced by f_i^l following the convention adopted in the previous section. This approach whereby the fugacity coefficient and the activity coefficient are respectively used to characterize non-idealities in the vapour and liquid phases is known as the

combined method of VLE and is discussed in more detail in Section 3.9.1 Substituting for f_i^l, the liquid fugacity using Equation (3-21), the following equation is obtained:

$$y_i \Phi_i P = x_i \gamma_i P_i^{sat} \tag{3-48}$$

where

$$\Phi_i = \frac{\hat{\phi}_i}{\phi_i^{sat}} \exp\left[-\frac{V_i^L \left(P - P_i^{sat} \right)}{RT} \right] \tag{3-49}$$

When the ϕ_i '*s* are substituted using Equation (3-26), Equation (3-49) transforms to:

$$\Phi_i = \exp\left[\frac{(B_{ii} - V_i^L)(P - P_i^{sat}) + P y_j^2 \delta_{ij}}{RT} \right] \tag{3-50}$$

where

$$\delta_{ij} = 2B_{12} - B_{11} - B_{22} \tag{3-27}$$

Equation (3-48) is the fundamental relationship relating liquid and vapour phases in equilibrium. It constitutes a set of two equations when written for a binary system that relate the equilibrium compositions to each other and to temperature and pressure. Application of the phase rule indicates that there are two degrees of freedom, thus whenever any two independent variables (from the set of x, y, T and P) are specified, the remaining two can be obtained by solving the set of equations given by Equation (3-48) provided that there is sufficient information for the evaluation of the activity coefficients – the only remaining unknowns in Equation (3-47). These activity coefficients are often calculated from models of excess Gibbs energy, a subject treated in more detail in Section 3.9

It should be observed that when both the liquid and vapour phases are assumed to be ideal (ideal gas and ideal solution) the activity coefficient and the fugacity coefficient become unity. Noting also that at low to moderate pressures, the Poynting correction differs from unity by only a few parts per thousand (Smith et al. [1996]) Equation (3-48) reduces to:

$$y_i P = x_i P_i^{sat} \tag{3-51}$$

an equation that expresses Raoult's Law. It is the simplest relation for VLE and fails to provide an accurate representation for most real systems. According to Prausnitz et al. [1986], for some systems, particularly carboxylic acid systems and those gases with a tendency to polymerise, large deviations (in the vapour phase) from ideality occur even at low pressures. The assumption of ideality in either phase should thus not be considered in order to accurately interpret vapour-liquid equilibria. This is the procedure that will be followed in this work. Raoult's law is however useful in gaining qualitative information about new systems yet to be analysed, for example, before measuring VLE data for any particular system, Raoult's law can be used to indicate the possible ranges of pressure and temperature for which the measurements are to be taken.

The main focus of the present work is on measuring and modeling low pressure vapour-liquid-liquid equilibria. We have so far looked at VLE and not VLLE. In the following section we discuss another form of phase equilibria, liquid-liquid equilibria, which will lead us to the phenomenon of vapour-liquid-liquid equilibrium.

3.7 Liquid-liquid equilibria (LLE)

An alternative criterion for phase equilibrium in a closed system is according to Smith et al. [1996] that *"the Gibbs energy should be a minimum with respect to all possible changes at a given temperature and pressure"*. Thus, when mixing two liquids at constant temperature and pressure, the Gibbs energy must decrease. If the system can achieve a lower Gibbs energy by forming two phases than by forming a single phase, then the system splits into two phases giving rise to the phenomenon known as liquid-liquid equilibrium (LLE).
Before giving any equations for the treatment of liquid-liquid equilibria, a brief look into the types of phase equilibria is presented.

There are usually two types of LLE reported in literature. The first type is the LLE of binary mixtures as a function of temperature. The second is the LLE of ternary mixtures at a fixed temperature. The first type, which is the subject of this section of the dissertation, finds its use in azeotropic distillation where the distillate forms two phases upon condensation. The second,

discussed in the following section, is more applicable to liquid-liquid extraction and is usually represented on an equilateral triangular graph known as a ternary phase diagram.

There are three common types of constant pressure binary LLE as shown if Figure 3-1 below.

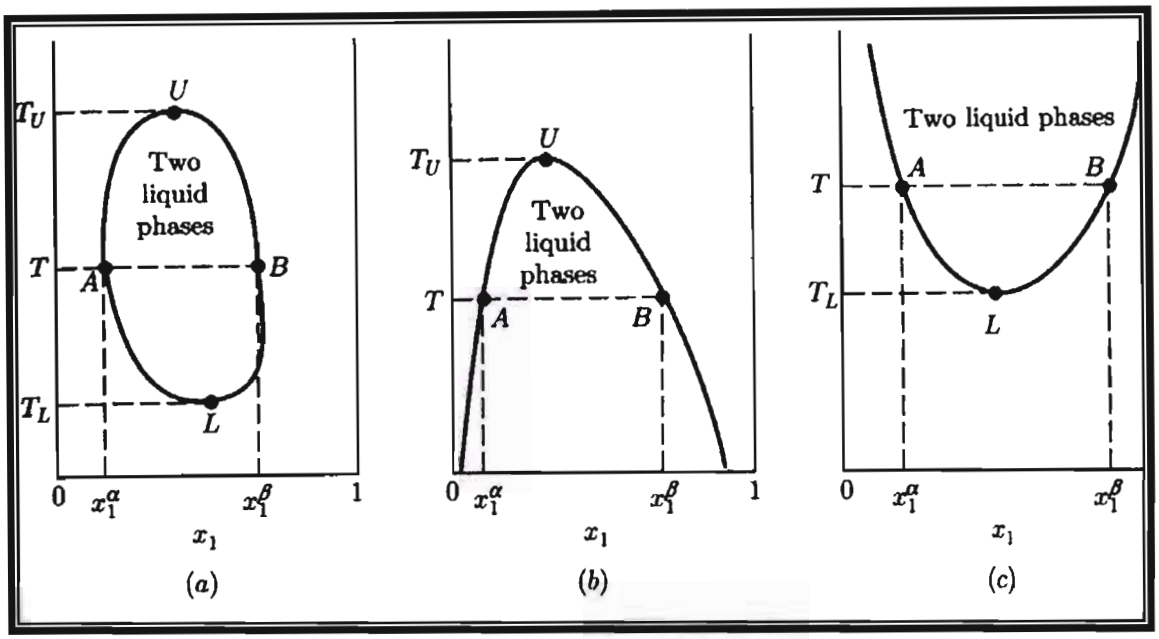

Figure 3 - 1: Three types of constant pressure liquid-liquid Equilibrium (Smith et al. 1996)

In the first diagram, which is seldom encountered (Smith et al. [1996]) there is both an upper critical solution temperature (UCST) and a lower critical solution temperature (LCST). These are the maximum and minimum temperatures between which LLE can exist respectively. The LCST may not exist if the liquid freezes at this temperature (Figure3-1b) and the UCST may not exist if the mixture bubble point is lower than the UCST (Figure 3-1c) (Raal and Muhlbauer [1999]). In all the three diagrams, equilibrium compositions x_1^α and x^β_1 (α and β representing the two phases in equilibrium) are given by the intersections of a horizontal tie line with the solubility curves (also known as binodal curves). When the binodal curves intersect both the freezing and bubble point curves, then a fourth type of behaviour is obtained as outlined by J.M Sorensen et al [1979a, 1979b, 1980], who give a comprehensive treatment of the subject.

3.7.1 Theoretical treatment of LLE

The same equilibrium criteria as for VLE are applicable to LLE, namely the equality of temperature, pressure and of the fugacity of each component in both phases. Denoting the two phases by α and β, Equation (3-14) gives:

$$f_i^{\alpha} = f_i^{\beta} \qquad (i = 1, 2.....N) \tag{3-52}$$

Equation (3-44), the defining equation for activity coefficients transforms the preceding equation to:

$$x_i^{\alpha}\gamma_i^{\alpha} = x_i^{\beta}\gamma_i^{\beta} \qquad (i = 1, 2.....N) \tag{3-53}$$

where the standard state fugacity f_i^{o} has been taken to be the same for the two components in the two phases. Equation (3-53) is the fundamental relation for LLE and when written for a binary system, two equations relating three variables (T, x_1^{α} and $x^{\beta}{}_1$) are obtained. Fixing one of these variables allows for the solution for the other two. The pressure is not included as one of the variables because LLE is a weak function of pressure at sub-critical pressures. This subject is further reviewed below (Section 3-10).

3.7.2 Ternary LLE

A brief introduction to ternary liquid-liquid equilibria was given in the previous section. In this section a look at the different types of ternary LLE and the equations for the reduction of such data are presented.

Ternary LLE data are usually measured at constant temperature and pressure. The data as has already been highlighted above are usually presented on equilateral triangular diagrams. Each vertex represents one of the pure components and the binodal curves separate single phase regions from the two-phase regions. Tie-lines connect two points corresponding to the compositions of the two liquids in equilibrium.

Triangular diagrams are classified into two major types, type 1 (see Figure 3-2 a), in which the 1-3 binary shows immiscibility and the 1-2 and the 2-3 binaries are completely miscible. The second type(see Figure 3-2 b), is type 2, in which both 1-3 and 2-3 binaries exhibit partial miscibility while binary 1-2 is completely miscible. Components 1 and 3 in Figure 3-2 are usually

considered solvents and component 2 is solute. Depending on the system being considered, the regions of immiscibility may be large enough such that they intersect and merge into a single two phase region. This results in variations of the triangular diagrams giving other behaviour in between the two cases already discussed. Sorensen et al. [1979 a] and Null [1980] give examples of all the possible cases.

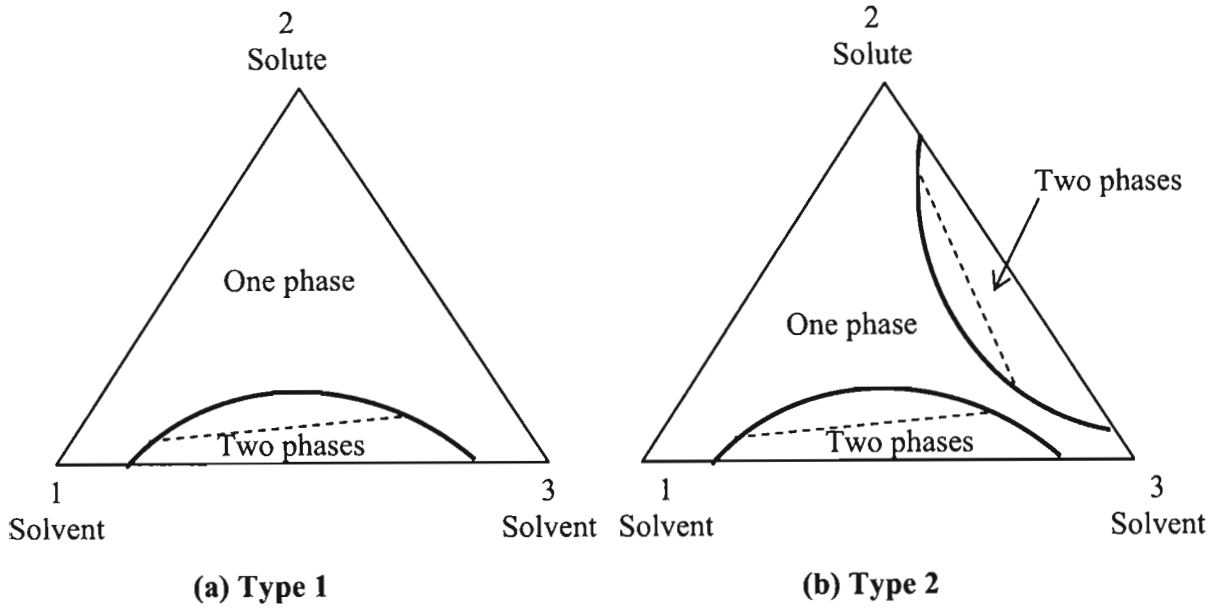

Figure 3 - 2: Two types of ternary phase diagrams.

According to Sorensen et al. [1979a and 1979b] who compiled a databank of LLE and evaluated its various aspects, out of a total of 405 ternary LLE systems they studied, 75 % were of type 1 and 20% were of type 2. The remaining 5% were the other variations discussed above.

3.7.3 Reduction of ternary LLE

For ternary LLE, the binodal curves and the tie line data are correlated separately. For the present work, three correlations will be used for the binodal curves and these are the Hlavaty correlation, the β function and the log-γ function. All these correlations have no thermodynamic basis and are based entirely on mathematical models. The model equations are given by Equations 3-54 to 3-56:

The Hlavaty (Hlavaty [1972]) Correlation:

$$x_2 = A_1 x_A \ln x_A + A_2 x_B \ln x_B + A_3 x_A x_B \tag{3-54}$$

The β function (Shultz et al [1973]):

$$x_2 = B_1 \left(1 - x_A\right)^{B_2} x_A^{B_3} \tag{3-55}$$

The log-γ function (Letcher et al [1989])

$$x_2 = C_1 \left(-\ln x_A\right)^{C_2} x_A^{C_3} \tag{3-56}$$

In all the above three equations, the quantities A_1, A_2, A_3, B_1, B_2, B_3, C_1, C_2 and C_3 are the parameters to be determined from the experimental data. x_A and x_B are given by:

$$x_A = \frac{\left(x_1 + \frac{1}{2}x_2 - x_1^o\right)}{x_{11}^o - x_1^o} \tag{3-57}$$

and

$$x_B = \frac{\left(x_{11}^o + x_1 - \frac{1}{2}x_2\right)}{x_{11}^o - x_1^o} \tag{3-58}$$

where x_1 refers to the mole fraction of the solute, x_2, refers to the mole fraction of the carrier and x_{11}^o and x_1^o are the values of x_1 on the binodal curve which cuts the $x_2 = 0$ axis

The tie line data will be regressed using the multicomponent form of the NRTL equation, (the NRTL equation is presented in Section 3.9 below). Non linear least squares regression (Section 3.9.1) will be used to obtain the 6* parameters in the equation with the following objective function:

$$S = \sum_{\text{All points}} \left\{ \begin{array}{l} \left[x_1^{'(Exp)} - x_1^{'(Cal)}\right]^2 + \left[x_2^{'(Exp)} - x_2^{'(Cal)}\right]^2 + \\ \left[x_1^{''(Exp)} - x_1^{''(Cal)}\right]^2 + \left[x_2^{''(Exp)} - x_2^{''(Cal)}\right]^2 \end{array} \right\} \tag{3-59}$$

The superscripts Exp and Cal denote experimental and calculated values respectively while prime and double prime denote the two phases in equilibrium.

* The non randomness parameter αij was set constant for all the 3 binaries of the systems contituents

The x's in this last equation are compositions, mole fractions, of the components specified by the corresponding subscripts.

3.8 Vapour-liquid-liquid equilibria (VLLE)

In Section 3.7 it was noted that the upper critical solution temperature will not exist if the binodal curves intersect the bubble point curve. When this happens, it gives rise to the phenomenon of vapour-liquid-liquid equilibrium (VLLE).

For a binary system existing in VLLE, there is only one degree of freedom according to the phase rule and thus having specified the pressure, the temperature and compositions of all the three phases in equilibrium are fixed. On a temperature composition diagram (see Figure 3-3 below) the three points representing the states of the three phases in equilibrium lie on a horizontal line at the equilibrium temperature. The two liquid phases in equilibrium are represented by points C and D and the vapour phase is represented by point E (azeotrope) in the diagram. Any binary mixture with overall composition between points C and D will split into two liquid phases and at equilibrium will give the same bubble point T^* with the three phases corresponding to VLLE being given by points C, D and E. Above the equilibrium temperature, T^*, VLE exists and below this temperature LLE is obtained.

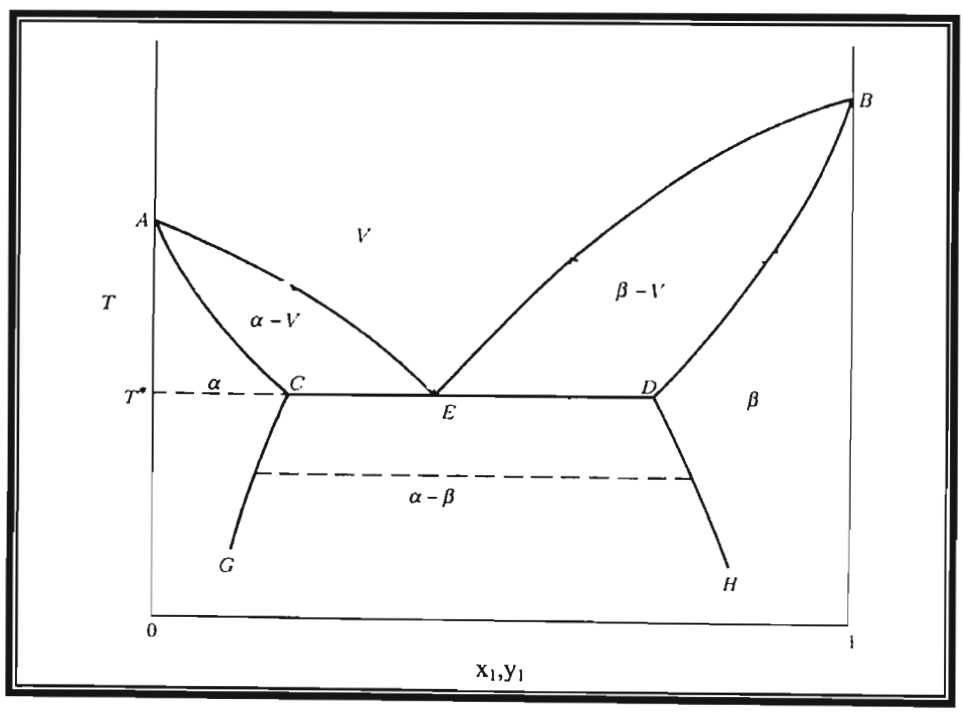

Figure 3 - 3: Txy diagram at constant P for a binary system exhibiting VLLE (Smith et al. [1996])

Depending on the temperature of the system and on overall composition, different phases are obtained at temperatures above T^*. The system may be a single liquid phase (regions β and α), two phases (regions α –V and β – V) or a single vapour phase (region V). When VLLE is measured at constant temperature, a similar phase diagram is obtained (see Figure 3-4). However, the boundaries separating the three liquid phase regions are nearly vertical because pressure has only a weak influence on liquid solubilities (Smith et al. [1996])

A look into Figure 3-3 indicates that complete description of binary VLLE over the entire composition range requires one to obtain curves AC, CG, DH AE, BE and BD. The following chapter, Chapter 4, is devoted to the equipment used in this work to obtain these curves experimentally. The experimental procedure is presented in Chapter 5.

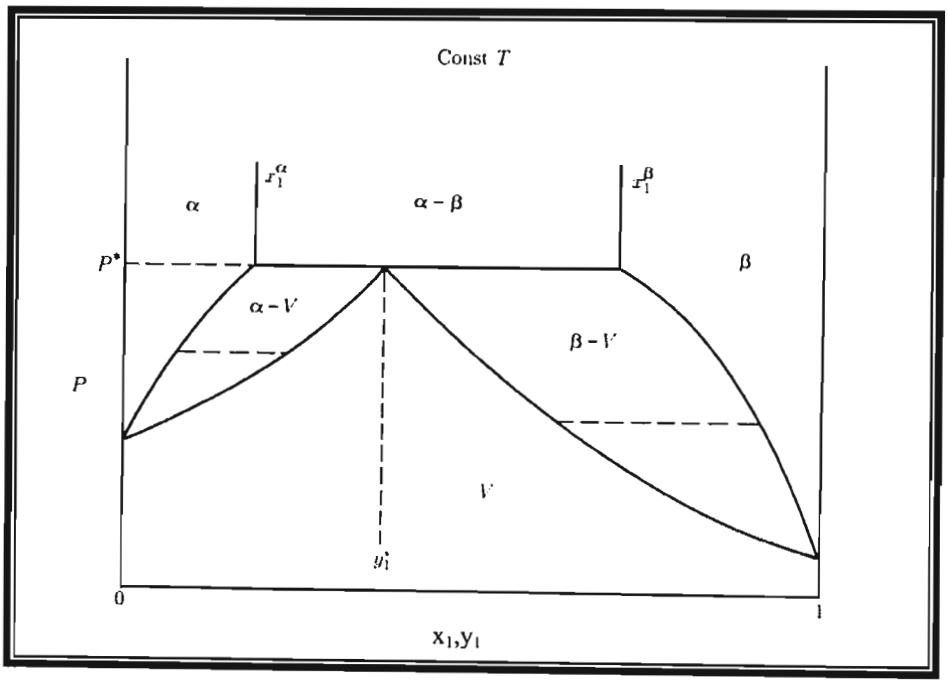

Figure 3 - 4: Pxy diagram at constant P for a binary system exhibiting VLLE (Smith et al. [1996])

The computation of low pressure VLLE is the same as that for VLE and thus the isofugacity criterion (Equation 3-14) is still applicable. The same equations presented above for VLE are used in the regions where a single liquid is in equilibrium with its vapour and for the regions where VLLE exist we have according to Equation (3-14):

$$\hat{f}_i^{\alpha} = \hat{f}_i^{\beta} = \hat{f}_i^{v} \qquad (3-60)$$

where α and β represent the two phases in equilibrium and v represents the corresponding vapour phase. Eliminating the liquid fugacities and the vapour fugacity in favor of the activity coefficients (Equation 3-44) and fugacity coefficients (Equation 3-16) respectively gives for a binary system the equations:

$$y_1\Phi_1 P = x_1^{\alpha}\gamma_1^{\alpha}P_1^{sat} = x_1^{\beta}\gamma_1^{\beta}P_1^{sat} \tag{3-61}$$

$$y_2\Phi_2 P = x_2^{\alpha}\gamma_2^{\alpha}P_2^{sat} = x_2^{\beta}\gamma_2^{\beta}P_2^{sat} \tag{3-62}$$

The Φ's in the above expressions are given by Equation (3-50) written for each component. Equations (3-61) and (3-62) constitute a total of four independent equations for VLLE which can be solved for any of the independent variables (x_1^{β}, x_1^{α}, y_1^{v}, T and P) whenever one of them has been specified.

At the beginning of this chapter it was stated that thermodynamic equations have been developed that allow minimum equilibrium data to be used to obtain equilibrium data at other conditions different to those at which the original data were measured. The basic equations for that purpose have thus far been presented. The remainder of this chapter discusses how the equations already presented are used in such calculations under the broad heading regression and correlation.

3.9 Data regression and correlation (VLE)

Equilibrium data are often correlated to models whereby a large data set is reduced to a set of parameters, which when used with the model, gives back the measured data. The ability to reproduce the measured values from these sets of parameters depends on how well the model describes the data. This reduction has the important advantage that it becomes possible to predict the equilibrium data at conditions other than those at which the data were measured. Furthermore, it makes possible the assessment of the quality of the measured data.

The models that are used are equations relating the Excess Gibbs energy to the liquid properties. According to Gess et al. [1991] the introduction of the excess properties allows one to obtain a physical sense of the activity coefficients. This is because the excess Gibbs energy is a function of measurable system properties such as temperature, pressure and composition. Excess properties are mixture properties and are the difference between a true value of a solution property and the value attributed to an ideal solution under the same conditions.

An equation that facilitates the use of these models in describing equilibrium between vapour and liquid phases is the fundamental excess property relation derived in great rigor by Smith et al. [1996]:

$$d\left(\frac{nG^E}{RT}\right)=\frac{nV^E}{RT}dP-\frac{nH^E}{RT^2}dT+\sum_i\frac{\overline{G}_i^E}{RT}dn_i \tag{3-63}$$

By using the definition:

$$\overline{G}_i^E = RT\ln\gamma_i \tag{3-64}$$

Equation (3-63) is transformed to:

$$d\left(\frac{nG^E}{RT}\right)=\frac{nV^E}{RT}dP-\frac{nH^E}{RT^2}dT+\sum_i\ln\gamma_i dn_i \tag{3-65}$$

It follows from the calculus of several variables that restricting the above equation to constant temperature, pressure and all the mole numbers except those of component i we obtain the equation:

$$\ln\gamma_i=\left(\frac{\partial\left(nG^E/RT\right)}{\partial n_i}\right)_{P,T,n_j} \tag{3-66}$$

This last equation shows that $\ln\gamma_i$ is a partial property with respect to G^E/RT and thus allows the calculation of γ_i from an expression for G^E as a function of composition. From the mathematics of partial properties the following equations hold for a two-component mixture:

$$\ln\gamma_1=\frac{G^E}{RT}+\frac{x_2 d(G^E/RT)}{dx_1} \tag{3-67}$$

$$\ln\gamma_2=\frac{G^E}{RT}-\frac{x_1 d(G^E/RT)}{dx_1} \tag{3-68}$$

An important equation that results from the fact that $\ln\gamma_i$ is a partial property with respect to G^E/RT is:

$$\frac{G^E}{RT} = \sum_i x_i d \ln \gamma_i \tag{3-69}$$

This last equation allows G^E to be calculated from activity coefficient data. Another yet imperative equation relating excess properties is the Gibbs Duhem Equation which is useful in checking experimental data for thermodynamic consistency. According to Van Ness [1995] data are only consistent if they conform to the Gibbs Duhem Equation, which when written in terms of excess properties becomes:

$$\sum_i x_i d \ln \gamma_i = \frac{\overline{V}^E}{RT} dP - \frac{\overline{H}^E}{RT^2} dT \tag{3-70}$$

Thermodynamic consistency is discussed in more detail later in this chapter.
Three different methods exist for regressing low pressure VLE data. These are:

1. The combined method (The gamma-phi formulation of VLE)
2. The direct method (The phi-phi formulation of VLE, The EOS method)
3. The model-independent methods

The third method for the computation of VLE is usually used to calculate VLE from P-x data, i.e. experimental data where only the total pressure and liquid composition are measured at constant temperature. The vapour phase composition is calculated by integrating one of the many different forms of the Gibbs Duhem equation (Sayegh and Vera [1980]). In this work, the compositions of all the phases in equilibrium are measured and thus this method will not be used nor discussed any further. For the reader interested in the subject, the papers by Ljunglin and Van Ness [1962], Mixon et al. [1965] and Sayegh and Vera [1980] are recommended.
The other two methods are discussed below.

3.9.1 The Combined method ($\gamma - \phi$ method)

In this method, introduced briefly in Section 3-6, an excess Gibbs energy model is used to account for non-idealities in the liquid phase while an equation of state (EOS) is used to account for non-idealities in the vapour phase (for the present work the Virial equation will be used to

account for non idealities in the vapour phase as outlined in Section 4.4.2 and given by Equation 3-26). Following the pioneering work of Barker [1953] the following steps are involved in regressing isothermal experimental VLE data (P-x data) to obtain parameters in the excess Gibbs free energy models (Raal and Muhlbauer [1998]):

1. A suitable expression is assumed for G^E as a function of composition. Barker in his original paper used the Scatchard [1949] polynomial, but any acceptable equation for G^E may be used to provide expressions for the γ_i
2. The system total pressure is then calculated from:

$$P = \frac{x_1 \gamma_1 P_1^{sat}}{\Phi_1} + \frac{x_2 \gamma_2 P_2^{sat}}{\Phi_2} \tag{3-71}$$

This last equation is obtained from Equation (3-48) by noting that $\Sigma x_i = \Sigma y_i = 1$

3. Equations for γ_1 and γ_2 obtained from the chosen G^E expression according to Equations (3-67) and (3-68) are substituted into Equation (3-71).
4. For the initial calculations the Φ_i's which are functions of the vapour composition, a parameter unknown at this point are set equal to 1. The vapour compositions are later found from Equation (3-72). The only remaining unknowns in the above equation are the fitting parameters in the equation for G^E chosen in step one. These are determined via an optimal regression technique designed to produce a best fit to the experimental P-x data over the entire composition range (see the following paragraphs).
5. Once the model parameters have been determined, the vapour compositions are calculated using:

$$y_i = \frac{x_i \gamma_i P_i^{sat}}{\Phi_i P} \tag{3-72}$$

The vapour phase correction factors Φi's are then found from Equation (3-50).

With isobaric data, the regression procedure is the same as that outlined above except that it becomes more involved as the temperature, an important parameter in determining mixture properties, is not constant, and its variation needs to be taken into account in the fourth step.

Step 4 above involves determining parameters in the activity coefficient equations from the G^E model chosen in step 1. These equations are generally of the form:

$$\gamma_i = \gamma\left(T, P, x_i, C_1, C_2 \ldots\ldots\ldots C_n\right) \tag{3-73}$$

where C_1, C_2 .... C_n are the parameters to be determined. In most circumstances the appropriate statistical criterion for adjusting the values of the parameters to best fit the experimental data is the least squares criterion (Marquardt [1959, 1963]. By the least squares criterion, the unknown parameters are to be adjusted until

$$S = \sum_{Alli}\left[Y^{Exp} - Y^{Cal}\right]^2 \tag{3-74}$$

is a minimum. In the above expression S is known as the *Objective Function* (Van Ness and Abbott [1982]) and Y can be any of the measured experimental variables (x, y, P or T depending on whether the data are isothermal or isobaric). The superscripts Exp and Cal denote experimental and calculated (predicted) values respectively. The difference (Y^{exp}-Y^{cal}) is known as the *residual* and is denoted by δ. Other residuals that can be evaluated are $\delta\gamma_1$, $\delta\gamma_2$, $\delta \ln\left(\gamma_1/\gamma_2\right)$, and $\delta G^E/RT$. Use of only *P-t-x* data permits subsequent testing of the thermodynamic consistency by comparing the measured vapour composition with the calculated.

Barker [1953] minimized the pressure residual in her pioneering work. According to Van Ness et al. [1978] different objective functions will give different parameters for a given model except when the data are perfect. This implies that different objective functions should be tried and the one that gives the best fit chosen for each model. Van Ness et al. [1978] also compared all objective functions and conclude that the pressure residual is the simplest and most direct when regressing isothermal data.

When the dependence of γ on the unknown parameters is linear (parameters in the first degree) the solution for the unknown parameters is straightforward; the partial derivatives of S (Equation 3-74) with respect to each of the unknown parameters are set equal to zero and the resultant simultaneous linear equations solved giving the desired parameters. However, if the relationship is non-linear (a case that is usually encountered in the modeling of VLE), the most economical way is to minimize S directly. This procedure is given in more detail by Marquardt [1959, 1963]

and by Gess et al. [1991]. The calculations are best effected with the aid of a personal computer. Applications like MATLAB, FORTRAN and C+ have built-in routines that allow such calculations to be performed with relative ease. In this work the MATLAB programming language has been used for the modeling process. The different calculations carried out depend on whether the data are isothermal or isobaric. For isothermal data, the parameter calculation procedure will involve *Bubble-Pressure iteration* (see Figure 3-5 below) for each experimental point while isobaric data necessitates calculation of the temperature and vapour composition, *Bubble-Temperature iteration* (see Figure 3-6 below).

The nature of Equation (3-73) will depend on the equation for G^E. Many expressions for the dependence of the excess Gibbs energy on composition and/or temperature have been proposed over the years. The composition has been expressed in terms of mole fractions although it has been suggested (Walas [1985]) that the use of volume fractions instead of mole fractions can better account for size differences. The most common of these equations are the Margules, Van Laar, Wilson, NRTL, UNIQUAC, UNIFAC and ASOG with the last two being of the *Group Contribution Class* and are used in predicting equilibrium data. They will not be discussed further and the reader is referred to Fredenslund et al. [1977] and Kojima et al. [1979] for a greater discussion on their development and use. Of the remaining five models only the NRTL and the UNIQUAC are capable of describing VLE for systems of limited liquid miscibility. The Margules and Van Laar equations however do predict liquid miscibility but because they have no explicit temperature dependence, they would have difficulty representing the usually strongly temperature dependent LLE (Raal and Muhlbauer [1998]).
These two models however can still be applied to those sections of VLLE where a single liquid phase is in equilibrium with a vapour phase and will thus be discussed further.

Before a discussion on the different activity coefficient models is presented, it is necessary to introduce the concept of stability, which explains why some models are incapable of describing VLE for systems of partial liquid miscibility.

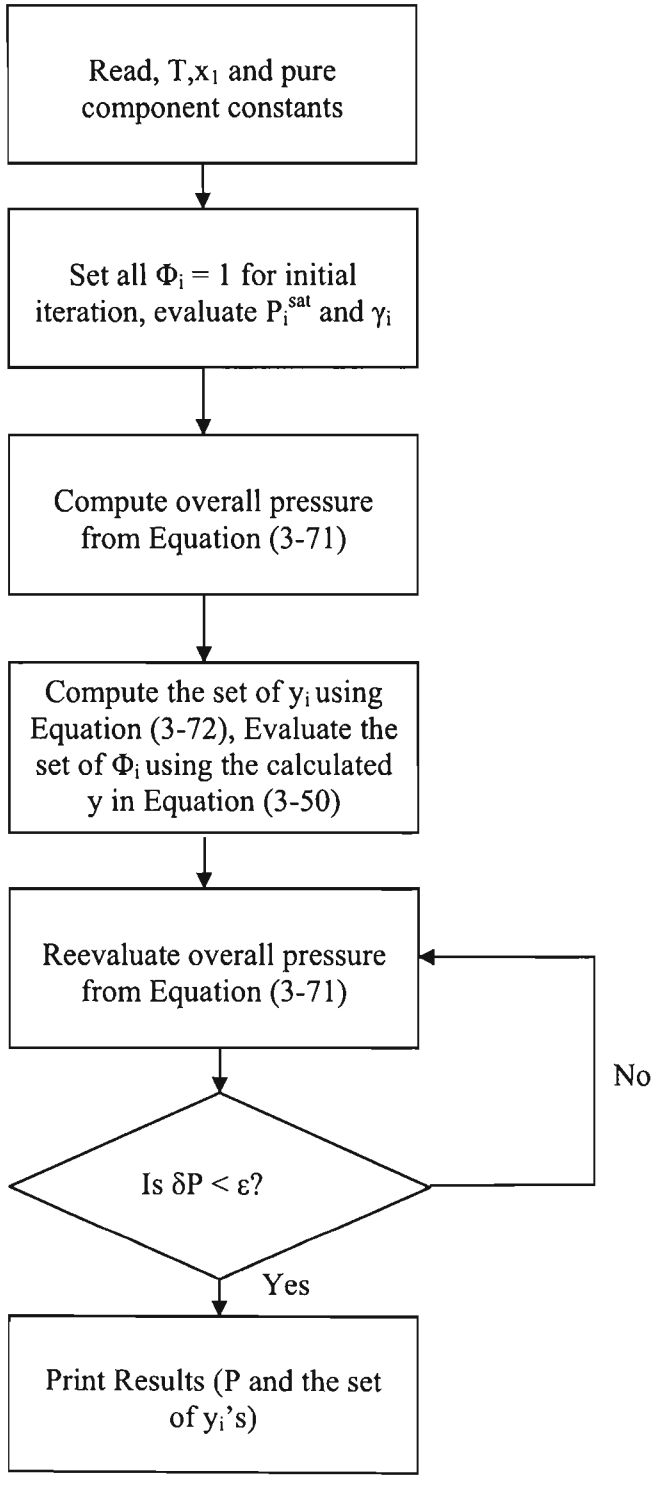

Figure 3 - 5: Computational procedure for the Bubble Pressure iteration using the combined method

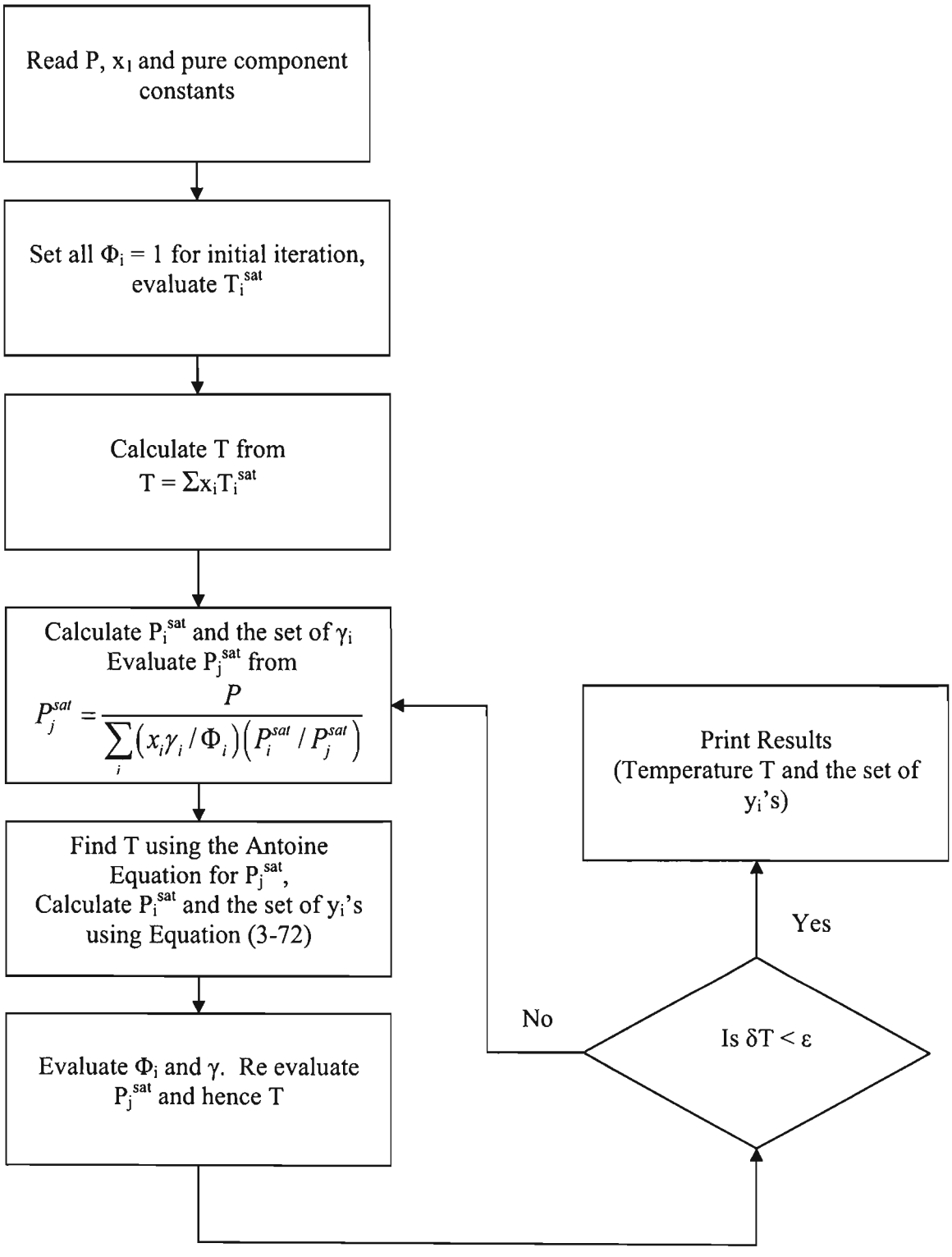

Figure 3 - 6: Computational procedure for the Bubble Temperature iteration using the combined method

3.9.1.1 Stability and the models of activity coefficient

Stability analysis is a complex subject and will not be discussed in detail here. The purpose of this section is to explain using stability why some models of excess Gibbs energy will not be suitable for partially miscible systems. The reader is referred to good discussions by Prausnitz et al [1986] and Abbott and Van Ness [1982].

At a fixed temperature and pressure, *a stable system is one that has a minimum Gibbs energy* (Prausnitz [1969]), thus stability analysis tells us that a liquid mixture will split into separate liquid phases if upon doing so it can lower its Gibbs energy.

Figure 3-7 below shows a typical curve for the Gibbs energy of mixing (defined by $\Delta G = G - \Sigma x_i G_i$, G being the mixture Gibbs energy and G_i the pure component values) for a binary partially miscible liquid at constant T and P.

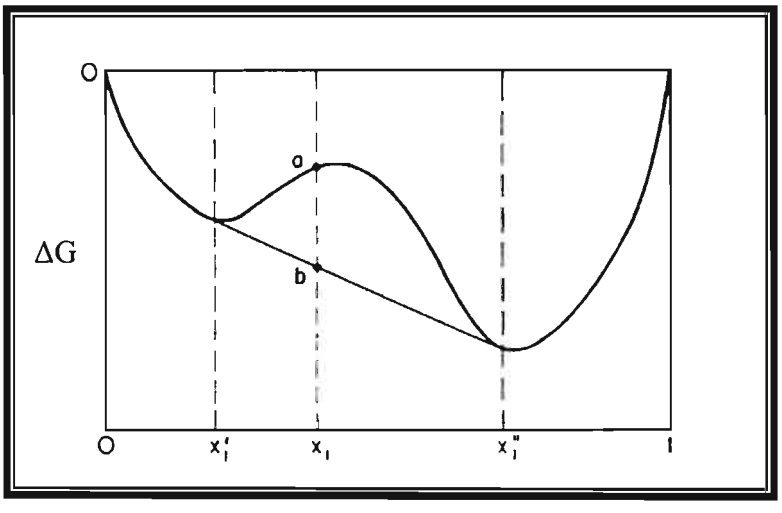

Figure 3 - 7: Molar Gibbs Energy of mixing for a partially miscible binary system (Prausnitz [1969])

A mixture with composition corresponding to point *a* will according to the stability criterion, split into separate phases having compositions x_1' and x_1'' and the molar Gibbs energy change upon mixing is given by point *b*. As seen in the above diagram point b represents the lowest possible Gibbs energy which the mixture may attain subject to the conditions of constant temperature, pressure and overall composition, x_1.

From the above plot we see that a decrease in Gibbs energy of a mixture can only occur if part of a plot of the Gibbs energy change of mixing is concave downward. Mathematically this condition for instability is:

$$\left(\frac{\partial^2 \Delta G}{\partial x^2}\right)_{T,P} < 0 \tag{3-75}$$

where ΔG is the Gibbs energy change of mixing

x in this equation can be either x_1 or x_2. In terms of excess Gibbs Energy the above relation is:

$$\left(\frac{\partial^2 G^E / RT}{\partial x^2}\right)_{T,P} + \frac{1}{x_1 x_2} < 0 \tag{3-76}$$

For an ideal solution, $G^E = 0$ and for all x between 0 and 1 the above inequality is never obeyed, thus we conclude that an ideal solution is always stable and cannot exhibit phase splitting.
The above equation can also be used to test the different expressions (models) for excess Gibbs energy to see if they can predict immiscibility. The expression for G^E for the particular model under test is substituted in Equation (3-76) and if values of its adjustable parameters can be found such that the inequality is obeyed then it can be concluded that such a model can predict partial miscibility. As has already been stated some models fail this test. An example is the Wilson [1964] model for which, when substituted in the above relation, no parameters Λ_{12} and Λ_{21} can be found which indicate the existence of two stable liquid phases (Prausnitz [1969]).

Following is a discussion on the earlier mentioned models (see Section3.9.1) i.e. those models that can describe equilibrium for both miscible and partially miscible systems). The discussion will include the modified Wilson equation – a model which also can describe VLE for systems of limited miscibility in the liquid phase. For more detail on these and other models the reader is referred to Walas [1985], Gess et al. [1991], Malanowski and Anderko [1992] and Sandler et al. [1994].

3.9.1.2 The Margules equations

The Margules equations are the oldest of all models that have been proposed for activity coefficients. Despite this, having been proposed in 1895, they are still very useful in their ability to correlate VLE data (Walas [1985]).

The simplest of the Margules equations is the two-suffix equation (second degree equation in composition, x):

$$\frac{G^E}{RT} = Ax_1x_2 \tag{3-77}$$

Application of Equations (3-67) and (3-68) gives the following expressions for the activity coefficients for a binary system:

$$\ln \gamma_1 = Ax_2^2 \tag{3-78}$$

$$\ln \gamma_2 = Ax_1^2 \tag{3-79}$$

The coefficient A in these equations is nominally independent of temperature but in practice it is usually found to depend on temperature.

The above equations predict a symmetric relationship between x and G^E and because most real systems exhibit asymmetric behaviour, the two-suffix Margules has limited applicability. Higher order equations were thus proposed to account for more complicated behaviour. This led to the three-suffix Margules equation which is defined as follows:

$$\frac{G^E}{RT} = x_1x_2\left[A_{12}x_2 + A_{21}x_1\right] \tag{3-80}$$

The corresponding activity coefficient equations are

$$\ln \gamma_1 = \left[A_{12} + 2\left(A_{21} - A_{12}\right) x_1 \right] x_2^2 \tag{3-81}$$

$$\ln \gamma_2 = \left[A_{21} + 2\left(A_{12} - A_{21}\right) x_2 \right] x_1^2 \tag{3-82}$$

Addition of one more constant, C in Equation (3-80) gives the more popular form of the Margules equations; the four-suffix Margules equation:

$$\frac{G^E}{RT} = x_1 x_2 \left[A_{12} x_2 + A_{21} x_1 - C x_1 x_2 \right] \tag{3-83}$$

Applying Equations (3-67) and (3-68), the following relationships are obtained:

$$\ln \gamma_1 = \left[A_{12} + 2\left(A_{21} - A_{12} - C\right) x_1 + 3C x_1^2 \right] x_2^2 \tag{3-84}$$

$$\ln \gamma_2 = \left[A_{21} + 2\left(A_{12} - A_{21} - C\right) x_2 + 3C x_2^2 \right] x_1^2 \tag{3-85}$$

An advantage of the Margules equations is that they are capable of predicting limited liquid-liquid miscibility (Abbott and Van Ness [1975]). Gess et al. [1991] evaluates the performance of each of the Margules equations and notes that the three-suffix equations have been applied to a larger number of systems than the two-suffix form.

3.9.1.3 The Van Laar equation

This model was proposed by Van Laar in 1910 and is given by the expressions:

$$\frac{G^E}{RT} = \frac{A_{12} A_{21} x_1 x_2}{x_1 A_{12} + x_2 A_{21}} \tag{3-86}$$

$$\ln \gamma_1 = A_{12} \left[\frac{A_{21} x_2}{x_1 A_{12} + x_2 A_{21}} \right]^2 \tag{3-87}$$

$$\ln \gamma_2 = A_{21} \left[\frac{A_{12} x_1}{x_1 A_{12} + x_2 A_{21}} \right]^2 \tag{3-88}$$

The Van Laar [1910] equations were developed so that they take into account the size differences between molecules. However they still fail to model highly non-ideal systems (Gess et al. [1991]). Another inadequacy of the Van Laar equations is that the effect of temperature on G^E is not addressed. This limits their applicability especially for systems of limited miscibility even though they do predict partial miscibility. An advantage though, of the Margules and Van Laar equations is mathematical simplicity.

A serious drawback of these equations, according to Smith and Van Ness [1996], is that they have no sound theoretical foundation and thus there is no rational basis for their extension to multicomponent systems.

3.9.1.4 The Wilson equation

The Wilson [1964] equation is based on the concept of local composition (as opposed to overall liquid compositions) and was developed following the independent work of Flory [1942] and Huggins [1942] on athermal solutions (solutions having zero enthalpy of mixing). These local compositions account for the short-range order and non-random molecular orientations that result from differences in molecular size and intermolecular forces (Perry [1997]). For a binary system, the excess Gibbs energy expression for the Wilson model is:

$$\frac{G^E}{RT} = -x_1 \ln\left(x_1 + x_2\Lambda_{12}\right) - x_2 \ln\left(x_2 + x_1\Lambda_{21}\right) \tag{3-89}$$

The equations for the activity coefficients are:

$$\ln\gamma_1 = -\ln\left(x_1 + x_2\Lambda_{12}\right) + x_2\left(\frac{\Lambda_{12}}{x_1 + x_2\Lambda_{12}} - \frac{\Lambda_{21}}{x_2 + x_1\Lambda_{21}}\right) \tag{3-90}$$

$$\ln\gamma_2 = -\ln\left(x_2 + x_1\Lambda_{21}\right) + x_1\left(\frac{\Lambda_{12}}{x_1 + x_2\Lambda_{12}} - \frac{\Lambda_{21}}{x_2 + x_1\Lambda_{21}}\right) \tag{3-91}$$

The parameters Λ_{12} and Λ_{21} are related to the pure component liquid volumes (obtained from the Rackett [1979] equation) by:

$$\Lambda_{ij} = \frac{V_i}{V_j} \exp\left[-\frac{\lambda_{ij} - \lambda_{ii}}{RT}\right] \tag{3-92}$$

where

V_i is the molar volume of pure liquid component at the system temperature

λ_{ij} is the interaction energy between components j and i

The parameters ($\lambda_{ij} - \lambda_{ii}$) represent the different molecular interactions between the components that make up a system and are the ones usually reported in literature (Walas [1985]).

Apart from the built-in temperature dependence of the Wilson parameters (Equation 3-92) an important advantage of the Wilson equation is that it can be readily applied to multi-component mixtures without the necessity of introducing parameters other than those for the constituent binaries.

Its drawback however, is its inability to predict limited liquid miscibility. Tsuboka and Katayama [1975] proposed a modified Wilson equation (T-K Wilson Equation) that allows systems of partial liquid miscibility to be modeled satisfactorily. Their equation is discussed in the following section.

3.9.1.5 The T-K Wilson equation

The excess Gibbs energy function of the T-K Wilson equation is:

$$\frac{G^E}{RT} = -x_1 \ln\left[\frac{x_1 + V_{12}x_2}{x_1 + x_2\Lambda_{12}}\right] + x_2 \ln\left[\frac{x_2 + V_{21}x_1}{x_2 + x_1\Lambda_{21}}\right] \tag{3-93}$$

The corresponding activity coefficient equations are:

$\sum x_i d\ln\gamma_i = 0$

$$\ln \gamma_1 = \ln\left[\frac{x_1 + V_{12}x_2}{x_1 + x_2\Lambda_{12}}\right] + \left[\beta - \beta_v\right]x_2 \tag{3-94}$$

$$\ln \gamma_2 = \ln\left[\frac{x_2 + V_{21}x_1}{x_2 + x_1\Lambda_{21}}\right] - \left[\beta - \beta_v\right]x_1 \tag{3-95}$$

where

$$\Lambda_{ij} = \frac{V_i}{V_j}\exp\left[-\frac{\lambda_{ij} - \lambda_{ii}}{RT}\right] \tag{3-96}$$

$$\beta = \frac{\Lambda_{12}}{x_1 + \Lambda_{12}x_2} - \frac{\Lambda_{21}}{x_2 + \Lambda_{21}x_1} \tag{3-97}$$

$$\beta_v = \frac{V_{12}}{x_1 + V_{12}x_2} - \frac{V_{21}}{x_2 + V_{21}x_1} \tag{3-98}$$

$$V_{ij} = \frac{V_j}{V_i} \tag{3-99}$$

The adjustable parameters Λ_{ij} in the above equations are given by the same equations (Equation 3-92) as those in the Wilson equation.

3.9.1.6 The NRTL (Non-RandomTwo Liquid) equation

Renon and Prausnitz [1968] proposed an improved local composition model which, unlike the Wilson equation is applicable to both partially miscible and completely miscible systems and has an additional term to account for the non-randomness in the solution. The NRTL equation is as follows:

$$\frac{G^E}{RT} = x_1x_2\left[\frac{\tau_{21}G_{21}}{x_1 + x_2G_{21}} + \frac{\tau_{12}G_{12}}{x_2 + x_1G_{12}}\right] \tag{3-100}$$

where

$$\tau_{ji} = \frac{g_{ji} - g_{ii}}{RT} \tag{3-101}$$

$$G_{ij} = \exp\left(-\alpha_{ji}\tau_{ji}\right) \tag{3-102}$$

g_{ji} is a parameter for interaction between components j and i

$\alpha_{ij} = \alpha_{ji}$ is a non randomness parameter and,

$(g_{ji} - g_{ii})$ are the adjustable parameters which together with α_i are usually reported in literature

The corresponding activity coefficients for a binary system are:

$$\ln \gamma_1 = x_2^2 \left[\tau_{21} \left(\frac{G_{21}}{x_1 + x_2 G_{21}} \right)^2 + \frac{G_{12}\tau_{12}}{\left(x_2 + x_1 G_{12}\right)^2} \right] \tag{3-103}$$

$$\ln \gamma_2 = x_1^2 \left[\tau_{12} \left(\frac{G_{12}}{x_2 + x_1 G_{12}} \right)^2 + \frac{G_{21}\tau_{21}}{\left(x_1 + x_2 G_{21}\right)^2} \right] \tag{3-104}$$

The NRTL equation has, like the Wilson equation, the advantage of limited parameter temperature dependence although this does not extend to the third parameter α_{ij}. This is not a serious issue as the values of the activity coefficients are generally insensitive to values of α_{ij} in the range -1 to 0.5 (Walas [1985]). According to Walas [1985] a value of $\alpha_{ij} = 0.3$ may thus be used for non-aqueous systems and that of $\alpha_{ij} = 0.4$ for those containing water. However according to Raal and Muhlbauer [1998] a suitable value of α_{ij} should be found from the experimental data through reduction rather than using a fixed value. Another advantage of the NRTL equation is its direct generalization for multi-component systems.

3.9.1.7 The UNIQUAC (Universal Quasi Chemical Theory) equation

The concept of local composition was incorporated by Abrams and Prausnitz [1975] who proposed a model more complex than the previous NRTL and Wilson models. In the UNIQUAC equation, the excess Gibbs energy consists of two parts, a *configurational or combinatorial* part,

which is due to differences in sizes and shapes of the molecules, and a *residual* part, which is due to energetic interactions between molecules. For a binary system the equation is as follows:

$$G^E = G^E\left(configurational\right) + G^E\left(residual\right) \tag{3-105}$$

Expressions for the configurational and residual parts are given respectively by:

$$G^E\left(configurational\right) = x_1 \ln\frac{\Phi_1}{x_1} + x_2 \ln\frac{\Phi_2}{x_2} + \frac{z}{2}\left(q_1 x_1 \ln\frac{\theta_1}{\Phi_1} + q_2 x_2 \ln\frac{\theta_2}{\Phi_2}\right) \tag{3-106}$$

$$\frac{G^E\left(residual\right)}{RT} = -q_1 x_1 \ln\left[\theta_1 + \theta_2\tau_{21}\right] - q_2 x_2 \ln\left[\theta_2 + \theta_1\tau_{12}\right] \tag{3-107}$$

where

z, the co-ordination number is set = 10

Φ, the *segment fraction* and θ, the *area fraction* are respectively given by:

$$\Phi_i = \frac{x_i r_i}{x_i r_i + x_j r_j} \tag{3-108}$$

$$\theta_i = \frac{x_i q_i}{x_i q_i + x_j q_j} \tag{3-109}$$

The terms r (*size parameter*) and q (*area parameter*) are pure component constants and are evaluated using contributions from molecular structure and various functional groups present in a system. Methods are available for their determination as given by Raal and Muhlbauer [1998] and Fredenslund et al [1977].

The two adjustable parameters τ_{ij} are given by:

$$\tau_{ij} = \exp\left[-\frac{u_{ij} - u_{ii}}{RT}\right] \tag{3-110}$$

In the above equation u_{ij} is the parameter of interaction between components i and j. The temperature dependence of τ_{ij} makes the UNIQUAC equation attractive for partially miscible

systems. Walas [1985] asserts that introducing a temperature-dependent co-ordination number would greatly improve the correlating abilities of the model. In this light, Skjold-Jorgensen et al [1980] proposed an equation in which Z has a quadratic dependence on temperature while Raal and Naidoo [1990] proposed a co-ordination number with Arrhenius type temperature dependence.

Expressions for the activity coefficients corresponding to Equation (3-105) are also in two parts and are given by:

$$\ln \gamma_i = \ln \gamma_i \left(configurational\right) + \ln \gamma_i \left(residual\right) \tag{3-111}$$

$$\ln \gamma_i \left(configurational\right) = \ln \frac{\Phi_i}{x_i} + \frac{z}{2} q_i \ln \frac{\theta_i}{\Phi_i} + \Phi_j \left(l_i - \frac{r_i}{r_j} l_j \right) \tag{3-112}$$

$$\ln \gamma_i \left(residual\right) = -q_i \ln \left(\theta_i + \theta_j \tau_{ji}\right) + \theta_j q_j \left(\frac{\tau_{ji}}{\theta_i + \theta_j \tau_{ji}} - \frac{\tau_{ij}}{\theta_j + \theta_i \tau_{ij}} \right) \tag{3-113}$$

where

$$l_i = \frac{z}{2}\left(r_i - q_i\right) - \left(r_i - 1\right) \tag{3-114}$$

The UNIQUAC equation is applicable to a wide variety of liquid mixtures containing both polar and non polar components. It can also be extendend to represent multi-component mixtures in terms of binary parameters alone and as has already been stated it can also describe partially miscible systems. The UNIQUAC equation has the drawback, however, of algebraic complexity and the unavailability of r and q parameters.

3.9.2 The Direct method for VLE (EOS Method)

This method presents an alternative to the combined method in modeling low pressure vapour-liquid equilibrium (Perry 1997]). An equation of state (EOS) is used to describe non-idealities in both the liquid and vapour phases. Application of the equilibrium criterion (Equation 3-14) to a vapour phase, V, in equilibrium with a liquid phase, L, gives:

$$\hat{f}_i^l = \hat{f}_i^v \tag{3-115}$$

Substituting for the fugacities using Equation (3-16) we get:

$$x_i \phi_i^v = y_i \phi_i^l \tag{3-116}$$

The fugacity coefficients in the above equation are determined from a suitable EOS together with appropriate mixing rules (which extend the pure component form of the EOS to mixtures) applicable to both phases using the thermodynamic relationships:

$$\ln \phi_i^v = \left(\frac{1}{RT}\right) \int_{V^v}^{\infty} \left[\left(\frac{\partial P}{\partial n_i}\right)_{(T,V,n_j)} - \frac{RT}{V^v} \right] dV - \ln \left[\frac{PV^v}{n_T RT} \right] \tag{3-117}$$

$$\ln \phi_i^l = \left(\frac{1}{RT}\right) \int_{V^l}^{\infty} \left[\left(\frac{\partial P}{\partial n_i}\right)_{(T,V,n_j)} - \frac{RT}{V^l} \right] dV - \ln \left[\frac{PV^l}{n_T RT} \right] \tag{3-118}$$

The solution of the above equations is facilitated through the use of the equilibrium ratio defined as:

$$K_i = \frac{y_i}{x_i} = \frac{\phi_i^l}{\phi_i^v} \tag{3-119}$$

The direct method has the advantage that it can also be applied to high-pressure systems. However according to Raal and Muhlbauer [1998] some of its difficulties are:

(a) Selecting from the hundreds of EOS available in the literature the most appropriate one for a particular system. The main criterion is that it should be flexible enough to fully describe a pure substance's P, V, T behavior for both phases in the temperature and pressure range under study.

(b) Selection of appropriate mixing rules so that the EOS can be applied to mixtures. Most mixing rules are somewhat empirical in nature and tend to be system specific.

(c) Locating the appropriate roots for liquid and vapour molar densities when higher than cubic equations of state are used.

The reduction of data to obtain parameters in the EOS's is similar to that discussed for the combined method although a bit more involved. Again bubble pressure and bubble temperature iterations are carried out as part of the reduction process as illustrated in Figures 3-8 and 3-9 respectively. The use of the method is treated in greater detail by Raal and Muhlbauer [1998], Sandler [1994] and Walas [1985].
Following is a discussion on the EOS's that will be used in this work.

3.9.2.1 The Soave Redlich Kwong cubic equation of state

Soave [1972] modified the Redlich and Kwong [1949] cubic equation of state, which was not satisfactory for the liquid phase (Walas [1985]), and proposed the equation:

$$P = \frac{RT}{(V-b)} - \frac{a(T,\omega)}{V(V+b)} \tag{3-120}$$

where

$$a = 0.42747\left(R^2T_c^2 / P_c\right)\alpha \tag{3-121}$$

$$\alpha = \left[1+\left(1-T_r^{0.5}\right)\left(0.48+1.57\omega-0.176\omega^2\right)\right]^2 \tag{3-122}$$

$$b = 0.08664RT_c / P_c \tag{3-123}$$

In the above equations b is a constant and is known as the *Van der Waals* volume and is related to the size of the molecules. It is assumed to be temperature-independent as given by Equation (3-123). *a* is a measure of the intermolecular attraction force and is a function of temperature and the accentric factor as given by Equations (3-121) and (3-122).
When used to calculate fugacity coefficients through Equations (3-117) and (3-118), the Soave EOS is more conveniently written as a polynomial in terms of the compressibility factor, Z (Z = PV/RT):

$$Z^3 - Z^2 + Z\left(A-B-B^2\right) - AB = 0 \tag{3-124}$$

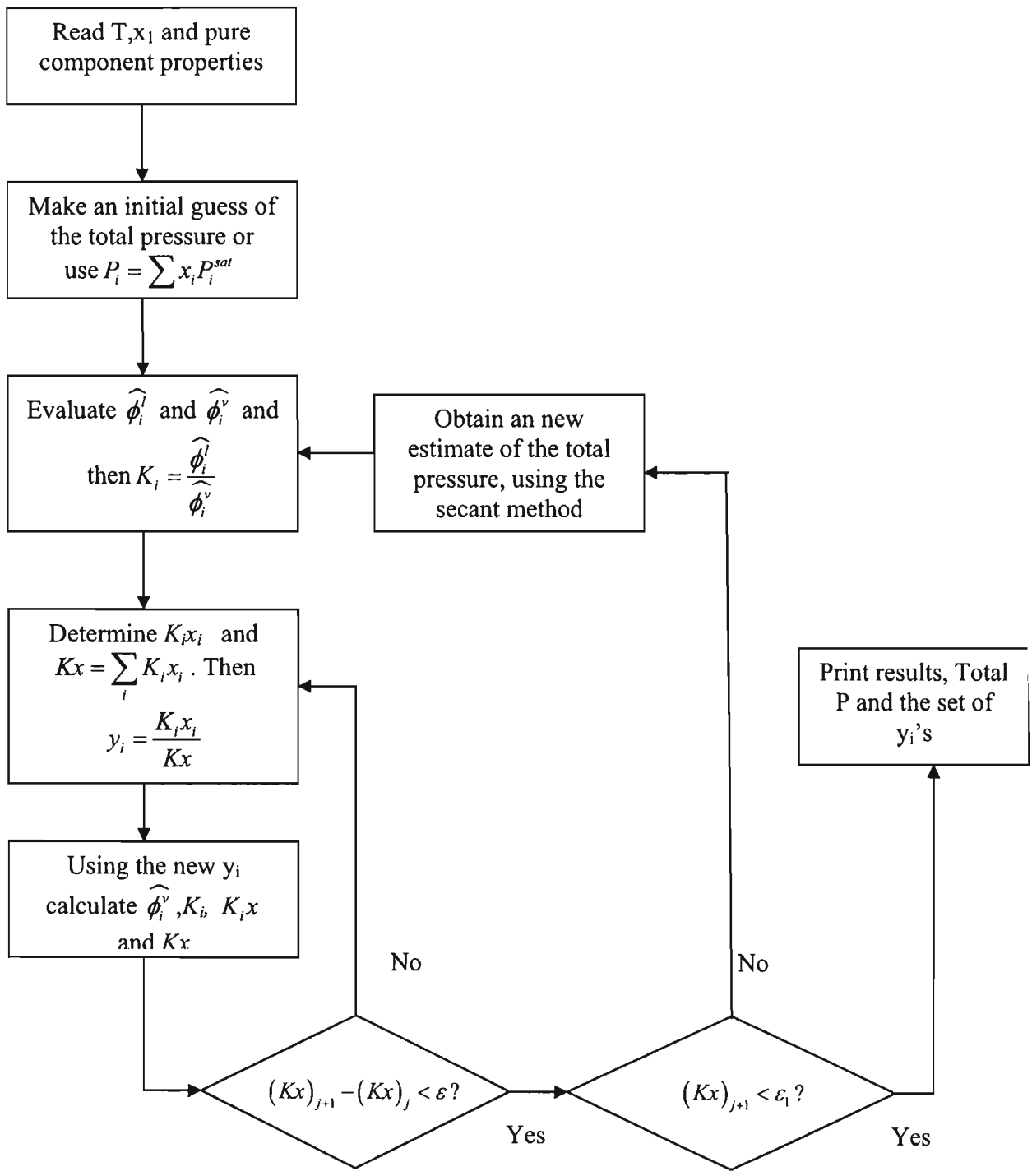

Figure 3 - 8: Computational procedure for the Bubble Pressure iteration using the Direct Method

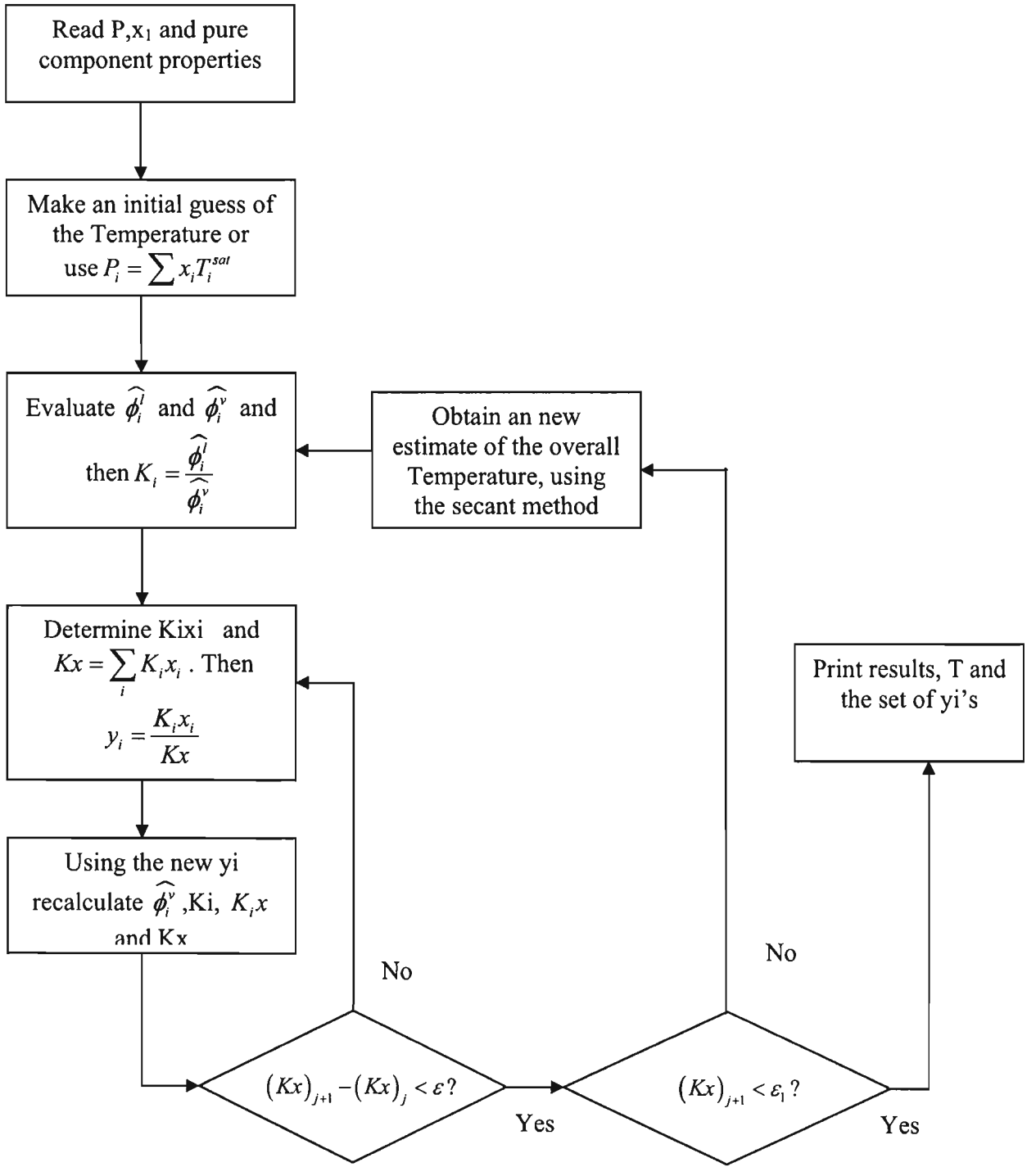

Figure 3 - 9: Computational procedure for the Bubble Temperature iteration using the Direct Method

A and B in the preceding equation are given by:

$$A = \frac{aP}{R^2T^2} \tag{3-125}$$

$$B = \frac{bP}{RT} \tag{3-126}$$

The above equation in Z when solved will give three roots; the largest (greater than zero) is taken to be the vapour phase compressibility and the smallest (greater than zero) gives the liquid phase compressibility. The third root is a mathematical consequence of the equation but has no theoretical significance. The partial fugacities are then given by the following equation:

$$\ln\hat{\phi}_i = \frac{B_i}{B}(Z-1) - \ln(Z-B) + \frac{A}{B}\left(\frac{b_i}{b} - 2\frac{\sum_{j=1}^{n} y_j a_{ij}}{a}\right)\ln\left(1+\frac{B}{Z}\right) \tag{3-127}$$

where A_i and B_i are pure component parameters and are given by Equations (3-125) and (3-126). A and B are mixture parameters and are calculated from a_i and b_i using the same mixing rules as in the Redlich and Kwong [1949] EOS:

$$a = \sum_i \sum_j y_i y_j a_{ij} \tag{3-128}$$

$$b = \sum_i y_i b_i \tag{3-129}$$

y_i in the last three equations can be the vapour or liquid phase composition depending on which fugacity is being calculated. a_{ij} is a cross parameter and is calculated from:

$$a_{ij} = (1-k_{ij})(a_i a_j)^{0.5} \tag{3-130}$$

The term k_{ij}, known as the *interaction parameter* is unique to each binary pair and is found from experimental data using the same reduction techniques given in Section 3.9.1. It characterizes the binary formed by component i and component j.

The Soave EOS was further modified by Soave [1979] for strongly polar substances such as water and alcohols. He proposed a new alpha function (Equation 3-117) with two adjustable parameters which must be obtained from experimental vapour pressure data (Walas [1985]). The Soave equation fails to predict liquid densities at temperatures close to the critical point. The deviations of predicted values from literature data increase from about 7% at $T_r = 0.65$ to 27% at the critical point (Peng and Robinson [1976]). In order to address this weakness Peng and Robinson modified the Soave EOS and proposed a more robust equation discussed below.

3.9.2.2 The Peng and Robinson equation of state

The Peng-Robinson EOS is similar to that of Soave and is given by:

$$P = \frac{RT}{(V-b)} - \frac{a(T,\omega)}{(V+b)+b(V-b)} \tag{3-131}$$

where

$$a = a_c \alpha \tag{3-132}$$

$$a_c = 0.45724 \frac{R^2 T_c^2}{P_c} \tag{3-133}$$

$$\alpha = \left[1+\kappa\left(1-\sqrt{T_r}\right)\right]^2 \tag{3-134}$$

$$b = 0.07780 \frac{RT_c}{P_c} \tag{3-135}$$

$$\kappa = 0.3764 + 1.54226\omega - 0.2699\omega^2 \tag{3-136}$$

For the determination of the fugacity coefficients a cubic equation in Z similar to Equation (3-124) is used:

$$Z^3-(1-B)Z^2+Z\left(A-3B^2-2B\right)-\left(AB\right)-B^2-B^3)=0 \tag{3-137}$$

Where A and B are given as in the Soave EOS by Equations (3-125) and (3-126) respectively. The fugacity coefficients equation is:

$$\ln\hat{\phi}_i=\frac{b_i}{b}(Z-1)-\ln(Z-B)-\frac{A}{2\sqrt{2}B}\left(\frac{2\sum_k y_k a_{ki}}{a}-\frac{b_i}{b}\right)\ln\left[\frac{Z+\left(1+\sqrt{2}\right)B}{Z+\left(1-\sqrt{2}\right)B}\right] \tag{3-138}$$

The mixture parameters are obtained from the following mixing rules:

$$a=\sum_i\sum_j y_i y_j a_{ij} \tag{3-128}$$

$$b=\sum_i y_i b_i \tag{3-129}$$

where

$$a_{ij}=\left(1-\delta_{ij}\right)\left(a_i a_j\right)^{0.5} \tag{3-139}$$

δ_{ij} is the empirically determined binary interaction parameter. The Peng and Robinson EOS has the advantage over the Soave EOS in that it predicts improved liquid density values. It also gives accurate vapour pressures and equilibrium ratios (Peng and Robinson [1976]).

3.9.2.3 The Stryjek and Vera modified Peng and Robinson EOS

In an effort to come up with an EOS applicable to a wide variety of substances (non-polar, polar associating and non-associating alike), Stryjek and Vera [1986] modified the dependence of the attractive term of the Peng-Robinson EOS on temperature and on the acentric factor. They retained Equations (3-131) to (3-135) for the Peng-Robinson EOS but proposed a new equation for κ. the new expression is:

$$\kappa = \kappa_o + \kappa_1\left(1+T_r^{0.5}\right)\left(0.7-T_r\right) \tag{3-140}$$

where

$$k_o = 0.378893+1.4897153\omega-0.17131848\omega^2+0.0196554\omega^3 \tag{3-141}$$

In the above expression, κ_1 is an adjustable parameter characteristic of each pure compound and is found from regressing vapour pressure data. Stryjek and Vera [1986] tabulated values of this parameter for a number of compounds, which were obtained through correlation of vapour pressure data at reduced temperatures.

The same mixing rules and expressions for the fugacities are used as in the Peng-Robinson EOS.

3.9.2.4 The Wong and Sandler mixing rule

The above three equations of state (Soave [1972], Peng and Robinson [1976] and Stryjek and Vera modified Peng and Robinson [1986]) use similar mixing rules when applied to mixtures. These mixing rules are known as the *Van der Waal one fluid theory classical mixing rules* and the mixture a_m and b_m parameters are respectively given by:

$$a = \sum_i \sum_j y_i y_j a_{ij} \tag{3-128}$$

$$b = \sum_i y_i b_i \tag{3-129}$$

where for the original Soave [1972] EOS the cross parameter a_{ij} is given by:

$$a_{ij} = \left(1-k_{ij}\right)\left(a_i a_j\right)^{0.5} \tag{3-130}$$

and for the other two:

$$a_{ij} = \left(1-\delta_{ij}\right)\left(a_i a_j\right)^{0.5} \tag{3-139}$$

The foregoing classical mixing rules, although having been used successfully for some highly non-ideal and complex systems are not generally applicable and are limited in that they do not have predictive capabilities. In this light Wong and Sandler [1992] developed a mixing rule which when used in conjunction with any cubic equation of state (CEOS) can be used to predict high-pressure vapour-liquid equilibrium from VLE data measured at low pressures. Their mixing rule when applied to a CEOS gives second virial coefficients which have quadratic composition dependence and thus is consistent with statistical mechanics (Wong and Sandler [1992]). The correct use of the excess Helmholtz energy at infinite pressure in the mixing rule produces the correct low and high densities without being density dependent.

The density-independent Wong and Sandler mixing rule is one of the five *novel* classes of mixing rules as described by Raal and Muhlbauer [1998]. These include the density-dependent mixing rules (DDMR), classical mixing rules (CMR), composition-dependent mixing rules (CDMR), density-independent mixing rules (DIMR) and local composition mixing rules (LCMR). Incorporation of the local composition theory into three of the above mixing rules produces three other mixing rules, increasing the list to eight. Clearly it is not possible within the scope of this work to adequately discuss all these mixing rules and indeed an attempt to do so is not made. Only the Wong and Sandler mixing rule will be discussed and the reader is referred to the above mentioned text for a greater and more detailed discussion on this and the rest of these mixing rules.

The Wong and Sandler mixing rule gives the mixture parameters a_m and b_m as:

$$\frac{a_m}{RT} = \frac{QD}{(1-D)} \tag{3-142}$$

and

$$b_m = \frac{Q}{(1-D)} \tag{3-143}$$

with Q and D being given by the equations:

$$Q = \sum_i \sum_j x_i x_j \left(b - \frac{a}{RT} \right)_{ij} \tag{3-144}$$

$$D = \sum_i x_i \frac{a_i}{b_i RT} + \frac{A_\infty^E}{cRT} \tag{3-145}$$

The fugacity coefficient is then computed from any CEOS by substituting it in the equation:

$$\ln \phi_i = \int_V^\infty \left[\frac{1}{RT} \left(\frac{\partial P}{\partial n_i} \right)_{T,V,n_j} - \frac{1}{V} \right] dV - \ln \left(\frac{PV}{RT} \right) \tag{3-146}$$

When evaluating fugacities using the above equation, the partial derivatives of the mixture a_m and b_m parameters are needed. These are given by the equations:

$$\frac{\partial n b_m}{\partial n_i} = \frac{1}{(1-D)} \left(\frac{1}{n} \frac{\partial n^2 Q}{\partial n_i} \right) - \frac{Q}{(1-D)^2} \left(1 - \frac{\partial nD}{\partial n_i} \right) \tag{3-147}$$

$$\frac{1}{RT} \left(\frac{1}{n} \frac{\partial n^2 a_m}{\partial n_i} \right) = D \frac{\partial n b_m}{\partial n_i} + b_m \frac{\partial nD}{\partial n_i} \tag{3-148}$$

The corresponding partial derivatives of Q and D are given respectively by:

$$\left(\frac{1}{n} \frac{\partial n^2 Q}{\partial n_i} \right) = 2 \sum_j x_j \left(b - \frac{a}{RT} \right)_{ij} \tag{3-149}$$

and

$$\frac{\partial nD}{\partial n_i} = \frac{a_i}{b_i RT} + \frac{\ln \gamma_i^\infty}{c} \tag{3-150}$$

with c being a constant and:

$$\ln \gamma_i^\infty = \frac{1}{RT} \frac{\partial n A_\infty^E}{\partial n_i} \tag{3-151}$$

Wong and Sandler [1992] showed that A^E is much less pressure dependent than G^E (an advantage which allows for the prediction of high pressure VLE from low-pressure VLE), thus:

$$\overline{G}^E (T, x, P = low) = \overline{A}^E (T, x, P = low) = \overline{A}^E (T, x, P = \infty) \tag{3-152}$$

From this relation, any expression of G^E at low pressure can be substituted for A^E in Equation (3-151). When the NRTL equation is used for this purpose we have:

$$\frac{A_\infty^E}{RT} = \sum_i x_i \left(\frac{\sum_j x_j \tau_{ji} g_{ji}}{\sum_k x_k g_{ki}} \right) \tag{3-153}$$

and

$$\ln \gamma_i^\infty = \frac{\sum_j x_j \tau_{ji} g_{ji}}{\sum_k x_k g_{ki}} + \sum_j \frac{x_j g_{ij}}{\sum_k x_k g_{kj}} \left(\tau_{ij} - \frac{\sum_l x_l \tau_{lj} g_{lj}}{\sum_k x_k g_{kj}} \right) \tag{3-154}$$

The following equation is used in Equation (3-144) for the evaluation of the cross parameters:

$$\left(b - \frac{a}{RT} \right)_{ij} = \frac{\left(b_i - \frac{a_i}{RT} \right) + \left(b_j - \frac{a_j}{RT} \right)}{2} (1 - k_{ij}) \tag{3-155}$$

In the above equation the parameter k_{ij} is obtained by regression of data for binary mixtures following the procedure detailed in Section 3.9.2. In addition to this parameter, the coefficients in the expression chosen for the Helmholtz free energy are needed, for example if the NRTL model is used, a total of four parameters would be needed.

According to Wong and Sandler [1992] their mixing rule is equally applicable to and accurate for simple mixtures containing hydrocarbons and inorganic gases and mixtures containing polar, aromatic and associating species over a wide range of pressures. In this work, the Wong and Sandler mixing rule will be used with the NRTL equation in the above three EOS.

3.9.3 Data regression and correlation (LLE)

An introduction to systems of partial liquid miscibility was presented in Section 3.7. The different types of LLE exhibited by binary systems were also presented and it was shown that the iso-

fugacity criterion also holds for LLE. The method and the equipment description for measuring LLE are presented in Chapter 4. In this section we look at the correlation of LLE using the activity coefficient models. We seek to answer the question "given the values of the equilibrium phase compositions, x_I^{α} and x_I^{β}, how can the constants in the equation for G^E be determined?" These constants when available can be used to predict equilibrium at other conditions remote from those at which they were determined. This subject is treated further below.

The application of the equilibrium criterion to the two phases and the use of Equation (3-66) to give the activity coefficients from the chosen G^E expression allow the constants to be found. Thus when Equation (3-53) is written for each of the two components in the two phases we have respectively:

$$\gamma_1 x_1 = \gamma_1^* x_1^* \tag{3-156}$$

$$\gamma_2 x_2 = \gamma_2^* x_2^* \tag{3-157}$$

where in order to simplify notation, the quantities in phase β have been denoted by an asterisk and those in phase α are left without a superscript (Raal and Muhlbauer [1998]). As in the modeling of VLE, application of Equation (3-60) to the chosen G^E model gives an equation of the form:

$$\gamma_i = \gamma\left(T, P, x_i, C_1, C_2\right) \tag{3-158}$$

In the above equation, only those models with two arbitrary constants can be used in representing LLE because at any given temperature there are only two experimental data points available for regression. Substitution of this last equation in Equations (3-156) and (3-157) gives two equations in two unknowns, the arbitrary parameters in the G^E model:

$$\gamma\left(x_1, T, P, C_1, C_2\right) x_1 = \gamma\left(x_1^*, T, P, C_1, C_2\right) x_1^* \tag{3-159}$$

$$\gamma\left(x_2, T, P, C_1, C_2\right) x_2 = \gamma\left(x_2^*, T, P, C_1, C_2\right) x_2^* \tag{3-160}$$

These equations can in principle be solved for the two arbitrary parameters. Once the parameters have been obtained, they can be used to calculate activity coefficients for the two components making the binary system in the two miscible regions (Prausnitz [1969]). Mutual solubility can thus be used to predict VLE. This subject is treated further in the following section.

Raal and Muhlbauer [1998] suggest that the calculations should be done for at least two mutual solubility data sets at different temperatures so that the temperature dependence of the parameters can be determined.

Equations (3-159) and (3-160) can be written for the Margules Van laar and NRTL Gibbs energy models. The resulting equations are presented in Appendix 2. For the NRTL equation, the third parameter, the non-randomness parameter must be fixed to allow for the solution of the equations. Prausnitz [1969] suggests that a value of α should be obtained from experimental results of the same class of compounds as those under study. Because of the algebraic complexity of the NRTL equation the solution for its parameters is tedious. For this reason Renon and Prausnitz [1969] published the results for the calculations in a graphical form. In these graphs, two parameters S and D are obtained from the mutual solubility data and are related to the NRTL coefficients by the equations:

$$S = \frac{1}{2}(\tau_{21} + \tau_{12}) \tag{3-161}$$

$$D = \frac{1}{2}(\tau_{21} - \tau_{12}) \tag{3-162}$$

Their graphs are also presented in Appendix 2.

LLE, like VLE, can also be described by the direct method using EOS's. However this approach is only important in modeling high-pressure LLE where the effect of pressure on the equilibria can no longer be neglected (Ohta et al. [2004], Raal and Muhlbauer [1998]). The use of the direct method in describing LLE (and hence VLLE) will not be discussed any further as this work is concerned with atmospheric and sub-atmospheric pressures, where LLE is generally independent of pressure. The reader interested in greater detail on the method can refer to Englezos et al. [1990a, b, 2005], Liu et al. [2002] and (Ohta et al. [2004].

3.10 Combined VLE and LLE (VLLE)

The prediction of VLE from LLE was highlighted in the previous section. It was indicated that the parameters in the model equations for the excess Gibbs energy obtained from LLE data alone can be used to predict VLE in the miscible regions. This section looks into the reverse process, that of predicting LLE from VLE. Thus we assume that the parameters in the G^E model have been found (for example by regressing the VLLE data for the single liquid phase regions or from predictive methods like the UNIFAC) and the task is to compute mutual solubilities.

The criterion of stability introduced in Section (3.9.1.1) allows these calculations to be made (Prausnitz [1969], Raal and Muhlbauer [1998]). A plot similar to Figure (3-7) of ΔG calculated from:

$$\frac{\Delta G}{RT} = \frac{G^E}{RT} + \sum_i x_i \ln x_i \qquad (3\text{-}163)$$

is made against x_1 and examined. If part of the curve is concave downward (as in Figure (3-7)) then a tangent drawn joining the ends of the convex part of the curve gives the equilibrium compositions of the two liquid phases. These values are approximate and more accurate values can be found by differentiating Equation (3-163) after substituting for G^E and then equating the resultant equation to the slope of the tangent line obtained above. The resulting equation can be solved by iterative methods with the earlier obtained values providing the starting values in the trial and error procedure (Raal and Muhlbauer [1998]).

An alternative procedure is presented by Null [1980] where the mutual solubilities are obtained from a plot of the product $\gamma_1 x_1$ against $\gamma_2 x_2$ for a choice of increasing x_1 and x_2 and from a plot of $\gamma_1 x_1$ vs. x_1. The equilibrium compositions are read off the second plot at a value of $\gamma_1 x_1$ corresponding to that from the first plot where the curve intersects itself (The looping and intersection of the curve is a necessary condition for the existence of a solution).

3.11 Thermodynamic consistency testing

Thermodynamic consistency testing, a topic that wraps up this chapter, was introduced in Section (3-7). The Gibbs Duhem equation (Equation 3-70) was also presented and it was highlighted that it is an important equation in thermodynamics on which many tests of consistency were developed. The different tests pertinent to this work are discussed below.

3.11.1 The Point test

Recirculating equilibrium stills (see Chapter 2), similar to the one used in this work allow for the measurement of temperature, pressure and both liquid and vapour compositions. This is an *over determination* of VLE because any one of these variables can be determined from the other three using the Gibbs Duhem Equation. In the Point Test of Van Ness et al. [1973], the vapour phase composition or (pressure for isothermal data) is computed from the remaining variables and the results compared with the measured values. This comparison generates residuals Δy (or ΔP) which for consistent data should scatter evenly about the zero axis over the full composition range. When isobaric data is to be tested, the Δy and ΔT residuals need to be examined. Van Ness and Abbot [1982] and Hirata [1975] discuss the choice of objective functions when using this test. Fredenslund et al. [1975] and Danner and Gess [1990] provide a quantitative criterion for acceptance of data and they propose that the absolute average deviation should be less than 0.01. This is the criterion that will be used in this work.

3.11.2 The Area test

The area test proposed independently by Herington [1947] and by Redlich and Kister in 1948 derives directly from the Gibbs Duhem equation:

$$\sum_i x_i d\ln\gamma_i = \frac{\overline{V}^E}{RT}dP - \frac{\overline{H}^E}{RT^2}dT \qquad (3\text{-}70)$$

Integration of the left and right hand terms of the above equation for a binary mixture at constant pressure and temperature gives respectively:

$$\int_{x_1=0}^{1} \ln\frac{\gamma_1}{\gamma_2} dx_1 = -\int_{x_1=0}^{1} \frac{H^E}{RT^2} dT \tag{3-164}$$

and

$$\int_{x_1=0}^{1} \ln\frac{\gamma_1}{\gamma_2} dx_1 = -\int_{x_1=0}^{1} \frac{V^E}{RT} dP \tag{3-165}$$

For consistent data, the two areas in the above equations should be equal. The two areas in practice would never be exactly equal and the criterion in general use is that the net area (determined by regarding the sign) should be no more than 10% of the total area. However, according to many researchers (Raal and Muhlbauer [1998] and Van Ness [1995]), the test may pass data sets that are inconsistent. Van Ness [1995] concludes that the test is a necessary but insufficient condition for consistency, thus data failing the test are thermodynamically inconsistent.

The area test has two other drawbacks. The first is that the heat of mixing data required for isobaric data are often unavailable for most systems. The right hand side of Equation (3-164) has thus been taken to be zero, an assumption that is not valid and cannot be justified even if the H^E term is divided by the square of the temperature (Raal and Muhlbauer [1998]). However for isothermal data, the RHS of Equation (3-165) can justifiable be set to zero.

The second disadvantage of the test is that the measured total pressure cancels in the ratio of the activity coefficients (see Equation 3-48). This is one of the most important and accurately measured variables but disappears in this test. Because of these inadequacies, Van Ness [1995] proposed the *direct test*. This test is discussed further below.

3.11.3 The Direct test

Van Ness [1995] describes this test as *being a long sought goal – a simple direct test of thermodynamic consistency for each point of a VLE data set with respect to the Gibbs Duhem equation itself.* The formulation of this test is long and will not be presented here and the reader interested in great detail should refer to Van Ness [1995]. The formulation results for a binary system in the equation:

$$\delta \ln \frac{\gamma_1}{\gamma_2} = x_1 \frac{d \ln \gamma_1^{Exp}}{dx_1} + x_2 \frac{d \ln \gamma_2^{Exp}}{dx_1} - \varepsilon \tag{3-166}$$

The superscript Exp denotes values obtained from measured experimental data and ε depends on whether the data are isothermal or isobaric. It is given by the equations:

$$\varepsilon = \frac{V^E}{RT} \frac{dP}{dx_1} \tag{3-167}$$

and

$$\varepsilon = \frac{-H^E}{RT^2} \frac{dT}{dx_1} \tag{3-168}$$

for the two cases respectively. When applying the test, a VLE data set is reduced using $\Sigma (\delta g)^2$ (where $g = x_1 \ln \gamma_1 + x_2 \ln \gamma_2$) as the objective function. For consistent data, the RHS of Equation (3-166) is required to be zero. The residual on the left is thus a measure of deviations from the Gibbs Duhem Equation and the extent to which the residual fails to scatter about the zero axes provides a measure of the departure of the data set from consistency (Van Ness [1995]). Van Ness [1995] also provides a quantitative criterion for the test. He gives a table of indices (see Table 3-1 below) calculated from the above mentioned residual (Equation 3-166) and they start from 1 for excellent data and go to 10 for poor data.

Index	RMS $\delta \ln (\gamma_1/\gamma_2)$	
1	>0	≤ 0.025
2	>0.025	≤ 0.050
3	>0.050	≤ 0.075
4	>0.075	≤ 0.100
5	>0.100	≤ 0.125
6	>0.125	≤ 0.150
7	>0.150	≤ 0.175
8	>0.175	≤ 0.200
9	>0.200	≤ 0.225
10	>0.225	

Table 3 - 1: Consistency table for the direct test (Van Ness [1995])

4

Chapter Four

Equipment Description

The equipment that was used in this project has already been mentioned in the previous chapters. This chapter is devoted to a complete description of the experimental apparatus which comprised two parts. The first part was for VLE measurents and the second for the corresponding LLE measurements which together gave the complete VLLE for the systems measured. The VLE measurents were conducted in a modified Raal and Muhlbauer [1998] still that had been adapted for systems of partial liquid miscibility and the LLE measurements were conducted in an all-glass jacketed cell maintained at the required temperatures by circulating water from a constant temperature bath. The aspects of the experimental equipment that will be covered are as follows:

1. The VLE Apparatus
    - The VLE equilibrium still
    - Temperature measurement and control
    - Pressure measurement and control
    - Sampling and composition analysis

2. The LLE Apparatus
    - The LLE cell
    - Temperature measurement and control
    - Sampling and composition analysis

4.1 The VLE apparatus.

Figure 4.1 below shows a schematic diagram of the VLE apparatus. The experimental equipment comprises the VLE dynamic cell , which is described in more detail below, a 50 litre ballast tank, a Julabo FT 200 cold finger, a WIKA model P10 pressure transmitter, a WIKA model 5001 6 ½ digit pressure display, a WIKA Model 4003 4 ½ digit temperature display, a Labotech water bath complete with a pump and cooling water, 4 x AC Voltage regulators for powering up heaters, 3 x DC power supplies (two for the magnetic stirrers and one for actuating a solenoid valve that is connected to the vacuum pump on the vapour sampling line), a BUCHI Model B-721 pressure controller, a Vacuum pump, a CN-40 temperature controller and a FUTEK SSR 40 DA solid state relay.

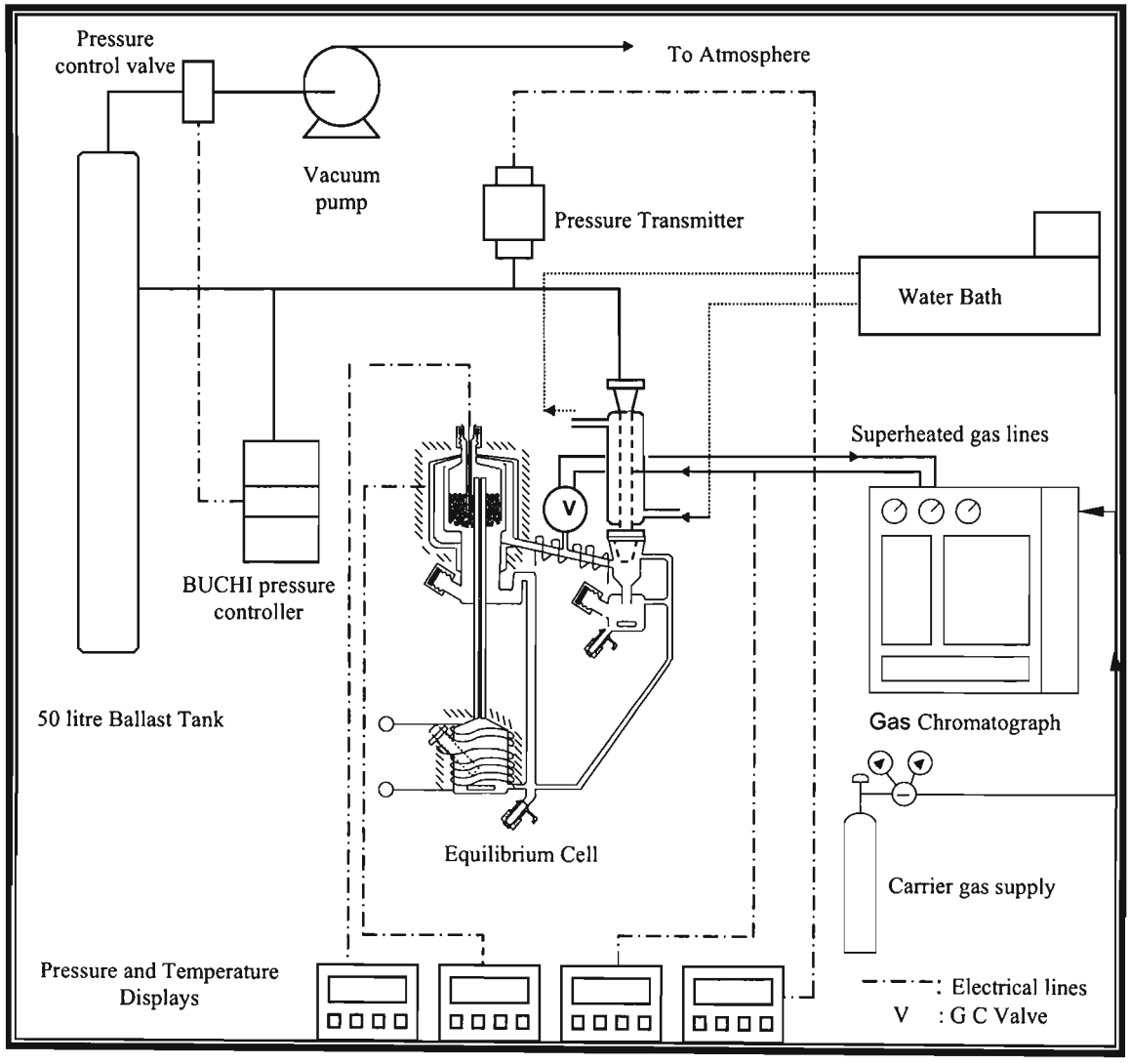

Figure 4 - 1: Schematic Diagram of VLE Apparatus

In the above setup, the pressure measuring device (WIKA P10 Pressure transmitter) is connected to the equilibrium cell via the condenser. The pressure controller, connected to the same line as the measuring device, drives a two-way control valve leading to the vacuum pump. This arrangement allowed for precise control of the pressure at the desired values. Another noteworthy feature in the above diagram is the superheated take-off of the vapour samples directly to the gas chromatograph. This arrangement is a special modification for systems of partial liquid miscibility, for which the vapour forms a two-liquid phase upon condensation. This setup together with the pressure measuring train is described in more detail below.

The VLE still is mounted onto a wooden support provided with a Perspex shield – an important safety feature incorporated in the equipment design. Figure 4-2 shows a picture of the experimental setup presented above.

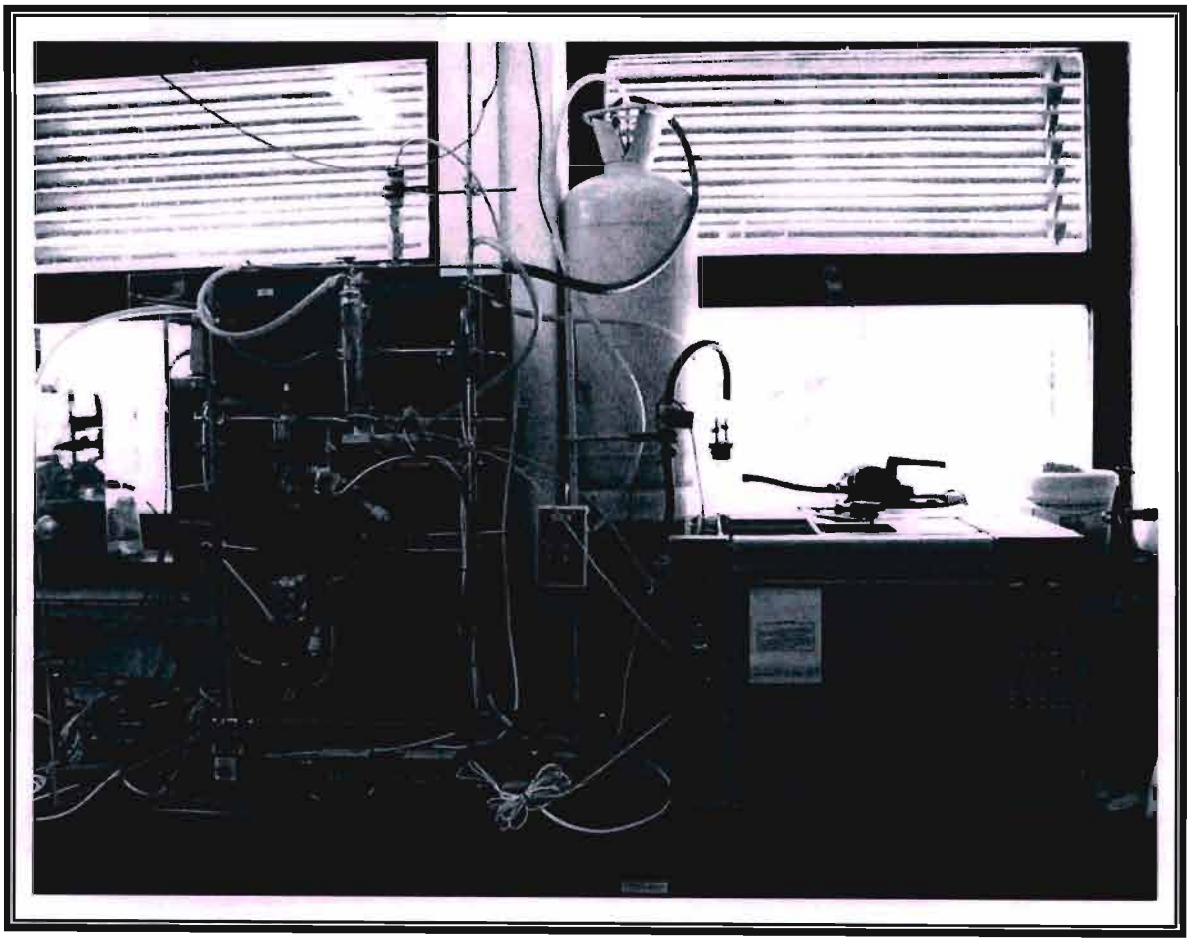

Figure 4 - 2: Front View of the VLE Apparatus

4.1.1 The vapour liquid equilibrium still

The all glass VLE dynamic still designed by Raal and Muhlbauer [1998] was described briefly in Chapter 2 (Section 2.2.1.5). The still was constructed by a glass blower; Mr. P Siegling operating in Durban where this work was conducted. Figure 4-3 gives a detailed view of the still which is based on the designs of Heertjies [1960] and Yerazunis [1964], who successfully used a packed equilibrium chamber where the liquid and vapour phases are forced downward co currently to achieve rapid and dynamic equilibrium. The original Raal and Muhlbauer [1998] still was used as further modified by Joseph et al [2001].

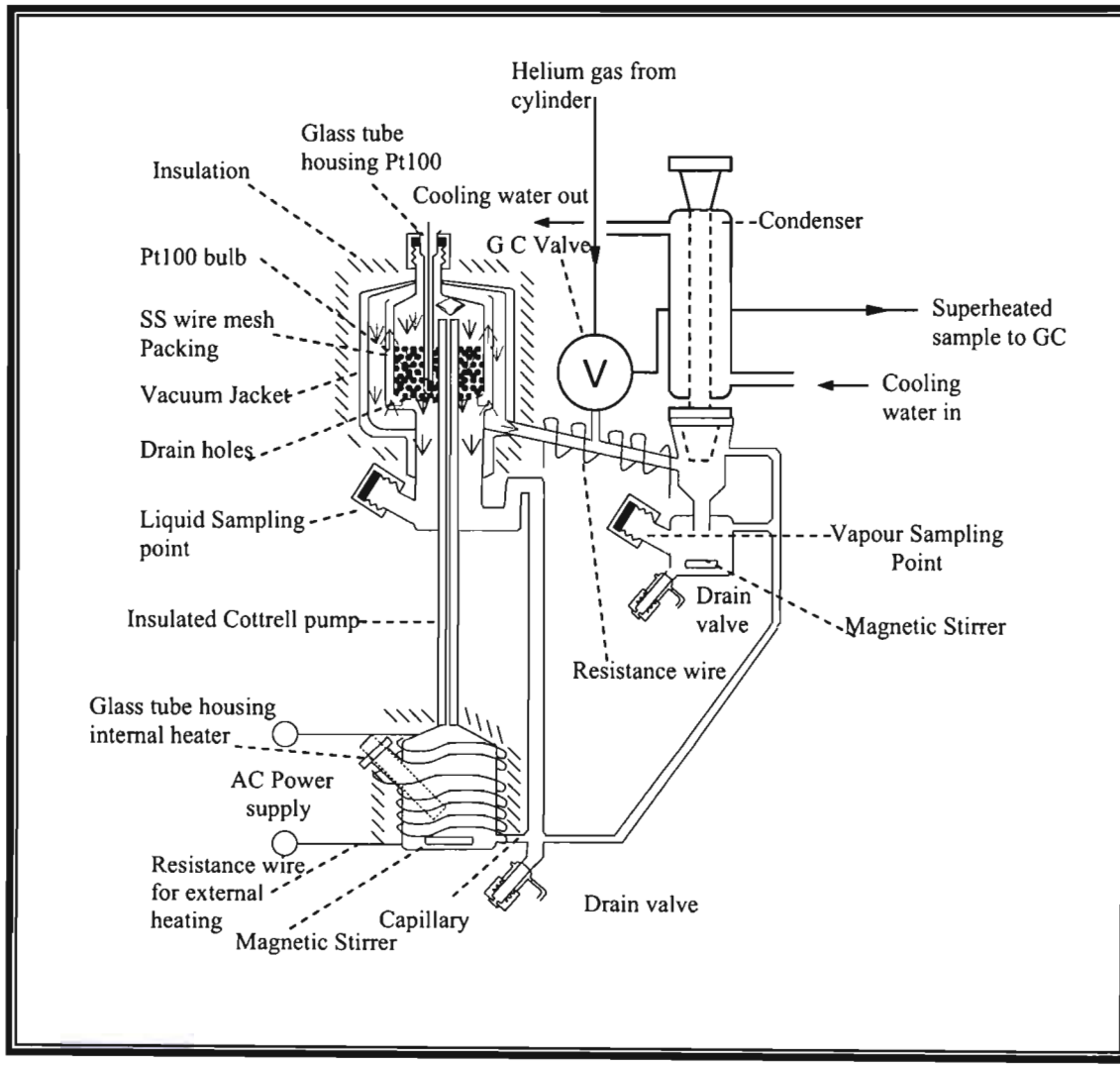

Figure 4 - 3: Schematic diagram of the VLE Still

The central feature of the still is the packed equilibrium chamber that is concentric around a vacuum-insulated Cottrell pump. During operation a liquid mixture is charged into the boiling chamber which is heated both internally and externally. Internal heating is achieved through a heater cartridge which provides the actual impetus for heating. Heat losses to the environment are accounted for through external heating which is provided by resistance wire wound around the boiling chamber. The glass tube housing the internal heater has its surface roughened to provide nucleation sites for smooth boiling and control of the circulation rate.

When boiling commences, a vapour-liquid mixture from the boiling chamber is forced upward through the Cottrell tube whereupon it flows downward through the packing made of stainless steel wire mesh cylinders of 3 mm diameter. The packing provides a large interfacial area and thus establishes intimate contact between the vapour and liquid phases flowing down the equilibrium chamber. An immediate advantage of this arrangement is the rapid attainment of equilibrium even in systems of high relative volatility. Before the mixture leaves the chamber through holes at the bottom of the equilibrium chamber it flows onto a Pt-100 temperature sensing element which is directly connected to a display which gives the equilibrium temperature. Liquid and vapour phases disengage at this point and the liquid flows down into a small trap, where a sample may be withdrawn for analysis, before overflowing from the trap to the boiling chamber.

The vapour rises up and around the equilibrium chamber to the condenser where it collects in the condensate receiver before overflowing to the boiling chamber via a standpipe leg.

The movement of the vapour around the chamber provides an important role of thermal lagging of the equilibrium chamber. It was realized though, during the operation of the still that the downward third pass of the vapour in the equilibrium chamber results in partial vapour condensation due to contact with the outside walls which were a few degrees below the equilibrium temperature. However, unlike in homogeneous systems where the partial condensation of the vapour in the line before the condenser does not affect the vapour composition (this is so because for such systems a vapour sample is withdrawn after total condensation where the composition should be constant), in systems of limited liquid miscibility, minute condensation of the vapour before sampling should be avoided as this would necessarily change the compositions.

To overcome this problem, the outside walls of the equilibrium chamber were kept at 5 degrees Celsius above the equilibrium temperature. This was achieved through a CN-40 temperature controller connected to a FUTEK SSR 40 DA solid state relay which regulated the power to an

electrical wire wound around the equilibrium chamber. The choice of the 5 degree temperature difference was arrived at by comparing successive vapour compositions for a homogeneous system measured at different wall temperatures. The wall temperature of the equilibrium chamber was raised in successive runs and at each run the composition of a sample sent directly through the sampling lines (described in more detail below) was compared to that taken from the condensate receiver using a syringe until the results agreed. The sampling of the vapour phase using a syringe was possible as the homogeneous system for which the measurements were carried out formed only a single liquid phase upon condensation.

The other special features of the still are that:

- The Cottrell tube is not depended on as a means of establishing equilibrium since the equilibrium chamber increases the transfer of mass between the vapour and liquid phases, thus allowing for rapid attainment of equilibrium.
- The direct analysis of the vapour composition by gas chromatography eliminates the difficulties encountered in analyzing the two-phase condensate that is formed a few degrees below the boiling point.
- The small volumes of the condensate receiver and the boiling chamber make it possible for magnetic stirring to completely emulsify the two-phase liquid mixture obtained in systems of partial miscibility.
- Efficient magnetic stirring in both the condensate receiver and the boiling chamber eliminates temperature and any possible concentration gradients that may affect reproducibility of the sample concentrations. Stirring in the boiler also ensures that the returning condensate is thoroughly mixed with the rest of the liquid and thus prevents flashing
- The packing is easily accessible through the top of the still. The advantage of this is that the height and type of the packing can both be adjusted/altered which allows for the handling of highly volatile systems including those that may have difficulty in attaining equilibrium.

4.1.2 Temperature measurement and control

Several temperatures were measured during the operation of the VLE apparatus. These are

- The equilibrium temperature
- The equilibrium chamber wall temperature
- The vapour sample loop and take-off line temperatures

In each case, a class A Pt-100 resistance sensor connected to a temperature display was used as the measuring device and the temperature was read off directly from the display. A number of other temperatures at different positions on the equilibrium chamber wall and sampling lines were also measured so as to give the actual state of the apparatus at any given time. All these additional temperatures were also measured using Pt100 temperature sensors but were all connected to a single display via a selector switch. The selector switch had up to 12 positions and thus allowed up to 12 temperatures to be measured using a single display. The Pt100 sensors had to be calibrated to give the actual reading. This subject is treated in the following chapter.

For isothermal runs the equilibrium temperature was controlled at fixed values manually by adjusting the pressure in the still appropriately. Raising the pressure increases the temperature and lowering the pressure had the effect of lowering the temperature. With the preceding temperature measurement and control strategy, the overall accuracy of the measured temperature was estimated to be ± 0.02 °C and the accuracy of the temperature control varied between 0.01 and 0.05 °C. Figure 4.4 below shows the housing and position of the Pt-100 sensor in the equilibrium chamber.

4.1.3 Pressure measurement and control

The pressure in the VLE still was measured using a WIKA model P10 pressure transmitter. Pressure control was effected with a BUCHI model B-721 pressure controller which had a vent to the atmosphere and utilized a two way solenoid valve connected to a vacuum pump. Figure 4-1 shows the connections in the pressure measuring train. The 50 litre ballast tank was used for smoothing out pressure fluctuations. Overall pressure accuracy was estimated at 0.03 kPa and when the still was operated at constant pressure, the controlled pressure was within 0.01 kPa

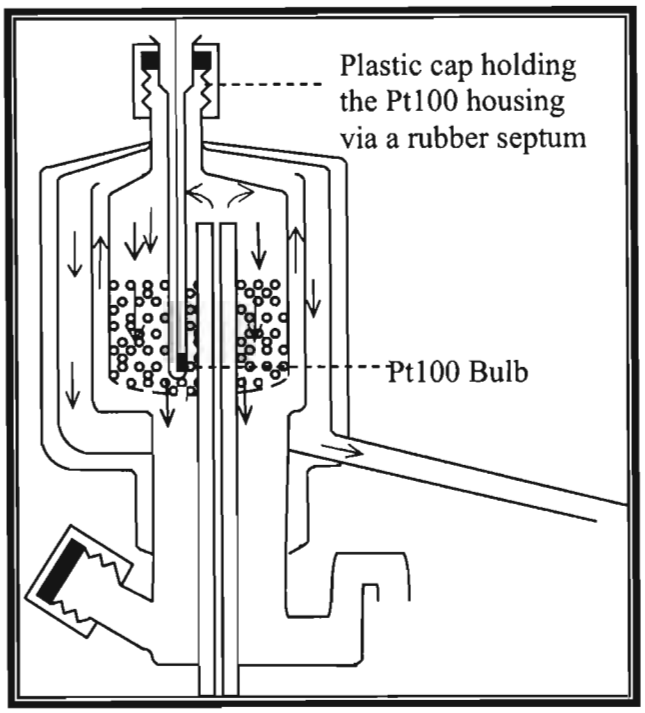

Figure 4 - 4: Schematic diagram of the equilibrium chamber showing the position of the Pt-100 temperature sensor

4.1.4 Sampling and composition analysis.

Liquid samples were taken directly from the liquid trap as in the case for homogeneous systems, using a gas-tight syringe through chemically resistant septa (See Figure 4.3 above). For the vapour phase, as has already been indicated above, a sampling mechanism was designed for systems of limited miscibility in the liquid phase. A vapour sample was taken from the still before condensation and sent to a gas chromatograph (GC) via a superheated gas line. A six-port GC valve was used in conjunction with a solenoid valve connected to a vacuum pump for this purpose. Figure 4.5 below shows the connection of the valves and the stages in the sampling process. In this arrangement, tried initially, the sample loop is evacuated through the use of the vacuum pump (Diagram 3) after which the position of the three way solenoid valve is changed allowing the vapour to be sucked into the loop (Diagraml) and finally the sample is flushed by the GC carrier gas after switching the position of the GC valve (Diagram 2).

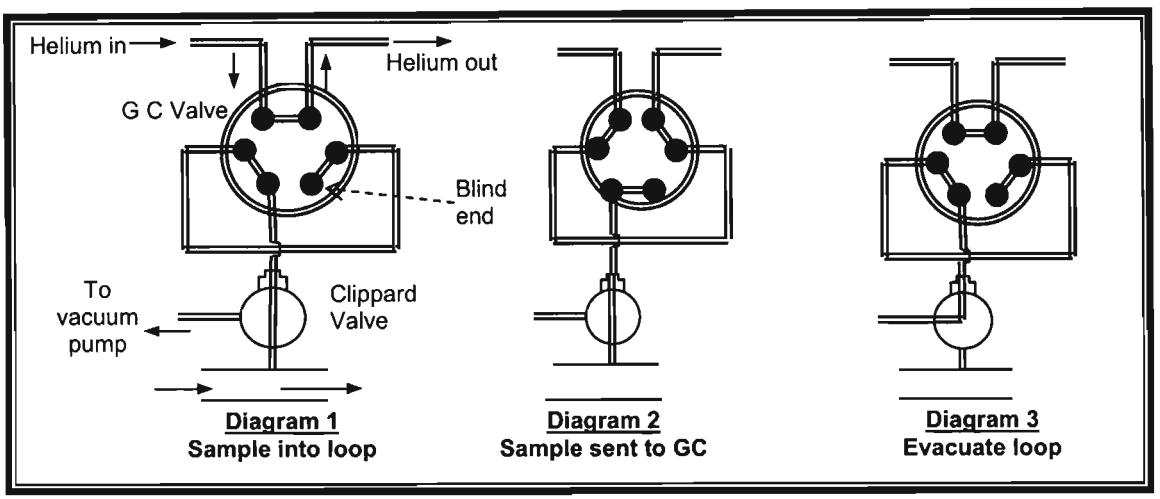

Figure 4 - 5: Stages in the Vapour Sampling Process (Initial Set up)

Problems were however, encountered in sending a sample through to the GC when the still was operated at low pressures. The driving force for transfer of the vapour from the still to the sampling loop, (which is the difference in the pressure in the still and that in the sampling loop) diminishes as the pressure in the still is lowered. This led to an alternative arrangement, shown in Figure 4.6, which relied solely on the vacuum pump for the sampling process. The new arrangement had an added advantage that it eliminated the need for heating the solenoid valve.

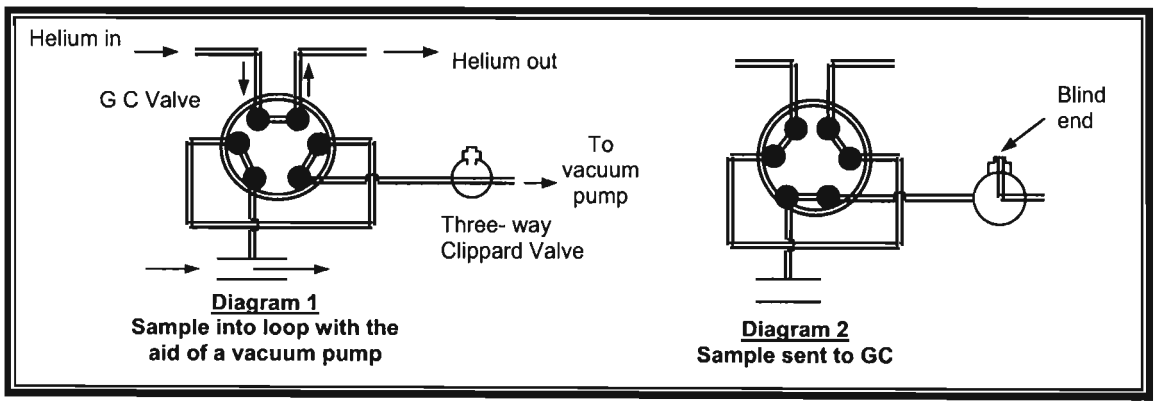

Figure 4 - 6: Stages in the Vapour Sampling Process (Alternative setup)

To prevent partial condensation of the vapours in the sampling train, which would alter the composition, the two sampling valves (the six-port GC valve and Clippard valve) were mounted onto an aluminium block that was heated using two 10mm D x 40mm L heater cartridges, each

rated at 200 Watts. Figure 4-7 below shows a 3D diagram of the heating block with all the pertinent dimensions.

An important point to note with the above sampling arrangement is that the carrier gas is metered in the GC (measuring and control of carrier gas flowrate and pressure) before diverting to the sampling valves from where it is routed directly to the GC injector. This prevents the condensation of the vapour sample in the cold GC parts that would occur if the carrier gas went to the valve prior to metering. The gas line is also preheated before and after flushing out the vapour sample, all this being done to prevent condensation in the lines. Several Pt-100 temperature sensors were placed on the lines as described in Section 4.1 2.

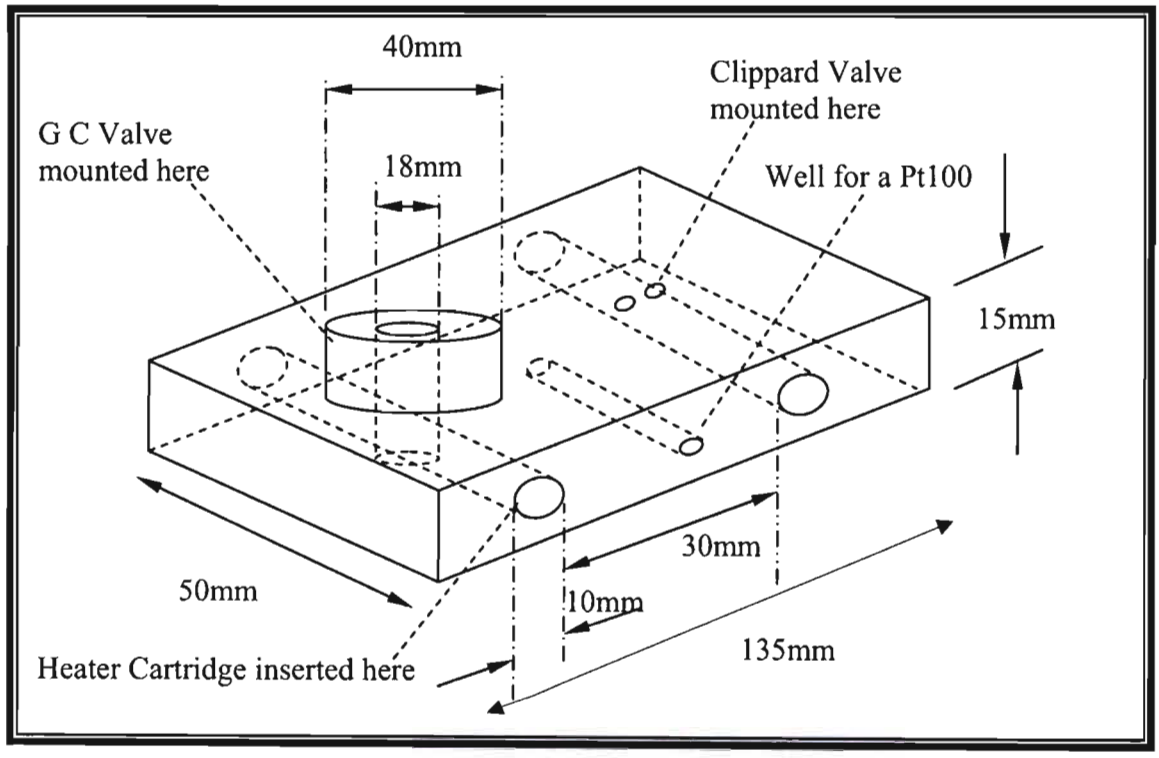

Figure 4 - 7: Heating Block for the Sampling Valves

Figure 4-8 below shows pictures of the heating bock with the sampling valves together with their connection onto the VLE still.

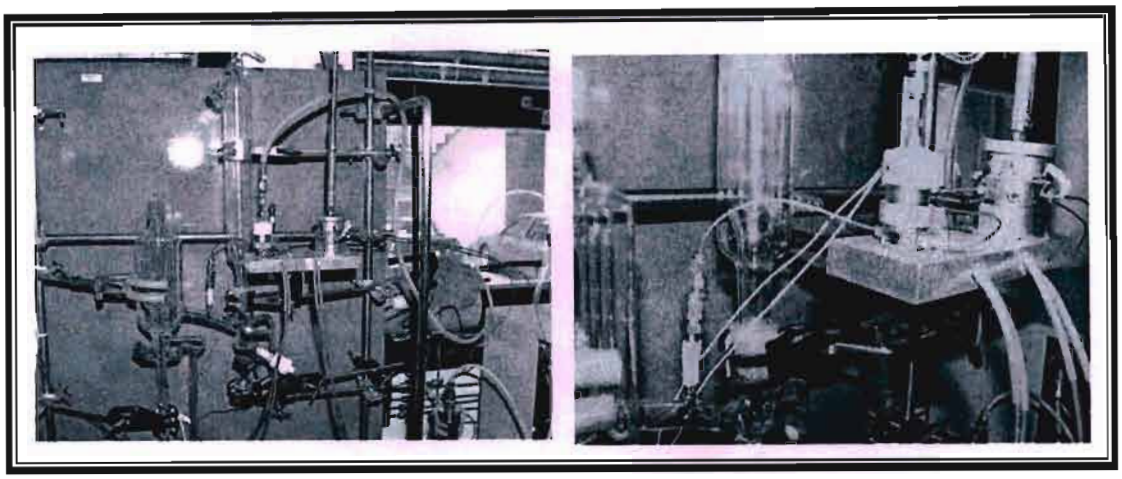

Figure 4 - 8: Vapour sampling for the VLE still

4.1.4.1 Composition analysis

A Hewlett Packard 5890 Series II Gas Chromatograph was used to obtain accurate compositions of the equilibrium liquid and vapour samples. The GC was operated with a thermal conductivity detector (TCD) and a 2.5m long stainless steel column (2.2 mm in diameter) packed with 80 to 100 mesh Poropak Q. The composition measurements were estimated to be accurate to within 0.001 of a mole fraction. The operation of the GC together with its calibration and sampling procedures are presented in the following chapter.

4.2 The liquid-liquid equilibrium (LLE) apparatus.

The stirred analytical cell used for LLE measurements is shown in Figure 4.9 below together with other peripheral devices that make up the apparatus. These auxiliary devices are a Labcon water bath complete with a pump and cooling water, 2 x Pt-100 temperature sensors with corresponding 2 x 4 ½ temperature displays and a magnetic stirrer complete with a DC power pack.

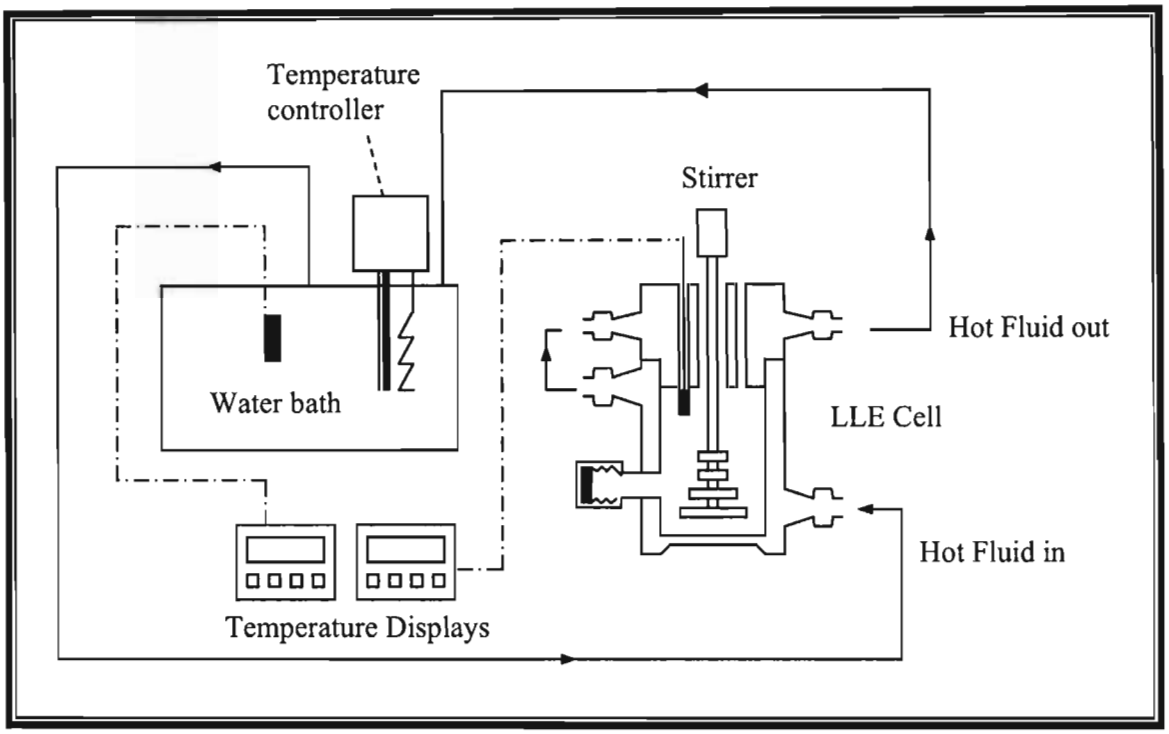

Figure 4 - 9: Schematic diagram of the LLE Apparatus

During operation, the pump circulates water maintained at the required temperature from the water bath through the jacketed cell (described in more detail below). A two-phase liquid mixture placed initially in the cell is mixed for a sufficient time to reach equilibrium and then allowed to settle so that the two phases separate. Liquid samples of the two phases are thereafter withdrawn for analysis in a GC using a gas-tight syringe from the two sampling points provided for this purpose (see Figure 4-11 below). The procedure was repeated at a series of temperatures over the interval of interest. Figure 4-10 shows a picture of the apparatus.

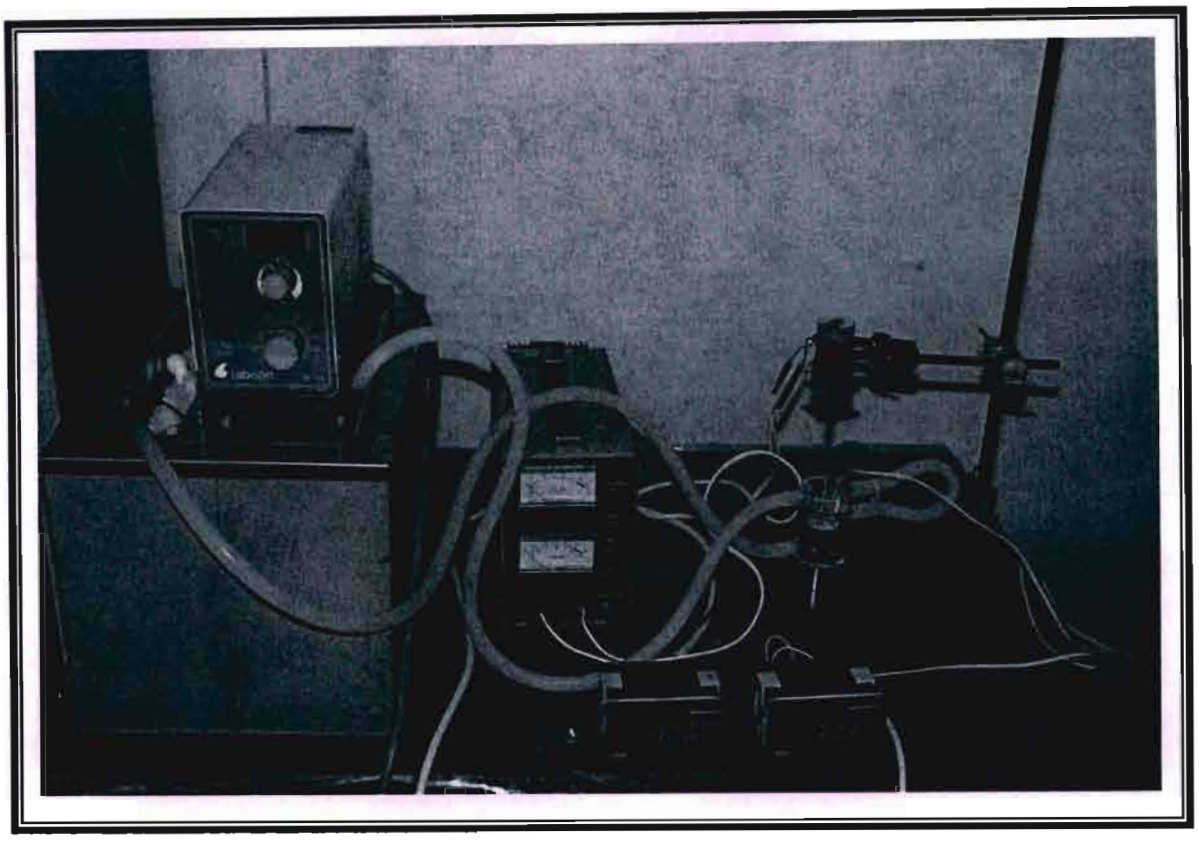

Figure 4 - 10: Front View of the LLE Apparatus.

4.2.1 The LLE cell

Figure 4-11 shows a schematic view of the all-glass LLE cell. The jacketed cell has provision for a hot fluid to be circulated through the header which has a thermo-well in which a Pt-100 temperature sensor is placed. The stirrer is driven by a miniature variable speed DC motor. An important feature of the cell is that two different sampling points are provided for the two phases in equilibrium. This, unlike in previous designs which had a single sampling point, results in higher accuracy in the LLE measurements as contamination of the samples is avoided.

The contact between the header which houses the Pt-100 and the rest of the LLE cell was a ground glass joint and this had the important advantage of completely sealing the cell which thus prevented contamination of the cell contents from the surroundings. A Teflon bush, visible in Figure 4-10 but not shown in Figure 4-ll, held the stirrer in the upright position. This did not only prevent wobbling of the shaft as the stirring action began but also helped in the sealing of the apparatus.

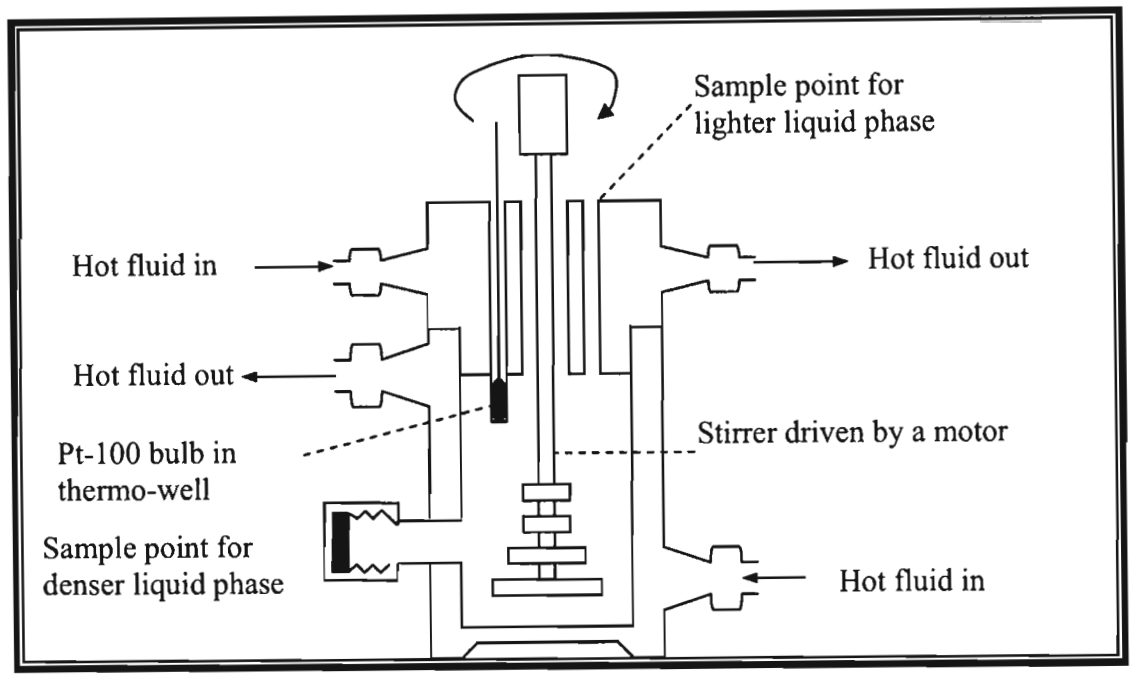

Figure 4 - 11: The LLE Cell

4.2.2 Temperature measurement and control

Two temperatures were measured in this apparatus which are

- Bath temperature and
- Equilibrium temperature.

As in the VLE apparatus described above, class A Pt-100 temperature sensors were used to measure these temperatures. The Pt-100 sensor for the bath temperature was fitted into a thin walled stainless steel tube and fully immersed into the bath while that for the equilibrium temperature was placed in a thermo-well on the cell (see Figure 4-11 above). A drop of oil was put into the thermo-well to increase the contact area between the sensor and the glass wall.
The pump was fitted with a heater and temperature controller; an arrangement which allowed for fine temperature control and had an overall accuracy estimated at 0.02 °C.

4.2.3 Sampling and composition analysis

Gas-tight syringes were used to sample the two liquid phases in equilibrium. The resultant compositions were measured using the same Hewlett Packard 5890 Series II gas chromatograph described above for the VLE apparatus. Calibration of the GC is treated in detail in the following chapter.

5

Chapter Five

Experimental Procedure

This chapter presents a discussion on the operating procedures of the equipment that was discussed in the preceding chapter. Thus the methods of operation of both the VLE apparatus and the LLE apparatus will be outlined. It should be noted that these procedures are a result of successive trial runs that were carried out with the aim of obtaining reproducible and accurate experimental results. As was indicated in the introductory chapters of this thesis, these trial runs were done for two test systems, the first being the homogeneous cyclohexane (1) + ethanol (2) system at 40kPa and the second being the heterogeneous water (1) + MBE (2) system at 97.2 kPa. The results for these test systems are presented and analysed in the following chapter.

The material in this chapter is covered under the headings Preparation, Calibration and Operation for each apparatus

5.1 The VLE apparatus

5.1.1 Preparation

5.1.1.1 Leak detection and elimination

Precise pressure measurement and control is only possible if the system is completely free of leaks. Thus the first stage in the operation of the VLE apparatus was the identification and successful elimination of all leaks. In this project all the pressure measurements were at conditions less than the atmospheric pressure. This coupled with the fact that the equilibrium still was made of glass and thus higher than atmospheric pressures could not be conveniently applied to the equipment, meant that leak detection would be a problem. The usual method of leak detection which involves pressurising the equipment and then using a soapy solution, for which bubbles would be seen when a leak is present, could therefore not be used.

The determination of the presence of leaks in the apparatus was thus achieved though evacuating the still using a vacuum pump followed by complete isolation of the vacuum pump using valves on the connecting lines. The pressure reading on the display was then noted and the equipment left in that condition for about 2 hours. Any leaks in the system were manifested in an increase in the pressure reading.

As a way of detecting the individual leaks, points on the apparatus suspected of having leaks were sprayed with a small amount of acetone (or any volatile chemical). The presence of a leak was then seen by a slight fluctuation in the system pressure which occurs as a result of the acetone vaporizing causing a slight increase in pressure before stabilization occurs. The identified leaks were then eliminated by using vacuum grease on ground glass joints and vacuum seals on steel pipe joints.

Leak detection on the lines conveying the vapour samples to the GC was simple as the whole sampling mechanism was made of steel and thus could be isolated and pressurized, after which a soapy solution was used as described above.

All the leaks were thus eliminated by repeating the foregoing procedures.

5.1.1.2 Cleaning of the equilibrium still

Cleaning of the still before any run was necessary as any contaminants present could greatly affect the VLE data produced. In the cleaning process, acetone (supplied by Merck at 99.5 volume % purity) was allowed to circulate at constant pressure in the still for approximately one hour, with the exact duration depending on the systems measured. The still was then emptied and the process (circulation of acetone in the still) repeated until only the acetone peak remained after a GC analysis of the spent acetone. After the cleaning stage, any remaining acetone in the still was drawn off through the aid of the vacuum pump. The pressure in the still was kept at very low values (1kPa) at which pressures all the acetone vaporized and was sucked out by the vacuum pump.

5.1.2 Calibration

The equilibrium temperature and pressure measuring devices together with the GC had to be calibrated prior to their use in the VLE measuring process. The discussion on the calibration of these units follows below (Sections 5.1.2.1 – 5.1.2.3).

5.1.2.1 Pressure transmitter calibration

Equilibrium temperature sensor calibration is dependent on the system pressure and therefore pressure calibration had to be done first. The WIKA P10 pressure transmitter was calibrated by using a mercury manometer connected to the still and a NIST certified electronic barometer (VAISALA Model PTB 100A) which together gave the actual pressure in the still. The BUCHI pressure controller (see Section 4.1.3) was set to give a constant pressure in the still after which the differential height of the mercury manometer was measured using a cathetometer. This height corresponded to the pressure difference between the pressure of the atmosphere, given by the barometer, and that in the still. Simple addition gave the actual pressure in the still which was then compared to the pressure displayed by the transmitter. This procedure was repeated for a series of pressures over the anticipated experimental pressure range after which a linear plot of the actual pressure against displayed pressure gave the required calibration curve (see Figure 5.1 below)

5.1.2.2 Temperature sensor calibration

The equilibrium temperature measurement using a class A Pt100 temperature sensor was discussed in detail in Chapter 4 (Section 4.1.2). In situ calibration of the sensor was carried out using two pure components, one low boiling and the other high boiling. The use of the two chemicals (n-hexane and n-dodecane) was to ensure that a large range of temperatures was covered. In the calibration process, the still was operated at constant pressure over a range of pressures and for each pressure, the actual temperature corresponding to that predicted from the Antoine equation for the test chemicals (coefficients obtained from Reid et al [1988]) was compared to that given by the display connected to the temperature sensor. As in the case above for the pressure transmitter calibration, a plot of the actual temperature against the displayed temperature gave the desired relationship (see Figure 5.2)

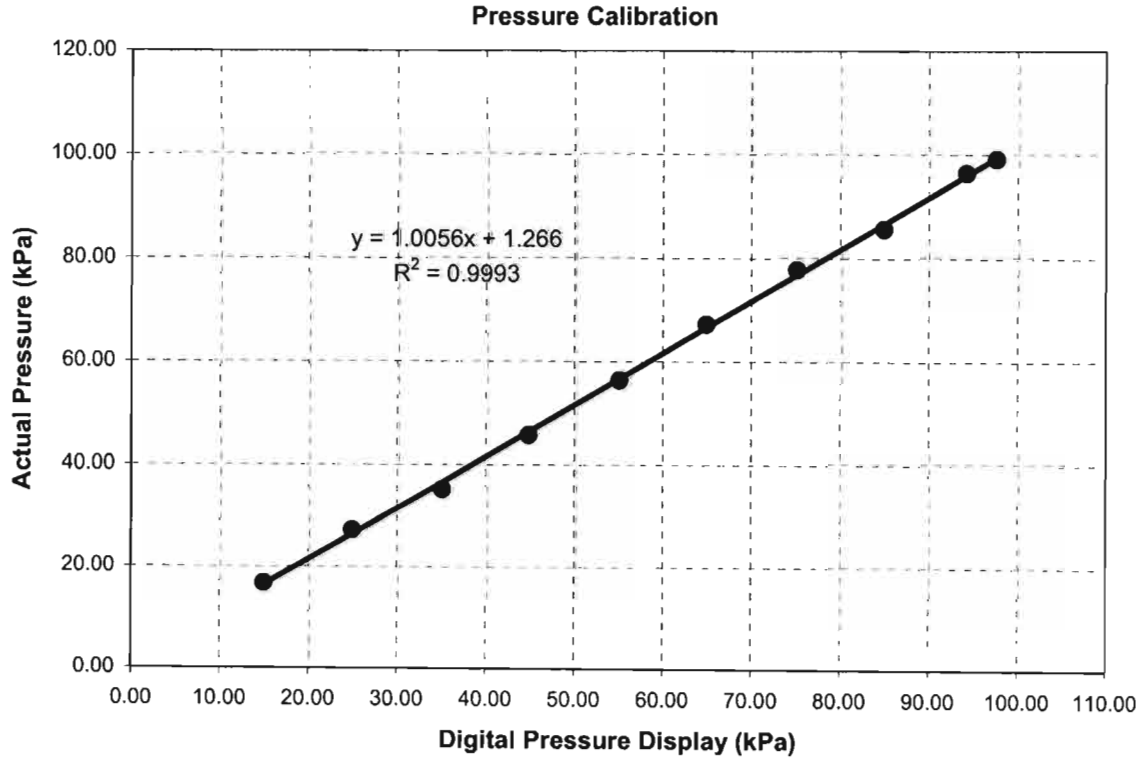

Figure 5 - 1: Pressure Transmitter Calibration curve for the VLE Still.

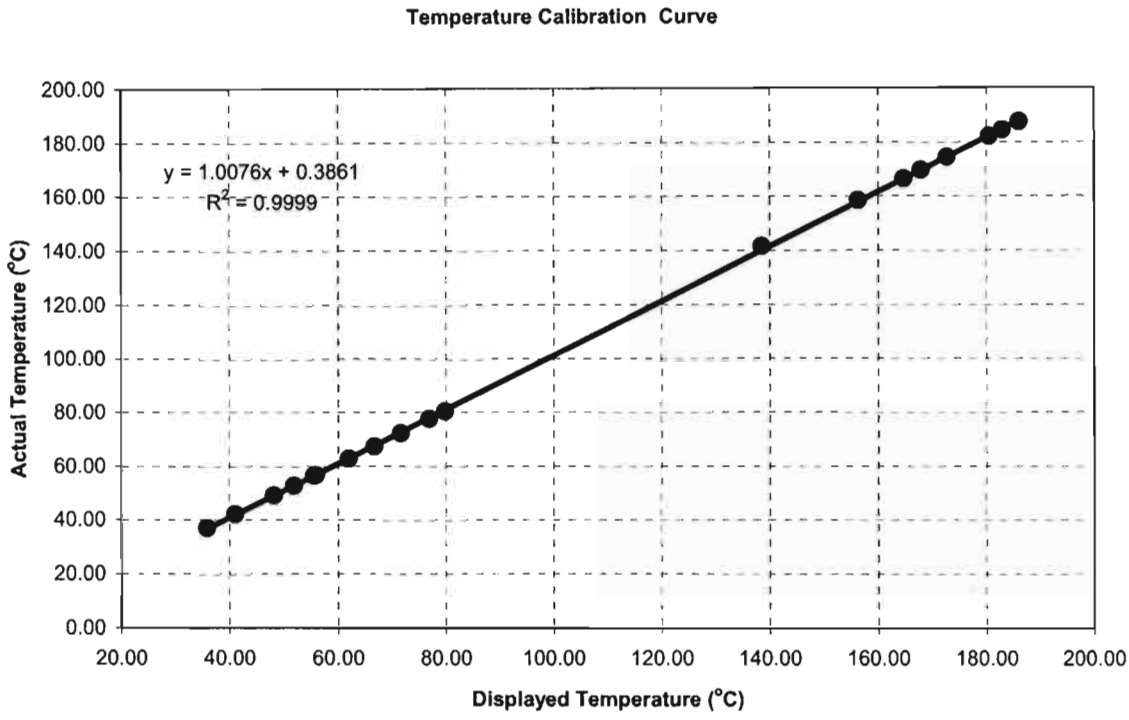

Figure 5 - 2:Temperature Sensor Calibration curve for the VLE Still.

5.1.2.3 Gas chromatograph calibration

The HP 5890 series II gas chromatograph (see Section 4.1.4.1) that was used in this project was calibrated following the area ratio method advocated by Raal and Muhlbauer [1998].

In a GC, the number of moles of a component i, n_i, passing the detector is proportional to the peak area, A_i, thus:

$$n_i = A_i F_i \tag{5-1}$$

where F_i is the proportionality constant . Raal and Muhlbauer [1998] suggest that since A_i is not constant, as it depends on the generally irreproducible injected volumes, it is more advisable to work with area ratios which for a binary system are given by:

$$\frac{n_1}{n_2} = \left(\frac{A_1}{A_2}\right)\left(\frac{F_1}{F_2}\right) = \frac{x_1}{x_2} \tag{5-2}$$

Another advantage of working with the area ratios is that the F ratios in the above equation are more likely to be concentration independent as opposed to the single response factors which depend on the amount injected. This results in greater reproducibility of the compositions measured.

When calibrating a GC, standard gravimetric samples are prepared to cover the entire composition range and then injected into the GC to give the response factor ratio, F_1/F_2. These response factors are obtained from a plot of composition ratios against area ratios for example A_1/A_2 vs. x_1/x_2. When the plot is linear over the whole composition range, then the slope of the curve should be equal to the inverse of that obtained from a plot of A_2/A_1 vs. x_2/x_1 and both curves should also pass through the origin - which is a test of the calibration procedure (Raal and Muhlbauer [1998]). The shape of the calibration curves depends on the detector type and on the system being studied. Non-linear relationships are thus not uncommon (especially in a GC fitted with a thermal conductivity detector) although even in such cases the curves should still pass through the origin.

Figures 5.3 and 5.4 show typical calibration curves for the system water (1) + MBE (2-methyl - 3 buten -2 ol) (2) that was used as a test system in this project (see the following chapter for a greater discussion on the test systems). Once the calibration curves have been obtained, the determination of the actual composition of a sample injected into the GC is simple and straight forward. For example, in a binary system, if the mole fraction ratio, x_2/x_1, found from the area ratio obtained from the GC (or from Equation 5-2) is, a, then:

$$1 + \frac{x_2}{x_1} = \frac{1}{x_1} = 1 + a$$

and hence

$$x_1 = \frac{1}{1+a} \tag{5-3}$$

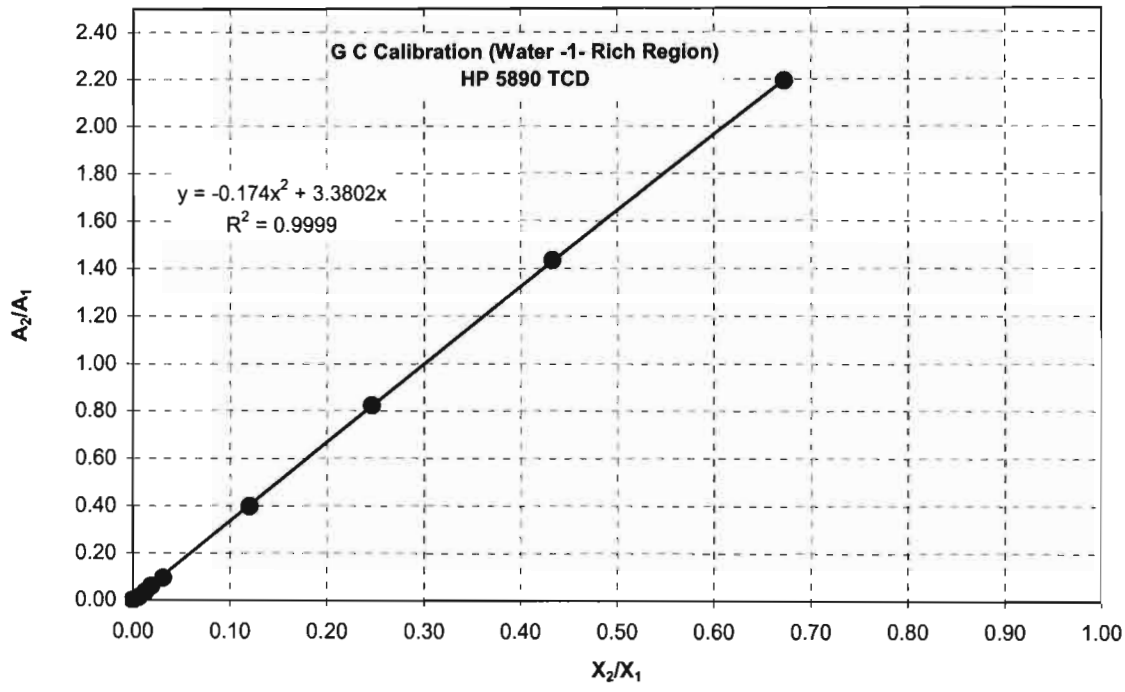

Figure 5 - 3: G C Calibration Curve for the Water (1) + MBE (2) system (MBE dilute region)

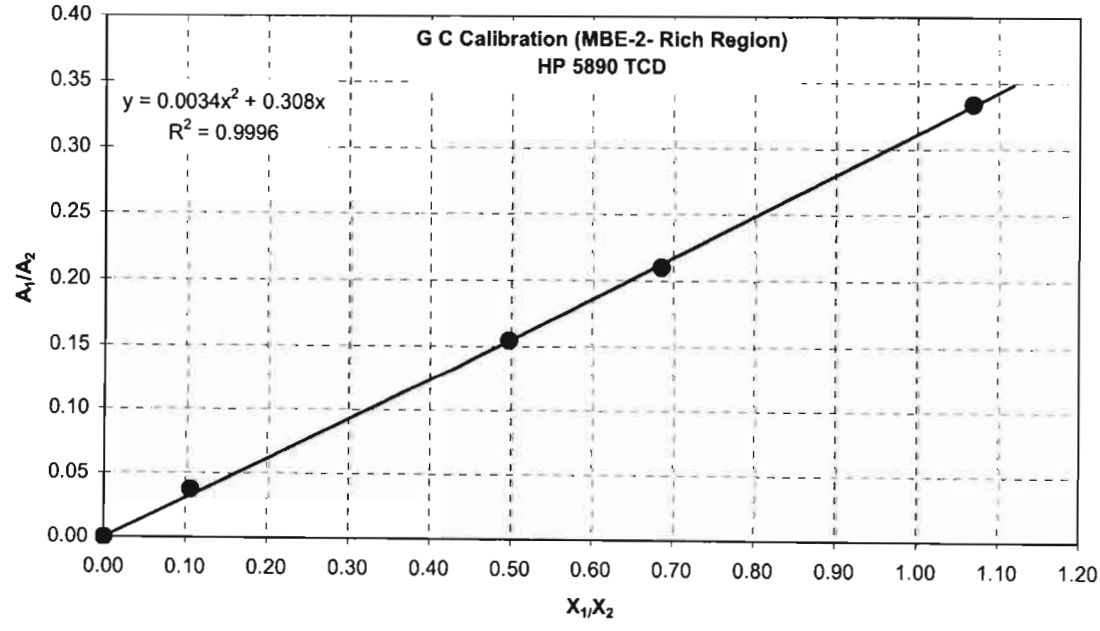

Figure 5 - 4: G C Calibration Curve for the Water (1) + MBE (2) system (MBE rich region)

In a multicomponent mixture the response factors are determined for the constituent binaries and the generalized form of the above result is used:

$$x_1 = \frac{1}{1+\sum_{2}^{n}\left(\frac{x_i}{x_1}\right)} \tag{5-4}$$

Table 5.1 shows the operating conditions of the GC that were used for the test systems measurements.

Operating Condition	System	
	Cyclohexane + Ethanol	**Water + MBE**
Gas Flowrate (ml/min)	30	30
Oven Temperature Profile		
Initial Temperature(°C)	160	160
Hold Time (min)	-	-
Temperature Ramp (°C/min)	-	-
Final Temperature (°C)	-	-
Hold Time (min)	-	-
Deterctor Profile		
Deterctor Type	**TCD**	**TCD**
Temperature (°C)	180	180
Attenuation	1	1
Range	-	-
Injector Profile		
Temperature	180	180

Table 5 - 1 Operating Conditions of the Hewlett-Packard 5890 Series II Gas Chromatograph.

5.1.3 Operating procedures

5.1.3.1 Isobaric procedure

The isobaric measurements began with the switching on of the power supplies to the stirrer motors, temperature and pressure displays, pressure controller and the vacuum pump. 10 ml Plastic syringes were then used to add into the clean still one or the other of the pure components for which the measurements were to be conducted. The addition of the pure component was continued until both the liquid and vapour condensate receivers were full and the level in the liquid chamber had risen to such a point (about 3 centimetres above the boiling chamber) that

material would be forced up the Cottrell pump once boiling began. Allowance was also made for the increase in the liquid volume which occurs as a result of expansion when heating begins. The pressure controller was then set to the required operating pressure, at which point, the pressure in the still dropped to the set value.

The next stage was heating, which began by turning on the power supply to all the heaters (both internal and external heaters), heater cartridges on the sampling valve block together with the electrical wires wound around the vapour sampling lines and the equilibrium chamber. When boiling in the still commenced, the power to the internal heater was then adjusted until the plateau region was attained (Kneisl et al. [1989]). The plateau region is the stage where the boiling temperature does not change with small changes in the power input, a point at which the superheating of the liquid which occurs as a result of the hydrostatic head acting on the fluid in the Cottrell pump offsets the subsequent cooling due to evaporation in the equilibrium chamber (Kneisl et al. [1989]). The temperature at this stage is the equilibrium temperature, but before any measurements were taken, the temperature controller regulating the heat to the outside wall of the equilibrium chamber was set to a temperature 5 degrees Celsius above the equilibrium temperature. This was also the case with the temperatures of the sampling valves and the superheated vapour lines taking the vapour sample to the GC which were adjusted manually by carefully varying the voltage to the heater cartridges and electrical wires. It should be remembered that this superheating was done so as to prevent any vapour condensation which would necessarily alter the composition (see Section 4.1.4 of Chapter 4). The whole heating exercise took approximately 1 ½ hours before thermal equilibrium was attained.

Once the system had reached equilibrium (after approximately 45 to 50 minutes), which was judged by constancy of temperature, pressure and composition, the temperature was recorded and samples were withdrawn for analysis. Liquid samples were withdrawn using syringes and placed in stoppered sampling bottles before analysis. Three injections to the GC were conducted for each sample and the average area was used in the subsequent calculations for the compositions. Vapour samples were taken prior to condensation using the sampling system designed for systems of partial liquid miscibility described in great detail in chapter 4 (see section 4.1.4). Again three samples were sent to the GC and the average was used in the computations.

The second component was then added to the still in a small enough quantity to alter the composition, after which the system was again brought to equilibrium and the liquid and vapour samples withdrawn and analysed. This process was repeated until the half way point in the equilibrium curve was reached, at which point the still was stopped, cleaned, and filled this time

with the second component. The whole process then began again with the first component now being added to alter the composition until the entire range of compositions had been covered.
This measuring process had two important advantages. The first is that it provides a test of the measuring method in that the two halves of the equilibrium curves must coincide if the measurements are to be accepted as accurate. The second is that it allows a number of points to be measured in the dilute regions of both components. These are the important areas in any VLE curve as it is usually where the greatest deviation from ideality is seen.

5.1.3.2 Isothermal procedure

The measurements at constant temperature depended on the successful operation of the apparatus at constant pressure. Thus, the following procedure assumes that the isobaric measurements are carried out first and the apparatus can be operated as described above.
In order to get isothermal measurements, the pressure in the still was set to a value such that when equilibrium was reached, the equilibrium temperature was close to the required operating temperature. The isobaric operation was then stopped and the temperature adjusted manually to its desired value. This was done manually by carefully increasing or lowering the pressure which had the effect of raising or decreasing the temperature. (see Section 4.1.2).

5.2 The liquid-liquid equilibrium apparatus.

5.2.1 Preparation

5.2.1.1 Cleaning

The cleaning of the LLE cell was simple and straightforward. Unlike in the VLE still, the LLE cell could be easily dismantled and reset up in a few minutes. Thus when cleaning was desired, for example before data for a new system was measured, the cell was dismantled and all the pieces taken to a sink where they were cleaned. Acetone was used as the cleaning liquid and was later allowed to evaporate from the clean still in a fume hood.

5.2.2 Calibration

5.2.2.1 Cell temperature calibration

A standard temperature probe was used to calibrate the cell temperature sensor (see Section 4.2.2). The cell was set up as described in Chapter 4 and water was allowed to circulate around the cell through the cell jacket. The cell was filled with water and the standard probe was placed in the cell to give the water temperature. The whole setup up was left to attain thermal equilibrium after which the two temperatures, one given by the standard probe and the other by the temperature sensor in the thermo well on the LLE cell, were recorded. The circulating water temperature was then raised and the whole process repeated until a set of temperatures over the anticipated range for the measurements was obtained. The standard temperatures were then plotted against the cell temperatures to give a relationship which was then used to compute the actual temperatures from the measured cell temperatures.

5.2.2.2 Bath temperature sensor calibration

The water bath temperature sensor was calibrated following the same procedure outlined for the cell temperature sensor using a standard probe.

5.2.2.3Gas chromatograph calibration

The same HP 5890 Series II gas chromatograph discussed in Section 5.1.2.3 above was used for the LLE measurements, thus it was not necessary to calibrate the GC again. The same calibration curves obtained for the VLE apparatus were used for the LLE measurements.

5.2.3 Operating procedure for LLE measurements

The LLE measurements began by adding both components into the clean cell in such a way that immiscible liquids were formed. The pure components were added into the cell to such a level that the interface between the two liquid phases was above the sampling point of the denser liquid (see Figure 4-11). The temperature on the controller was then set to the lowest value for which measurements were to be determined after which the pump and stirrer were switched on. Mixing was allowed for about twenty minutes after which it was stopped and the two liquids allowed to settle and to separate. Samples of one or the other phase were then taken using gas tight syringes and injected to the GC. The compositions were calculated and once the composition remained constant equilibrium was judged completed and the temperature was then recorded. The other phase was then sampled and analysed. Approximately 30 to 50 minutes were required to reach equilibrium with the actual time taken depending on the system studied.

The water bath temperature was afterwards raised and the whole process repeated. This was done for a number of temperatures over the interval of interest. For each run due care was take to ensure that the mixing speed was slow enough to avoid emulsification.

At the end of the measurements, the pump, the controller and the still are switched off and the cell contents allowed to cool after which the whole apparatus was dismantled and cleaned.

6

Chapter Six

Test Systems: Results and Analysis

The experimental procedure presented in Chapter 5 was derived after numerous runs were carried out on two test systems. These test systems, already highlighted in the previous chapters were the cyclohexane (1) + ethanol (2) system at 40 kPa and the water (1) + 2-methyl 3-buten-2-ol (2) (MBE) system at 97.2 kPa. The first system is completely miscible over the entire composition range and the second forms partially miscible liquids and is thus heterogeneous. The main criteria used in choosing these systems were that they should be non-ideal and that consistent literature data on the systems be available. Both systems satisfied these criteria. The chemicals were also available at sufficiently high purity at reasonable cost and were also stable – which are other properties desired in test chemicals.

Equilibrium data were measured for the two test systems mentioned above and the results obtained were rated by thermodynamic consistency tests and compared to literature data. Any discrepancies necessitated changes in the measuring procedures until the results agreed with the literature data. This chapter presents the results for the test systems. It also gives an analysis of the measured data. The discussion of the results is presented in Chapter 8 together with that for the previously unmeasured systems. The material presented here is on chemical purity, vapour pressures, vapour-liquid equilibria, vapour-liquid-liquid equilibria and thermodynamic consistency testing.

6.1 Chemical purity

All the chemicals used in the test systems were liquids at room temperature and pressure. They were all purchased from Merck (except water which was not purchased but distilled in our laboratory). GC Analysis, following the method of Raal and Muhlbauer [1998] and assuming constant F ratios, and refractive index measurements were used to verify the purity of the chemicals. The GC analyses gave no significant impurities and the chemicals were thus used without further purification. Table 6-1 gives the nominal purities of the test chemicals together with literature values of the refractive indices. The methanol, also shown in Table 6-1, was used in making heterogeneous MBE +water mixtures homogeneous in GC calibration (See Chapter 5).

Table 6 - 1: Chemical purities and Refractive indices

Reagent	Refractive Index		G C Analysis (Mass %)	Min Purity specified by supplier (Mass %)
	Experimental	Literature*		
Ethanol	1.3612	1.3611	99.8	99.5
Cyclohexane	1.4267	1.4266	99.8	99.5
MBE	1.4159	1.4163	99.5	98
Methanol	1.329	1.339	99.8	99.5

6.2 Vapour pressures.

The vapour pressures were the first to be measured for all the test chemicals. These are presented in Tables 6-2 to 6-3 and plotted in Figures 6-1 to 6-3. Also shown in Figures 6-1 to 6-3 are the literature values to which the vapour pressure data are compared.

* obtained from Weast et al [1983 -1984]

Table 6 - 2: Vapour pressure data for Ethanol

Measured P kPa	T K	ΔP_{Wagner} kPa	ΔP_{Ant} kPa
99.12	350.59	0.0884	0.0698
89.18	348.00	0.0802	0.0419
69.30	341.95	0.0605	0.0733
59.34	338.35	0.0112	0.0848
49.40	334.22	0.0309	0.0169
39.46	329.29	0.0602	0.0189
29.53	323.20	0.0815	0.1262
24.83	319.47	0.0321	0.0765
Average Deviations		0.0556	0.0635

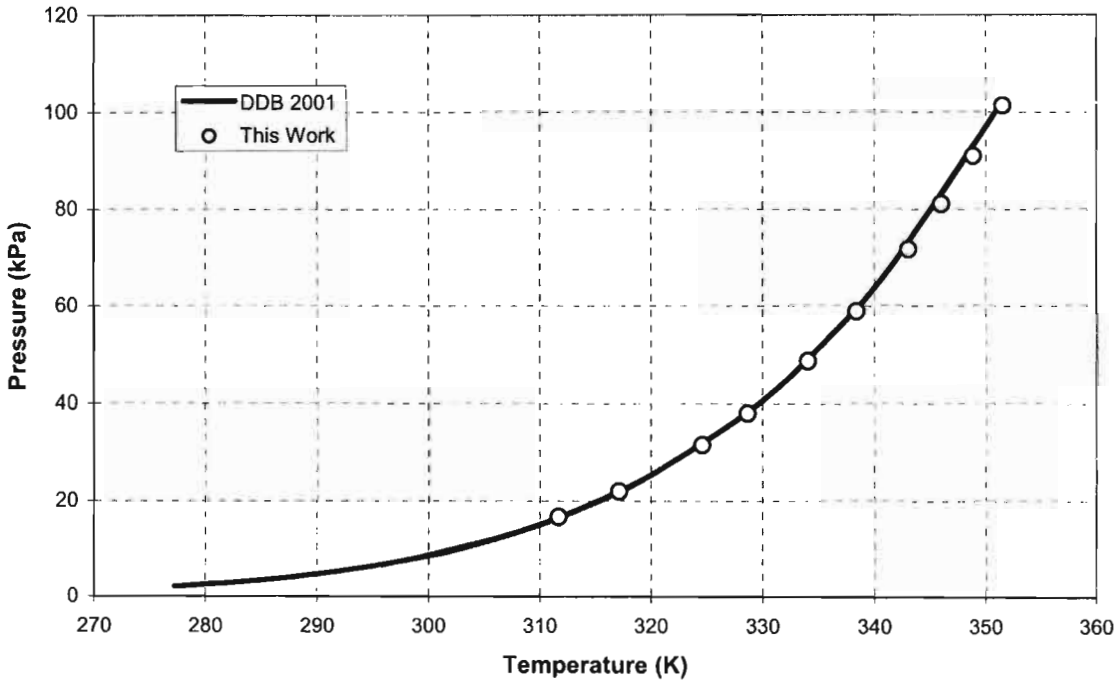

Figure 6 - 1: Vapour pressure data of Ethanol together with literature data

Table 6 - 3: Vapour pressure data for Cyclohexane

Measured P kPa	T K	ΔP_{Wagner} kPa	ΔP_{Ant} kPa
100.24	353.09	0.1602	0.0444
89.77	349.6	0.0667	0.1213
79.37	345.73	0.0683	0.0253
69.29	341.58	0.0794	0.0100
59.35	336.96	0.0149	0.0793
49.41	331.68	0.0249	0.0909
39.46	325.48	0.0296	0.0468
29.54	317.84	0.0536	0.0200
19.59	307.78	0.0404	0.0950
9.67	291.74	0.0038	0.0171
Average Deviations		0.0542	0.0550

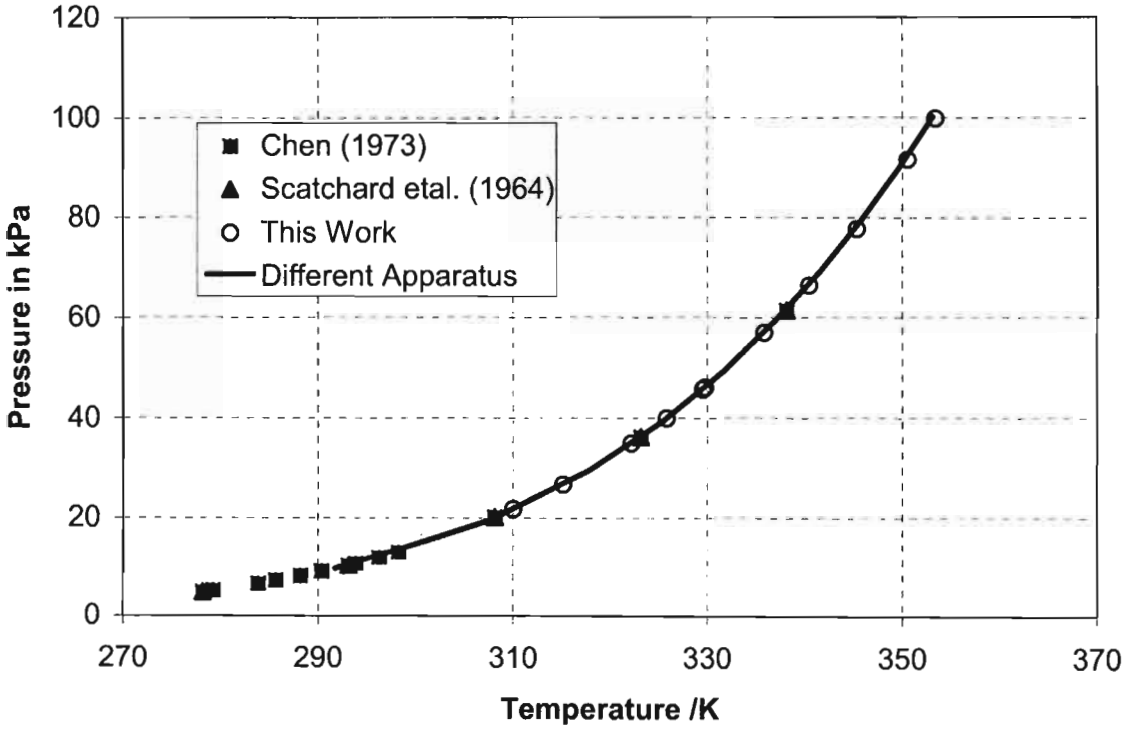

Figure 6 - 2: Vapour pressure data for Cyclohexane together with literature data

Table 6 - 4: Vapour pressure data for MBE

Measured P kPa	T K	ΔP_{Wagner} Kpa	ΔP_{Ant} Kpa
101.44	370.45	0.2020	0.0042
91.02	367.39	0.0030	0.0777
79.15	363.55	0.0426	0.0467
67.35	359.41	0.2474	0.1351
61.40	356.94	0.0710	0.1994
47.24	350.53	0.1287	0.0214
35.10	343.53	0.1344	0.1489
24.11	335.15	0.0961	0.0316
16.10	327.17	0.1044	0.1666
95.33	368.68	0.0233	0.0541
Average Deviations		0.1053	0.0866

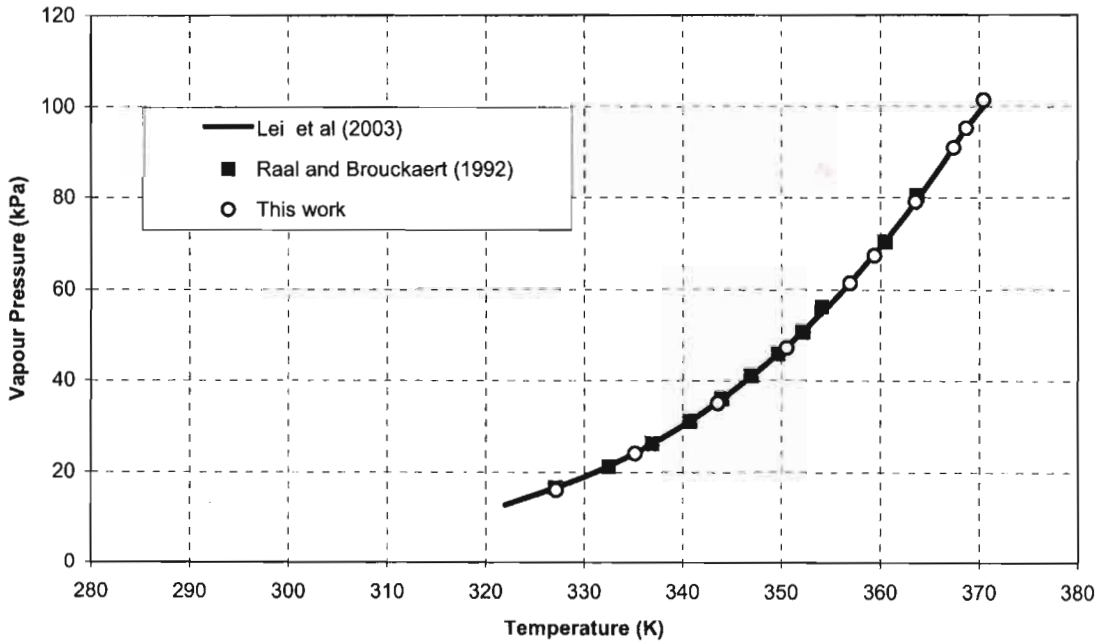

Figure 6 - 3: Vapour pressure of MBE together with literature data

6.2.1 Analysis of vapour pressure data.

The measured vapour pressure data were regressed to obtain parameters for both the Antoine and Wagner (Reid et al. [1988]) equations. The Antoine and Wagner equations are respectively:

$$\log P = A + \frac{B}{T + C} \tag{6-1}$$

and

$$\ln \frac{P}{P_C} = (1 - x)^{-1} \left[Ax + Bx^{1.5} + Cx^3 + Dx^6 \right] \tag{6-2}$$

where

$$x = 1 - \frac{T}{T_C} \tag{6-3}$$

and A, B, C and D are parameters to be determined. The pressure is measured in kPa and the temperature in Kelvin. The regression was carried out in Matlab following the procedure outlined in Section 3.9. The pressure residuals, δP, i.e. the differences between the experimentally measured pressures and the calculated pressures were minimised in the regression. The programs named Antoine and Wagner in Appendix 3 were used for these calculations. (NB. Sample programs used in this work are presented in Appendix 3).

In addition to the experimentally measured vapour pressures, Tables 6-1 to 6-3 give the absolute values of the residuals between the experimental vapour pressures and those predicted from the Antoine and Wagner equations while Tables 6-5 and 6-6 give the parameters in the two equations for all the test chemicals for which the vapour pressure was measured. The average absolute deviations are also presented in Tables 6-5 and 6-6.

Table 6 - 5: The Antoine coefficients for the test systems' chemicals

Reagent	A	B	C	$\frac{1}{n}\sum\lvert\Delta P\rvert$
Ethanol	8.0838	-2102.3685	-5.2224	0.0635
Cyclohexane	6.615	-1581.9568	-9.9317	0.0550
MBE	5.8901	-986.3742	-116.4853	0.0866

Table 6 - 6: The Wagner vapour pressure equation coefficients for the test systems chemicals

Reagent	A	B	C	D	$\frac{1}{n}\sum\lvert\Delta P\rvert$
Ethanol	-31.224	58.3258	-116.1812	377.6688	0.0556
Cyclohexane	-9.9307	8.8136	-15.7567	29.888	0.0542
MBE	21.1549	-62.8018	79.7687	-131.3177	0.1053

6.3 Vapour-liquid equilibria (Cyclohexane (1) + Ethanol (2) system at 40 kPa)

The first aspect in the measurement of VLE data for any system is GC calibration (provided that gas chromatography is the chosen method of composition analysis). The procedure followed has already been discussed (see Section 5.1.2.3). This system was completely miscible for the entire composition range and thus presented no difficulties in the calibration process. Figures 6-4 and 6-5 below show the GC calibration curves.

The VLE data measured are shown in Table 6-7 and Figures 6-6 and 6-7 give T-x-y and x-y plots respectively. Also shown in Figures 6-6 and 6-7 are the literature data of Joseph et al. [2001] to which the data measured in this work were compared.

For this system the vapour phase was sampled using two different methods. The first was using a gas tight GC syringe and the second was using the new sampling mechanism designed for

systems of partial liquid miscibility (see Chapter 4), thus in the second case, the vapour phase was sampled before condensation and the sample sent directly to the GC. The composition obtained was then compared to that of the sample sent manually. This served the purpose of ascertaining if the sampling mechanism would give the desired results. The compositions obtained for the two sampling procedures are also shown in Table 6-7.

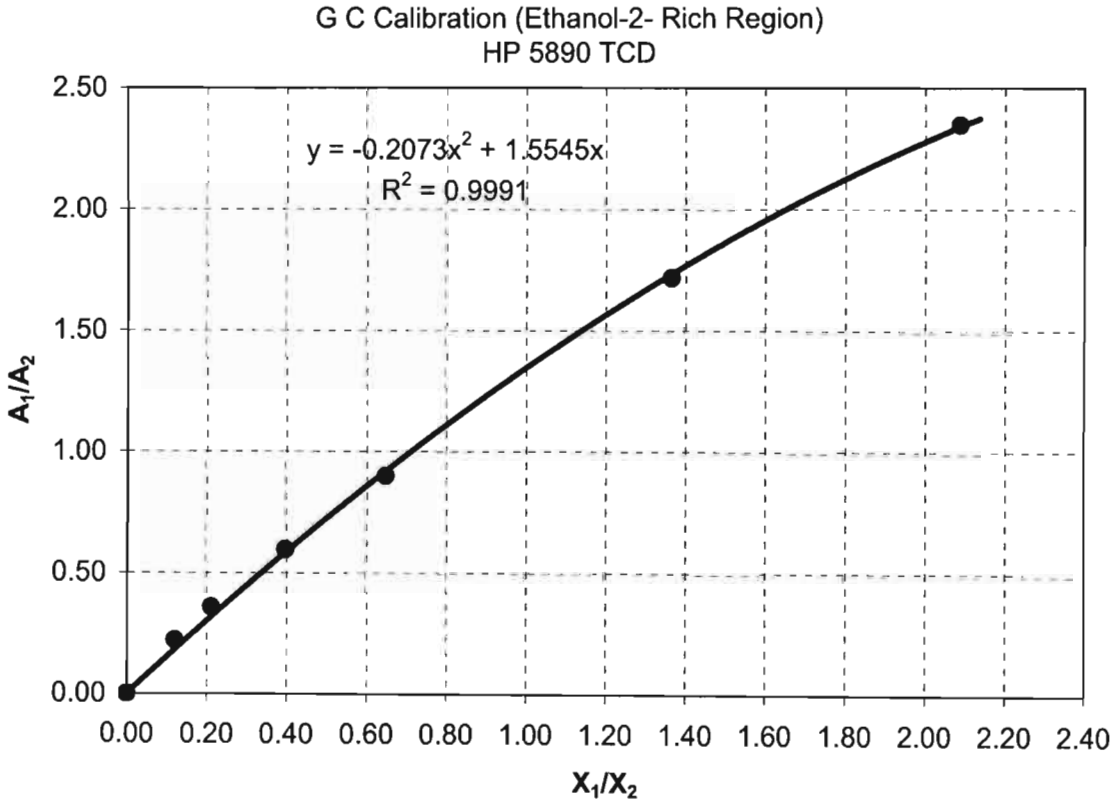

Figure 6 - 4: GC Calibration curve for the Cyclohexane (1) + Ethanol (2) system (Dilute Cyclohexane region)

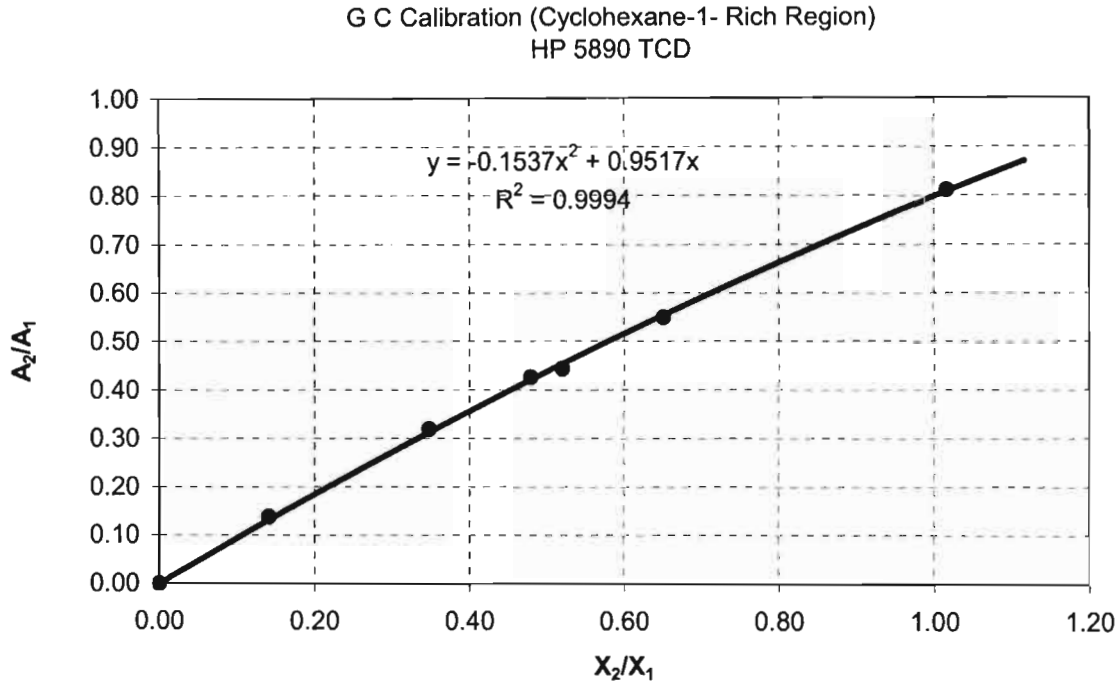

Figure 6 - 5: GC Calibration curve for the Cyclohexane (1) + Ethanol (2) system (Rich Cyclohexane region)

Table 6 - 7: VLE data for the Cyclohexane (1) + Ethanol (2) system at 40Kpa

T °C	x_1	y_1 Manual	y_1 Auto
52.87	1.0000	1.0000	1.0000
47.15	-	0.8314	0.8342
46.46	-	0.8087	0.8087
46.16	-	0.7939	0.7997
49.22	0.9987	0.8847	0.8855
43.80	0.9756	0.7160	0.7162
42.91	0.9511	0.6987	0.6903
41.82	0.8870	0.6584	0.6550
43.50	0.1934	0.5201	0.5210
44.09	0.1617	0.5007	0.5000
44.29	0.1511	0.4812	0.5031
45.77	0.1133	0.4398	0.4514
47.64	0.0840	0.3753	0.3772
48.53	0.0671	0.3483	0.3447
49.12	0.0574	0.3160	0.3147
56.61	0.0000	0.0000	0.0000

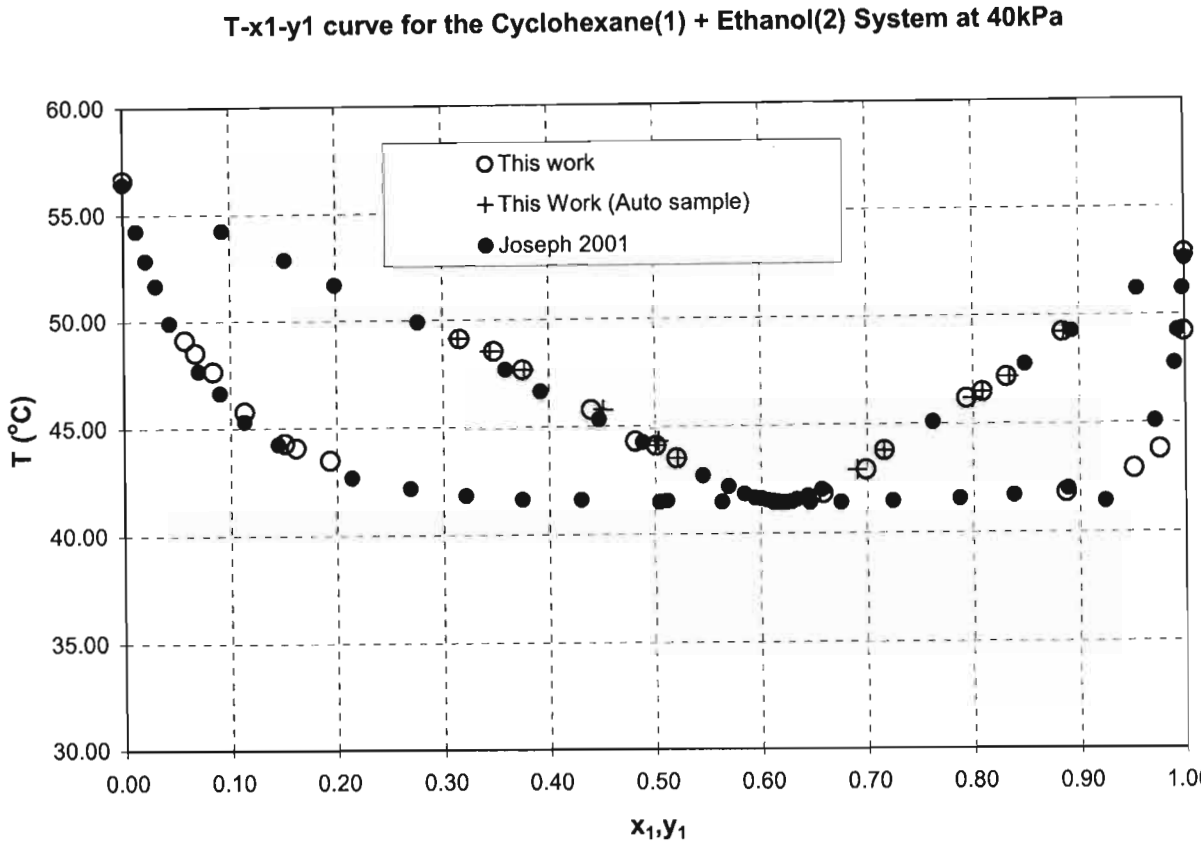

Figure 6 - 6:T-x-y curve for the Cyclohexane (1) + Ethanol (2) system at 40 kPa With Literature Data

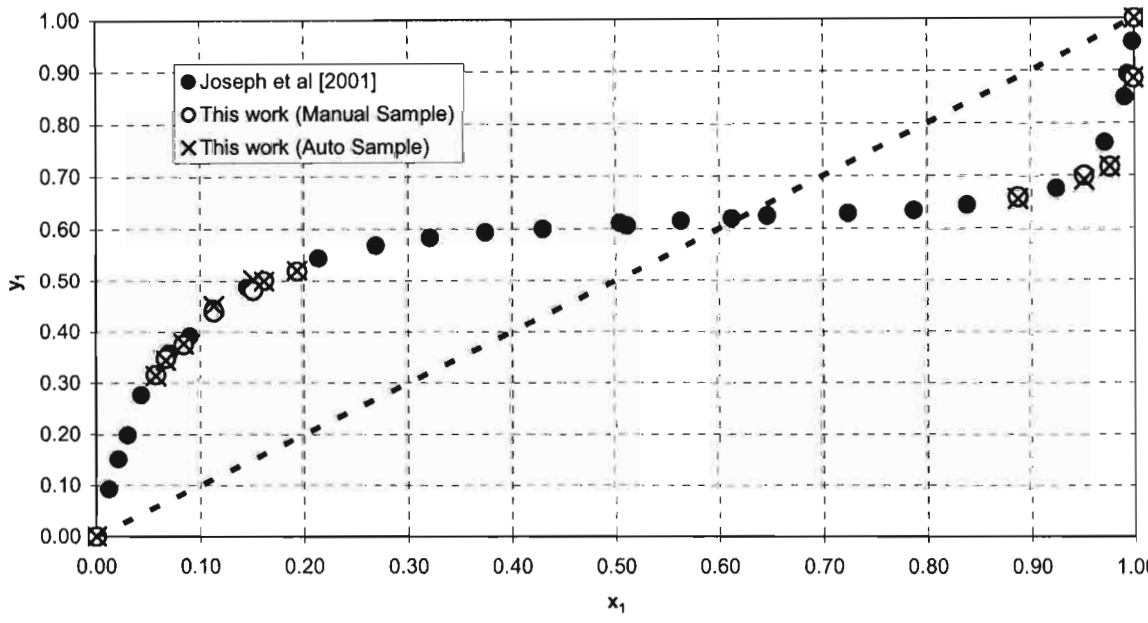

Figure 6 - 7: x-y curve for the Cyclohexane (1) + Ethanol (2) system at 40 kPa With Literature Data

6.3.2 VLE analysis

The isobaric VLE data for the system; cyclohexane (1) + ethanol (2), were regressed to obtain parameters for the NRTL, and modified Wilson (T-K Wilson) models following the procedure presented in great detail in Chapter 3 (see Section 3.9). However, before any computations were carried out, the pure component critical parameters had to be determined. (NB – only the Combined Method will be used in the analysis in this chapter. This analysis served the purpose of validating the experimental methods used in the project and thus there was no need to go into detailed analysis – However, for the previously unmeasured systems discussed in the next chapter both methods will be used including an additional activity coefficient model; the UNIQUAC model).

6.3.2.1 Pure-component properties.

Table 6-8 gives the pure component critical parameters for both ethanol and cyclohexane. These were obtained from either the Korean Data Bank of Thermo physical Properties (KDB) or the Dortmund Data Bank (DDB).

Table 6 - 8: Pure-component critical parameters for Ethanol and Cyclohexane.

	V_c	Z_c	T_c	ω	P_c
	cm^3/mol		K		kPa
Ethanol	308.00	0.27	553.80	0.21	4080.00
Cyclohexane	168.00	0.24	514.00	0.64	6137.00
Mixture	230.98	0.26	533.53	0.43	4936.84

Also presented in Table 6-8 are mixture parameters. These cross parameters were calculated using the mixing rules proposed by Prausnitz [1986] as outlined in Section 3.4.2.1.

Experimental activity coefficients

Activity coefficients were calculated from the measured T-x-y data by re-arranging Equation (3-48) :

$$y_i \Phi_i P = x_i \gamma_i P_i^{sat} \tag{3-48}$$

to give:

$$\gamma_i = \frac{y_i \Phi_i P}{x_i P_i^{sat}} \tag{6-4}$$

In the above equation, the only unknowns are the vapour phase correction factors, Φi , and the saturated vapour pressures, P_i^{sat}. The Φ_i's were calculated from the Virial equation using Equation (3-50) with the Virial coefficients being evaluated at the measured temperatures from the Pitzer and Curl [1957] correlation. Liquid molar volumes were estimated from the Rackett [1970] equation (Equation 3-22) also at the experimental temperatures. P_i^{sat} values were computed from the Antoine equations. For ease of calculation, programs were written in Matlab for calculating Virial coefficients and molar volumes at any temperature. All the user does is to enter the required temperature and the program then computes the desired values. These programs (known as functions in Matlab) are presented in Appendix 3 and are named MolarV and Virial for the molar volumes and virial coefficients respectively. Table 6-9 shows the calculated experimental activity coefficients.

Table 6 - 9: Experimental activity coefficients for the system Cyclohexane (1) + Ethanol (2) at 40 kPa.

P = 40 kPa		
x_1	γ_1	γ_2
0.9987	0.9922	123.9671
0.9756	1.0096	21.2020
0.9511	1.0460	11.7332
0.8870	1.1027	6.0802
0.1934	3.7416	1.1000
0.1617	4.2110	1.0693
0.1511	4.2975	1.0864
0.1133	4.9491	1.0440
0.0840	5.3062	1.0286
0.0671	5.9617	1.0092
0.0574	6.1846	1.0190

6.3.2.2 VLE data reduction (The Gamma-Phi [γ - ϕ] method)

The parameters in the NRTL and T-K Wilson equations were obtained by minimizing the sum of the squared differences between the experimental and calculated temperatures, δT:

$$\delta T = \sum_{All i} \left(T_i^{Exp} - T_i^{cal} \right)^2 \tag{6-5}$$

At each stage of the iteration, the variation of the activity coefficients with temperature was taken into account. This process was simple when one takes into consideration that programs had already been written for the evaluation of the virial coeffcicients and liquid molar volumes at any temperature. The only task at hand was thus to incorporate the above Matlab functions as subprograms in the iteration programs. The program that was used for the NRTL equation is also appended in Appendix 3 and is named Isobaricnrtl. Table 6-10 gives the model parameters and values of the absolute average deviations in temperature and vapour composition for the two models.

Table 6 - 10: Model Parameters (evaluated from average Experimental Temperatures) and Absolute Deviations from Experimental T-x-y data for the Cyclohexane (1) + Ethanol (2) system at 40 kPa.

Quantity	NRTL	T-K Wilson
$\lambda_{12} - \lambda_{11}$ (J/mol)	2255.2895	444.811
$\lambda_{12} - \lambda_{22}$ (J/mol)	1679.0456	9510.3083
α	-1.2435	-
ΔT (K)	0.2435	0.2444
Δy	0.013	0.0085

Figures 6-8 and 6-9 below summarise these results and compares the experimental temperature and vapour compositions to values predicted from the model parameters.

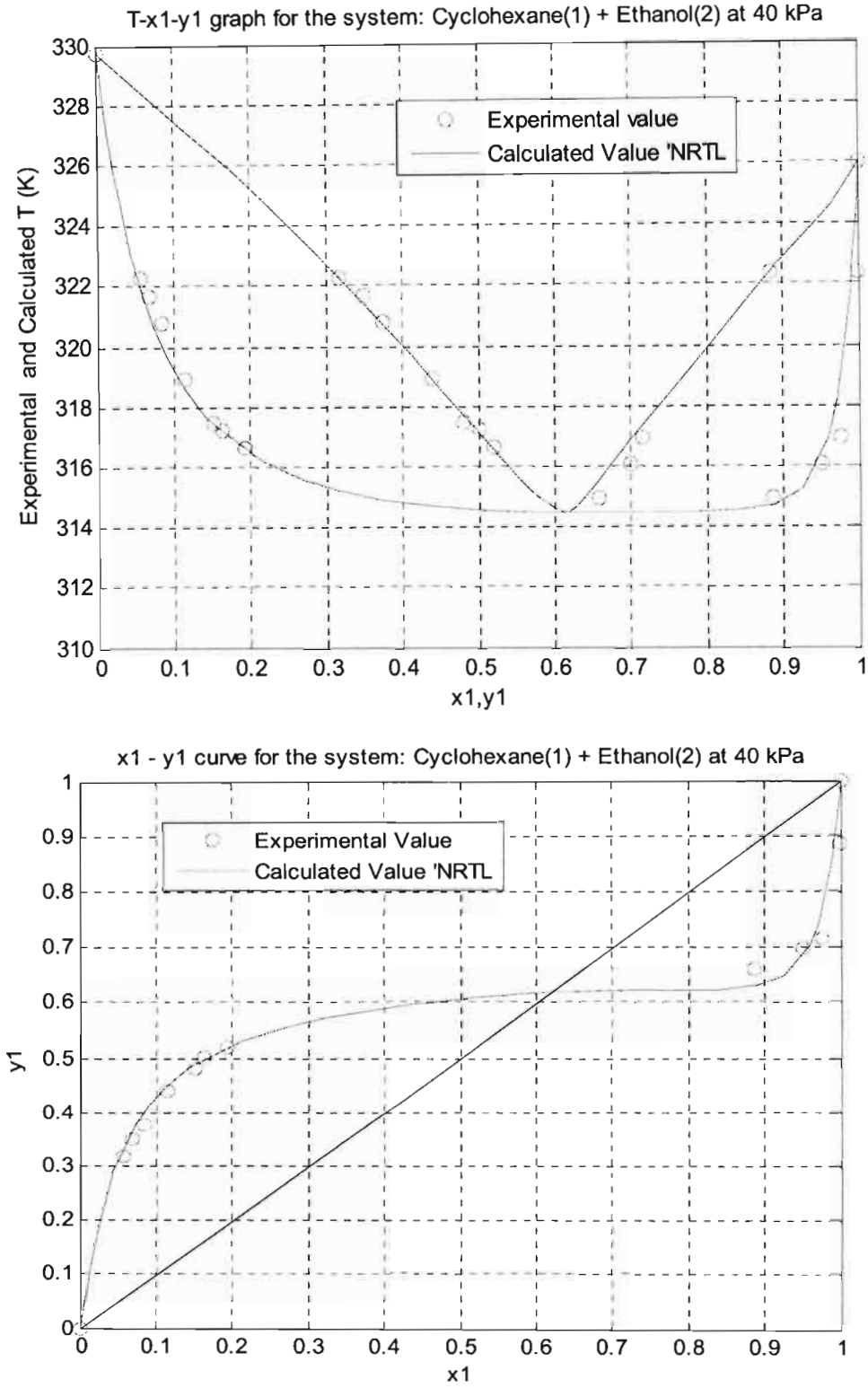

Figure 6 - 8: NRTL model fitted to Experimental T-x-y data for the Cyclohexane (1) + Ethanol (2) System at 40 kPa

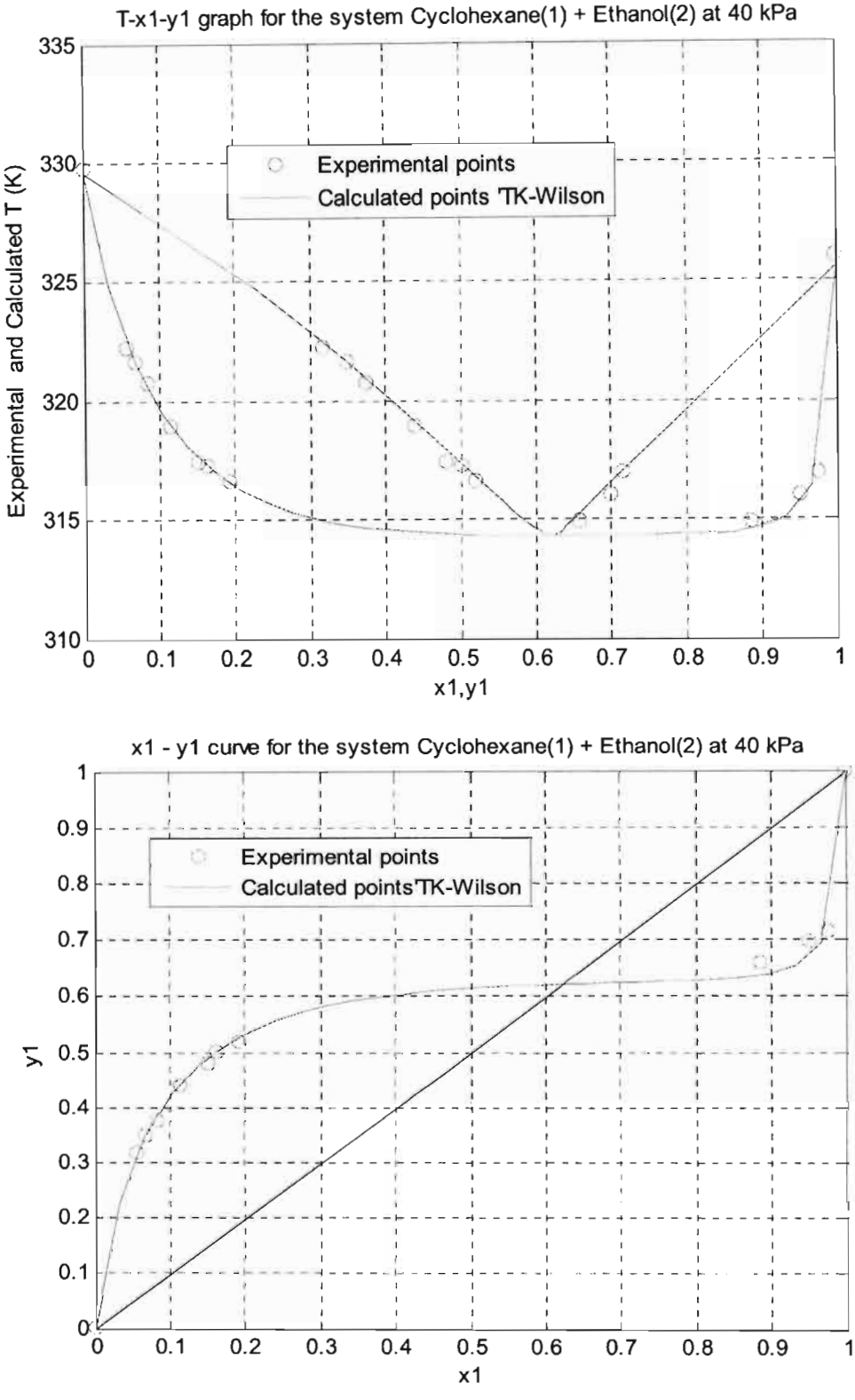

Figure 6 - 9: TK-Wilson model fitted to T-x-y data for the Cyclohexane(1) + Ethanol (2) System at 40 kPa

6.3.2.3 Thermodynamic consistency testing

The VLE data for the cyclohexane (1) + ethanol (2) system was tested using the Point Test of Van Ness et al. [1973] and the Area test of Herington [1951]. For the previously unmeasured systems presented in the next chapter, the Direct Test of Van Ness [1995] is also used in addition to these two tests.

The Point Test of Van Ness et al. [1973]

The application of this test was discussed in detail in Chapter 3 (see Section 3.12). In this case, we have isobaric data, and thus temperature differences between experimental and calculated values were minimized and Δy residuals were computed and examined. For consistent data, the residuals should scatter about the zero axis and the absolute average deviation should be less than 0.01 (Fredenslund et al. [1975]).

Figure 6-10 shows the deviations in the T and y values computed from the NRTL equation and Table 6-11 gives the absolute average deviations in y.

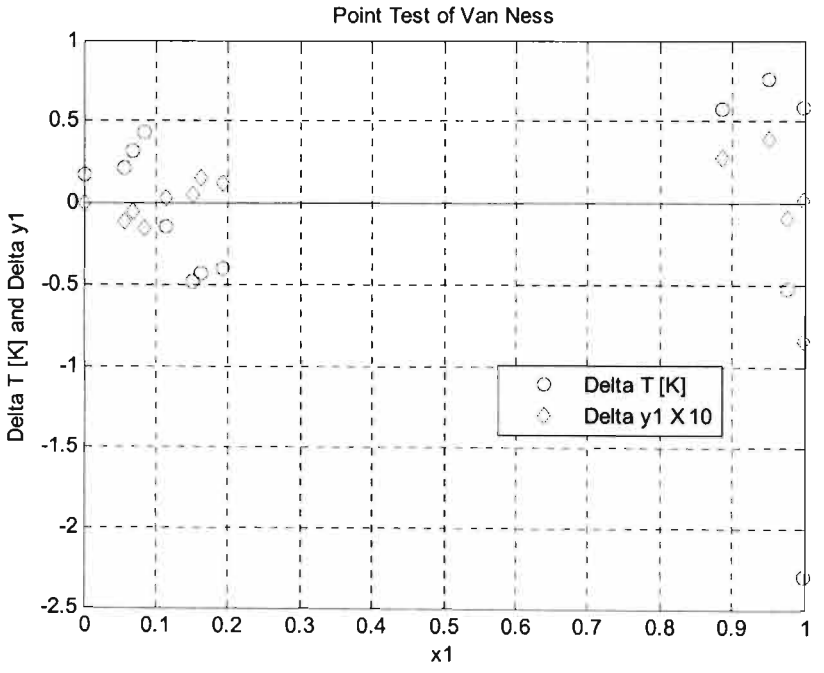

Figure 6 - 10: Δy and ΔT residuals from the reduction of T-x-y data for the Cyclohexane (1) + Ethanol (2) system at 40 kPa using the NRTL equation.

Table 6 - 11: Absolute deviations in vapour compositions from the reduction of T-x-y data for the Cylohexane (1) + Ethanol (2) system at 40 kPa using the NRTL Equation.

Experimental y_1	Calculated y_1	Δy_1 (Absolute)
0.8847	0.9683	0.0836
0.7160	0.7250	0.0090
0.6987	0.6590	0.0397
0.6584	0.6308	0.0276
0.5201	0.5075	0.0126
0.5007	0.4851	0.0156
0.4812	0.4763	0.0049
0.4398	0.4360	0.0038
0.3753	0.3900	0.0147
0.3483	0.3533	0.0050
0.3160	0.3273	0.0113

The Herington [1951] Area Test

The area test was also presented in great detail in Section 3.12 of Chapter 3. It was shown that for consistent isobaric binary data the areas corresponding to the LHS and RHS of Equation (3-145) should be the same.

$$\int_{x_1=0}^{1} \ln\frac{\gamma_1}{\gamma_2}dx_1 = -\int_{x_1=0}^{1}\frac{H^E}{RT^2}dT \tag{3-145}$$

Instead of making the invalid and unjustifiable assumption that the RHS of the above equation is zero in the absence of heat of mixing data, Herington [1951] proposed that quantities D and J given by the equations:

$$D = \frac{\left|\int_0^1 \ln\left(\frac{\gamma_1}{\gamma_2}\right)dx_1\right|}{\int_0^1\left|\ln\left(\frac{\gamma_1}{\gamma_2}\right)\right|dx_1}\times 100 = \frac{|A'-B'|}{|A'|+|B'|}\times 100 \tag{6-6}$$

and

$$J = \frac{T_{Max}-T_{Min}}{T_{Min}}\times 150 \tag{6-7}$$

where A' and B' are the positive and negative areas surrounded by the natural logarithmic values of the ratio of the liquid phase activity coefficients and the zero (x_1) axis. T_{min} and T_{max} are the lowest and highest boiling points observed in the composition range $x_1 = 0$ to $x_1 = 1$, in degrees K.

should be calculated from the experimental data and examined. He suggested the following criterion for consistency:

If (D – J) < 10, the data are consistent
If (D – J) >10 the data are inconsistent.

The foregoing test was applied to the cyclohexane (1) + ethanol (2) data by first fitting the activity coefficient data to the Redlich-Kister expansion and then integrating the resultant equation to find the areas above and below the zero axes. Table 6-12 below gives the coefficients in the Redlich and Kister expansion:

$$\ln\left(\frac{\gamma_1}{\gamma_2}\right) = a' + b'(x_2 - x_1) + c'(6x_1x_2 - 1) + d'(x_1 - x_2)(8x_1x_2 - 1) \qquad (6\text{-}8)$$

The two areas above and below the zero axis were found to be 0.52757 units^2 and 0.53775 units^2 respectively. From these values the quantities D and J were calculated with T_{min} = 314.56 K and T_{max} = 329.59 K. Figure 6-11 summarises the test results .

Table 6 - 12: Coefficients in Equation (6-8) and results of the Herington's Area Test.

System	a'	b'	c'	d'	D-J
Cyclohexane - Ethanol	-0.0089	2.0932	0.4488	0.5098	-6.21

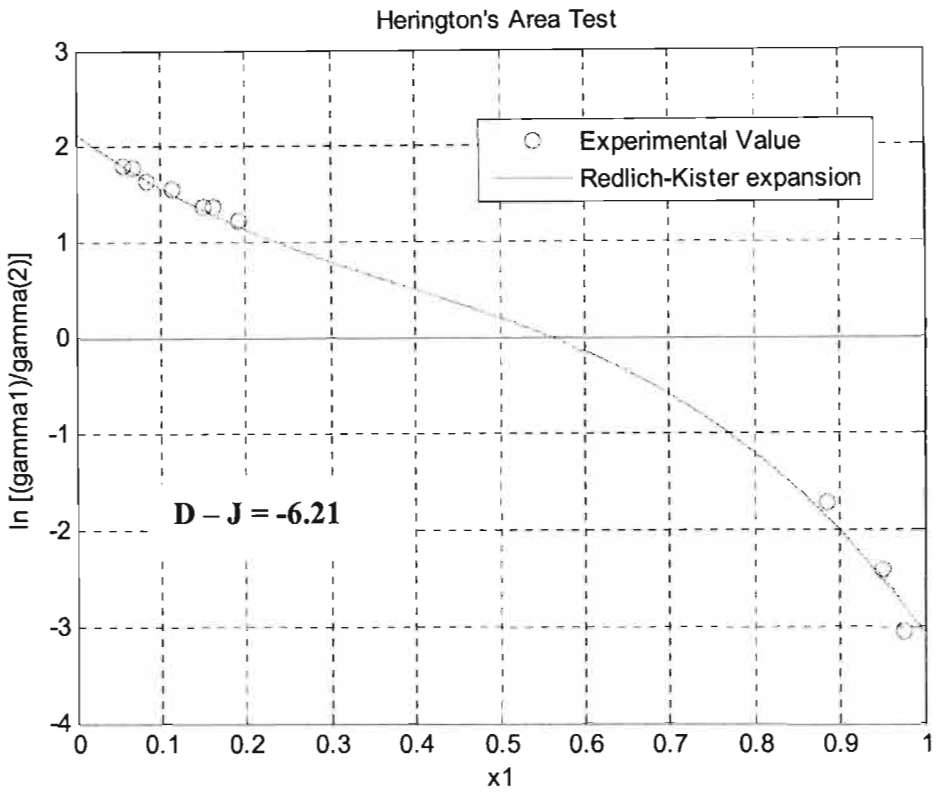

Figure 6 - 11: Herington's Area Test for the system Cyclohexane (1) + Ethanol (2) at 40 kPa

6.4: Vapour-liquid-liquid equilibria (Water (1) + MBE (2) system at 97.2 kPa)

The water-MBE system forms a heterogeneous azeotrope because of its partial miscibility in the liquid phase. It was thus fitting to measure data for this system to test the experimental apparatus as it falls into the class of systems for which this project is all about, and indeed a class for which the equipment described in Chapter 4 was designed.

The chemical purity and vapour pressure of MBE have already been presented and analysed above (see Sections 6-1 and 6-2). In this section we look at the computation of its vapour-liquid-liquid equilbria.

6.4.1 VLLE analysis

GC calibration.

As in the cyclohexane (1) + ethanol (2) system, the VLLE measurements began with the GC calibration. Mixtures of the two chemicals were gravimetrically prepared and analysed following the method of Raal and Muhlbauer [1998]. Heterogeneous water + MBE mixtures were made homogeneous by adding sufficient pure methanol to produce a single liquid phase. These samples were then injected into the HP 5890 GC to give areas for the entire composition range. The methanol peak was ignored in the analysis that followed. Figures 6-12 and 6-13 give the calibration curves for the dilute and rich MBE regions respectively.

6.4.1.1 Pure-component properties.

All the pure component parameters for water were taken from the DDB. However, for MBE, none of the data was available and had to be estimated. The critical properties were computed by using the Lydersen Group contribution method given in Reid et al [1988]. The accentric factor was computed from the vapour pressure data using Equation (3-30). Table 6-13 gives these parameters for both water and MBE.

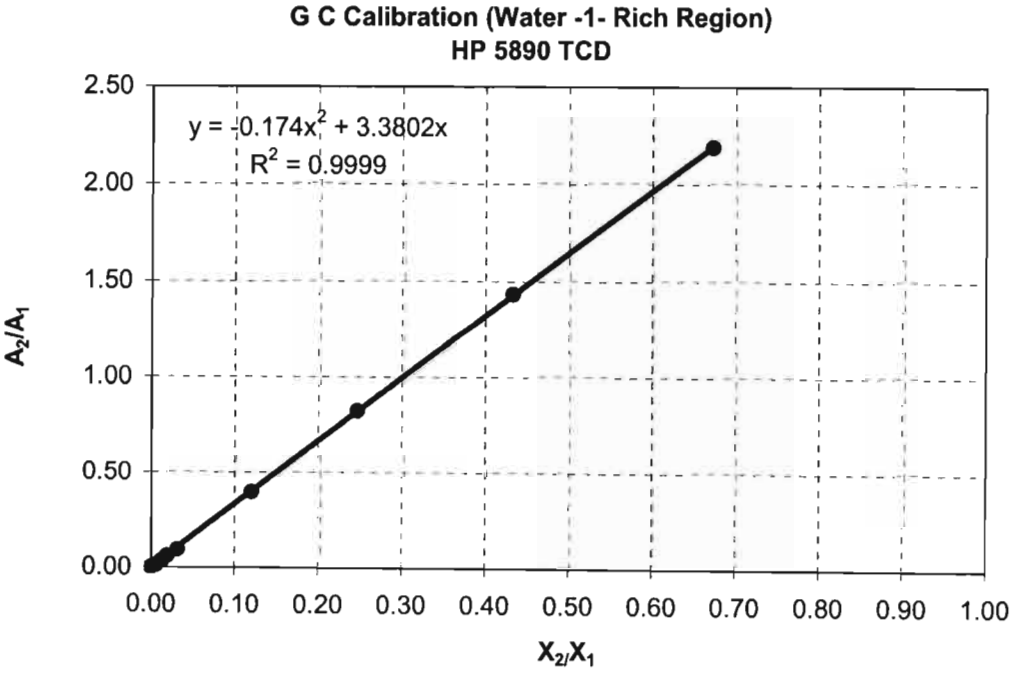

Figure 6 - 12: GC Calibration curve for the Water (1) + MBE (2) system (Dilute MBE region)

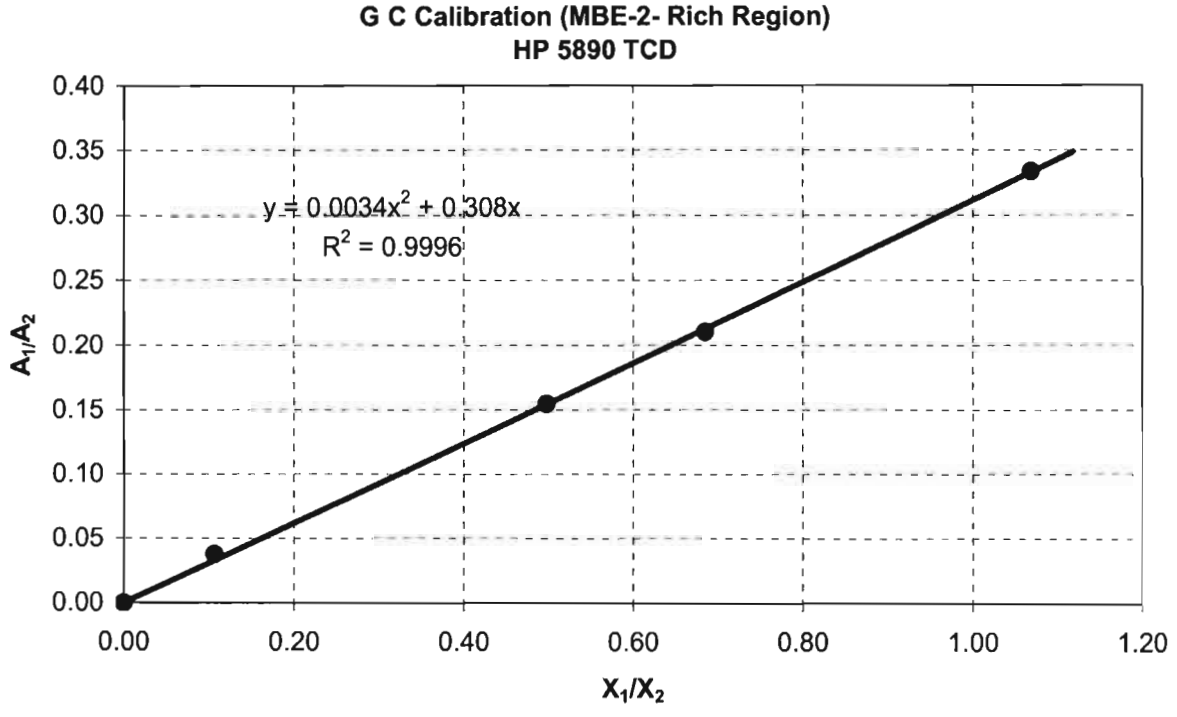

Figure 6 - 13: GC Calibration curve for the Water (1) + MBE (2) system (Rich MBE region)

Table 6 - 13: Pure component parameters for Water and MBE

	V_c cm^3/mol	Z_c	T_c K	ω	P_c kPa
Water	217.6	0.229	647.3	0.344	22055
MBE	299.0	0.282	529.6	0.3996	4148.2

VLLE data

Experimental VLE data were measured for both homogenous water and MBE regions and the results obtained are presented in Table 6-14 and Figure 6-14. In order to determine the complete VLLE data for the heterogeneous water + MBE system, the LLE of the system had to be measured. Table 6-15 and Figure 6-15 give the LLE results and in Figure 6-10 the results are compared to the literature data of Raal and Bouckaert [1992].

Table 6 - 14: Isobaric VLE and VLLE data for the Water (1) + MBE (2) system at 97.2 kPa. (asterisks, * indicate VLLE data)

T [K]	x_1	y_1	T [K]	x_1	y_1
369.17	0.0000	0.0000	357.89*	0.9616*	0.6190*
364.63	0.0886	0.2240	357.93	0.6083	0.5885
364.04	0.0992	0.2540	361.77	0.9885	0.6828
361.38	0.1838	0.3813	362.96	0.9915	0.7109
361.18	0.1917	0.3925	365.72	0.9955	0.8052
360.89	0.2104	0.4077	367.39	0.9973	0.8554
359.90	0.2930	0.4514	371.14	0.9996	0.9787
358.23	0.4306	0.5488	371.34	0.9996	0.9842
357.89*	0.5995*	0.6190*	371.63	1.0000	1.0000

The three phase temperature and vapour composition were determined by first fitting the T-y data for both homogeneous MBE and water regions to fourth order polynomials and then extrapolating the resultant equations to the point were they meet. The LLE at the boiling point was then read off or extrapolated from the measured LLE data. These three points (the three phase vapour composition and the composition of the associated two liquids in equilibrium) together with data from the homogeneous regions give a complete description of the VLLE for the system studied. The three-phase compositions are indicated by asterisks in table 6-14.

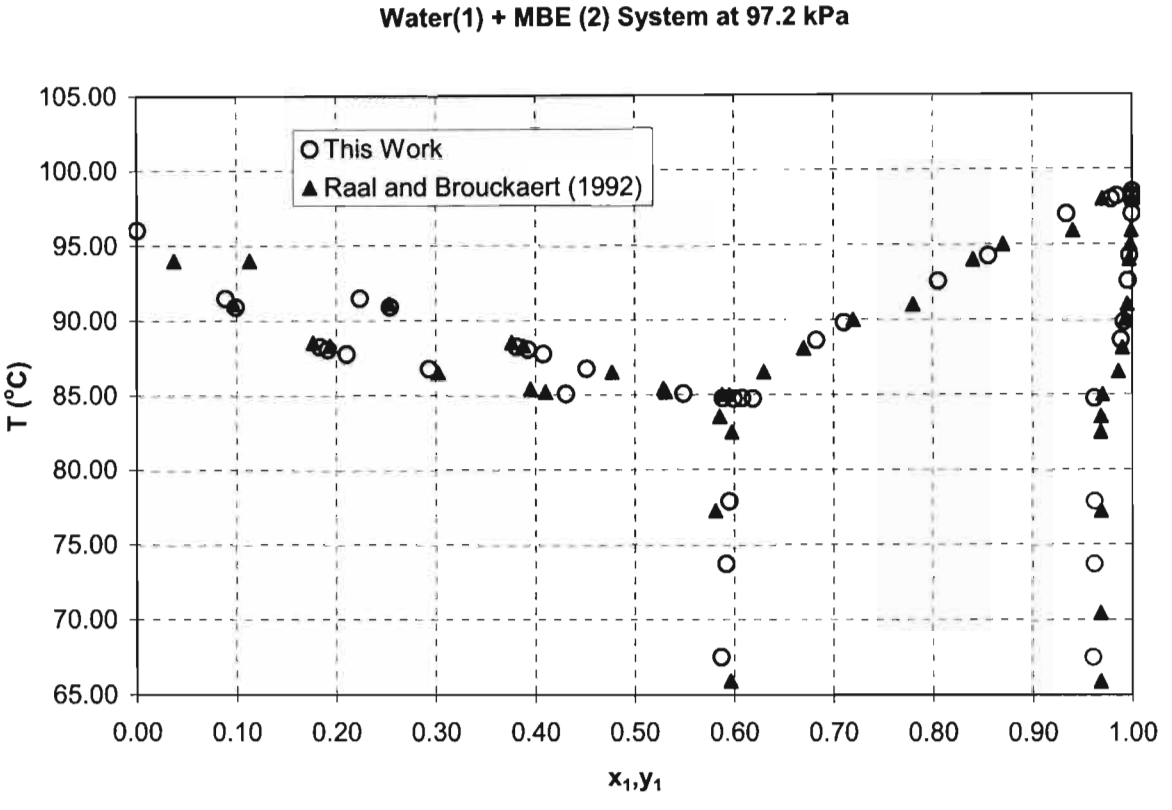

Figure 6 - 14: Isobaric VLE and VLLE data for the Water (1) + MBE (2) system at 97.2 kPa together with literature data

Table 6 - 15: LLE data for the Water (1) + MBE (2) system

T [K]	x_1^{alpha}	x_1^{beta}
301.92	-	0.946
311.87	0.624	0.952
320.94	0.596	0.955
331.18	0.590	0.960
340.65	0.587	0.960
346.85	0.592	0.961
350.99	0.595	0.962

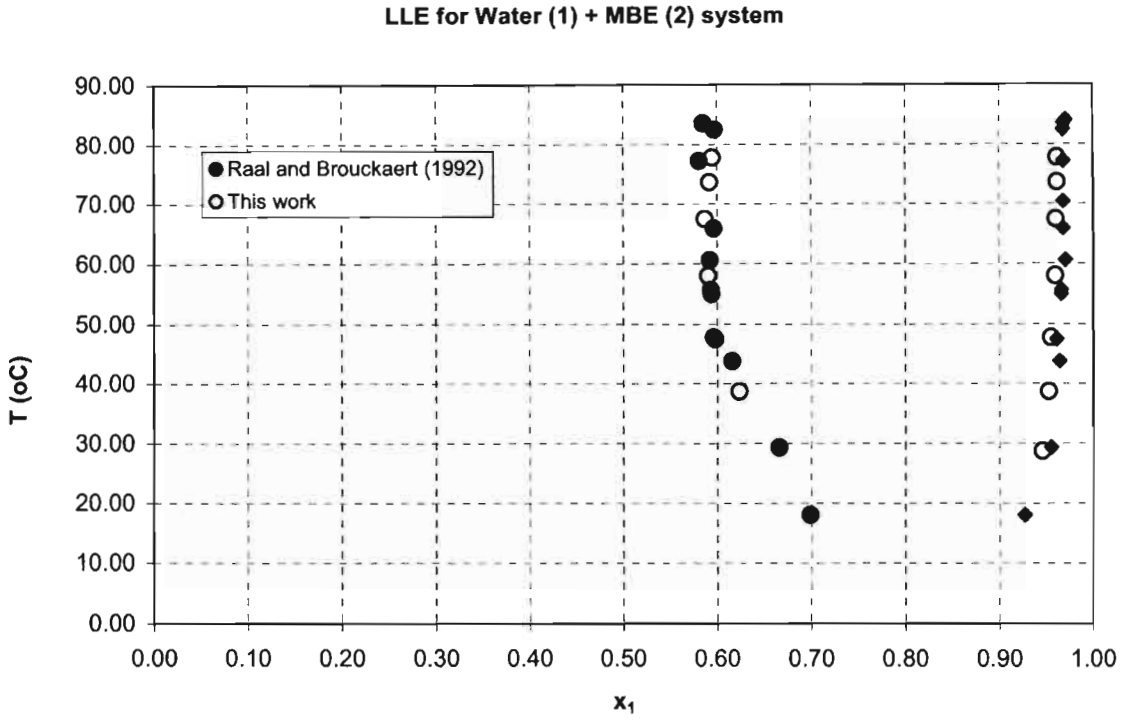

Figure 6 - 15: LLE data for the Water (1) + MBE (2) system at 97.2 kPa together with literature data

Experimental activity coefficients

The experimental activity coefficients were computed following the same procedure as for the cyclohexane (1) + ethanol (2) system discussed above. The results are shown in Table 6-16 below.

Table 6 - 16: Experimental activity coefficients for the system Water (1) + MBE (2) at 97.2 kPa

x_1	γ_1	γ_2	x_1	γ_1	γ_2
0.0886	3.3136	1.0086	0.9616*	1.0934	15.1503
0.0992	3.4314	1.0025	0.6083	1.6407	1.6017
0.1838	3.0769	1.0131	0.9885	1.0092	36.3279
0.1917	3.0602	1.0120	0.9915	1.0010	42.8495
0.2104	2.9287	1.0212	0.9955	1.0175	49.2819
0.2930	2.4194	1.0968	0.9973	1.0140	57.4078
0.4306	2.1362	1.1942	0.9996	1.0090	50.0106
0.5995*	1.7535	1.4530	0.9996	1.0073	36.8405

6.4.1.2 VLLE data reduction (The Combined method)

It was indicated in chapter 3 that the treatment of VLLE is the same as that for VLE. Thus, the same equations used for the cyclohexane (1) + ethanol (2) system at 40 kPa were used for the water (1) + MBE (2) system at 97.2 kPa. It is important to note that only those models that can predict liquid immiscibility should be used. The NRTL and the T-K Wilson models do predict partial miscibility and were thus used to regress first the VLE data in the homogenous MBE and Water regions and then the entire VLLE data set including the three-phase compositions (see Table 6-17). Figure 6-16 presents the T-x-y data for the entire region fitted to the NRTL equation. Similar graphs for the other cases considered are presented in the appendix to this chapter together with those from the TK-Wilson model. The model parameters are however all shown in Table 6-17. For comparison, data fitted to the restricted regions only are also shown since the parameters may give better correlation in these regions.

Table 6 – 17: Model parameters for the Water (1) + MBE (2) system at 97.2 kPa

Quantity	NRTL	TK-Wilson
	Homogeneous Water Region	
$\lambda_{12}-\lambda_{11}$ (J/mol)	935.4169	4281.1367
$\lambda_{12}-\lambda_{22}$ (J/mol)	3785.1018	-2068.7448
α	-7.3061	-
ΔT (K)	0.1516	0.3108
Δy	0.0110	0.011
	Homogeneous MBE Region	
$\lambda_{12}-\lambda_{11}$ (J/mol)	2712.9247	4828.4951
$\lambda_{12}-\lambda_{22}$ (J/mol)	862.3607	-3378.2635
α	-1.5604	-
ΔT (K)	0.1104	0.1506
Δy	0.013	0.0116
	Entire VLLE Data Set	
$\lambda_{12}-\lambda_{11}$ (J/mol)	2604.4452	4669.7595
$\lambda_{12}-\lambda_{22}$ (J/mol)	941.2518	-3790.9228
α	-1.7015	-
ΔT (K)	0.2864	0.5568
Δy	0.011	0.0187

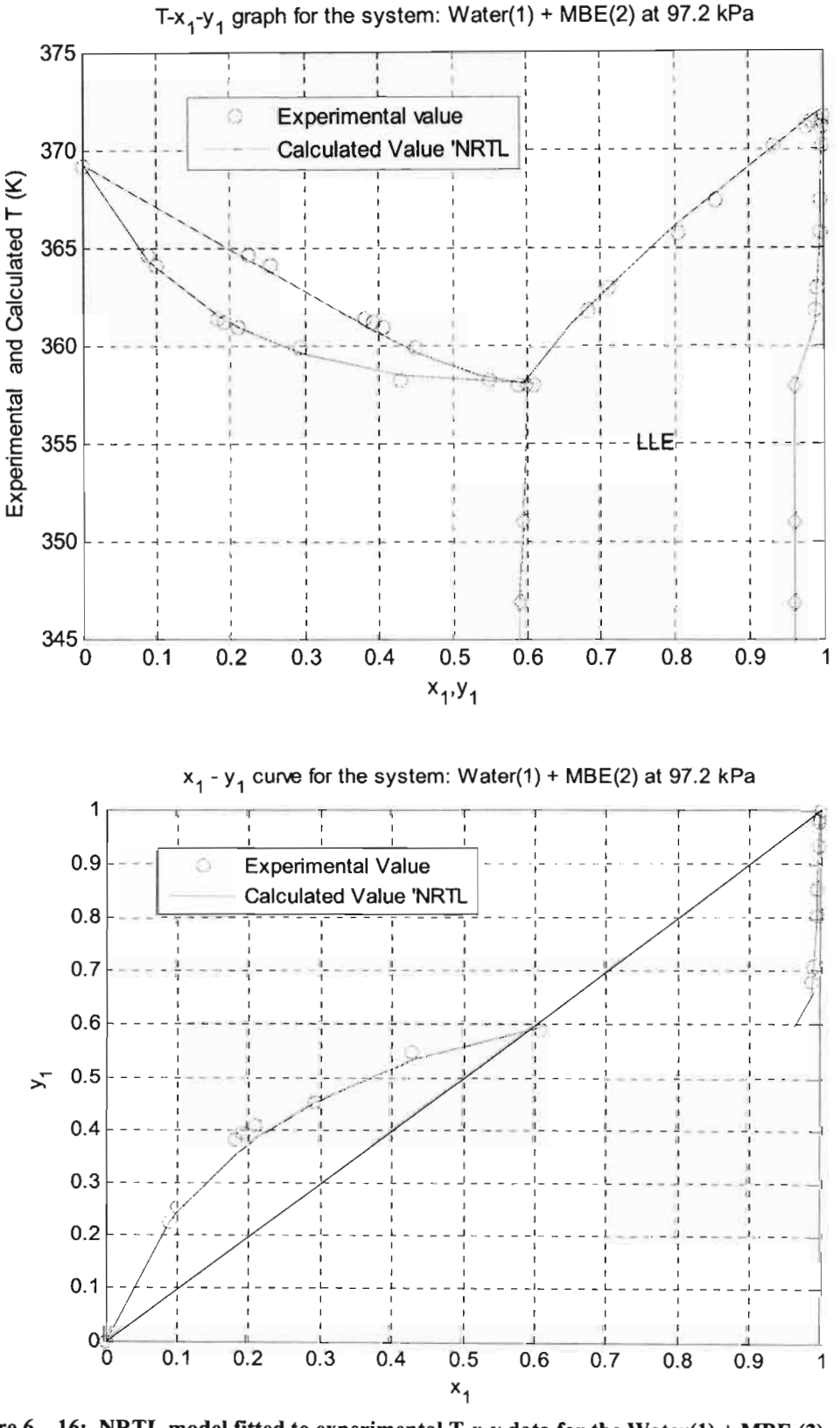

Figure 6 – 16: NRTL model fitted to experimental T-x-y data for the Water(1) + MBE (2) system at 97.2 kPa

6.4.1.3 Thermodynamic consistency testing

The two tests applied to the VLE data for the cyclohexane (1) + ethanol (2) system above were also used to test the VLLE data for consistency. The Point test of Van Ness [1973] was applied to data on both homogeneous water and MBE rich regions while the area test of Herington was applied to the entire VLLE data set. Figures 6-17 and 6-18 and Table 6-19 and summarise the results.

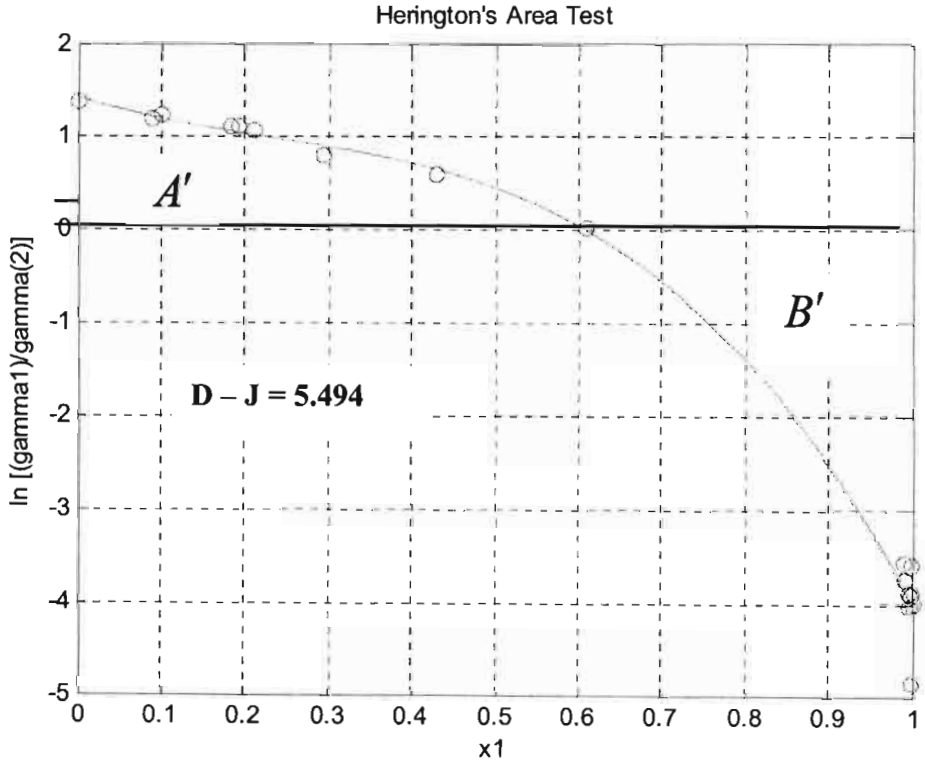

Figure 6 – 17: Herington's area test applied to the VLLE data for the Water (1) + MBE (2) system at 97.2 kPa

Table 6 – 18: Coefficients in equation (6-8) and results of the Herington's area test.

System	a'	b'	c'	d'	D-J
Water (1) + MBE(2)	0.0804	1.7689	1.2236	1.1553	5.494

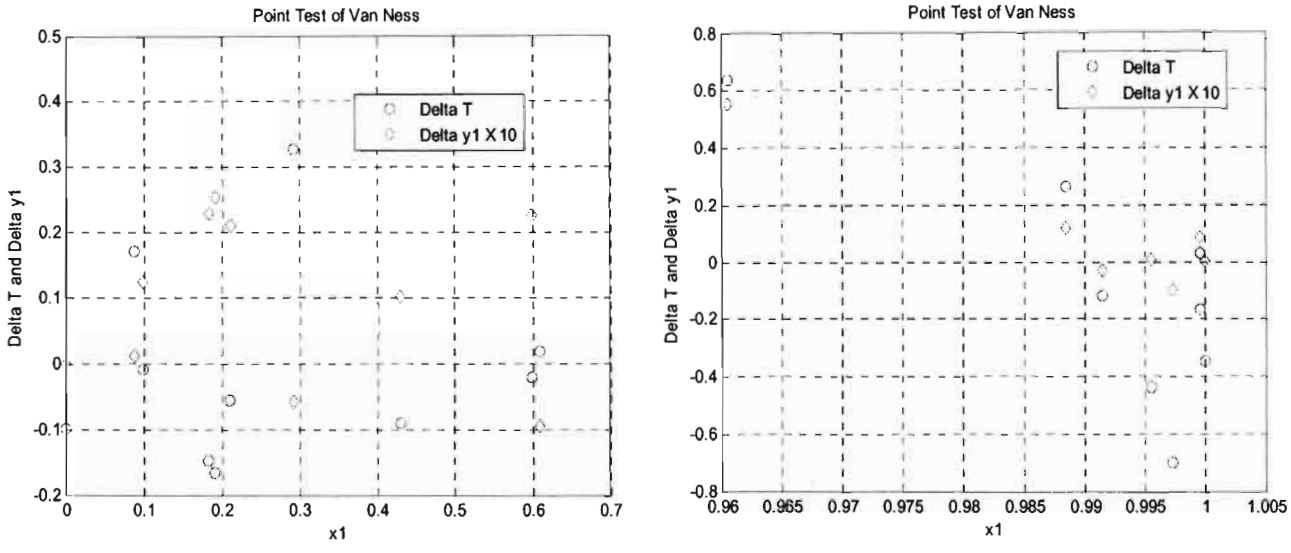

(a) (b)

Figure 6 – 18 Point test applied to the homogeneous MBE (a) and Water (b) regions for the system Water (1) + MBE(2) at 97.2 kPa.

Table 6 – 19: Absolute deviations in vapour compositions from the reduction of T-x-y data for the Water (1) + MBE (2) system at 97.2 kPa using the NRTL equation. (a)Homogeneous MBE region (b) Homogeneous Water region

Experimental y_1	Calculated y_1	Δy_1 (Absolute)	Experimental y_1	Calculated y_1	Δy_1 (Absolute)
0	0	0	0.619	0.5638	0.0552
0.224	0.2228	0.0012	0.6828	0.6711	0.0117
0.254	0.2415	0.0125	0.7109	0.7142	0.0033
0.3813	0.3583	0.023	0.8052	0.8044	0.0008
0.3925	0.367	0.0255	0.8554	0.8655	0.0101
0.4077	0.3864	0.0213	0.9787	0.9756	0.0031
0.4514	0.4572	0.0058	0.9842	0.9756	0.0086
0.5488	0.5386	0.0102	1	1	0
0.5885	0.598	0.0095			
0.619	0.5962	0.0228			

(a) **(b)**

The very good results obtained for the above two test systems indicated satisfactory performance of both the equipment and operating procedures and was therefore followed by measurements on new systems.

Appendix to Chapter 6

Test Systems: Results and Analysis.

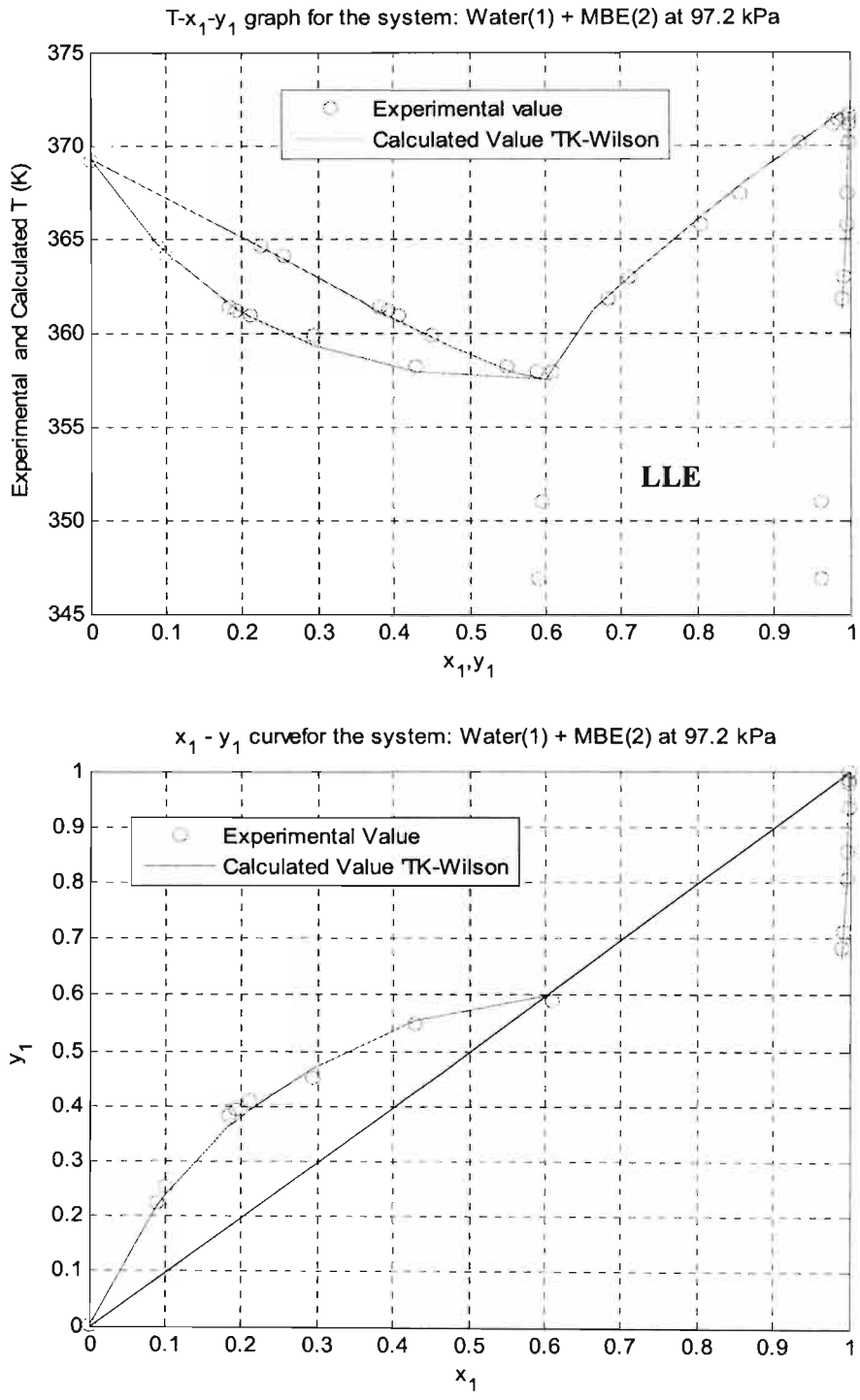

Figure A6 - 1: TK Wilson model fitted to the entire VLLE data set for the system Water(1) + MBE (2) at 97.2 kPa.

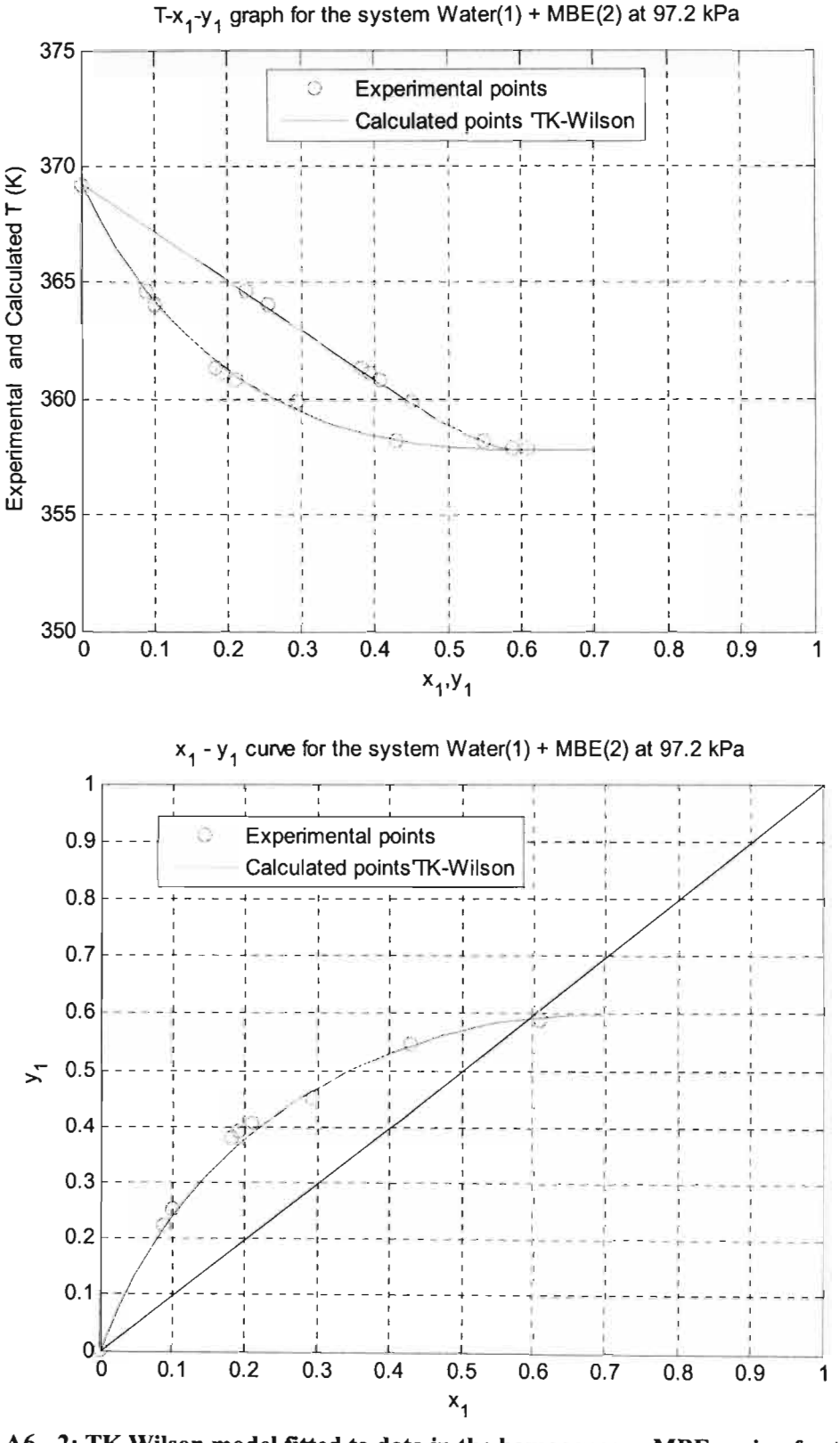

Figure A6 - 2: TK Wilson model fitted to data in the homogeneous MBE region for the system: Water (1) + MBE (2) at 97.2 kPa.

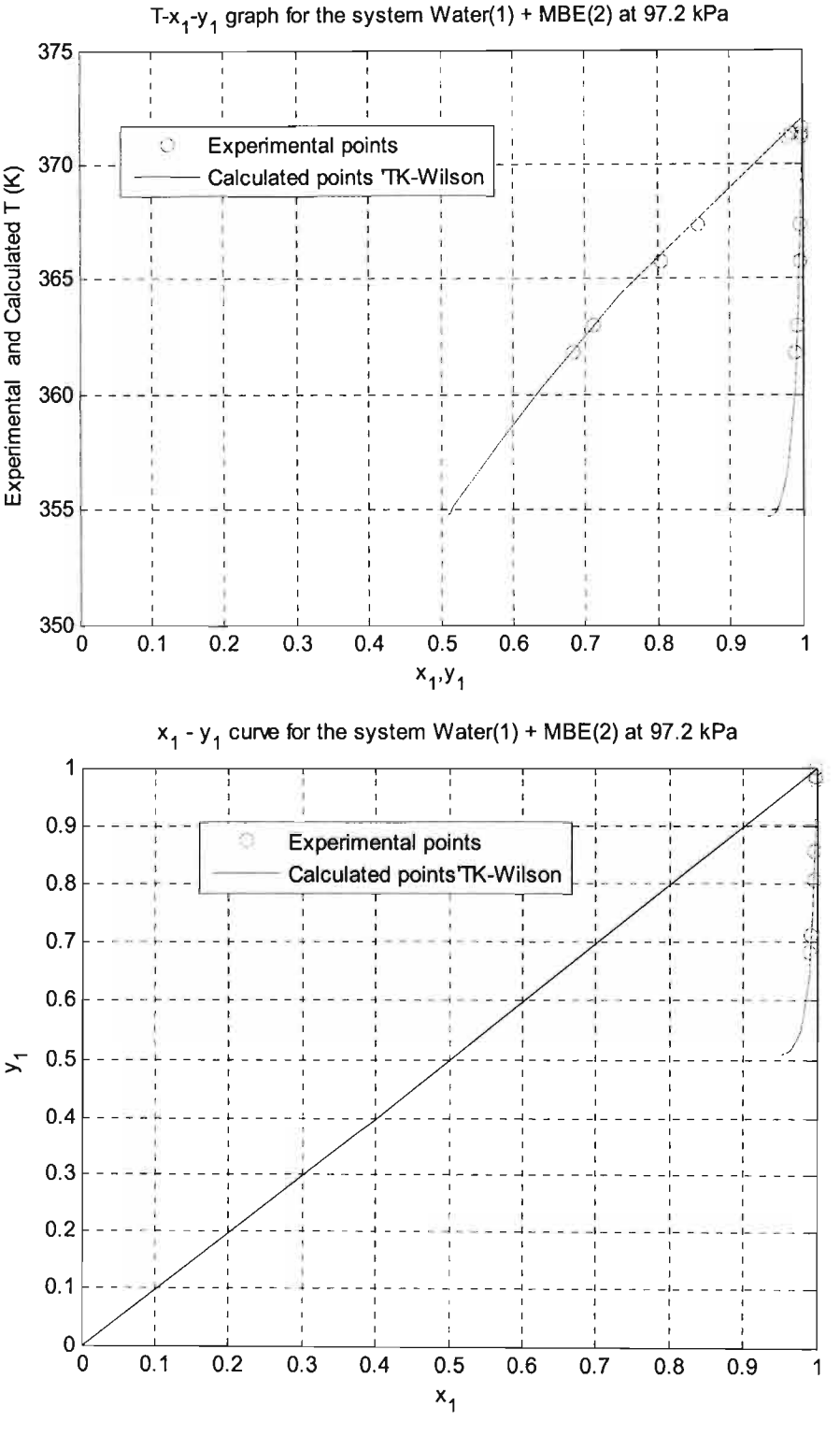

Figure A6 - 3: TK Wilson model fitted to data in the homogeneous Water region for the system: Water (1) + MBE (2) at 97.2 kPa.

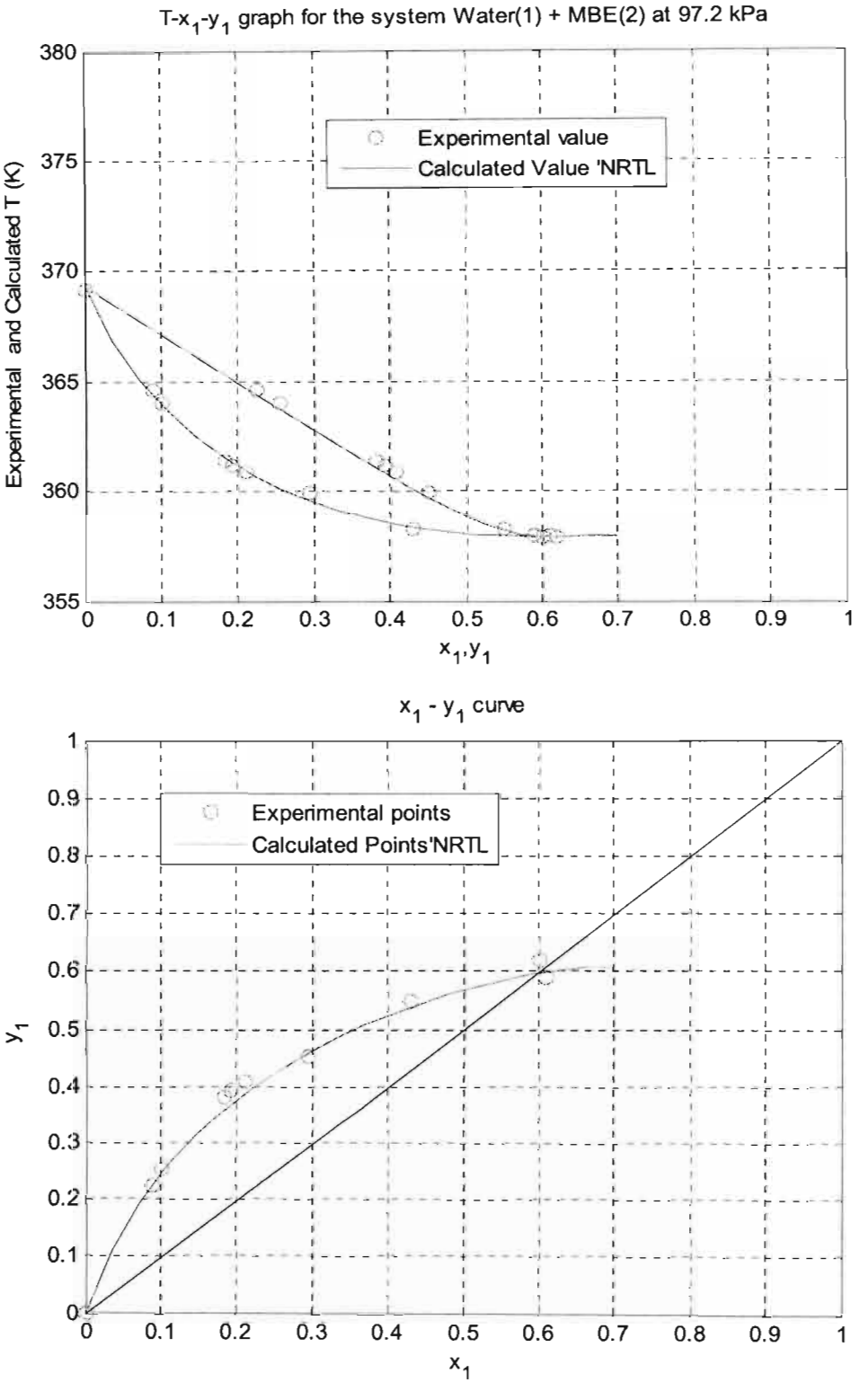

Figure A6 - 4: NRTL model fitted to data in the homogeneous MBE region for the system: Water (1) + MBE (2) at 97.2 kPa.

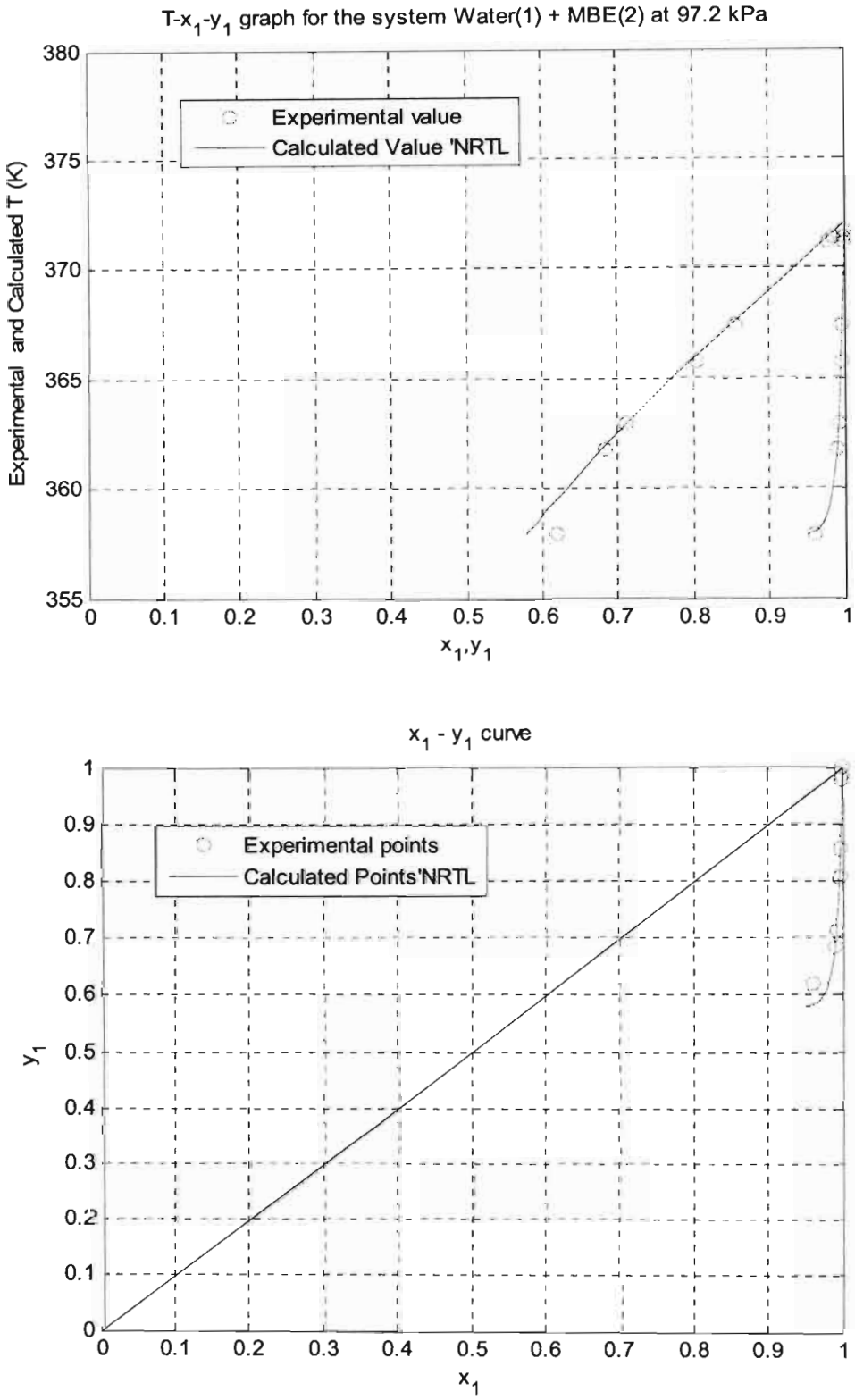

Figure A6 - 5: NRTL model fitted to data in the homogeneous Water region for the system :Water(1) + MBE (2) at 97.2 kPa.

7

Chapter Seven

New (Previously Unmeasured) Systems: Results and Analysis

Chapter 6 presented the results for the systems that were used to test the equipment that was used in this project and hence to come up with the equipment operating procedures. This chapter, like Chapter 6, presents the VLE, VLLE and LLE results and analyses for the new systems that were measured in this work. These were previously unmeasured systems – systems which had no available data in the literature at the time of writing of this dissertation. These systems, which were either homogeneous or partially miscible, are:

1. m-Cresol (1) + Naphthalene(2) at 55 kPa (Homogeneous)
2. m-Cresol (1) + Naphthalene (2) at 393.15 K (Homogeneous)
3. m-Cresol(1) + Naphthalene (2) at 383.15 K (Homogeneous)
4. m-Cresol (1) + Water (2) at 55 kPa (Heterogeneous)
5. o-Tolunitrile (1) + Water (2) at 55kPa (Heterogeneous)
6. m-Cresol (1) +Water (2) + Naphthalene (3), LLE at 253.15 K and 263.15 K

The analysis presented here follows the same style as that in Chapter 6. The material purities are presented first, and are followed by the measured vapour pressures. VLE and or VLLE analysis follows, and for each system, ends with thermodynamic consistency testing and finally LLE Analysis concludes the chapter. However in this chapter, a more detailed analysis of the results is presented. The Gamma - Phi method is used in conjunction with the NRTL, Wilson, T-K Wilson and UNIQUAC activity coefficient models. For the homogeneous

systems, the alternative analysis using Equations of State (EOS) is also used. The Peng and Robinson [1976] EOS (PR-EOS), the Soave Redlich Kwong [1972] EOS (SRK-EOS) and the Stryjek and Vera [1986] modified Peng and Robinson EOS (PRSV-EOS) are all used first with the classical mixing rules and then with the more rigorous density-independent Wong and Sandler [1992] mixing rules. For the ternary LLE measurements, the binodal curves are correlated to the Hlavaty [1972] equation, the β- function (Shultz et al. [1973]) and the log-γ function (Letcher et al. [1989]). The corresponding tie-line data are correlated to the NRTL model. All these results are discussed in the following chapter, Chapter 8.

7.1 Chemical purities

Other than water which was not purchased, all the chemicals were bought from Merck. Table 7-1 gives the nominal purities together with the measured and literature values of the refractive indices, a method that was used to check the purities of the chemicals. GC analysis of all the chemicals, as was described in Section 6.1, indicated no significant impurities and thus the chemicals were used without further purification.

Table 7 - 1: Chemical purities and Refractive indices

Reagent	Refractive Index		G C Analysis (Mass %)	Min Purity specified by supplier (Mass %)
	Experimental	Literature[♣]		
m-Cresol	1.5442	1.5438	99.9	99.9
o-Tolunitrile	1.5266	1.5279	99.5	98.0
Naphthalene	1.5906	1.5898	99.9	99.9
Benzene	1.5006	1.5011	99.9	99.9
Ethanol	1.3612	1.3611	99.9	99.9

Benzene, also shown in the table above, was used to dissolve solid naphthalene in m-cresol in GC calibration, while ethanol was used in making both gravimetrically prepared heterogeneous water + m-cresol and water + o-tolunitrile mixtures homogeneous, also in GC calibration. (see Chapter 5). (NB- Henceforth the names m-cresol and cresol will be used interchangeably. This will also be the case with the names o-tolunitrile and tolunitrile).

[♣] obtained from Weast et al [1983 -1984] and David et al [1992 – 1994]

7.2 Vapour pressures.

Vapour pressures were measured for m-cresol, o-tolunitrile and water. The data are presented in Tables 7-2 to 7-4. The same data are plotted in Figures 7-1 to 7-3 where they are compared to data obtained from the Dortmund Databank for Thermo Physical Properties (DDB). Also shown in Tables 7-2 to 7-4 are absolute deviations between measured vapour pressures and those computed from the Antoine and Wagner (Reid et al. [1988]) equations. How these values were obtained is the subject of the following section.

Table 7 - 2: Vapour Pressure Data for m-Cresol

Measured			
P	T	ΔP_{Wagner}	ΔP_{Ant}
kPa	K	kPa	kPa
3.23	373.69	0.0094	0.0022
4.14	379.54	0.0251	0.0260
4.81	383.47	0.0075	0.0105
6.10	389.51	0.0091	0.0172
7.44	394.65	0.0039	0.0148
8.74	398.88	0.0084	0.0033
11.28	405.83	0.0012	0.0107
16.01	415.71	0.0253	0.0233
18.09	419.24	0.0285	0.0201
21.18	423.77	0.0433	0.0608
26.03	430.02	0.0128	0.0426
28.16	432.43	0.0146	0.0481
31.32	435.76	0.0137	0.0229
36.41	440.50	0.0017	0.0362
42.59	445.53	0.0377	0.0563
51.38	451.78	0.0272	0.0603
56.12	454.00	0.1006	0.1771
56.12	454.80	0.0804	0.0168
Average Deviations		0.0250	0.0361

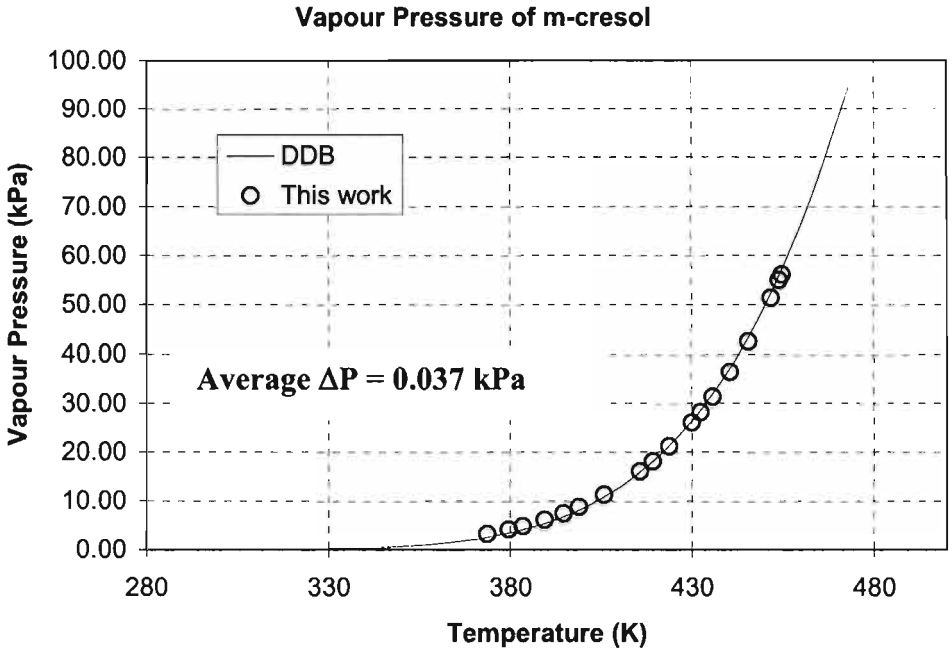

Figure 7 - 1: Vapour Pressure Data of m-Cresol together with Literature Data

Table 7 - 3: Vapour Pressure Data for o-Tolunitrile

Measured P kPa	T K	ΔP_{Wagner} kPa	ΔP_{Ant} kPa
6.41	456.11	0.0092	0.0219
8.31	452.79	0.0208	0.0305
11.29	452.49	0.0052	0.0295
17.58	448.05	0.0553	0.0427
21.66	441.60	0.0047	0.0039
30.79	434.15	0.0333	0.0190
38.20	422.36	0.0093	0.0526
45.63	415.51	0.1427	0.1086
51.60	401.80	0.0801	0.0990
52.41	392.63	0.3047	0.2808
56.91	384.88	0.0701	0.1622
Average Deviations		0.0669	0.0774

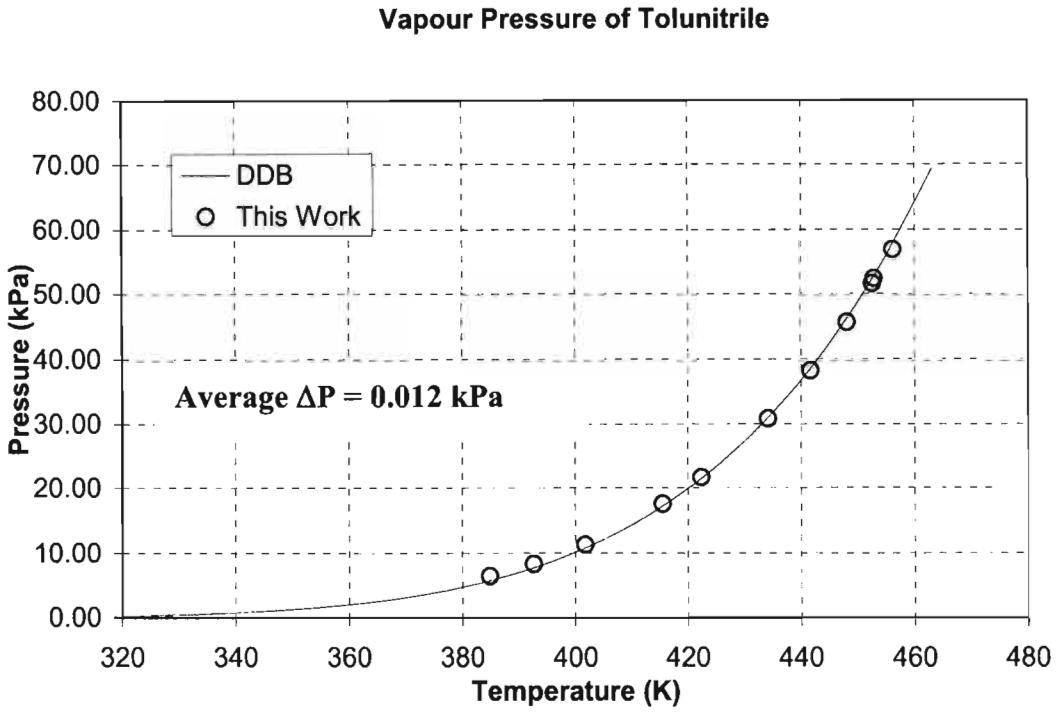

Figure 7 - 2: Vapour Pressure Data of Tolunitrile together with Literature Data

Table 7 - 4: Vapour Pressure Data for Water

Measured P kPa	T K	ΔP_{Wagner} kPa	ΔP_{Ant} kPa
11.10	319.99	0.0101	0.0006
16.17	328.15	0.1032	0.0897
21.38	334.03	0.1981	0.2186
31.46	343.36	0.1036	0.0958
41.65	350.21	0.0778	0.0951
54.94	357.27	0.0959	0.1386
68.62	363.01	0.2081	0.1651
76.91	366.13	0.1137	0.0877
100.74	373.69	0.1493	0.0400
Average Deviations		0.1178	0.1035

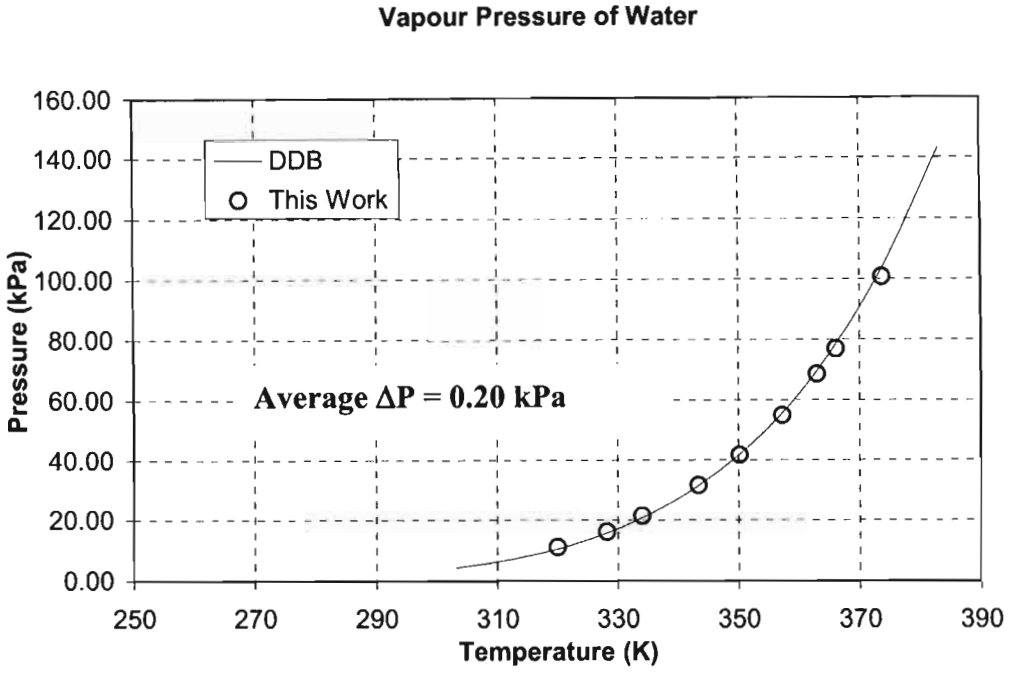

Figure 7 - 3: Vapour Pressure Data of Water together with Literature Data

The three vapour pressure curves shown above indicate good agreement between the measured data and the literature data. The excellent agreement led to the conclusion that the equipment pressure and temperature calibrations were correct as vapour pressure is a strong function of temperature.

7.2.1 Analysis of vapour pressure data

As in the treatment of the test systems' data, the measured vapour pressure data were regressed to obtain parameters for the Antoine and Wagner Equations (Reid et al. [1988]). The procedure followed has already been discussed in Section 6.2.1. Tables 7-5 and 7-6 show the regressed parameters. The absolute deviations between vapour pressures calculated from these sets of parameters and those experimentally determined, mentioned in the previous section, are shown in Tables 7-2 to 7-4.

Table 7 - 5: The Antoine Coefficients for the New Systems Chemicals

Reagent	A	B	C	$\frac{1}{n}\sum\lvert\Delta P\rvert$
m-Cresol	8.3973	-3426.4957	60.7048	0.0365
Tolunitrile	8.8240	-4212.879	141.739	0.0774
Water	7.7163	-2136.211	0.2354	0.1035

Table 7 - 6: The Wagner Vapour Pressure Equation Coefficients for the New Systems Chemicals

Reagent	A	B	C	D	$\frac{1}{n}\sum\lvert\Delta P\rvert$
m-Cresol	-5.6509	-3.7063	-1.566	16.5935	0.0250
Tolunitrile	-9.1667	4.8535	-12.0173	40.9151	0.0669
Water	15.9885	-41.7212	34.1634	-34.911	0.1178

A closer look at the last column in the two tables above shows that the Wagner equation was generally better that the Antoine equation in correlating the measured vapour pressures.

7.3 Vapour-liquid equilibria (m-Cresol (1) + Naphthalene (2) system)

The VLE measurements for this system were carried out at 55kPa, 383.15 K and 393.15 K. They began by calibrating the GC. Naphthalene is a solid at room temperature (melting point of 80°C) and thus could not dissolve in cresol at room temperature. As was the case for the water + MBE test system (see Chapter 5) which was heterogeneous and methanol had to be used to make the gravimetrically prepared samples homogeneous, benzene was used for that purpose in this system. Benzene, sufficient to dissolve the naphthalene in cresol was added to the mixtures and its chromatography peak ignored in the analysis that followed. Figures 7-4 and 7-5 below show the calibration curves for both dilute and rich cresol regions. As can be seen in the figures non-linear response factor relationships were obtained. A further discussion on these graphs is presented in Chapter 8 (Section 8.1).

The measured VLE data are shown in Table 7-7 and Figures 7-6 to 7-8 show the T-x-y and x-y plots for the three data sets. The gap in the Naphthalene rich regions in Figures 7-6 to 7-8 was a result of difficulties in sampling the liquid phase in these regions, as further discussed in Section 8.1.

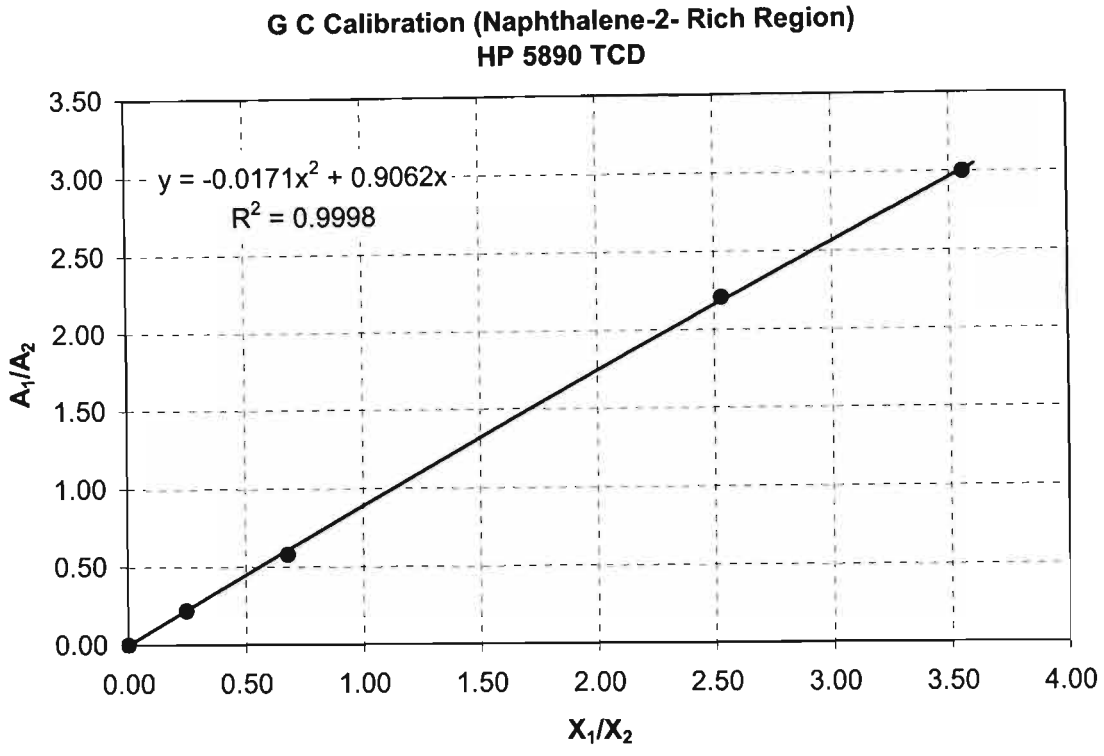

Figure 7 - 4: GC Calibration Curve for the m-Cresol (1) + Naphthalene (2) System (Dilute Cresol Region)

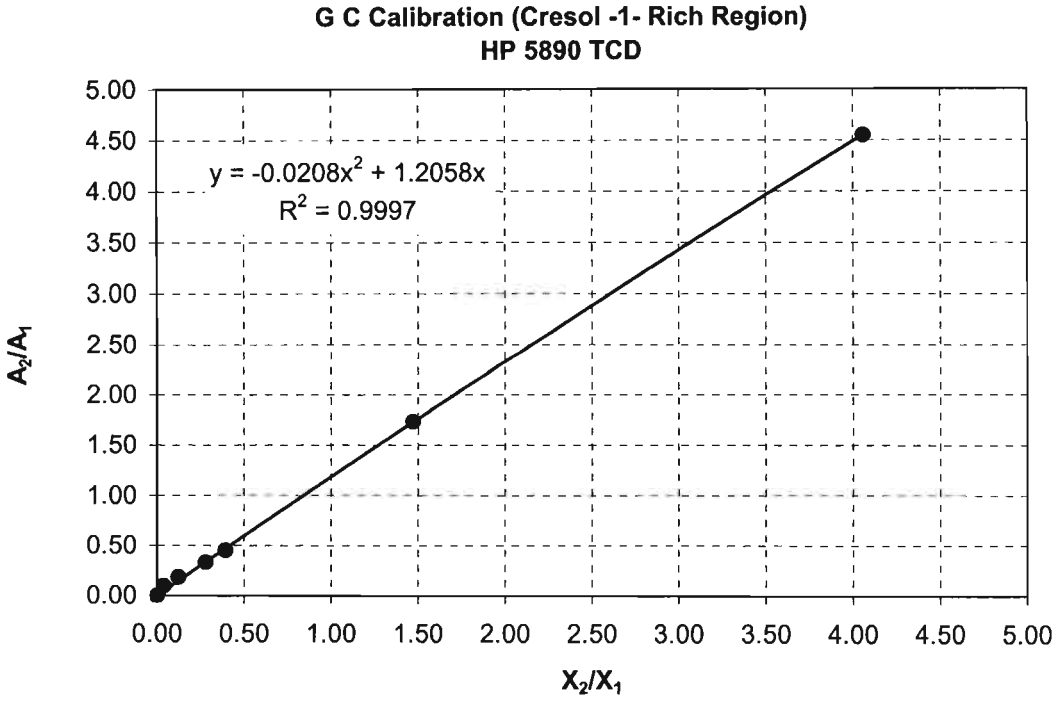

Figure 7 - 5: GC Calibration Curve for the m-Cresol (1) + Naphthalene (2) System (Dilute Cresol Region)

Table 7 - 7: Measured VLE Data for the m-Cresol (1) + Naphthalene (2) system

P = 55 kPa			T = 383.15 K			T = 393.15 K		
T [K]	x_1	y_1	P [kPa]	x_1	y_1	P [kPa]	x_1	y_1
467.00	0.0000	0.0000	5.49	0.0000	0.0000	3.74	0.0000	0.0000
459.54	0.1953	0.3039	7.53	0.3868	0.4407	5.23	0.4330	0.4600
458.33	0.2574	0.3677	7.63	0.4382	0.4852	5.32	0.4940	0.5110
457.32	0.3099	0.4213	7.82	0.5660	0.5668	5.38	0.5600	0.5550
456.52	0.3786	0.4812	7.80	0.6563	0.6292	5.31	0.6670	0.6290
455.71	0.4748	0.5490	7.74	0.6921	0.6653	5.24	0.7100	0.6660
455.61	0.4751	0.5516	7.65	0.7417	0.7009	5.19	0.7510	0.6940
454.90	0.5617	0.6213	7.51	0.8195	0.7758	5.09	0.8100	0.7520
454.50	0.6301	0.6720	7.40	0.8865	0.8427	4.93	0.8950	0.8450
454.40	0.6559	0.6910	7.00	1.0000	1.0000	4.48	1.0000	1.0000
454.10	0.7139	0.7338						
453.80	0.7347	0.7486						
453.49	1.0000	1.0000						

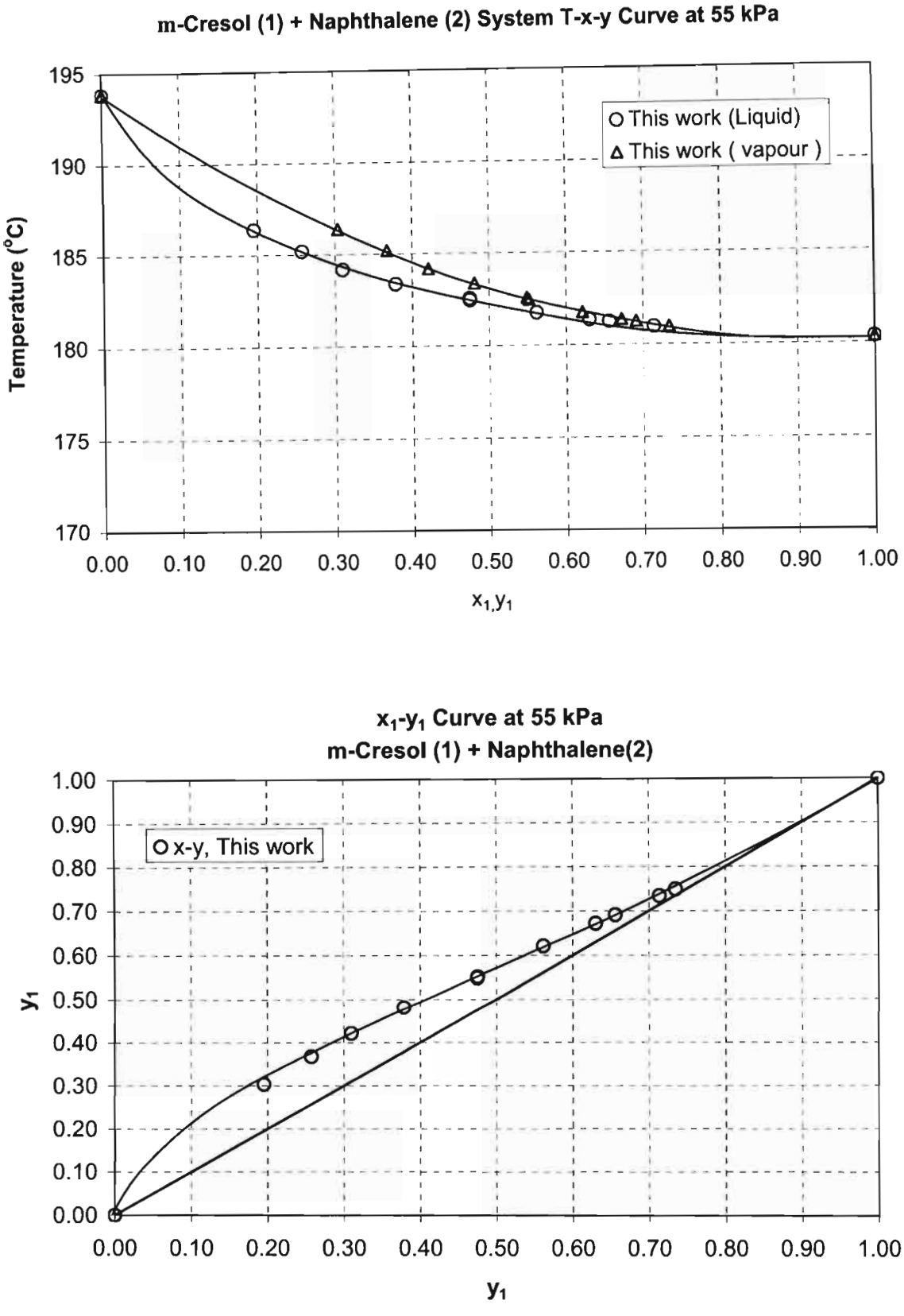

Figure 7 - 6: T-x-y and x-y curves for the system m-Cresol (1) + Naphthalene (2) at 55kPa m

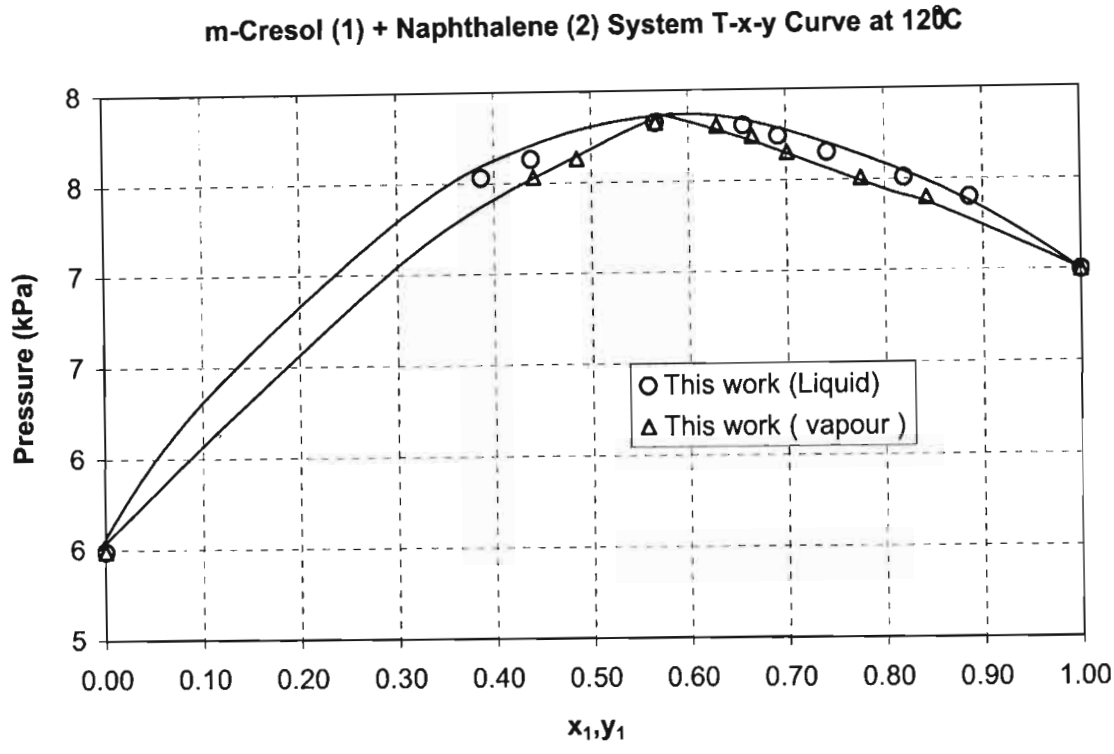

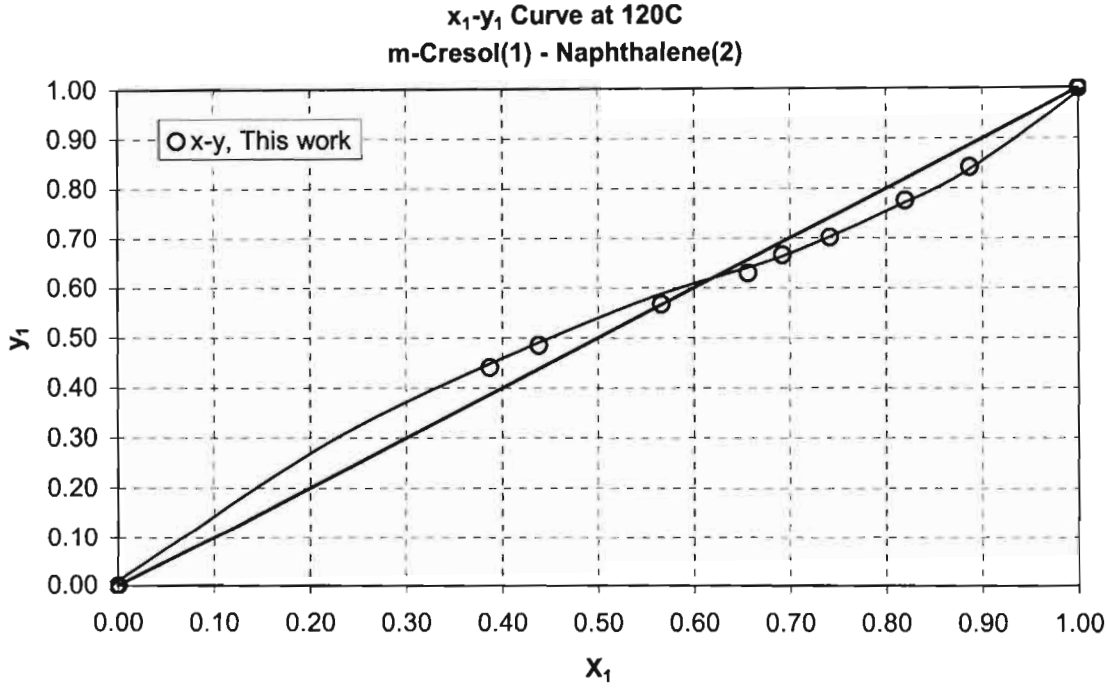

Figure 7 - 7: P-x-y and x-y curves for the system m-Cresol (1) + Naphthalene (2) at 393.15 K

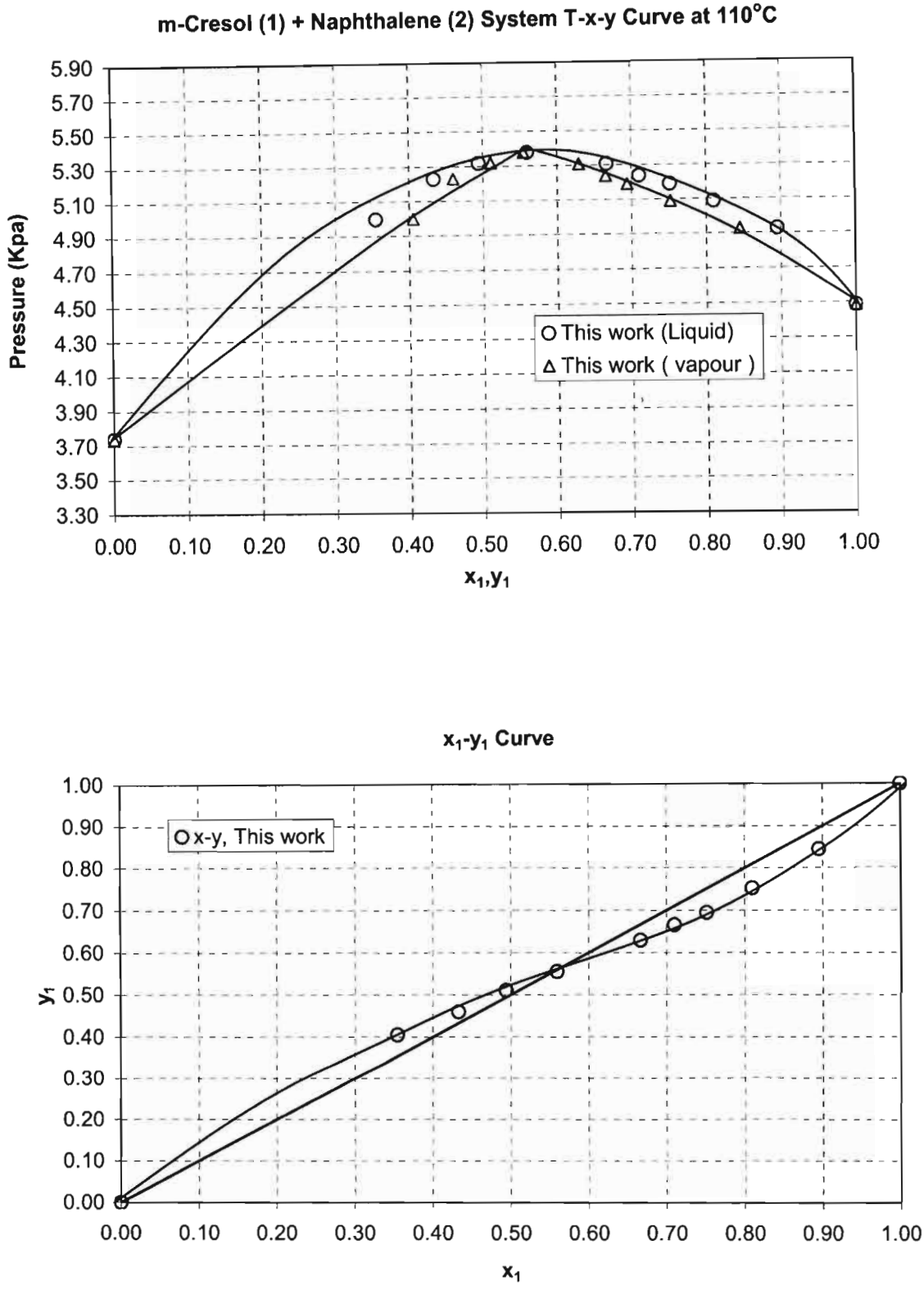

Figure 7 - 8: P-x-y and x-y curves for the system m-Cresol (1) + Naphthalene (2) at 393.15 K

7.3.1 VLE analysis

The measured VLE presented above were regressed to obtain parameters in the NRTL, Wilson, T-K Wilson and UNIQUAC activity coefficient models. As was the case in Section 6.3, the vapour phase imperfections were accounted for using fugacity coefficients evaluated from the Virial equation of state. This analysis was followed by the alternative analysis using Equations of State (EOS). The PR-EOS, SRK-EOS and the PRSV-EOS were used in the second approach first with the Van der Waal one-fluid mixing rules and then with the more rigorous density-independent Wong and Sandler [1992] mixing rules. The first step in the analysis of the data was determining the pure-component properties - a subject that is treated in the following section.

7.3.1.1 Pure-component properties

For both m-cresol and naphthalene, the pure-component properties, tabulated below, Table 7-8, were obtained from the DDB. The mixture properties were computed following the same procedure as in Section 6.3.3 using the mixing rules proposed by Prausnitz [1986].

Table 7 - 8: Pure component critical parameters for m-Cresol and Naphthalene

	V_c cm^3/mol	Z_c	T_c K	ω	P_c kPa
m-Cresol	310	0.2409	705.8	0.464	4559.63
Naphthalene	410	0.2671	748.4	0.302	4053
Mixture	357.7	0.2540	726.8	0.3830	4291

Experimental activity coefficients

These were calculated from the equation:

$$\gamma_i = \frac{y_i \Phi_i P}{x_i P_i^{sat}} \tag{6-4}$$

following the same procedure as in Section 6.3.2. Table 7-9 below shows the values obtained for the three data sets measured for the m-cresol (1) + naphthalene (2) system. Figure 7-9 shows the experimental activity coefficients for the 55kPa isobar. Similar graphs for the other

data sets are presented and discussed in Chapter 8. The graph indicates that the system shows positive deviations from Raoult's law.

Table 7 - 9: Experimental Activity Coefficients for the system m-Cresol (1) + Naphthalene (2)

P = 55 kPa			T = 393.15 K			T = 383.15 K		
x_1	γ_1	γ_2	x_1	γ_1	γ_2	x_1	γ_1	γ_2
0.0000	1.8844	0.9957	0.0000	2.7813	0.9957	0.0000	3.5445	1.0027
0.1953	1.2999	1.0482	0.3868	1.2236	1.2439	0.4330	1.2398	1.3305
0.2574	1.2346	1.0657	0.4382	1.2047	1.2666	0.4940	1.2283	1.3732
0.3099	1.2089	1.0784	0.5660	1.1160	1.4143	0.5600	1.1903	1.4530
0.3786	1.1564	1.0973	0.6563	1.0652	1.5252	0.6670	1.1183	1.5795
0.4748	1.0764	1.1536	0.6921	1.0596	1.5254	0.7100	1.0978	1.6110
0.4751	1.0840	1.1507	0.7417	1.0293	1.6064	0.7510	1.0713	1.7025
0.5617	1.0538	1.1864	0.8195	1.0116	1.6923	0.8100	1.0557	1.7730
0.6301	1.0277	1.2315	0.8865	1.0004	1.8611	0.8950	1.0403	1.9418
0.6559	1.0182	1.2504	1.0000	0.9945	2.0293	1.0000	1.0041	2.7861
0.7139	1.0023	1.3058						
0.7347	1.0021	1.3417						
1.0000	0.9923	1.3895						

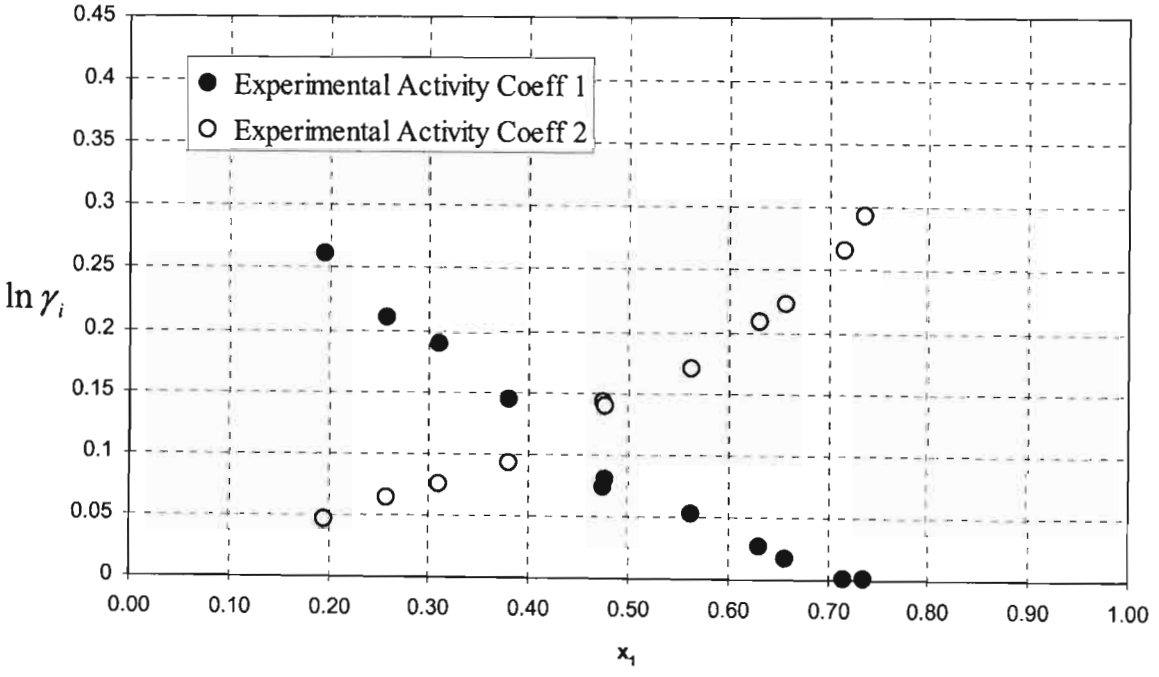

Figure 7 - 9: Experimental activity coefficients for the m-Cresol (1) + Naphthalene system at 55 kPa

7.3.1.2 VLE data reduction (The Gamma-Phi [γ -ϕ] method)

The objective function used to regress the experimental VLE data was:

$$\delta T = \sum_{Alli} \left(T_i^{Exp} - T_i^{cal} \right)^2 \tag{6-5}$$

for isobaric data and

$$\delta P = \sum_{Alli} \left(P_i^{Exp} - P_i^{cal} \right)^2 \tag{7-1}$$

for isothermal data.

For the isothermal data sets, the calculations were relatively simple as the Virial coefficients, saturated vapour pressures and molar volumes were constant and were determined once at the onset of the iterations. The parameters obtained for the four activity coefficients models used are shown in Table 7-10 below.

Table 7 - 10: Model Parameters and Absolute Deviations from Experimental T-x-y and P-x-y data for the m-Cresol (1) + Naphthalene (2) system.

Model	P = 55 kPa	T = 393.15 K	T = 383.15 K
NRTL			
$\lambda_{12}-\lambda_{22}$ (J/mol)	1893.2949	-1976.961	1865.7145
$\lambda_{21}-\lambda_{11}$ (J/mol)	-807.5927	5505.9436	2861.3611
α	-1.0602	0.14812	0.79708
ΔT or ΔP (K/kPa)	0.0926	0.0387	0.0276
Δy	0.0054	0.0087	0.0136
Wilson			
$\lambda_{12}-\lambda_{22}$ (J/mol)	5064.9807	6587.1977	3751.1703
$\lambda_{21}-\lambda_{11}$ (J/mol)	-2391.6623	-1537.5691	1528.8951
ΔT or ΔP (K/kPa)	0.0947	0.0549	0.0959
Δy	0.0053	0.0035	0.0102
T-K Wilson			
$\lambda_{12}-\lambda_{22}$ (J/mol)	5425.6273	6715.9632	2388.7111
$\lambda_{21}-\lambda_{11}$ (J/mol)	-2726.1605	-1689.8992	1631.148
ΔT or ΔP (K/kPa)	0.0976	0.0536	0.0566
Δy	0.0054	0.0034	0.0103
UNIQUAC			
$\lambda_{12}-\lambda_{22}$ (J/mol)	4009.5112	3585.7681	1744.1174
$\lambda_{21}-\lambda_{11}$ (J/mol)	-2494.1603	-1885.2491	-837.3616
ΔT or ΔP (K/kPa)	0.3149	0.0304	0.0373
Δy	0.0253	0.0174	0.0179

Figures 7-10 to 7-12 below summarize these results for the NRTL model and compares the experimental values to those calculated from the parameter sets. For the other models the graphs are presented in Appendix 1.

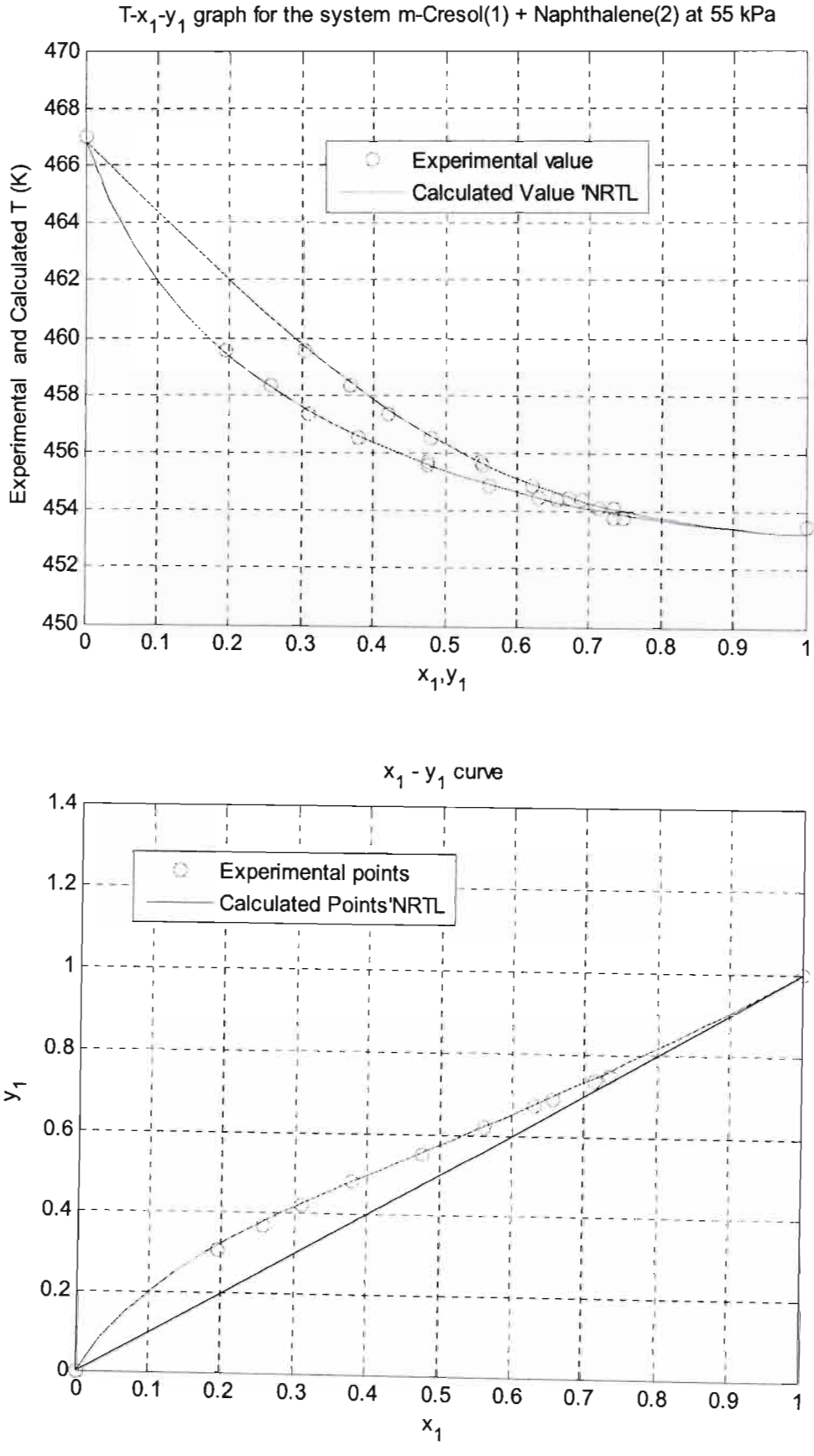

Figure 7 - 10: NRTL model fitted to Experimental T-x-y data for the + Cresol (1) - Naphthalene (2) System at 55 kPa

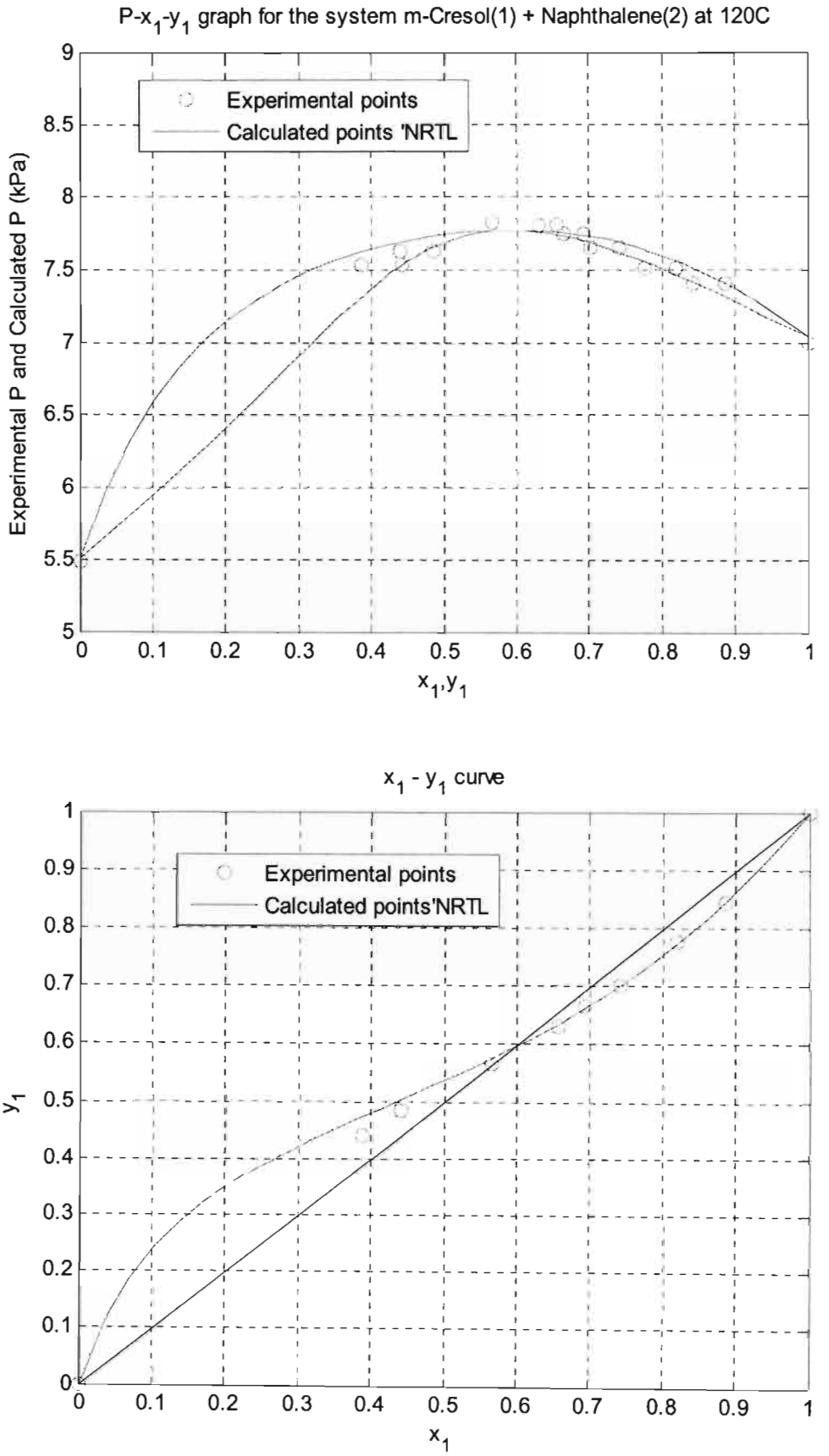

Figure 7 - 11: NRTL model fitted to Experimental T-x-y data for the + Cresol (1) - Naphthalene (2) System at 393.15 K

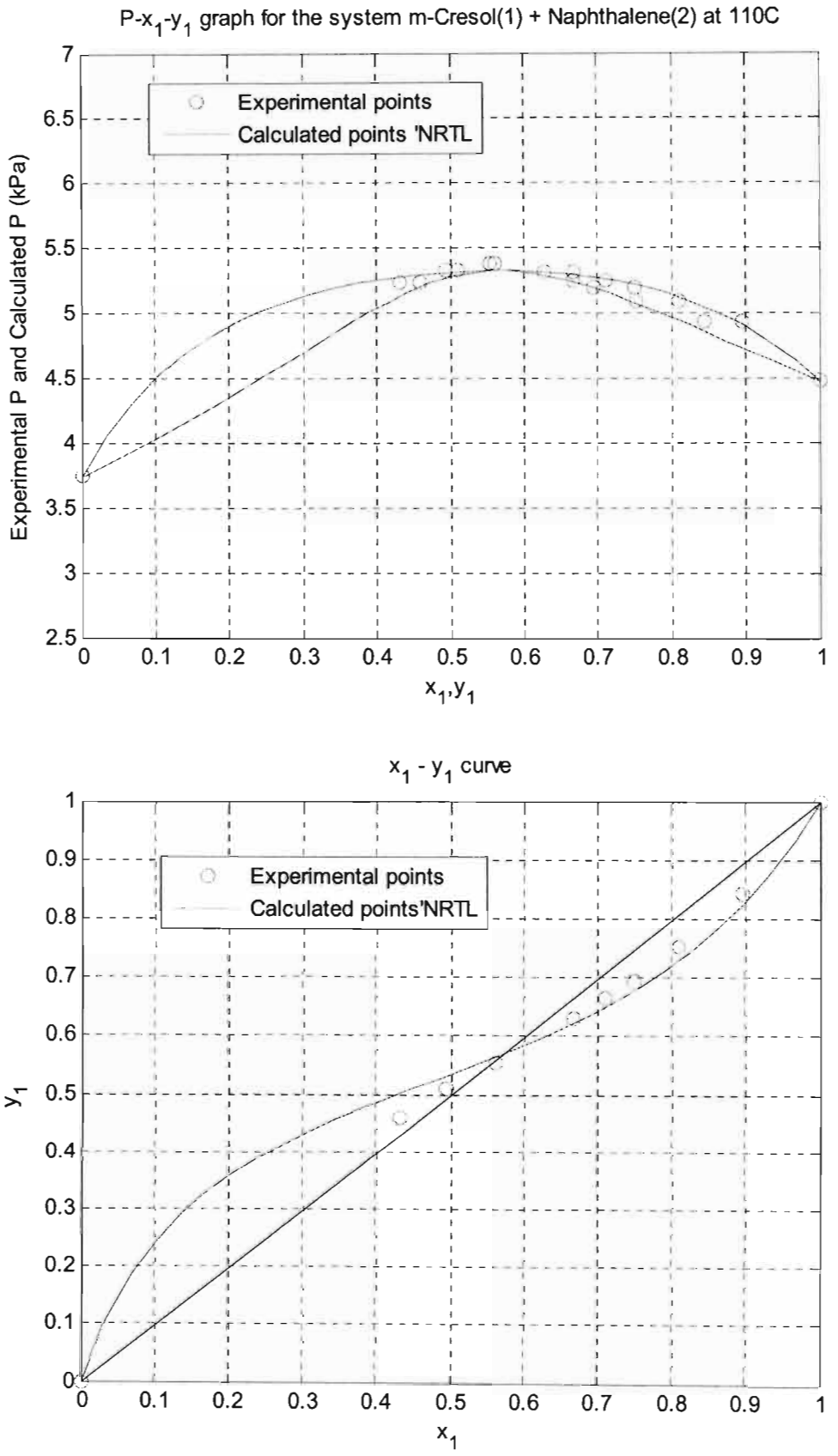

Figure 7 - 12: NRTL model fitted to Experimental T-x-y data for the + Cresol (1) - Naphthalene (2) System at 383.15K

7.3.1.3 VLE data reduction (The $\phi-\phi$ method)

The use of the Equation of State method in modeling VLE data was presented in great detail in Chapter 3 (see Section 3.9.2). As was the case with the Gamma-Phi method, non-linear least squares regression was used to adjust the parameters to best fit the experimental data. The same objective functions were used for the isobaric and isothermal cases viz:

$$\delta T = \sum_{All i} \left(T_i^{Exp} - T_i^{cal} \right)^2 \tag{6-5}$$

$$\delta P = \sum_{All i} \left(P_i^{Exp} - P_i^{cal} \right)^2 \tag{7-1}$$

Presented first is the analysis using the classical mixing rules and then that using the Wong and Sandler [1992] mixing rules in conjunction with the NRTL activity coefficient model.

7.3.1.3.1 Regression using Classical mixing rules (Van der Waal one-fluid mixing rules)

The three data sets for the m-cresol (1) + naphthalene (2) system were regressed to give the parameters in Table 7-12. For the PRSV EOS, the κ_1 parameter, which is one of the input parameters was unavailable and had to be estimated for cresol and tolunitrile. This parameter was obtained by regressing the measured vapour pressure data such that the equilibrium condition:

$$f_i^L = f_i^v$$

was satisfied along the vapour pressure curve (Peng and Robinson [1976]). The convergence criterion used was that:

$$\left| f_i^L - f_i^v \right| \leq 10^{-6} \text{ Kpa} \tag{7-2}$$

Table 7-11 shows the parameters obtained following the procedure just described together with those for water and naphthalene obtained from the paper by Stryjek and Vera [1986].

Table 7 - 11: κ_1 Parameters for the PRSV-EOS

Component	κ_1 Parameter
m-Cresol	0.00892
Naphthalene	0.03297
Tolunitrile	-0.19027
Water	-0.06635

Table 7 - 12: Model Parameters and Average Absolute Deviations from Experimental T-x-y and P-x-y data for the m-Cresol (1) + Naphthalene (2) system. Data regressed using the Van der Waal one fluid mixing rules

Model	P = 55 kPa	T = 393.15 K	T = 383.15 K
PR-EOS			
k_{ij}	0.02998	0.03725	0.04116
ΔT or ΔP (K/kPa)	0.4769	0.05861	0.04363
Δy	0.0046	0.01532	0.01676
PRSV-EOS			
k_{ij}	0.03001	0.04416	0.04871
ΔT or ΔP (K/kPa)	0.36598	0.03751	0.03279
Δy	0.00468	0.02069	0.02471
SRK-EOS			
k_{ij}	0.03175	0.05306	0.05868
ΔT or ΔP (K/kPa)	0.35132	0.07439	0.04075
Δy	0.00436	0.02930	0.03771

Figures 7-13 to7-15 summarise these results for the PR-EOS and compares the experimental values to those computed from the fitted parameters. For the other equations of state, similar graphs are presented in Appendix 1.

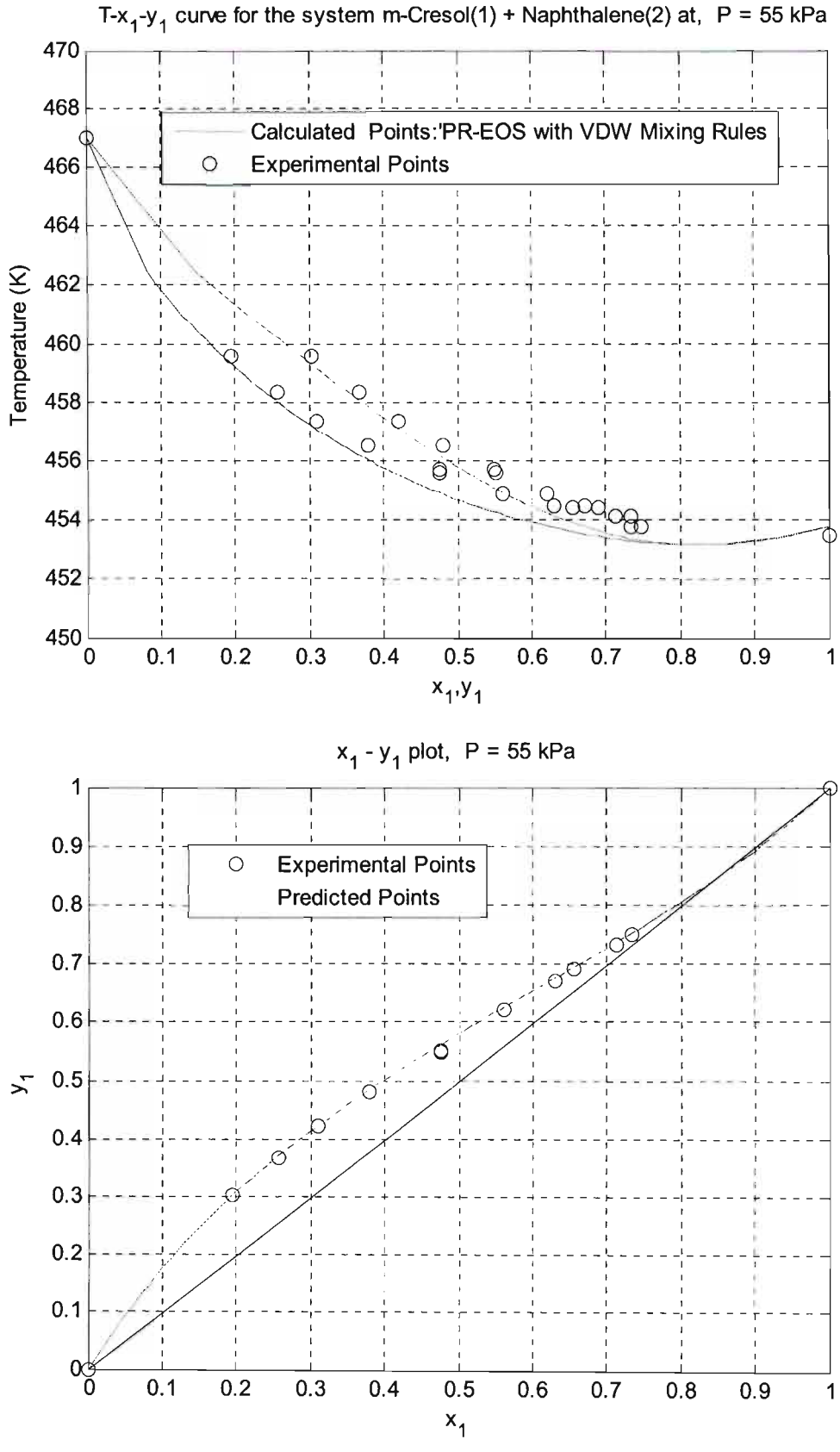

Figure 7 - 13: PR-EOS fitted to experimental VLE data for the system m-Cresol (1) + Naphthalene (2) at 55 kPa

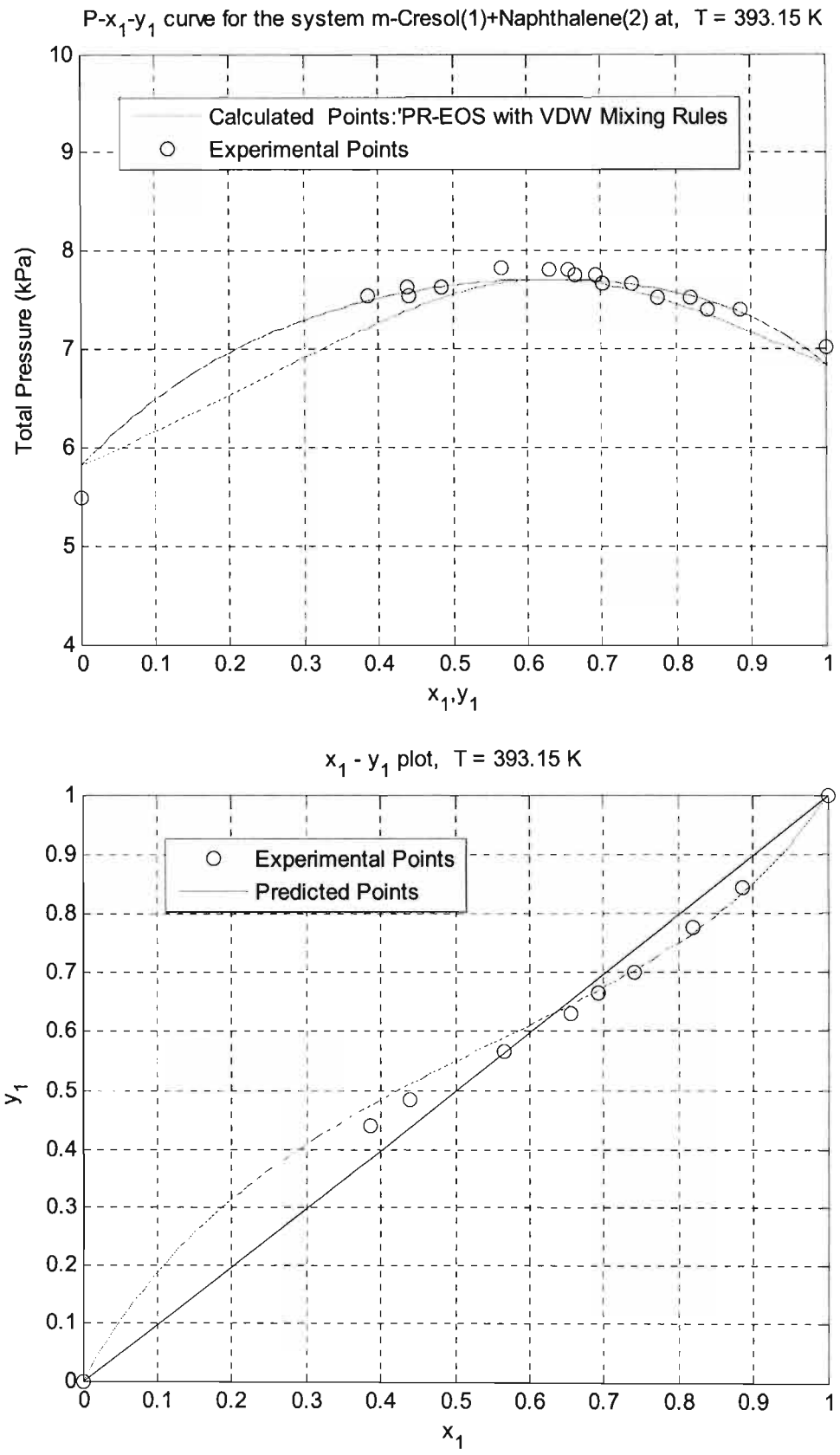

Figure 7 - 14: PR-EOS fitted to experimental VLE data for the system m-Cresol (1) + Naphthalene (2) at 393.15 K

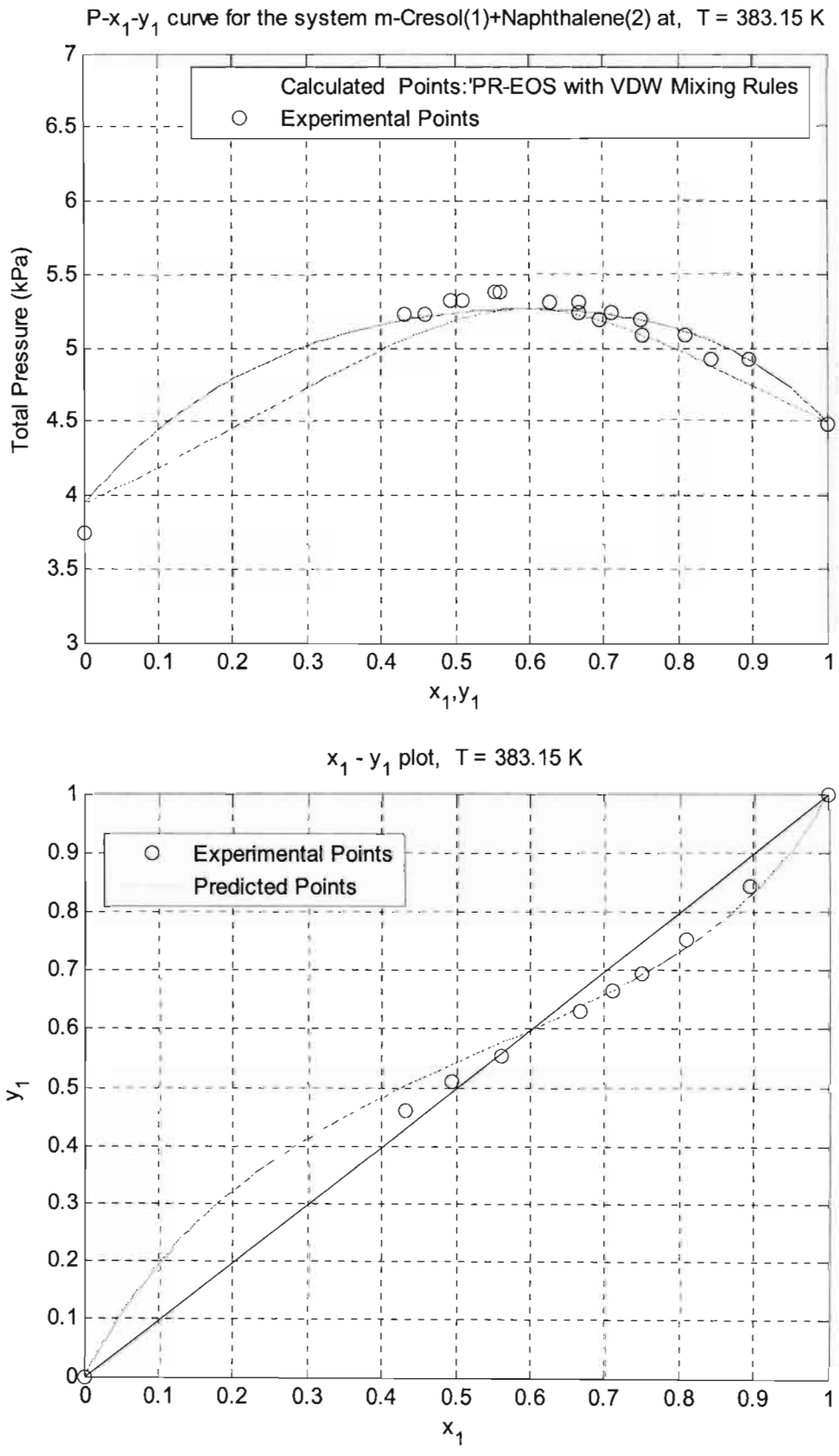

Figure 7 - 15: PR-EOS fitted to experimental VLE data for the system m-Cresol (1) + Naphthalene (2) at 383.15

7.3.1.3.2 Regression using the Wong and Sandler [1992] mixing rules.

The use of the theoretically correct mixing rule of Wong and Sandler [1992] requires in addition to the cross Virial coefficient interaction parameter, κ_{ij}, coefficients in the excess Helmholtz free energy model used. For the present study the NRTL model was chosen for use with the mixing rule and thus a total of four parameters had to be obtained from the measured equilibrium data. However, these parameters were reduced to a total of three after having set the non-randomness parameter (alpha). The value chosen for the constant was 0.14812, a value corresponding to that obtained from regression of equilibrium data for the same system using the gamma – phi method (see Table 7-10) as advocated by Walas [1985].

As has already been stated above, the measured VLE data for the cresol (1) + naphthalene (2) system were regressed using this mixing rule in the PR-EOS, PRSV-EOS and SRK-EOS. Table 7-13 shows the three parameters obtained for each data set and Figures 7-16 to 7-18 compares the experimental data to that obtained from the regression parameters. Also shown in Table 7-13 are the absolute average deviations in T or P and y.

Table 7 - 13: Model Parameters and Average Absolute Deviations from Experimental T-x-y and P-x-y data for the m-Cresol (1) + Naphthalene (2) system. Data regressed using the Theoretically correct Wong and Sandler [1992] mixing rule in conjunction with the NRTL Equation with alpha = 0.14812

Model	P = 55 kPa	T = 393.15 K	T = 383.15 K
PR-EOS			
$\lambda_{12} - \lambda_{22}$ (J/mol)	-20499.034	-23232.6704	-23986.9699
$\lambda_{21} - \lambda_{11}$ (J/mol)	22223.9848	26253.6523	27402.6391
k_{ij}	0.2335	0.26866	0.27171
ΔT or ΔP (K/kPa)	0.2595	0.04693	0.02988
Δy	0.00309	0.00312	0.002178
PRSV-EOS			
$\lambda_{12} - \lambda_{22}$ (J/mol)	-20059.5955	-23803.8331	-24582.7581
$\lambda_{21} - \lambda_{11}$ (J/mol)	21756.6571	27094.4531	28300.0312
k_{ij}	0.23379	0.26871	0.27172
ΔT or ΔP (K/kPa)	0.25217	0.04693	0.02989
Δy	0.00309	0.003116	0.002173
SRK-EOS			
$\lambda_{12} - \lambda_{22}$ (J/mol)	21651.745	-2697.6491	-2931.4728
$\lambda_{21} - \lambda_{11}$ (J/mol)	-19986.4939	2538.1662	2744.048
k_{ij}	0.23356	0.27334	0.30247
ΔT or ΔP (K/kPa)	0.25593	0.05117	0.049275
Δy	0.003086	0.013694	0.01322

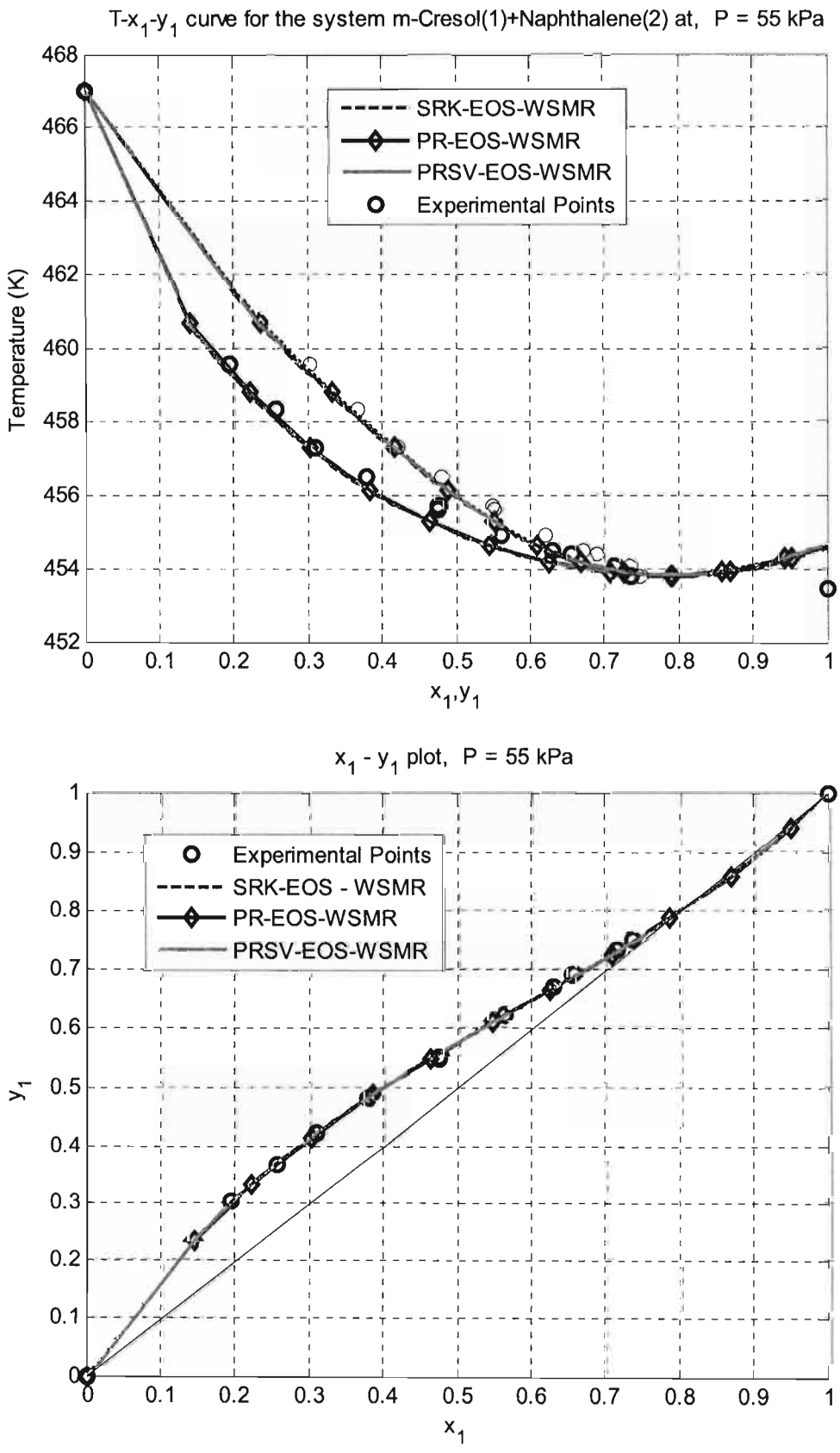

Figure 7 - 16: PR-EOS, PRSV-EOS and SRK-EOS fitted to experimental VLE data for the system m-Cresol (1) + Naphthalene (2) at 55 kPa.

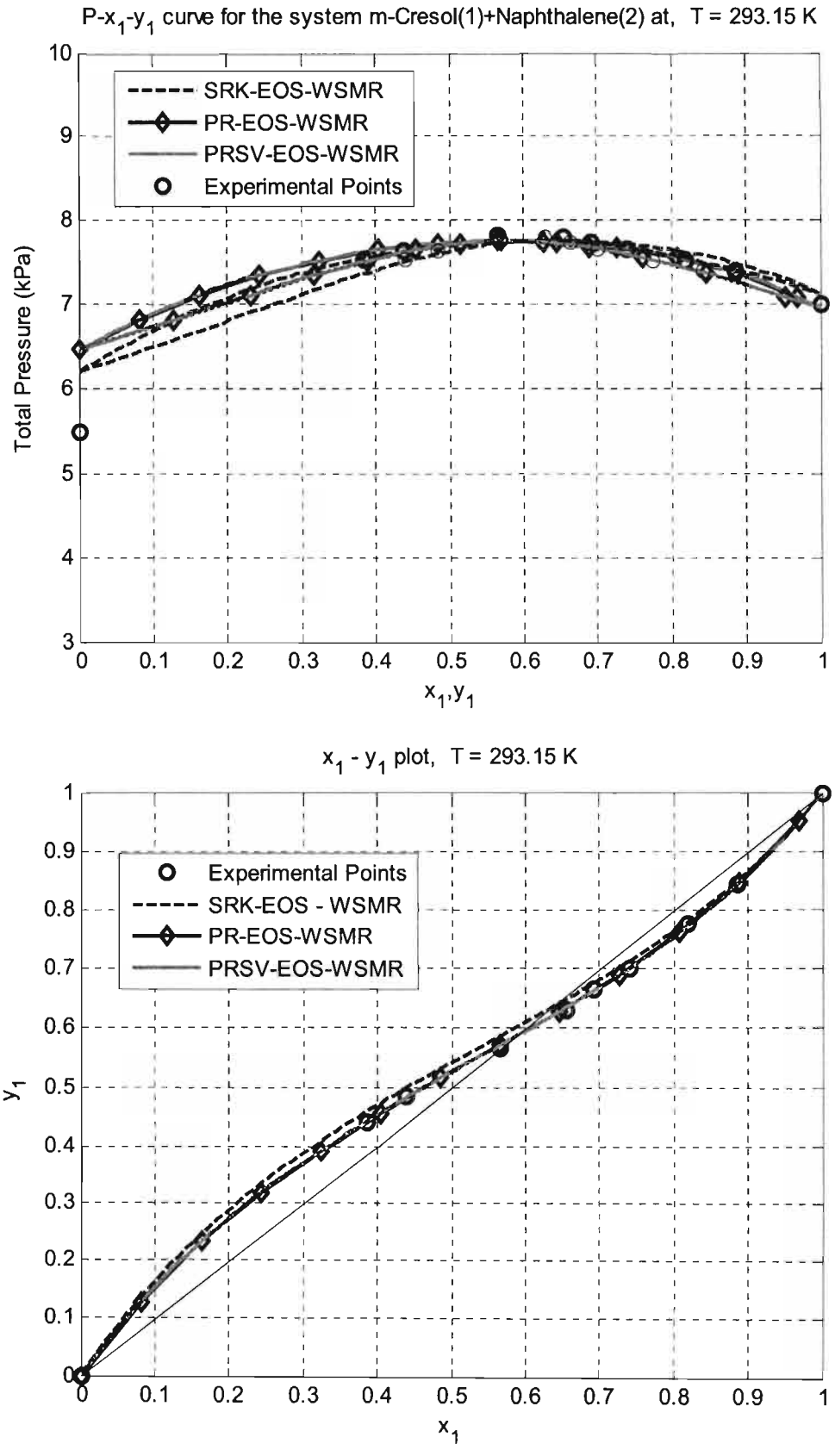

Figure 7 - 17: PR-EOS, PRSV-EOS and SRK-EOS fitted to experimental VLE data for the system m-Cresol (1) + Naphthalene (2) at 393.15 K

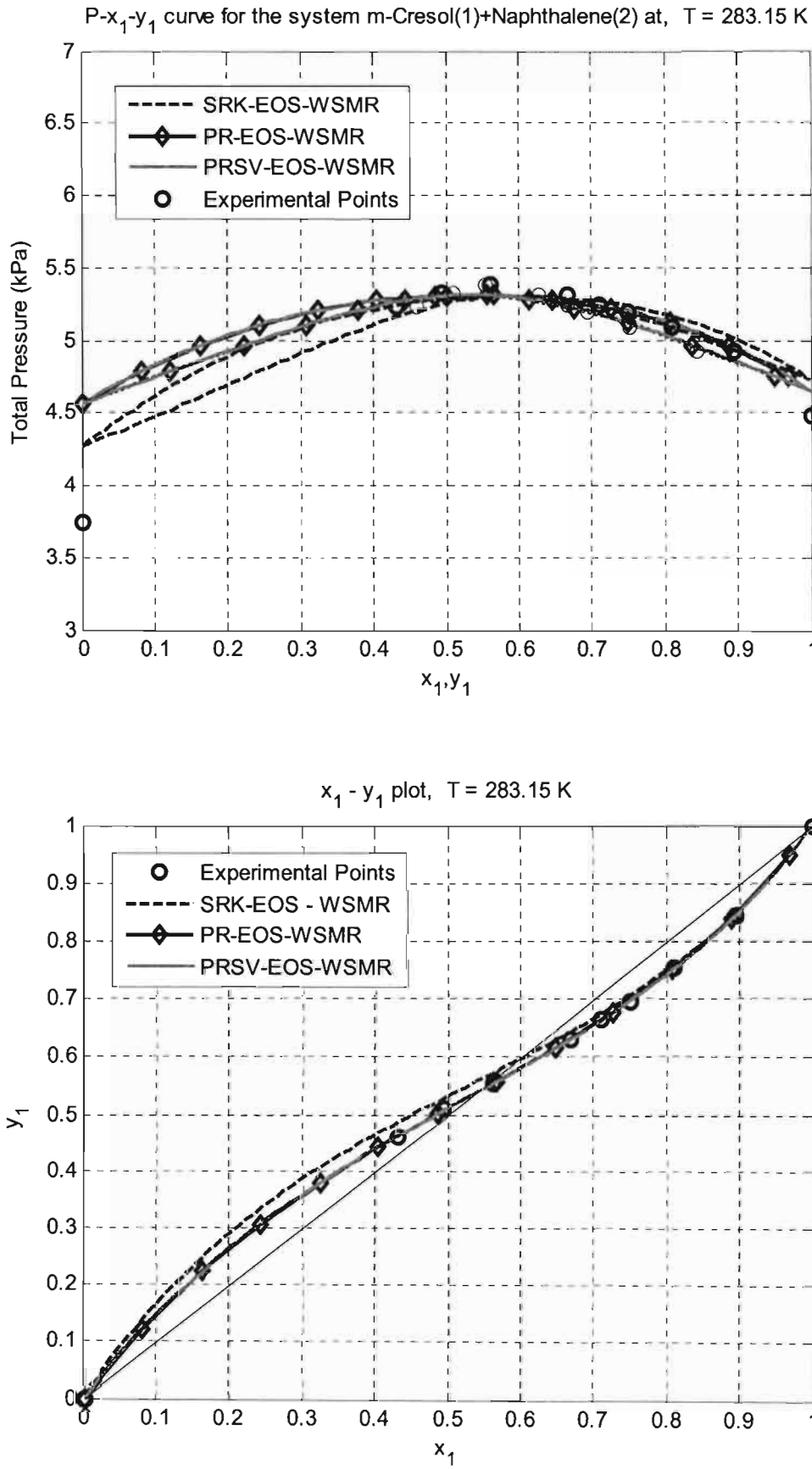

Figure 7 - 18: PR-EOS, PRSV-EOS and SRK-EOS fitted to experimental VLE data for the system m-Cresol (1) + Naphthalene (2) at 383.15

7.3.2 Thermodynamic consistency testing

The Area test of Herington [1951] and the Point test of Van Ness [1973] applied previously (Chapter 6) to the test systems data were also used to test the VLE data for the m-cresol (1) + naphthalene (2) binary system for consistency. Table 7-14 gives the coefficients used in the Redlich and Kister expansion in the Area test and Figures 7-19 to 7-21 summarise the results for both tests. An additional test, the Direct Test of Van Ness [1995] was also used. As outlined in Chapter 3, in order to apply this test the VLE data set is reduced using $\Sigma (\delta g)^2$ (where $g = x_1 \ln \gamma_1 + x_2 \ln \gamma_2$) as the objective function and the extent to which the residual $\delta \ln (\gamma_1/\gamma_2)$ fails to scatter about the zero axes provides an excellent measure of the departure of the data set from consistency (Van Ness [1995]). Van Ness [1995] also provides a quantitative criterion for the test. He gives a table of indices (see Section 3.12.3) starting from 1 for excellent data and going to 10 for poor data. Table 7-15 and Figures 7-22 and 7-23 summarise the results for this test.

Table 7 - 14: Coefficients in the Redlich and Kister Expansion for use in The Area Test.

Data set at	a'	b'	c'	d'
55Kpa	-0.0193	0.4556	-0.1541	0.0282
120 °C	-0.0572	0.7793	-0.2079	0.1005
110 °C	-0.0507	0.8463	-0.1871	0.2811

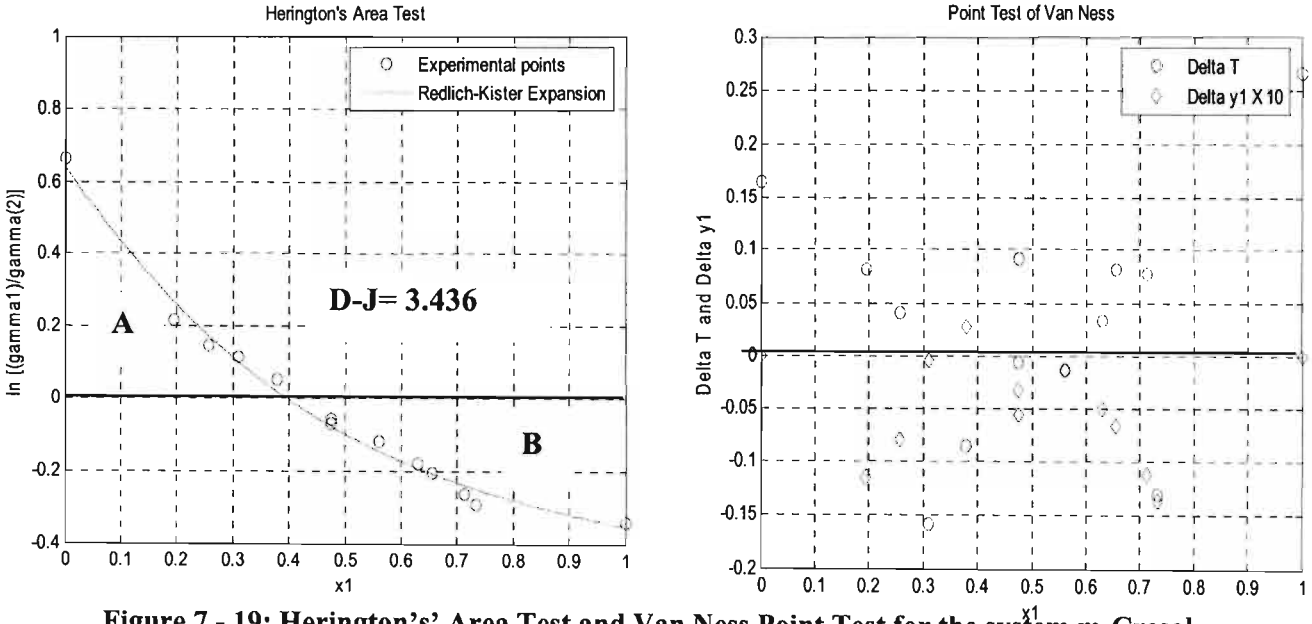

Figure 7 - 19: Herington's' Area Test and Van Ness Point Test for the system m-Cresol (1) + Naphthalene (2) at 55 kPa.

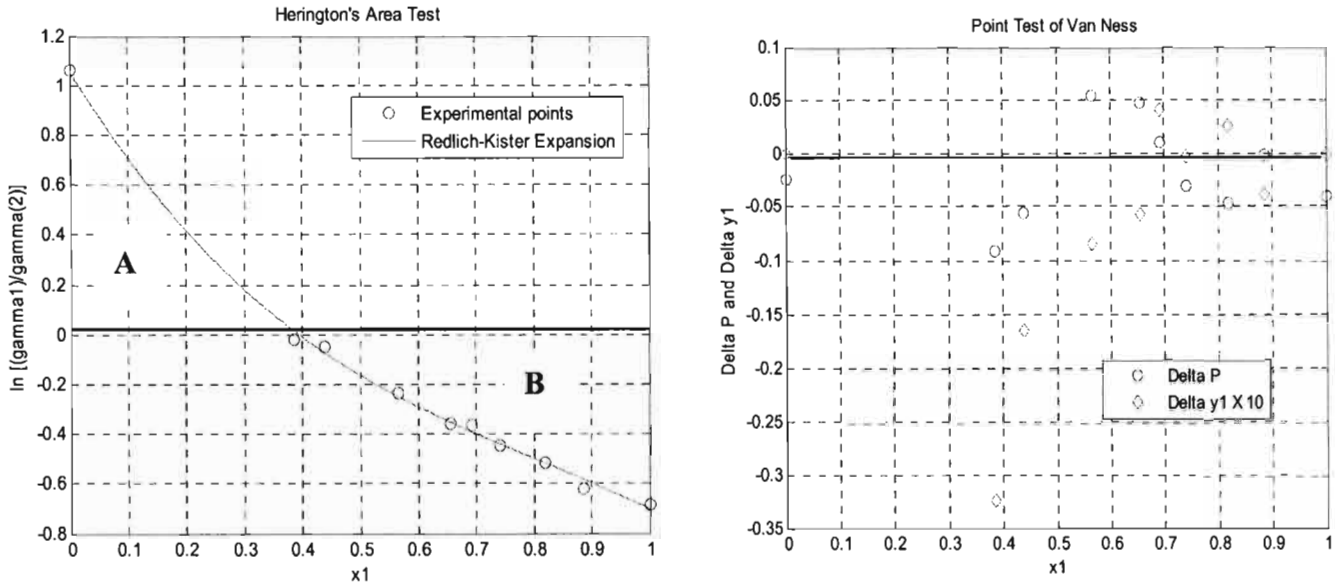

Figure 7 - 20: Herington's Area Test and Van Ness Point Test for the system m-Cresol (1) + Naphthalene (2) at 120°C.

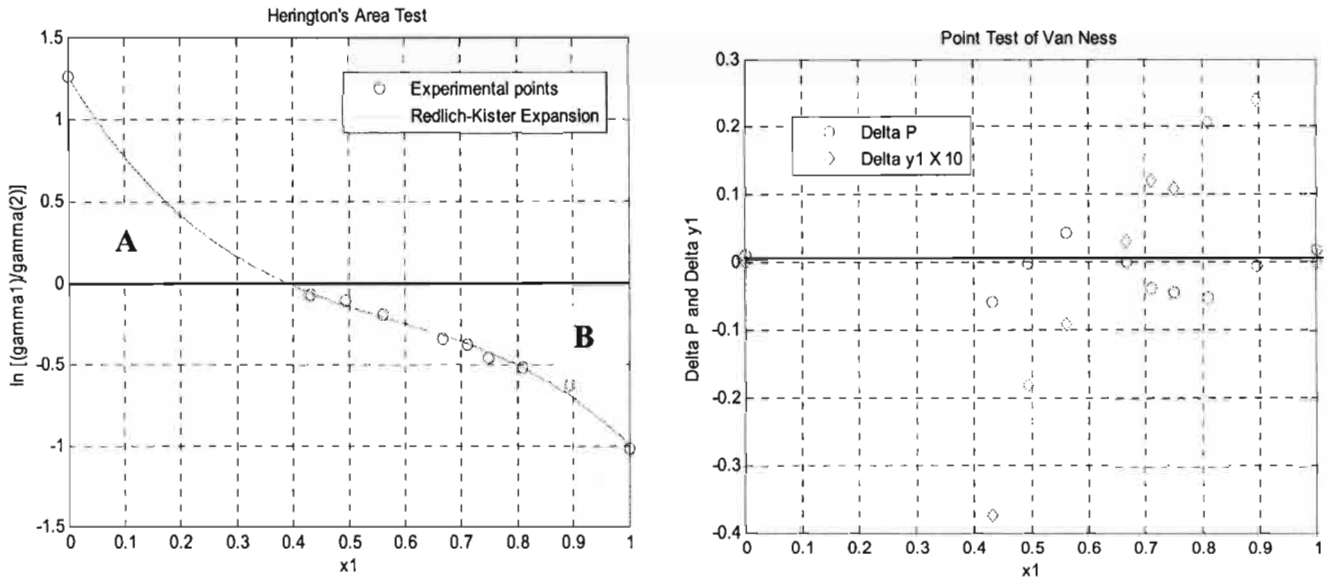

Figure 7 - 21: Herington's Area Test and Van Ness Point Test results for the system m-Cresol (1) + Naphthalene (2) at 110°C.

Table 7-15 below sumarises the results of the Direct test. It gives the RMS values of the residual $\delta \ln (\gamma_1/\gamma_2)$ together with the corresponding consistency index.

Table 7 - 15: Van Ness [1995] Direct Test (1 :Exellent Data , > :10 Poor data)

System at	RMS $\delta \ln (\gamma_1/\gamma_2)$	Consistency index
55Kpa	0.03385	2
120°C	0.04961	2
110°C	0.08756	4

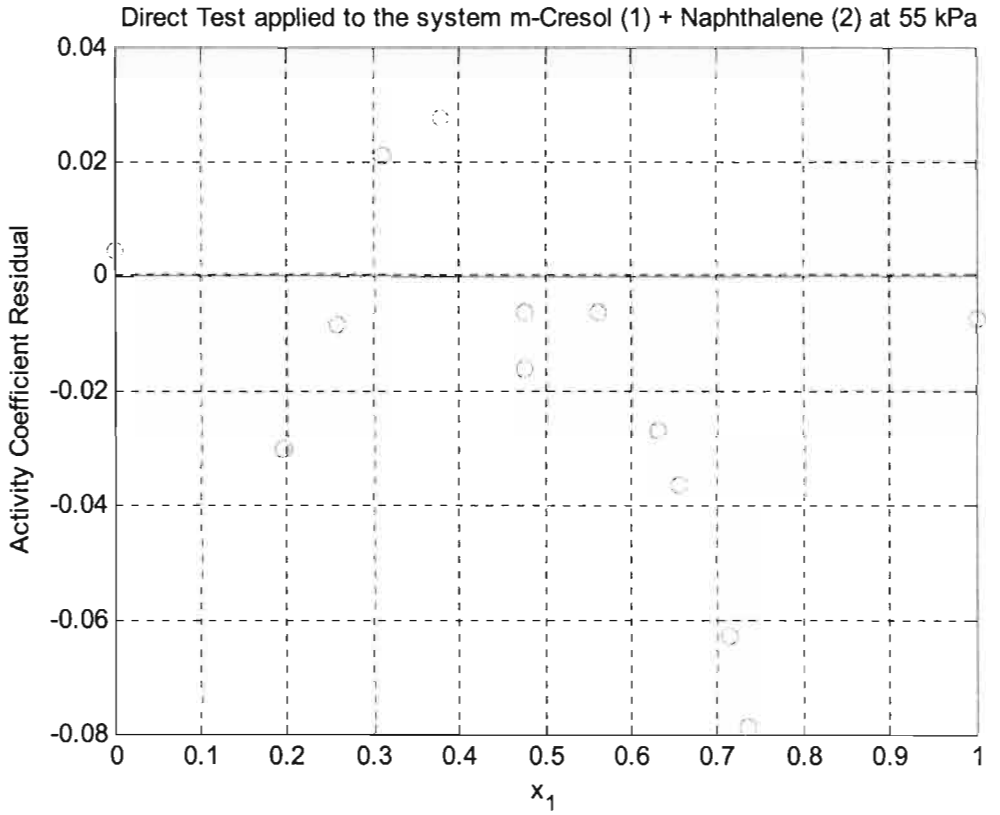

Figure 7 - 22 (a): The Direct Test Results ($\delta \ln (\gamma_1/\gamma_2)$ residuals) for the m-Cresol (1) + Naphthalene (2) system at 55 Kpa .

The low indices of 2, 2 and 4 in Table 7-15 indicate that the data are of high thermodynamic consistency. The thermodynamic consistency of all the data sets is discussed in more detail in Chapter 8.

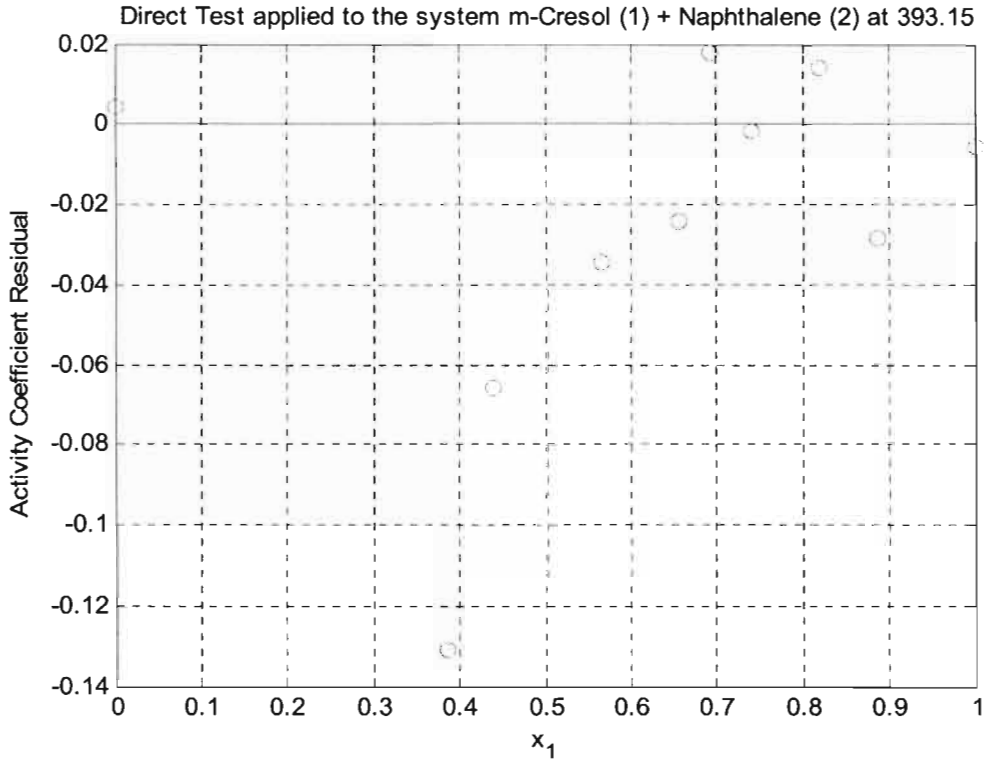

Figure 7-23 (a) The Direct Test Results ($\delta \ln (\gamma_1/\gamma_2)$ residuals) for the m-Cresol (1) + Naphthalene (2) system at 393.15 K.

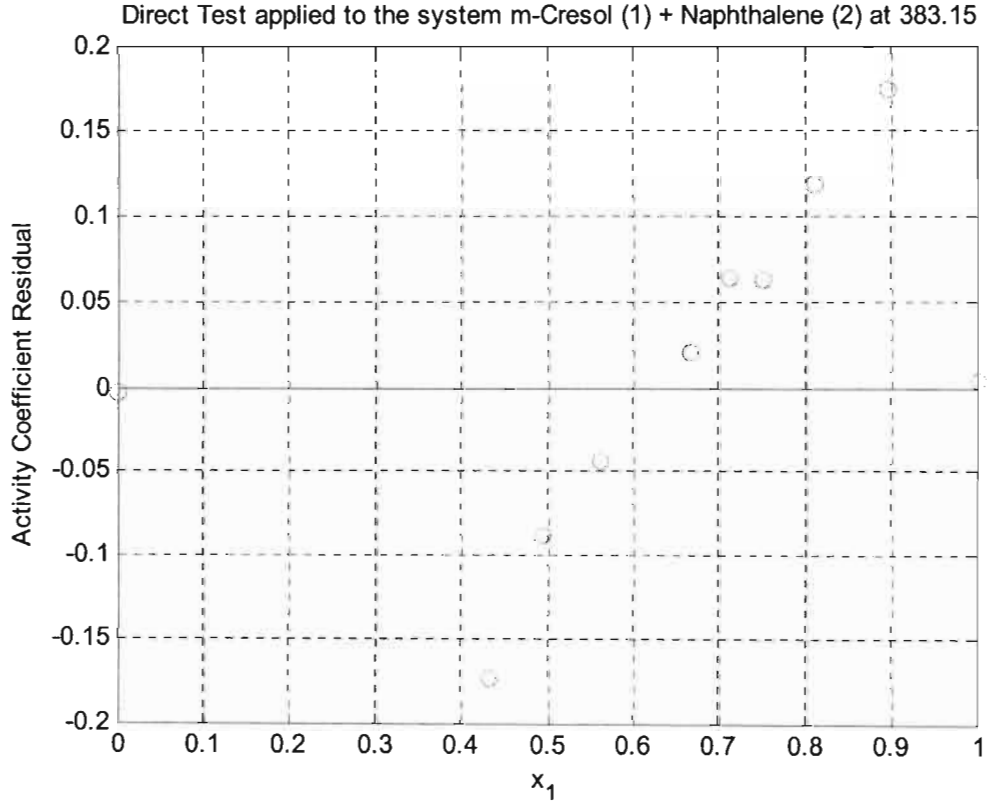

Figure 7 - 23 (b) :The Direct Test Results ($\delta \ln (\gamma_1/\gamma_2)$ residuals) for the m-Cresol (1) + Naphthalene (2) system at 383.15 K.

7.4: Vapour-liquid-liquid equilibria

7.4.1 VLLE analysis (m- Cresol (1) + Water (2) system)

The m-cresol (1) + water (2) system forms a partially miscible liquid mixture and thus gives rise to vapour-liquid-liquid equilibria. The vapour pressures for both components have been presented and analysed above (see Section 7.1). Following is the treatment of the systems' VLLE.

G C calibration

The use of pure ethanol in the calibration process has already been highlighted above. The corresponding GC calibration curves are shown in Figures 7-24 and 7-25. For this system linear response factors were obtained as seen in these figures.

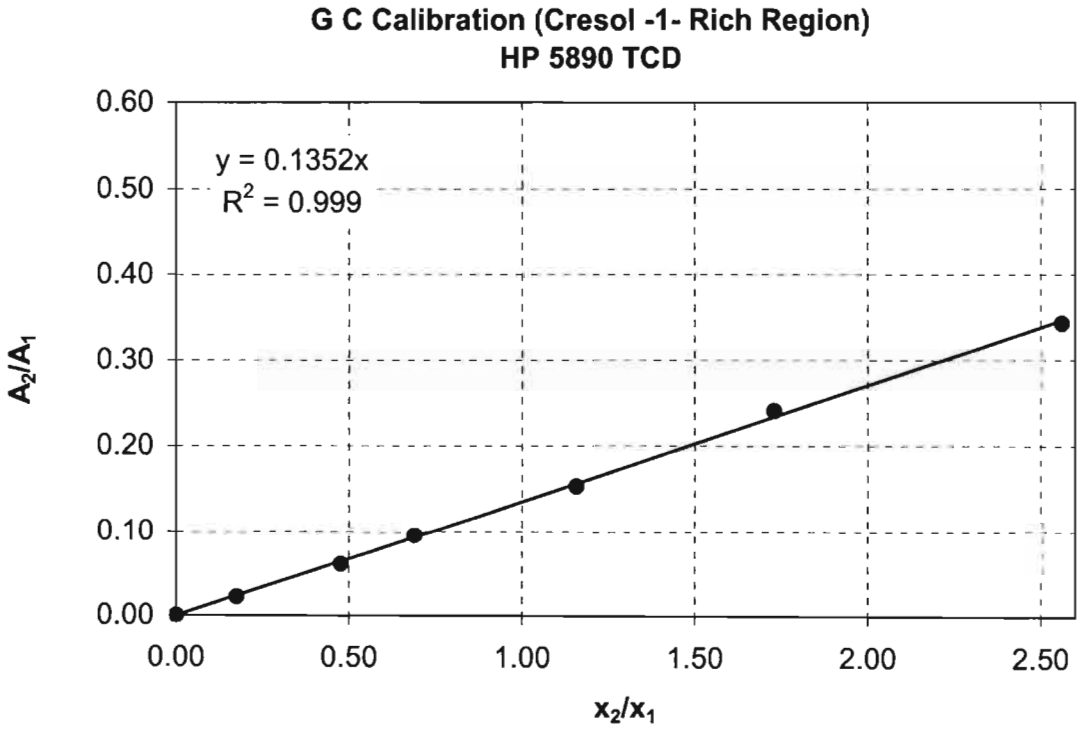

Figure 7 - 24: GC Calibration Curve for the m-Cresol (1) + Water (2) System

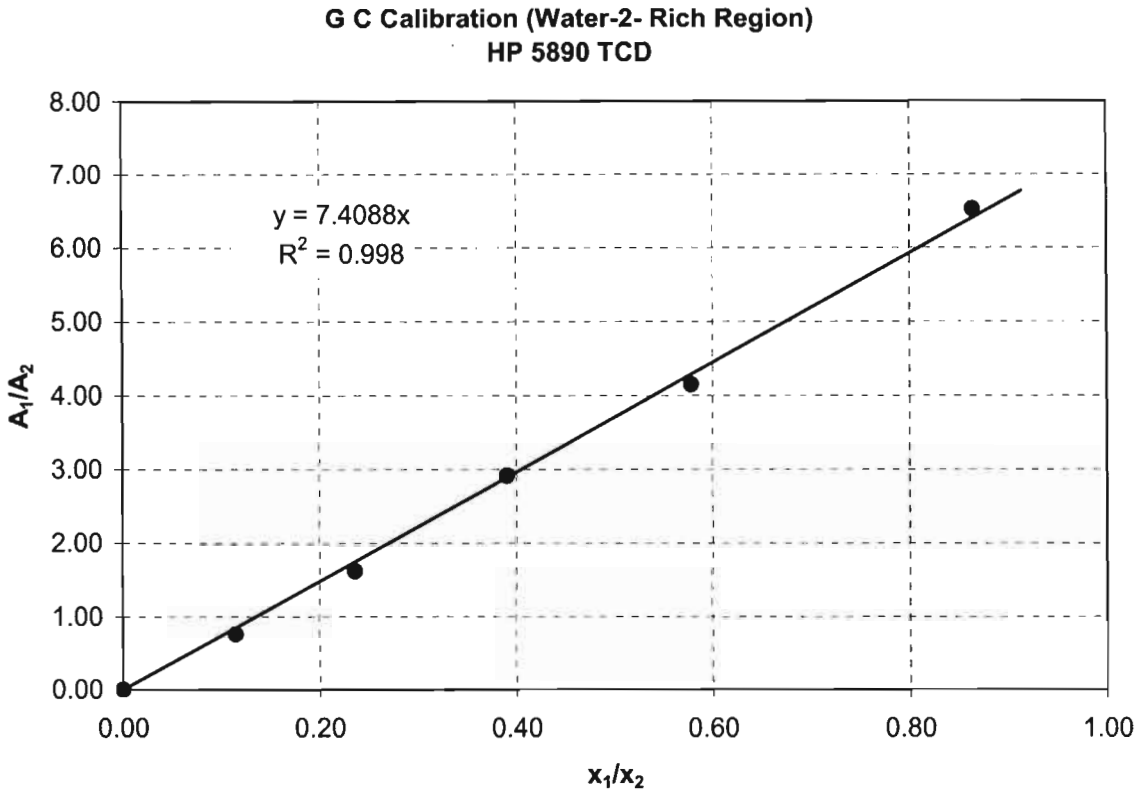

Figure 7 - 25: GC Calibration Curve for the m-Cresol (1) + Water (2) System (Dilute Cresol Region)

7.4.1 .1 Pure -component properties

The two components making this system have already been used in the systems analysed; water in Chapter 6 and cresol above. Their pure component critical parameters have thus been determined and are shown in Table 7 -16 below.

Table 7 - 16 Pure-component critical parameters for m-Cresol and Naphthalene

	V_c cm^3/mol	Z_c	T_c K	ω	P_c kPa
m-Cresol	310	0.2409	705.8	0.464	4559.625
Water	217.6	0.229	647.3	0.344	22055

VLLE data

As was the case for the heterogeneous water (1) + MBE (2) test system, the VLLE measurements were obtained by measuring first VLE data in both homogeneous m-cresol and water regions and then the LLE. The VLLE data are shown in Table 7-17. The data are also plotted in Figure 7-26. Table 7-18 and Figure 7-27 show only the LLE data.

Again, as was the case for the water + MBE test system, the three-phase temperature and vapour composition had to be determined. However unlike in the earlier case where these points were found by first fitting the T-y data for both homogeneous MBE and Water regions to fourth order polynomials and then extrapolating the resultant equations to the point were they met, such calculations could not be done for this system. This was a result of the observed very narrow homogeneous water-rich region for which only a single point was measured, which made it impossible to fit a polynomial to the data or any equation for that matter. Because smooth LLE and T-x data were obtained for the homogeneous cresol-rich region the alternative approach used was to fit both these data sets into polynomial equations and then solving them for the point of intersection. This gave the three-phase temperature and the composition of one of the two liquids in VLLE. The compositions of the corresponding vapour and the second liquid in equilibrium were then read off or extrapolated from the T –y and LLE data respectively. These three points (the three-phase vapour composition and the composition of the associated two liquids in equilibrium) together with data from the homogeneous regions give a complete description of the VLLE for the system studied. The compositions of these three phases in VLLE are indicated by asterisks in Table 7-14.

Table 7 - 17: Isobaric VLE and VLLE data for the Cresol (1) + Water (2) system at 55 kPa. (asterisks, * indicate VLLE data)

T [K]	x_1	y_1
357.97	0.0000	0.0000
357.17	0.0030	0.0074
357.53*	0.0049*	0.0112*
357.53*	0.3228*	0.0112*
360.79	0.5078	0.0108
365.13	0.5856	0.0112
378.53	0.7600	0.0207
383.67	0.7847	0.0248
453.49	1.0000	1.0000

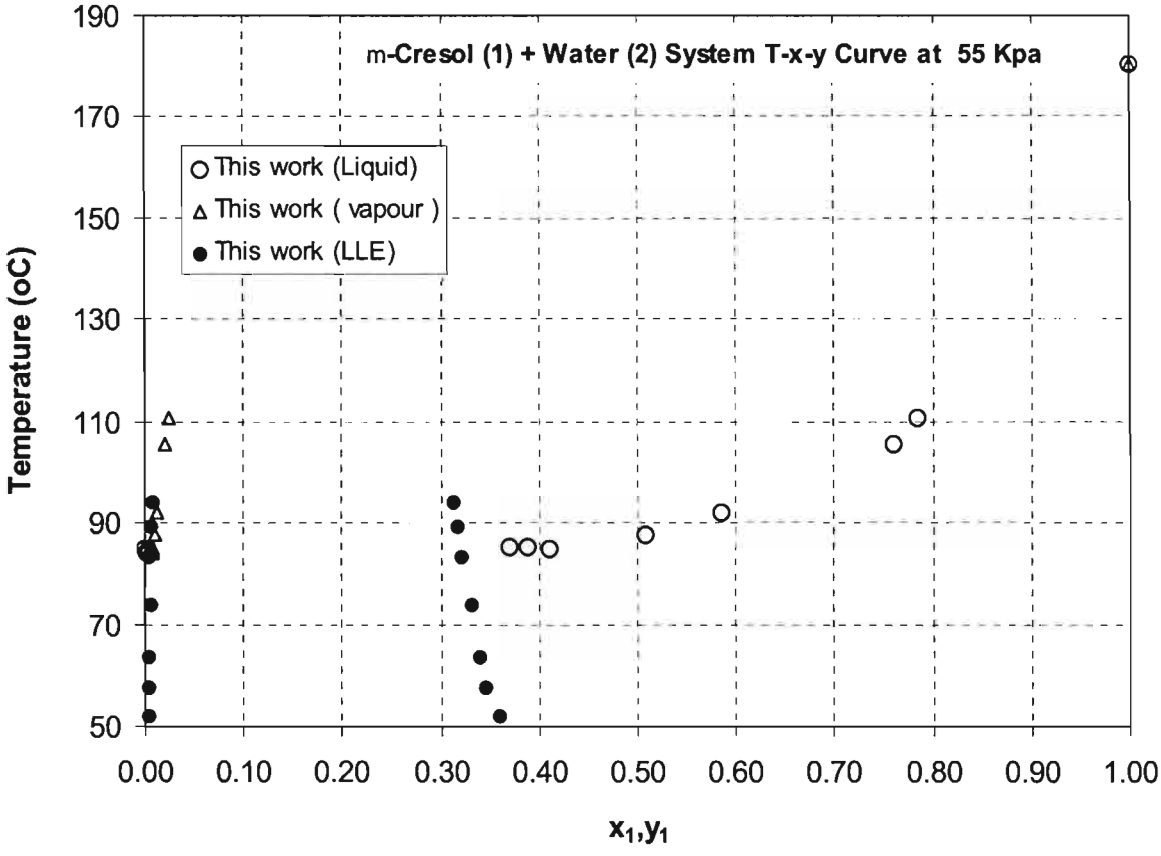

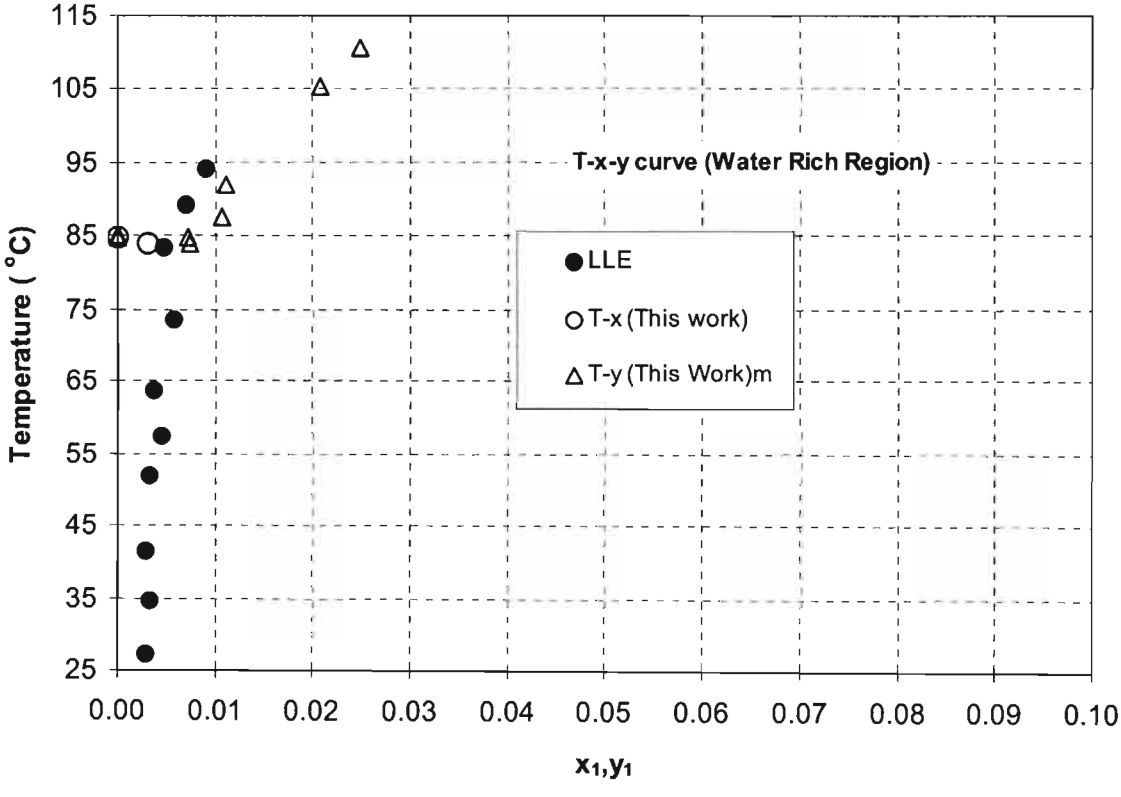

Figure 7 - 26: Isobaric VLE and VLLE data for the Cresol (1) + Water (2) system at 55 kPa

Table 7 - 18: LLE data for the m-Cresol (1) + Water (2) system

T [K]	x_1^{alpha}	x_1^{beta}
300.44	0.003	0.418
307.63	0.003	0.405
314.73	0.003	0.382
324.98	0.003	0.361
336.80	0.004	0.340
330.59	0.005	0.345
346.76	0.006	0.332
362.33	0.007	0.317
356.61	0.005	0.322
367.35	0.009	0.312

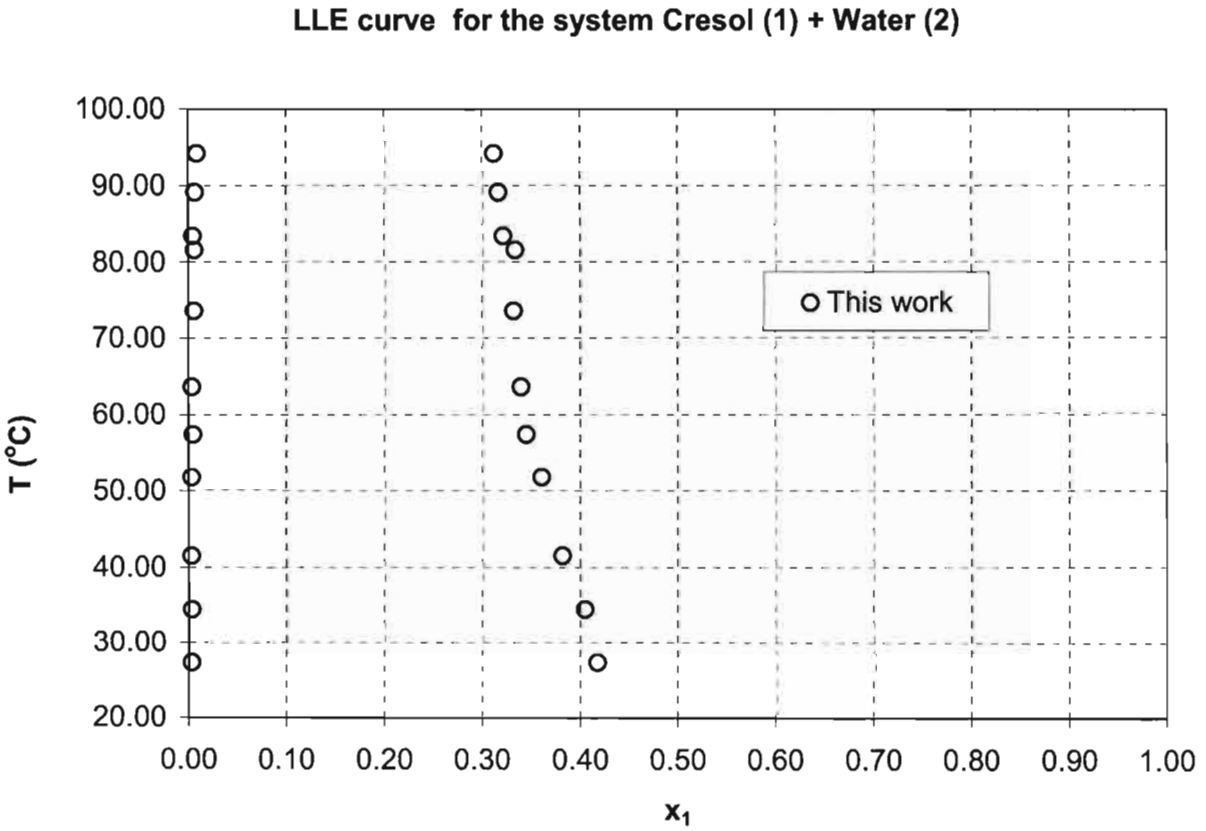

Figure 7 - 27: LLE data for the m-Cresol (1) + Water (2) system

The above figure shows that cresol is sparingly soluble in water. However, the solubility of water in cresol is quite appreciable.

Experimental activity coefficients

The computation of the experimental activity coefficients from the measured data has been dealt with in the earlier sections. The experimental activity coefficients obtained for the present system are shown in Table 7-19 below. The extreme non ideality of the system is evident from these activity coefficient values.

Table 7 - 19 Experimental Activity Coefficients for the system m-Cresol (1) + Water (2) at 55 kPa

x_1	γ_1	γ_2
0.0000	338.2995	0.9600
0.0030	132.3054	0.9853
0.5078	0.9274	1.7368
0.5856	0.6566	1.7617
0.7600	0.4689	1.9072
0.7847	0.4253	1.7969
1.0000	0.9923	1.8452

7.4.1.2 VLLE data reduction (The Gamma-Phi-method)

The NRTL, TK-Wilson and UNIQUAC equations are all applicable to systems of partial liquid miscibility. The measured data were regressed to obtain parameters in these models. However, unlike in the case for the water (1) + MBE (2) test system where the data were regressed first to give parameters for the homogeneous regions and then for the entire VLLE data set, for this system the regression could not be carried out on data in the homogeneous water region due to the narrowness of the observed single phase region. Only a single point could be measured in this region.

Figures 7-28 and 7-29 summarise the obtained results for the TK-Wilson model and compare the experimental data to the data predicted from the model using the regression parameters. The two graphs are for the regression using the entire data set and using data in the homogeneous cresol regions respectively. Similar graphs for the other models are, as before, presented in Appendix 1. The model parameters are shown in Table 7-20.

Table 7 - 20: Model Parameters for the m-Cresol (1) + Water (2) System at 55 kPa

Quantity	NRTL	TK-Wilson	UNIQUAC
	Homogeneous cresol Region		
$\lambda_{12}-\lambda_{22}$ (J/mol)	2396.6041	-6697.4343	1114.1758
$\lambda_{21}-\lambda_{11}$ (J/mol)	-656.1553	7605.4372	48019.7646
α	-2.3733	-	-
ΔT (K)	0.7195	2.4776	3.6971
Δy	0.0101	0.0070	0.0122
	Entire Data set		
$\lambda_{12}-\lambda_{22}$ (J/mol)	2394.7809	-6613.1635	2081.0216
$\lambda_{21}-\lambda_{11}$ (J/mol)	-675.4212	7509.2785	4231.8406
α	-2.269	-	-
ΔT (K)	0.7467	1.9832	5.3630
Δy	0.0087	0.0065	0.0663

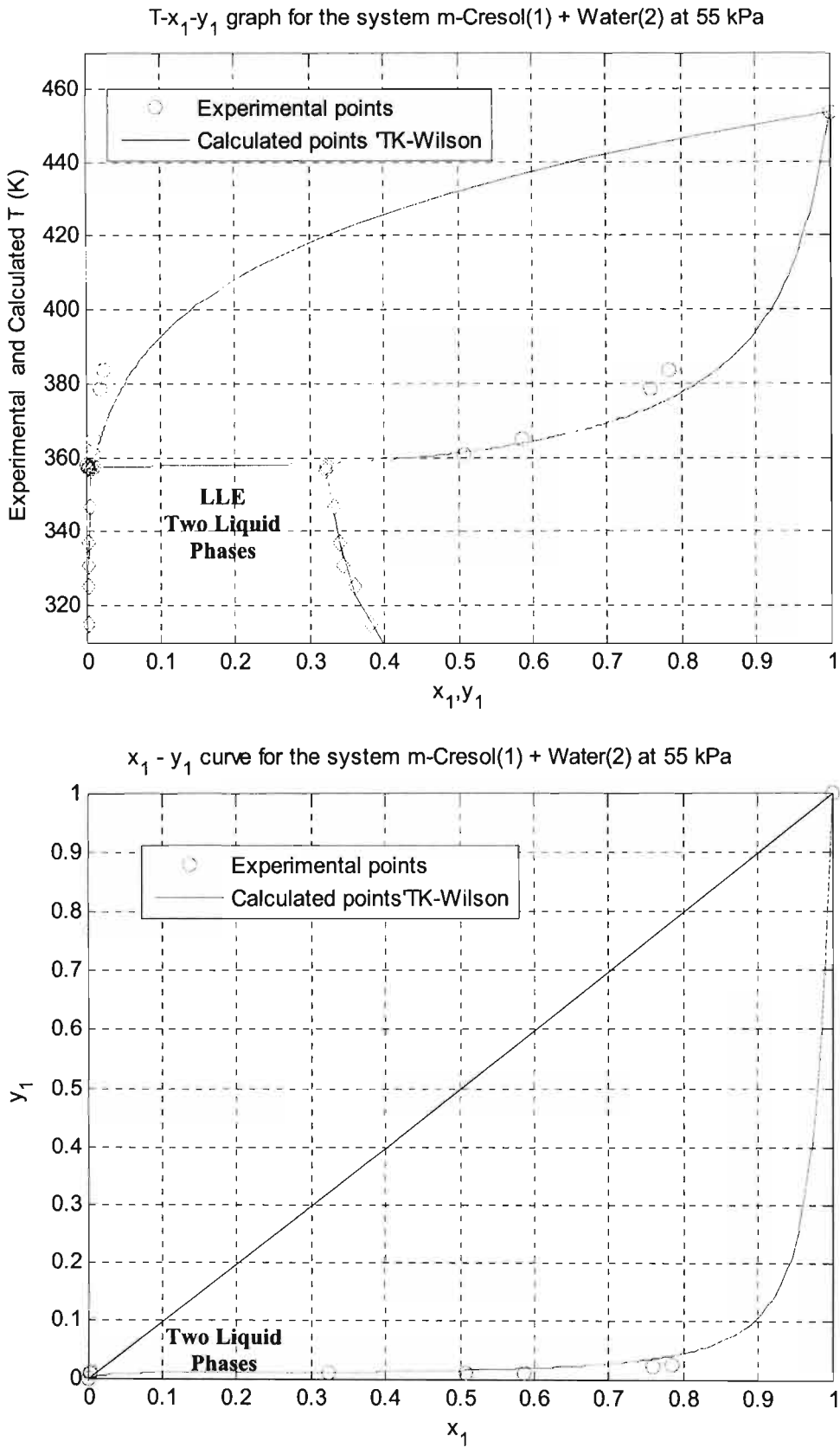

Figure 7 - 28: T-K Wilson model fitted to entire experimental P-x_1-y_1 data for the m-Cresol (1) + Water (2) System at 55 kPa

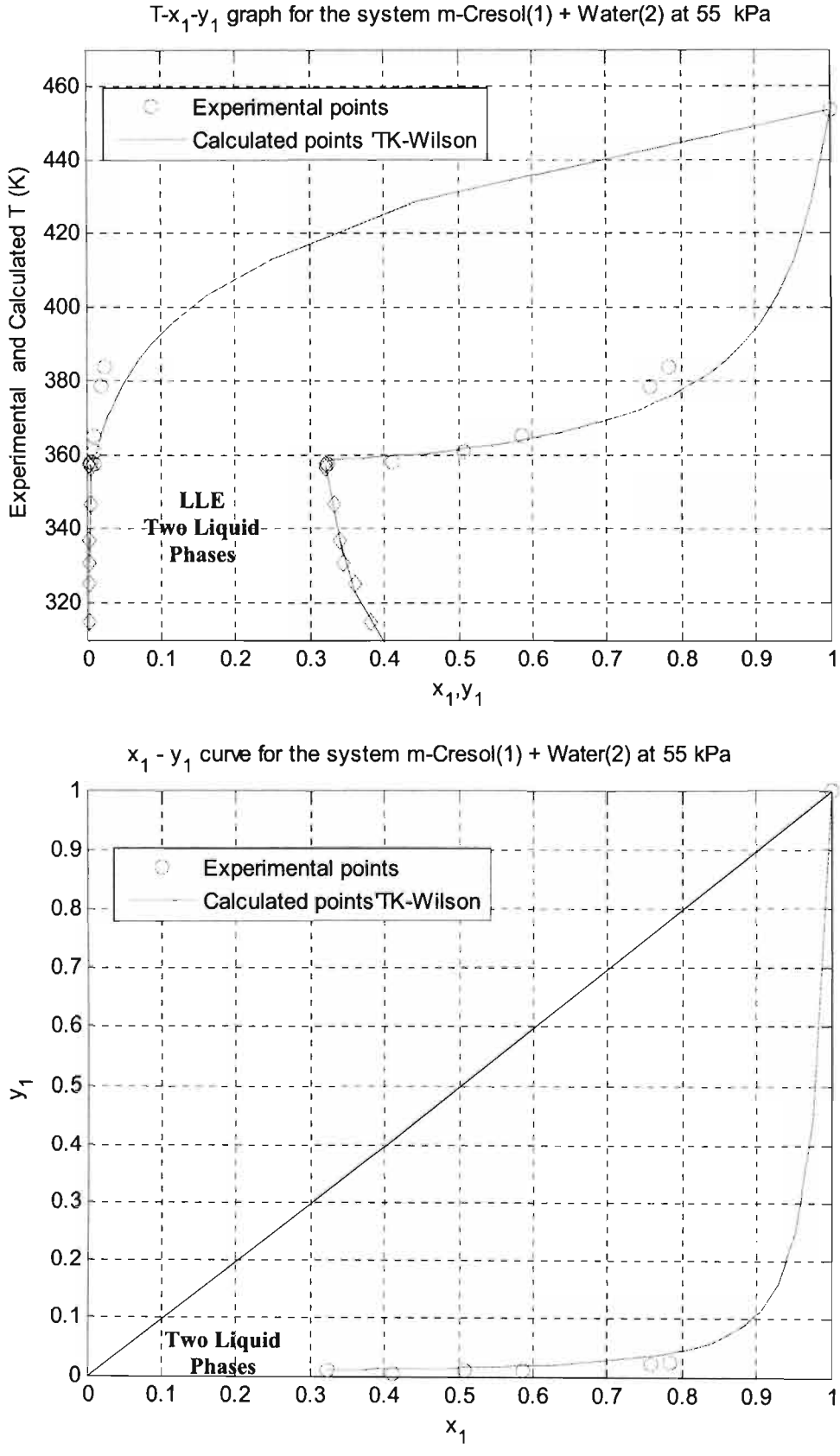

Figure 7 - 29: TK-Wilson model fitted to Experimental P-x_1-y_1 data for the m-Cresol (1) + Water (2) System at 55 kPa in the homogeneous Cresol Region

7.4.2 Thermodynamic consistency testing

The Point test, the Area test and the Direct test have already been discussed above. The point test was applied only to the data in the homogeneous m-cresol region while the other tests were applied to the entire data set including the three phase compositions. The results for the tests are summarized in Table 7-21 and Figures 7- 30 and 7-31.

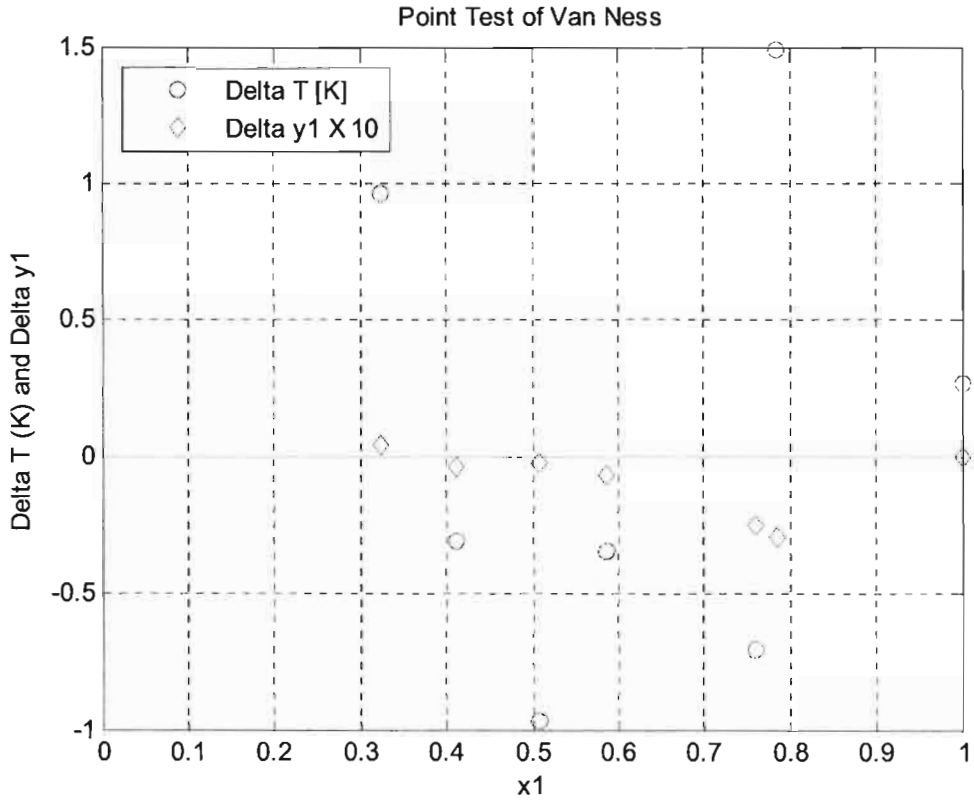

Figure 7 - 30: Van Ness [1972] Point Test applied to data in the Homogeneous Cresol Region for the System: m-Cresol + Water (2) at 55 kPa.

Table 7 - 21: Coefficients in the Redlich and Kister expansion for use in The Area Test for the System m-Cresol (1) + Water (2) at 55 kPa.

Data set at	a'	b'	c'	d'	D-J
55Kpa	-0.0660	2.7156	-1.2126	0.8619	-6.629

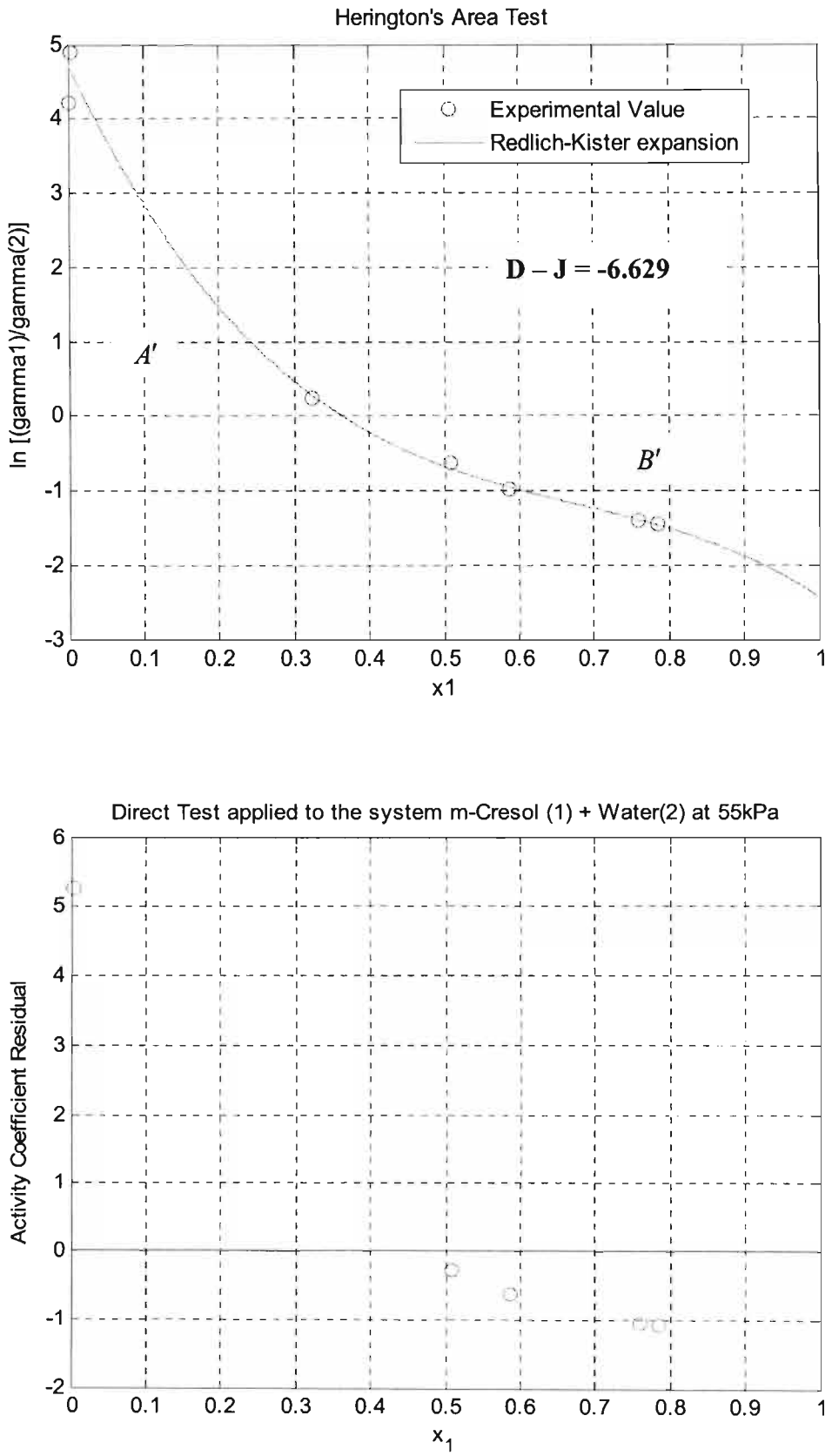

Figure 7 - 31: (a) Area Test and (b) Van Ness [1995] Direct Test applied to data in the Homogeneous Cresol Region for the System: m-Cresol + Water (2) at 55 kPa.

7.5 VLLE data (o-Tolunitrile (1) + Water (2) system)

For this system, VLE data could not be measured in either of the two homogeneous Water and o-tolunitrile regions. It was observed during the trial measurements that the equilibrium temperature would not be constant regardless of how long the system was left to attain equilibrium. The temperature kept on fluctuating and never attained a constant value. This was partly a result of the very large relative volatility of the system's components which have a boiling point difference of more than 100 degrees K at 55 kPa and partly a result of the large immiscibility region of the system (see Figure 7-34). The temperature fluctuations can then be explained in terms of 'flashing' of the more volatile component , water in this case, as the condensate returned to the boiling chamber, which was rich in the less volatile component (Tolunitrile) and hence at a temperature higher than the boiling point of water. Recommendations as to how to obtain data for such systems are presented in chapter nine.

The VLE data in the homogeneous regions were therefore computed from the LLE data. The prediction of VLE from LLE was presented in chapter three (see Section 3.10). It was shown that the LLE data can be regressed to give parameters in the excess Gibbs energy models and then the resultant parameters used to predict VLE in the miscible regions. This subject is treated further below, after a presentation of the GC calibration curves and LLE data.

GC calibration

The calibration process was similar to that for the m-cresol (1) + water (2) system. Ethanol was used in making the gravimetrically prepared heterogeneous mixtures of the system's components homogeneous. This has already been discussed above and the calibration curves for the dilute and rich tolunitrile regions are shown in Figures 7-32 and 7-33.

7.5.1 VLLE analysis

7.5.1.1 Pure-component properties

The only unknown pure component properties were those for tolunitrile. They were all obtained from the DDB except V_c (and hence Z_c) which was computed from the Lydersen group contribution method (Reid et al. [1988]) These parameters are tabulated below

Table 7 - 22: Pure component critical parameters for Tolunitrile

	V_c cm^3/mol	Z_c	T_c K	ω	P_c kPa
Tolunitrile	402.6	0.2695	709	0.402	3951.675

LLE data

LLE data were measured from 17 °C to 83°C. These data are shown in Table 7-23 and in Figure 7-34.

Table 7 - 23: LLE data for the Tolunitrile (1) + Water (2) system

T [K]	x_1^{alpha}	x_1^{beta}
290.68	0.0170	0.9795
296.50	0.0111	0.9574
303.69	0.0121	0.9382
315.61	0.0148	0.9331
325.57	0.0136	0.9016
344.98	0.0182	0.8725
351.09	0.0175	0.8291
355.92	0.0243	0.8014

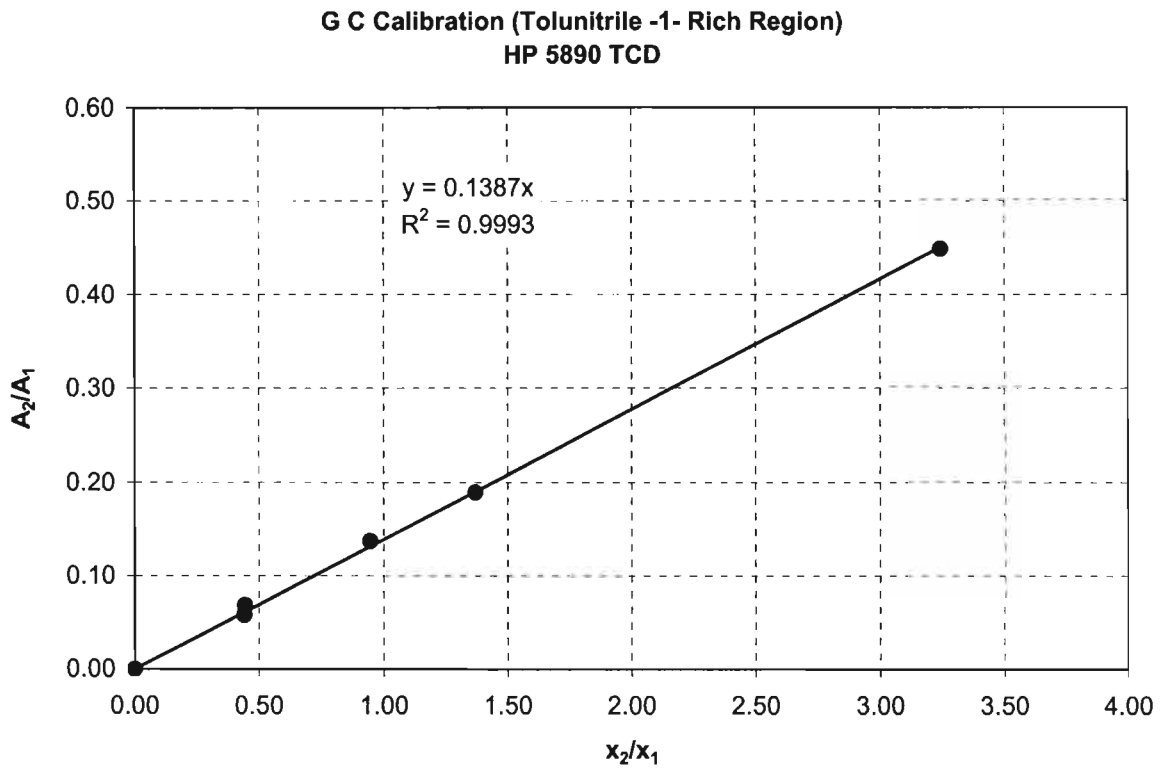

Figure 7 - 32: GC Calibration Curve for the Water (1) + Tolutintrile (2) System (Water dilute Region)

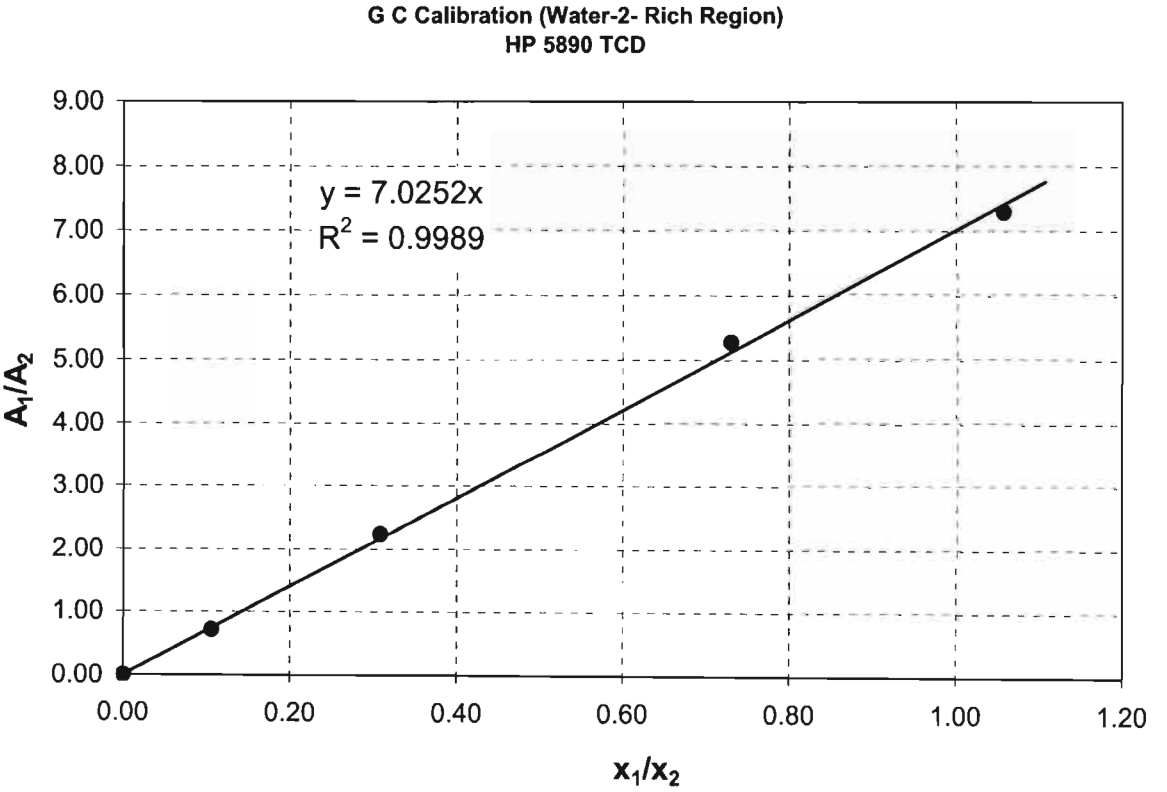

Figure 7 - 33: G C Calibration Curve for the Water (1) + Tolunitrile (2) system (Water rich region)

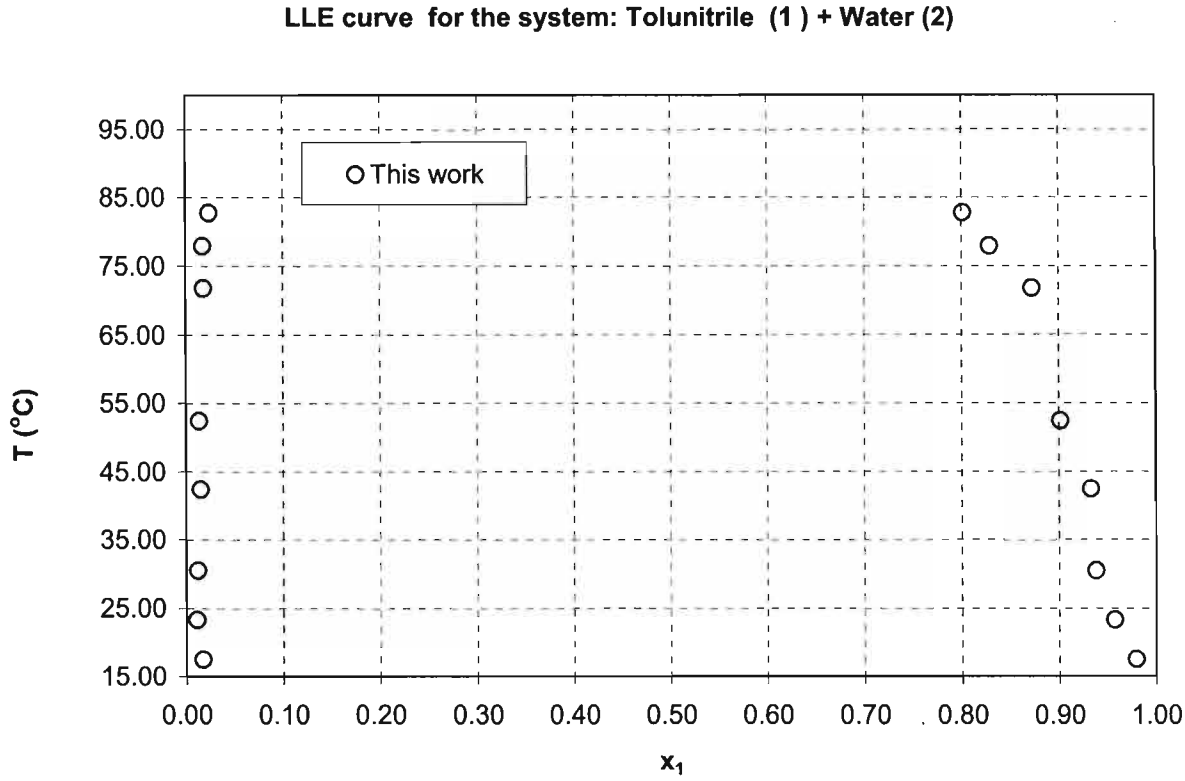

Figure 7 - 34: LLE data for the Tolunitrile (1) + Water (2) system

7.5.1.2 Prediction of VLE from LLE

In this section, the VLE in the miscible regions for the tolunitrile (1) + water (2) system are computed from the solubility data presented above. The procedure followed is given in Section 3.10 and in Appendix 2. The LLE data were fitted to the Three Suffix Margules, Van Laar and NRTL Models. The parameters obtained for each model are shown in Table 7-24. These model parameters were then plotted against the temperature to find their temperature dependence, which allowed for the extrapolation to give the parameters at 90°C - the temperature for which the VLE were predicted. Figures 7-35 to 7-37 show the parameter temperature dependence for the models while Table 7-25 gives the predicted VLLE which are also shown in Figures 7-38 and 7-39. Only data from the Van Laar Model are presented as it is the only one that correctly predicted phase separation.

Table 7 - 1: Model parameters from Solubility data for the system Tolunitrile (1) + Water (2)

Solubility Data			Model Parameters (J/mol)					
x_1^{α}	x_1^{β}	T [K]	Margules		Van laar		NRTL	
			A_{12}	A_{21}	A_{12}	A_{21}	$g_{12} - g_{22}$	$g_{21} - g_{11}$
0.0111	0.9574	296.50	4.6083	-3.4767	4.5818	3.5587	8381.3434	5423.2222
0.0121	0.9382	303.69	4.4836	-3.3643	4.4900	3.2422	8635.0850	4999.2597
0.0148	0.9331	315.61	4.3034	-3.2572	4.3002	3.2195	9000.2567	5169.2436
0.0136	0.9016	325.57	4.2658	-3.3997	4.3521	2.8535	9690.3045	4384.9981
0.0182	0.8725	344.98	3.9217	-3.3764	4.0543	2.7041	9579.6668	4072.7925
0.0175	0.8291	351.09	3.7401	-3.8053	4.0384	2.4257	10012.0406	3298.4274
0.0243	0.8014	355.92	3.3641	-3.7303	3.6918	2.4028	9469.1804	2959.1189

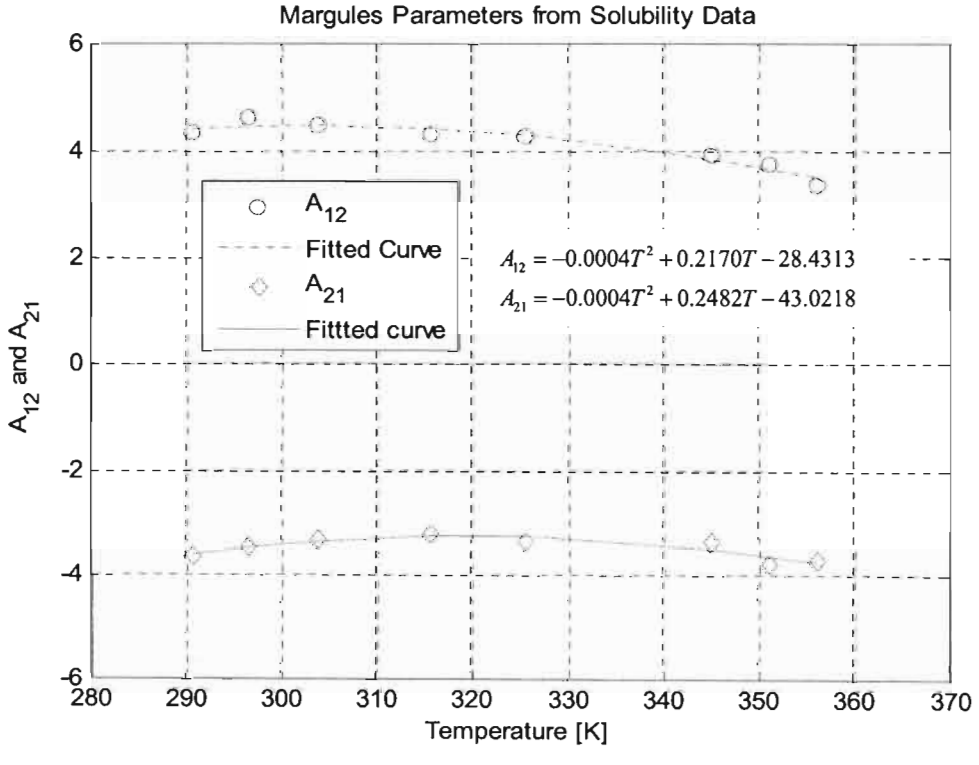

Figure 7 - 1: Temperature Dependence of the Margules Three Suffix Model parameters for the system Tolunitrile (1) + Water (2)

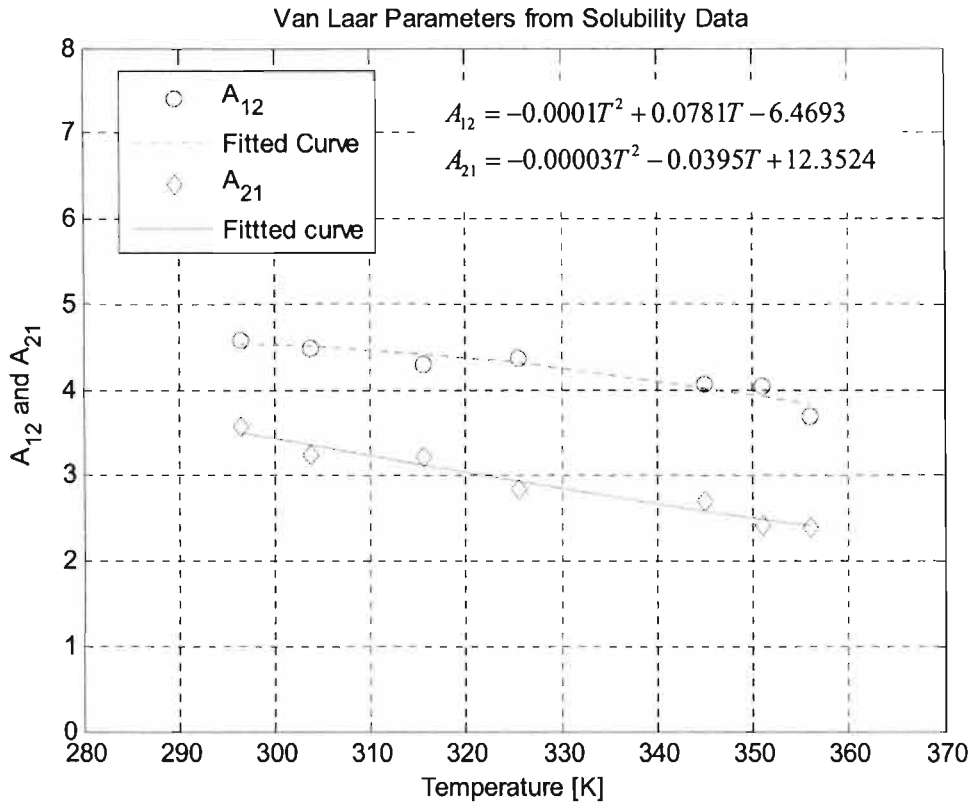

Figure 7 - 36: Temperature Dependence of the Van laar Model parameters for the system Tolunitrile (1) + Water (2)

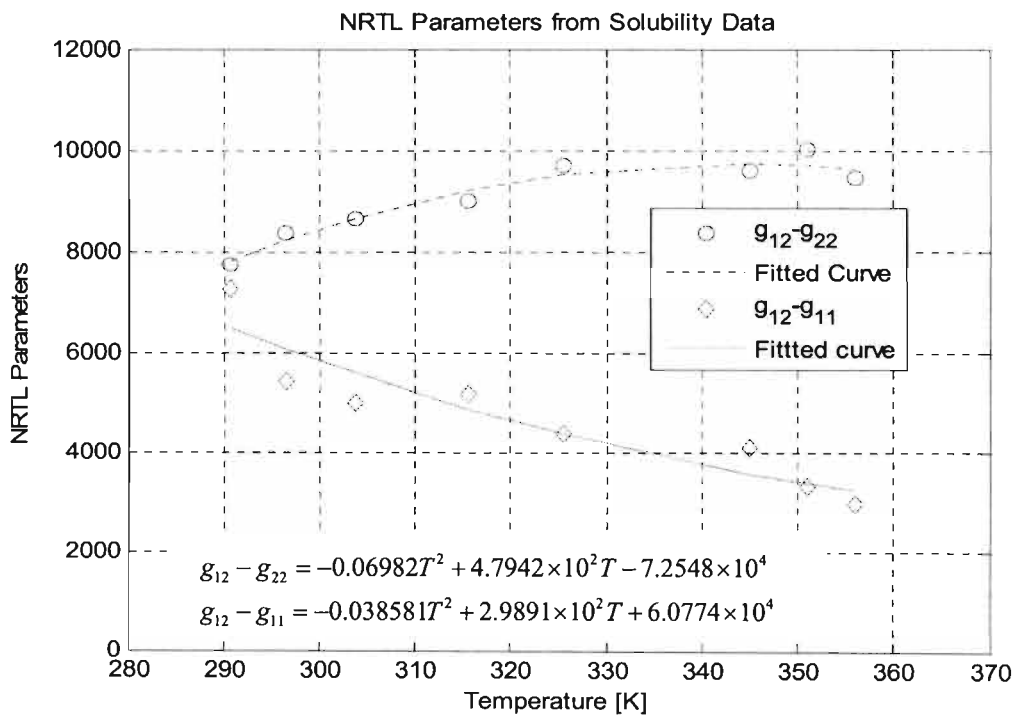

Figure 7 - 37: Temperature Dependence of the NRTL Model parameters for the system Tolunitrile (1) + Water (2)

Table 7 - 25: Predicted Isothermal VLE and VLLE data for the Tolunitrile (1) + Water (2) system at 90 °C (363.15K). (Asterisks, * indicate VLLE data)

P [kPa]	x_1	y_1
68.8130	0.0000	0.0000
67.4031	0.0714	0.0628
67.3605	0.1429	0.0675
67.4019*	0.0591*	0.0586*
67.4019*	0.8468*	0.0586*
64.8122	0.8571	0.0442
48.2802	0.9109	0.0606
41.2888	0.9286	0.0714
37.2233	0.9379	0.0794
25.5625	0.962	0.1167
16.1361	0.979	0.1859
3.0126	1.0000	1.0000

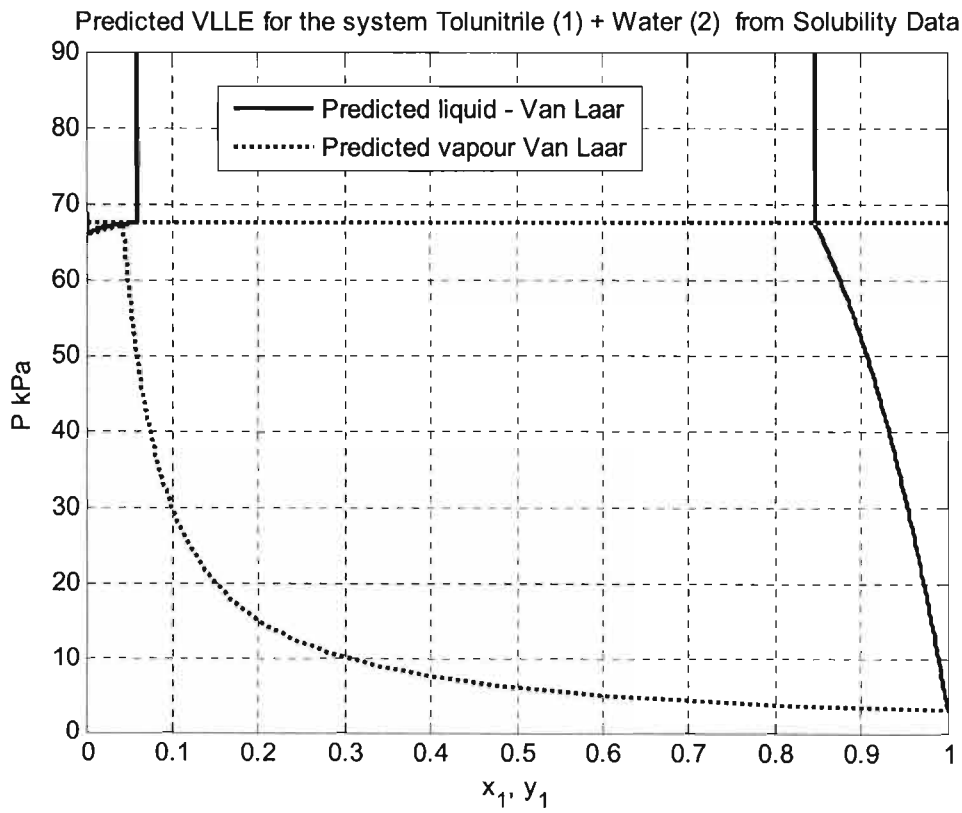

Figure 7 - 38: Predicted VLLE for the system Tolunitrile (1) + Water (2) system at 90°C from Solubility Data

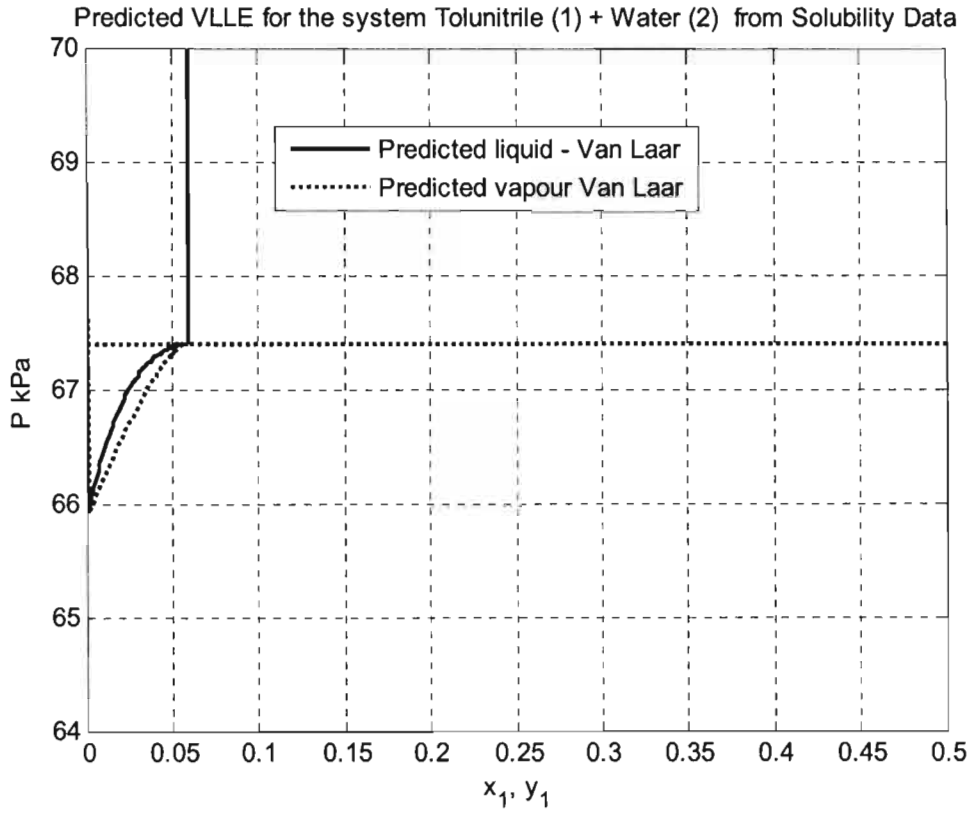

Figure 7 - 39: Predicted VLLE for the system Tolunitrile (1) + Water (2) system at 90°C from Solubility data (Water-Rich Region Expanded)

The above graphs show a very rapid rise in pressure with liquid composition in the tolunitrile rich region.

7.6 Ternary LLE (m-Cresol (1) + Water (2) + Naphthalene (3) system.

This section, which concludes this chapter, presents the LLE results and analysis for the ternary system m-cresol (1) + water (2) + naphthalene (3). Measurements were conducted at 80°C and 90°C. The measured data are shown in Figures 7-40 and 7-41 for the two temperatures respectively. The same data are shown in tabular form in Tables 7-26 and -727.

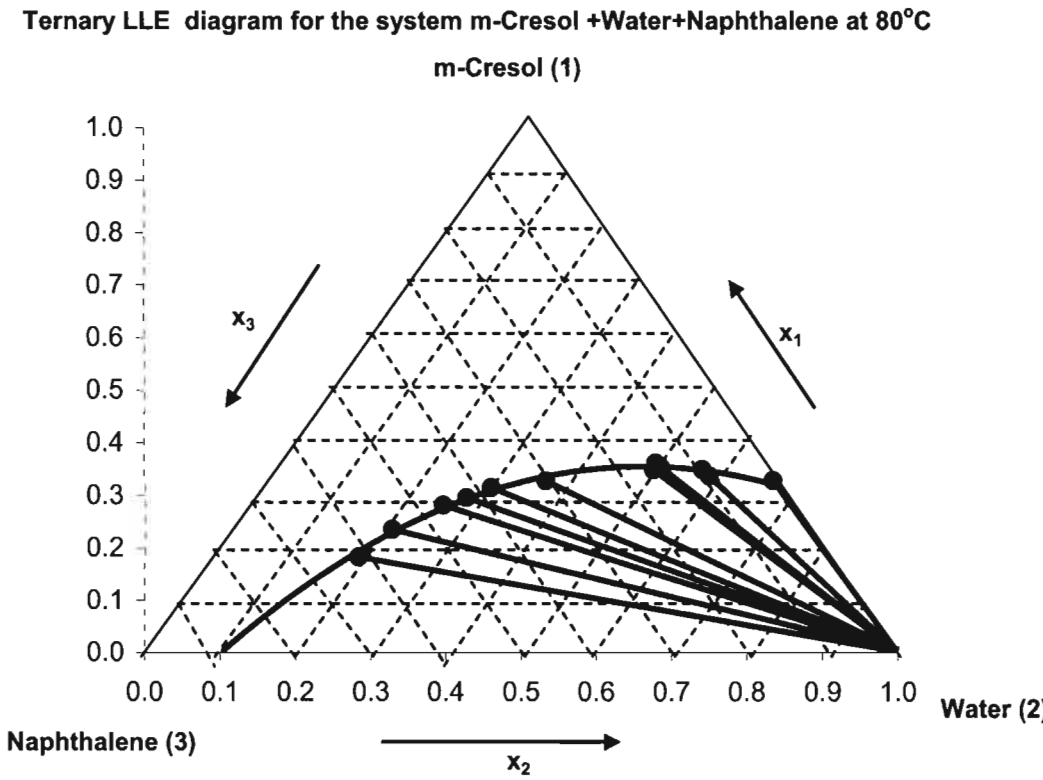

Figure 7 - 40: Ternary Phase diagram for the system m-Cresol (1) + Water (2) + Naphthalene (3) at 80 °C.

Table 7 - 26: Tie line compositions at 80°C

Organic Phase			Aqueous Phase		
x_1	x_2	x_3	x_1	x_2	x_3
0.3288	0.6712	0.0000	0.0120	0.9880	0.0000
0.3372	0.5821	0.0806	0.0217	0.9749	0.0035
0.3495	0.5670	0.0835	0.0124	0.9858	0.0018
0.3490	0.5023	0.1487	0.0135	0.9830	0.0034
0.3526	0.5107	0.1367	0.0253	0.9262	0.0484
0.3620	0.4989	0.1391	0.0174	0.9782	0.0045
0.3280	0.3694	0.3025	0.0139	0.9790	0.0071
0.2962	0.2801	0.4236	0.0078	0.9871	0.0051
0.3153	0.3033	0.3814	0.0076	0.9872	0.0051
0.2823	0.2557	0.4620	0.0066	0.9871	0.0063
0.2358	0.2114	0.5528	0.0061	0.9860	0.0079
0.1834	0.1929	0.6237	0.0047	0.9853	0.0100

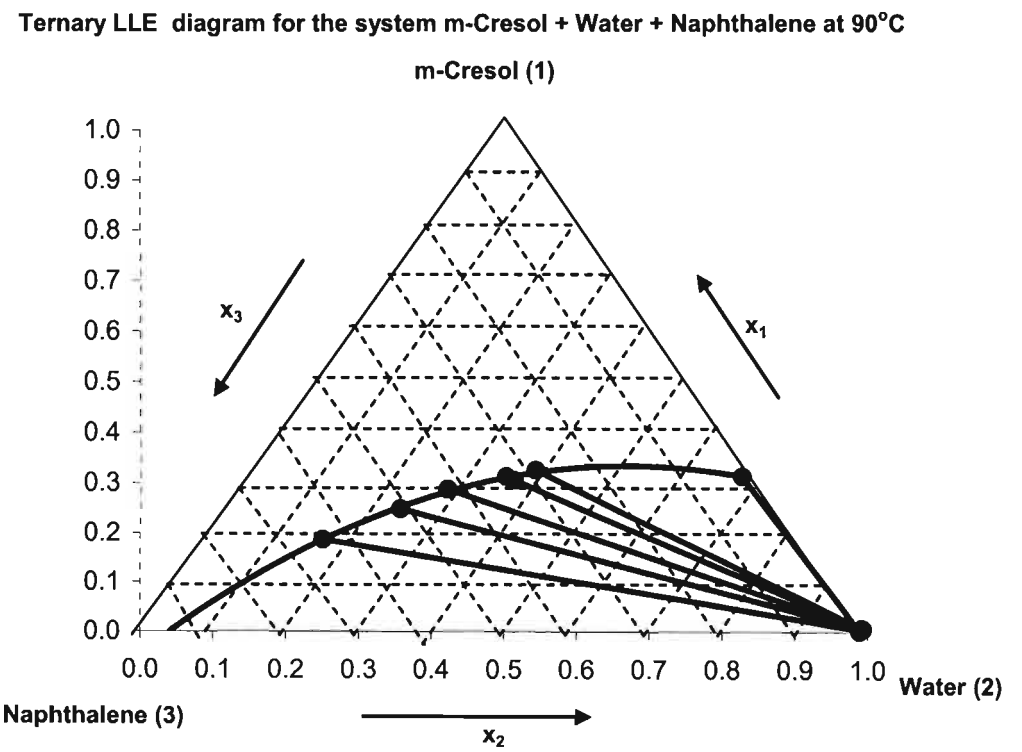

Figure 7 - 41: Ternary Phase diagram for the system m-Cresol (1) + water (2) + Naphthalene (3) at 90 °C.

Table 7 - 27: Tie line compositions at 90°C

Organic Phase			Aqueous Phase		
x_1	x_2	x_3	x_1	x_2	x_3
0.3133	0.6867	0.0000	0.0021	0.9880	0.0000
0.1864	0.1572	0.6563	0.0037	0.9890	0.0073
0.2485	0.2335	0.5180	0.0057	0.9889	0.0055
0.2879	0.2793	0.4328	0.0066	0.9880	0.0055
0.3056	0.3619	0.3326	0.0062	0.9904	0.0034
0.3125	0.3471	0.3404	0.0067	0.9894	0.0038
0.3253	0.3814	0.2933	0.0074	0.9883	0.0043

7.6.1 LLE correlation

The different types of ternary LLE phase diagrams are presented in Chapter 3 (see Section 3.7.2). Also presented in the same section are the equations which are used in this section to correlate the experimental data. These are the Hlavaty Equation, the β-function and the log-γ function for the binodal curves and the NRTL model for the tie line data. The correlations for the bimodal curves are:

The Hlavaty (Hlavaty [1972]) Correlation:

$$x_1 = A_1 x_A \ln x_A + A_2 x_B \ln x_B + A_3 x_A x_B \tag{7-3}$$

The β function (Shultz et al[1973]):

$$x_1 = B_1 \left(1 - x_A\right)^{B_2} x_A^{B_3} \tag{7-4}$$

The log-γ function (Letcher et al [1989])

$$x_1 = C_1 \left(-\ln x_A\right)^{C_2} x_A^{C_3} \tag{7-5}$$

In all the above three equations, the quantities A_1, A_2, A_3, B_1, B_2, B_3, C_1, C_2 and C_3 are the parameters to be determined from the experimental data. x_A and x_B are given by:

$$x_A = \frac{\left(x_2 + \frac{1}{2}x_1 - x_2^o\right)}{x_{22}^o - x_2^o} \tag{7-6}$$

$$x_B = \frac{\left(x_{22}^o + x_2 - \frac{1}{2}x_1\right)}{x_{22}^o - x_2^o} \tag{7-7}$$

and

where x_1 refers to the mole fraction of the solute, x_2, refers to the mole fraction of the carrier and x_{22}^o and x_2^o are the values of x_2 on the binodal curve which cuts the $x_1 = 0$ axis

Non-linear least squares regression was used to obtain the parameters which are presented in Tables 7-28 and 7-29 below. In fitting these correlations, x_1 was used as the dependent variable while x_A and x_B were used as independent variables. For the NRTL model the non-randomness parameter αij was set equal to a constant value for all the three binary pairs of the system's constituents (Walas [1985]). This reduced the regression parameters to 6. The value used for α was either 0.2 or 0.3 or 0.45. Calculations were done for all these values and the value that gave the best fit was then chosen for the data set being investigated.
Also shown in these tables are the standard deviation (Table 7-28) and root mean squared deviation (Table 7-29). The standard deviation was calculated using the equation:

$$\sigma = \left[\frac{\sum_{\text{All points}} x_2^{Exp} - x_2^{Calc}}{n-3}\right] \tag{7-8}$$

where n is the number of experimental points and 3 corresponds to the number of adjustable parameters in each model. The root mean squared deviation was calculated using the equation:

$$rmsd = \left\{\sum_i \sum_l \sum_m \frac{\left(x_{ilm}^{Exp} - x_{ilm}^{cal}\right)^2}{6k}\right\}^{1/2} \tag{7-9}$$

where x is the mole fraction and the subscripts i, l and m provide a designation for the component, the phase and the tie line, respectively. The value k designates the number of interaction components.

Table 7 - 28: Coefficients and standard deviations from the correlation of LLE binodal curve data for the system m-Cresol (1) + Water (2) + Naphthalene (3)

Correlation		System at	
		80°C	90°C
Hlavaty	A_1	-0.47967	-0.39616
	A_2	-1.14650	-1.42650
	A_3	-0.86893	-1.26380
	σ	0.01197	0.00834
β	B_1	0.77307	0.72926
	B_2	0.44220	0.38793
	B_3	0.72013	0.82408
	σ	0.01044	0.00706
log -γ	C_1	0.74417	0.70822
	C_2	0.42363	0.37525
	C_3	0.88353	0.97178
	σ	0.01005	0.00699

Table 7 - 29: NRTL Parameters from the regression of LLE data for the system m-Cresol (1) +Water (2) +Naphthalene (3)

NRTL Parameter	System at	
	80°C	90°C
$\lambda_{12} - \lambda_{22}$	-140.859	-597.1440
$\lambda_{21} - \lambda_{11}$	-491.6977	13316.3786
$\lambda_{13} - \lambda_{11}$	-519.2231	9136.5633
$\lambda_{31} - \lambda_{33}$	-922.0454	7473.6446
$\lambda_{23} - \lambda_{22}$	-514.8061	-919.0667
$\lambda_{32} - \lambda_{33}$	518.8312	1435.0509
α	0.45	0.2
rmsd	0.03328	0.026389

The standard deviation and rmsd' values presented in the above two tables show that all the correlations together with the NRTL model adequately described the experimental binodal curves and tie lines respectively.

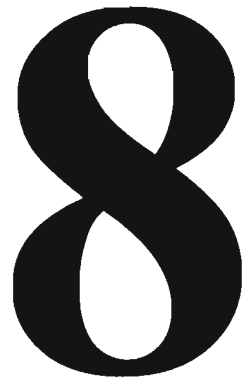

Chapter Eight

Discussion

Reference to this chapter has already been made in the previous two chapters which focused on the presentation and analyses of equilibrium data for both the test systems and new systems that were measured in this work. In this, the penultimate chapter of this dissertation, a discussion of the experimental results is presented. Much of the discussion will be on the accuracy to which the various models that were used to correlate the measured VLE, VLLE and LLE represent the experimental data.

The chapter material follows the same sequence as that in which the data and analyses in the earlier chapters were presented, thus the subject content will be under the following broad headings:

8.1 Experimental measurements
8.2 Vapour pressures
8.3 Vapour-liquid equilibria
8.4 Vapour-liquid-liquid equilibria and
8.5 Ternary liquid-liquid equilibria

8.1 Experimental measurements

Of all the systems that were measured, the m-cresol (1) + naphthalene (2) binary presented the greatest challenges during the data measurement process. These problems were a result of the fact that naphthalene is a solid at room temperature (having a melting point of 80°C). The

solid material, which could not dissolve in cresol under room temperature conditions, had to be introduced into the VLLE still by first melting it using a hot plate and then sucking it into the preheated still using a vacuum pump. Difficulties were still encountered while conducting measurements in the naphthalene rich region. The naphthalene would condense and solidify in the condenser and in the return line that sent the condensate to the bulk of the still. To avoid this, the condenser temperature was raised to about 50°C, a temperature that was high enough to avoid freezing of the naphthalene and at the same time preventing the loss of the other component, cresol, in the pressure measuring train (see Chapter 4). This possible loss of cresol however, was not a serious problem especially when one takes cognizance of the fact that the two components are relatively involatile (normal boiling points of 202.1 and 217.98 °C for cresol and naphthalene respectively). Another modification to the VLLE still for this particular system was that electrical heating wire was wound around the standpipe leg that sent the condensate to the reboiler. The electrical wire was also extended to the liquid return line from the liquid trap – so that any solid material which was formed, for example, when the still contents were allowed to cool to room temperature could be melted.
A consequence of these challenges was that few points were measured in the naphthalene rich regions (see Figures 7-6 to 7-8), as the liquid phase could not be sampled because the sample solidified in the sampling syringe. Subsequent melting of the solidified sample in the GC injector gave irreproducible results and as a result the measurements where stopped once enough points had been obtained from the cresol rich regions to allow extrapolation to the naphthalene rich regions

Another system that presented problems was the o-tolunitrile (1) + water (2) binary. These problems, which have already been highlighted in Section 7.5, led to inability of measuring VLE in the homogeneous regions for the system and were ascribed to the large immiscibility region coupled with the very large relative volatility of the system's constituents. VLE data for the system were therefore computed from the LLE data, for which the measurement presented no problems at all.

8.1.1 GC calibration

The HP 5890 series II gas chromatograph (see Section 4.1.4.1) that was used in this project was calibrated following the area ratio method advocated by Raal and Muhlbauer [1998]. Section 5.1.2.3 details the calibration process and Table 5.1 shows the operating conditions that were used for the test systems. For the other systems, the operating conditions are presented in Appendix 4.

Non-linear curves were obtained for the cyclohexane (1) + ethanol (2) system, for the water (1) + MBE (2) system and for the m-cresol (1) + naphthalene (2) system (see Figures 6-5, 6-5, 6-12, 6-13, 7-4 and 7-5). This meant that the response factor ratios were not constant over the composition ranges and thus due care had to be taken to ensure that the correct curves were used depending on whether the measurements were in the dilute or rich regions for any particular component. Quadratic relationships were chosen in favour of cubic and even higher order equations as these result in more than one solution and choosing the one to work with for a particular case then becomes no longer obvious.

For the linear graphs, (those for the cresol (1) + water (2) and tolunitrile (1) + water (2) binaries- see Figures 7-38, 7-39, 7-50 and 7-51), it was found that the response factor ratios, although constant in the dilute regions for each of the system's constituents, were not exactly constant over the entire composition range as the inverses of the response factor ratios (slopes of the curves) were not equal. The differences in these values were less than 1% but this figure was deemed large enough not to generalize the response factors as being constant over the entire composition range. Different curves were therefore used for the different regions along the composition range as was the case for the non linear-curves.

8.2 Vapour pressures.

Van Ness et al. [1973] argue that in thermodynamic computations, using saturated vapour pressures obtained from literature sources is a mistake which many researchers have been making. Vapour pressures are highly sensitive to experimental conditions and the purity of the chemicals used. They assert that in proper experimental determination of VLE, vapour pressures must be measured with the same apparatus and for the same lots of materials as are used for the other measurements so that they are an integral part of the data set. The use of inappropriate values will introduce non-random bias into the calculated thermodynamic properties (Van Ness et al. [1973]). In this light, pure component vapour pressures were measured for the components that were used in this work.

The measured data were presented and analysed in Sections 6.2 and 7.2. The data were regressed to obtain parameters in the Antoine and Wagner equations (Reid et al. [1988]). Tables 6-5, 6-6, 7.5 and 7.6 present the equations' parameters.

For all the components, save water and MBE, the Wagner equation was found to give superior correlation of the data to that of the Antoine Equation. Lower absolute average deviations between experimental and predicted pressures were obtained for the Wagner equation as seen in the parameter tables. The superior performance of the Wagner equation

was expected as the model has one more parameter than those in the Antoine equation. However, in the VLE and VLLE analyses that were carried out, the Antoine equation was preferred to the Wagner equation due to its explicit temperature dependence. The solution for the saturated temperature at any pressure is simple and straight forward and gives a single value for the Antoine equation.

8.3 Vapour liquid equilibria

Vapour Liquid Equilibrium data were measured for two homogeneous systems: for the cyclohexane (1) + ethanol (2) system and for the m-cresol (1) + naphthalene (2) system. The results and analyses for the two systems were presented in Sections 6.3 and 7.3 respectively. Below are separate discussions of the results for the two systems.

8.3.1 Cyclohexane (1) + Ethanol (2) system

This system was used to test the experimental apparatus and the measurements were conducted at 40 kPa.

Pure-component properties

The importance of accurate pure-component properties in the analysis of VLE cannot be overstated. Virtually all the thermodynamic quantities calculated will depend on these parameters. This fact therefore dictates that considerable effort should be placed in obtaining reliable values. For both ethanol and cyclohexane, the critical parameters, T_c, P_c, V_c and the acentric factors were all obtained from the Dortmund Data Bank (DDB). The same values were also available in the Korean Data Bank for thermo physical properties (KDB) and in the text by Reid et al. [1988]. These parameters are shown in Table 6.8.The cross parameters also shown in the table were calculated using the mixing rules proposed by Prausnitz [1986] as was outlined in Section 3.4.2.1. These pure-component parameters were then used to compute the virial coefficients using the Pitzer and Curl [1957] correlation. Liquid molar volumes were calculated using the Racket [1970] equation.

Experimental VLE data

The experimental VLE data for this test system are shown in Figures 6-6 and 6-7 where they are compared to the literature data of Joseph et al. [2001]. As can be seen in these figures

there is excellent agreement between the measured and the literature values. This showed that the still and the operating procedures employed were therefore operating as desired. It further suggested that any other data set obtained from the same still would thus be accepted as correct.

This same system was also used to test the vapour sampling mechanism that was devised specifically for systems of partial liquid miscibility. The vapour phase, as discussed in Section 6.3, was sampled using the new valve system and then also using a gas-tight syringe after the vapour had condensed. The two compositions thus obtained were then compared. The results are also shown in Figures 6-6 and 6-7, where the excellent agreement is also evident from the graphs and also from Table 6.7 which gives the two composition sets. It was therefore concluded that the sampling mechanism gave the expected results, at least for homogeneous systems. The proper functioning of the sampling valves for heterogeneous systems was tested using the partially miscible water (1) + MBE (2) system discussed later in this chapter (see Section 8.4.1).

Experimental activity coefficients

The calculation of these values from the experimental data has been detailed in Section 6.3. Figure 8.1 below shows a plot of the experimental liquid phase activity coefficients obtained from Table 6-9.

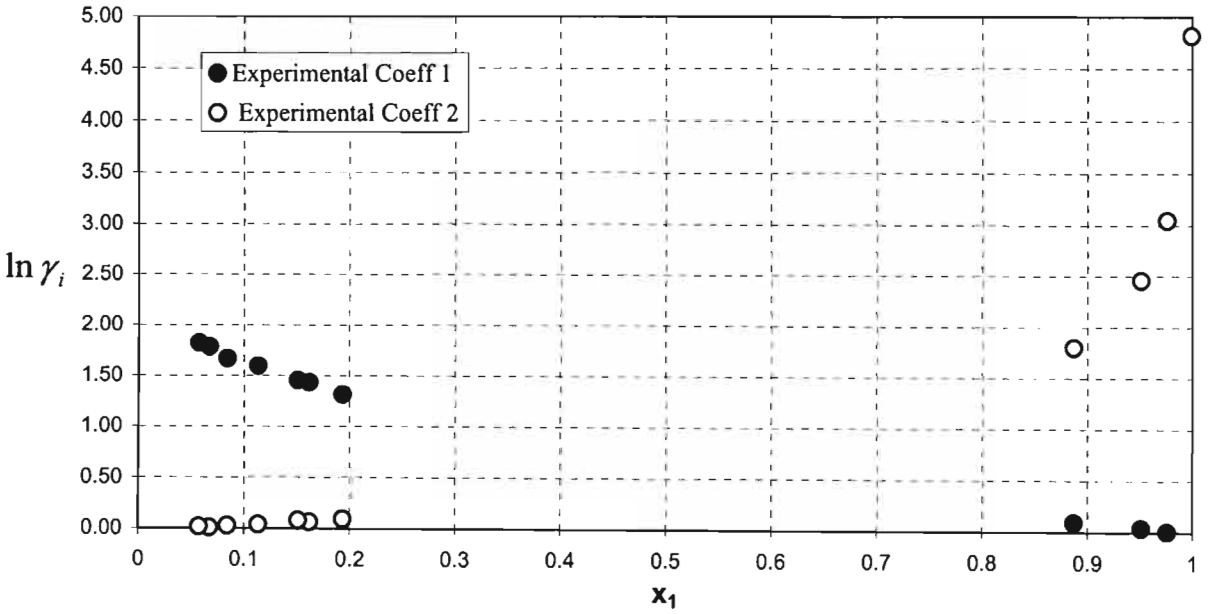

Figure 8 - 1: Experimental activity coefficients for the system Cyclohexane (1) + Ethanol (2) at 40 kPa (Dilute Regions)

The above figure indicates positive deviations from Raoults' law. The data also conform to the requirements of the Gibbs Duhem equation that the slope of the $\ln\gamma_1$ curve should always be of opposite sign to that of the $\ln \gamma_2$ curve (Smith et al. [1995]).

Data reduction

The measured VLE data for this system were regressed to give parameters in the NRTL and TK- Wilson models. The calculations are detailed in Section 6.3 and the parameters obtained for the two models are presented in Table 6-10. Figures 6-8 and 6-9 compare the experimental T-x-y data to that obtained from the parameters. As is evident from the graphs, both models represented the data satisfactorily. The T-K Wilson provided the best fit, which was judged from the relative magnitudes of the absolute average deviations in temperature and vapour compositions (ΔT and Δy). The NRTL model gave values of 0.2435 and 0.013 while the T-K

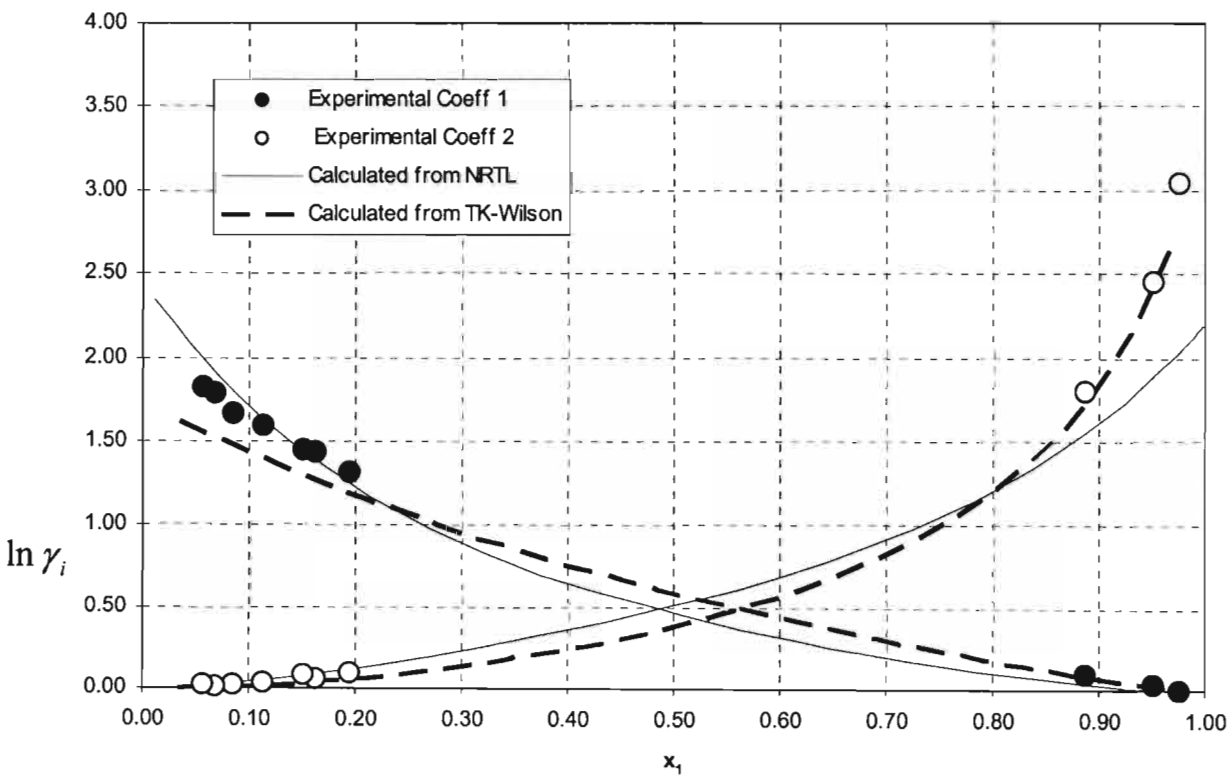

Figure 8 - 2: Comparison between experimental liquid phase activity coefficients and those predicted from the NRTL and T-K Wilson models.

Wilson model gave 0.2444 and 0.0085 for the two deviations respectively. Figure 8-2 below compares the experimental activity coefficients with those predicted from the model parameters.

Again as seen in this graph, the T-K Wilson model is superior to the NRTL model.

Thermodynamic consistency testing

Two thermodynamic consistency tests were applied to the data measured for this system. These were the Herington area test and the Point test of Van Ness. The measured data passed both tests as is seen from Figures 6-10 and 6-11. The area test is model-independent whereas the point test is not. This implies that one should not be quick in making conclusions based on the point test: that the data are consistent or inconsistent because for such a test model inadequacies can easily lead to a wrong conclusion. Instead different models should be tried until one finds one that best describes the data. This was found to be the case with data measured for this system. The NRTL model gave an average absolute deviation in y, Δy of 0.013, and thus failed the Point test, as the usual but rather subjective criterion is that Δy should be less that 0.01 if the data are to be deemed consistent. When the data were regressed using the T-K Wilson model a value of 0.0085 (< 0.01) was obtained and thus the data are consistent. This further confirms the point that an incorrect conclusion would have been made had the analysis been done using only the NRTL model.

8.3.2 m-Cresol (1) + Naphthalene (2) system.

This is one of the new systems that were measured in this work. Measurements were conducted at 55kPa, 120°C and 110°C.

Pure-component properties

As was the case for the above system, reliable pure component properties were obtained from the DDB. The cross parameters which were used to compute the virial coefficients were also computed using the mixing rules proposed by Prausnitz [1986].

Experimental VLE measurements

The measured VLE data for the three data sets are shown in Figures 7-6 to 7-8. For this system the measured data could not be compared to any data as there were none found for the system in the published literature. The three data sets show a minimum boiling azeotrope. The

azeotrope is clearly seen in the isotherms and has a composition of about 0.6 mole fraction. This composition is slightly higher in the isobar with a composition of 0.85.

Experimental activity coefficients

These values are shown in Table 7.9 and are plotted in Figures 8.3 to 8.5 below. The system also shows strong positive deviations from Raoult's law for the three data sets.

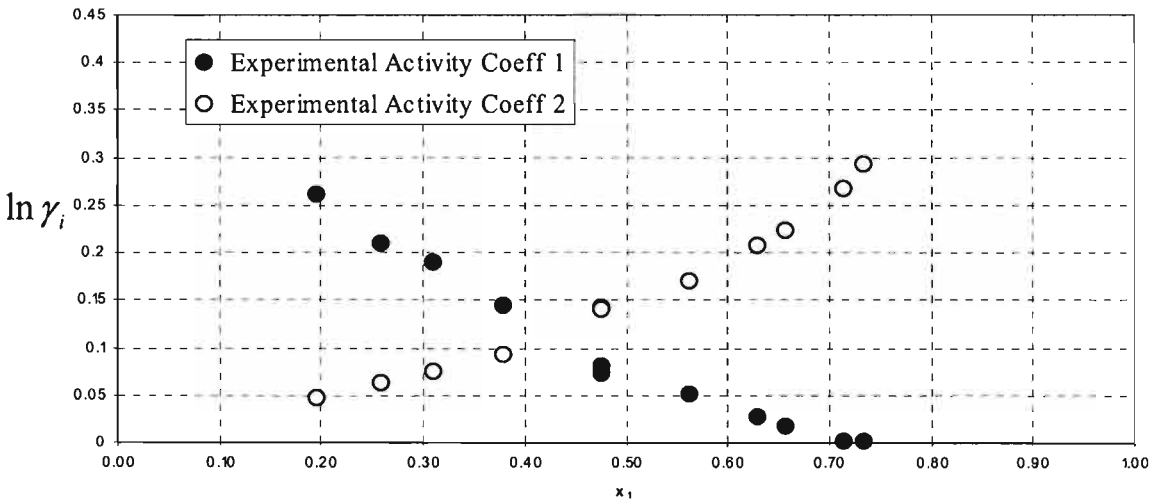

Figure 8 - 3: Experimental activity coefficients for the m-Cresol (1) + Naphthalene system at 55 kPa

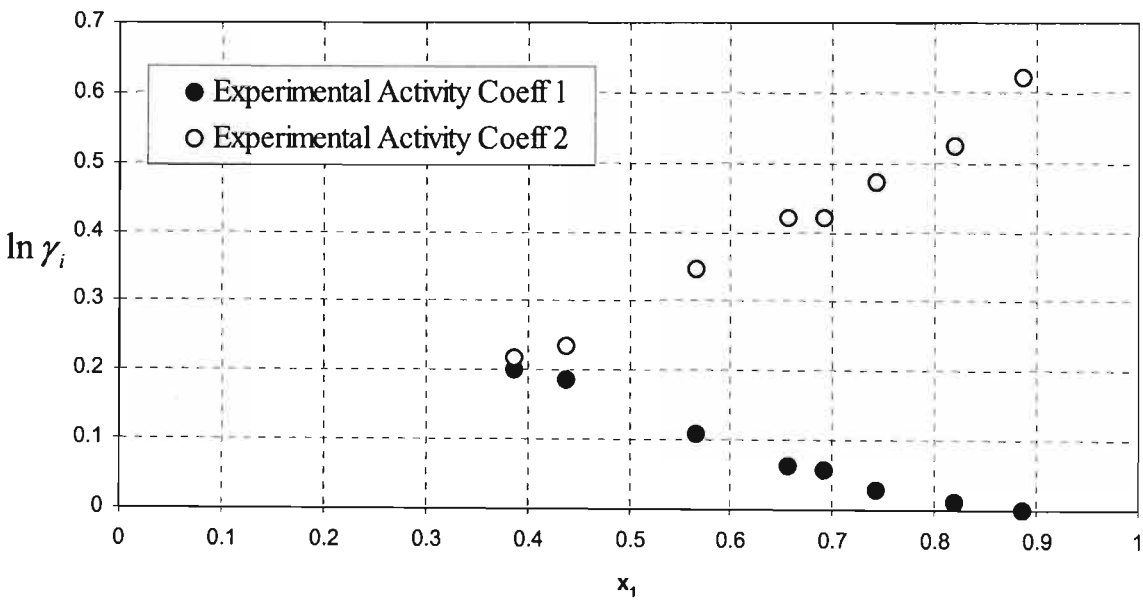

Figure 8 - 4: Experimental Activity Coefficients for the m-Cresol (1) + Naphthalene system at 120°C

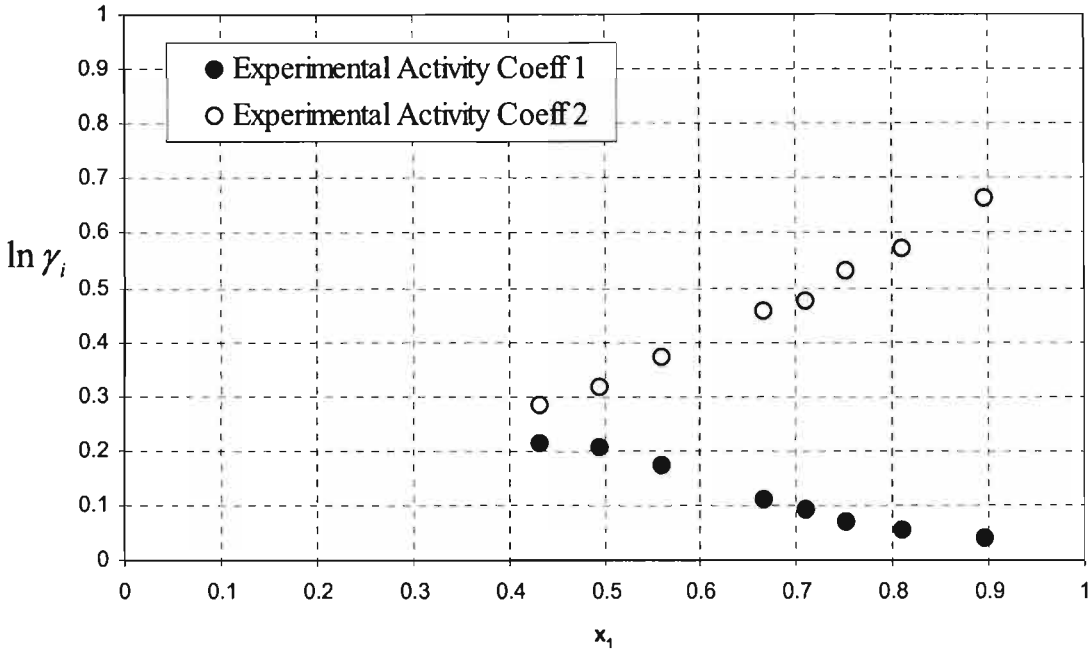

Figure 8 - 5: Experimental Activity Coefficients for the m-Cresol (1) + Naphthalene system at 55 Kpa

Data reduction

The VLE data for this system were regressed using both the Gamma-Phi and the EOS approaches. The analyses for both methods are presented in Sections 7.3.1.2 and 7.3.1.3.

The NRTL, Wilson, TK-Wilson and UNIQUAC models were used in the γ - ϕ method. Table 7-10 shows the model parameters and Figures 7-10 to 7-12 compare the experimental T-x-y and P-x-y data to data computed from the NRTL model parameters. A close look at the absolute average deviations from the four models revealed that for the 55 kPa isobar, the Wilson and NRTL models provided the best fit followed by the T- K Wilson model and lastly the UNIQUAC model. Examination of Figures 7-9, A1-1, A1-4 and A1-7 is also testament to the above conclusion, that the T-K Wilson and the UNIQUAC models were the worst fort this system.

For the 120°C Isotherm, similar analysis revealed a different scenario for the four models. The T-K Wilson proved to be the best, followed by the Wilson and then the NRTL. Again the UNIQUAC model proved remarkably poor in describing the VLE data set. Average absolute deviations in vapour compositions of 0.0034, 0.0035, 0.0087 and 0.0174 were obtained for the four models respectively. As shown above, this data set would fail the point test based on the UNIQUAC equation but pass it for the other three models.

For the 110 °C isotherm, a similar trend was observed. The order of the best fit of the models did not change from that of the 120 °C isotherm, thus the T-K Wilson still provided superior fit and the UNIQUAC the worst.

Figure 8-6 compares the experimental activity coefficients to those obtained from the model parameters for the 55 kPa data set. Similar graphs for the other two data sets are presented in the appendix to this chapter (Figures 8-12 and 8-13).

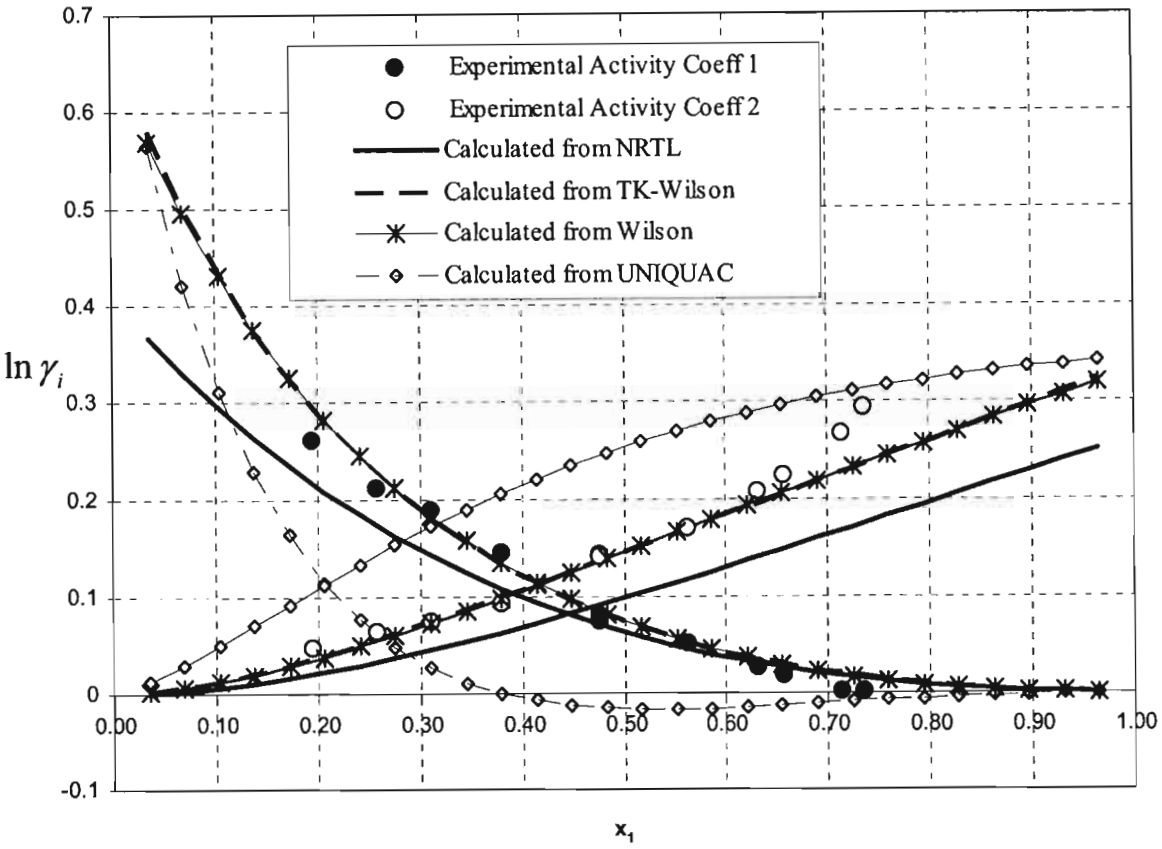

Figure 8 - 6: Comparison between experimental activity coefficients and those predicted from the model parameters for the m-Cresol (1) + Naphthalene system at 55 kPa

The three data sets for this system were also analysed using the EOS method. The calculations and the results obtained are presented in Section 7.3.1.3. Table 7-12 shows that for the 55 kPa data set, all the three EOS's performed reasonably well. The best representation was obtained from the SRK-EOS followed by the PRSV-EOS and then the PR-EOS. This result was rather unexpected as the Redlich-Kwong [1949] EOS and its modifications generally fail to generate satisfactory density values for the liquid even though the calculated densities of the vapour densities are generally acceptable (Peng and Robinson

[1976]). With the Peng and Robinson EOS, the results were as expected, as the PRSV- EOS provides better vapour pressure predictions when compared to the PR-EOS.

For the two isotherms, all three EOS failed to adequately describe the VLE data as evidenced by the rather large absolute deviations in the vapour compositions. The PR-EOS was the best followed by its modification and then lastly the SRK- EOS. This failure is due to the mixing rules that were used in the EOS. The classical mixing rules proved incapable of describing the VLE, a result that was expected given the high non-ideality of the system.

The use of the Wong and Sandler mixing rules clearly demonstrated their superiority over the classical mixing rules. Excellent correlation was obtained for all the EOS and for all the data sets with absolute deviations in vapour mole fractions being less that 0.005 for all the EOS in all the data sets save for the SRK-EOS in the 120°C and 110°C Isotherms. Table 7-13 and Figures 7-16 to 7-18 bear witness to this. This behaviour came as no surprise from the use of this mixing rule as it was shown by Wong and Sandler [1992] that their mixing rule is theoretically correct at both high and low pressure limits and is applicable and accurate for simple mixtures containing hydrocarbons and inorganic gases and mixtures containing polar, aromatic and associating species over a wide range of pressures.

Consistency testing

The Area test, the Point test and the Direct test were all applied to data for this system and as shown in Section 7.3.2, the three data sets passed these tests. Because of its inability to satisfactorily represent the VLE data sets, the UNIQUAC model faired poorest in the point test and gave absolute deviations in vapour compositions of 0.0253, 0.0174 and 0.0179 (all greater that 0.01 the threshold for the test) for the 55 kPa, 120°C and 110°C data sets respectively. Similar behaviour was obtained from the Direct Test for which the UNIQUAC also gave poor results. However for the NRTL and Wilson equations low indices (2, 2 and 4) were obtained for the data sets indicating that the data are of high thermodynamic consistency (Van Ness [1995]).

8.4 Vapour-liquid-liquid equilibria

Vapour-liquid-liquid equilibrium data were measured for three binary systems. These were the water (1) + 2- methyl-3 buten-2 ol (2) at 97.2 kPa, m-cresol (1) + water (2) at 55 kPa and tolunitrile (1) + water (2) at 90°C. The results for these systems were presented and analysed in Sections 6.4., 7.4 and 7.5 for the three data sets respectively. The results are discussed below.

8.4.1 Water (1) + 2- Methyl-3 buten -2 ol (2) at 97.2 kPa

This was the second test system used in this work and thus had available data in the published literature.

Pure-component properties

Reliable pure component properties for water were available from the DDB. However for MBE, the parameters were not available and had to be estimated by using Lydersen's group contribution method outlined in detail by Reid et al. [1988].

Experimental VLLE data

The data that were measured for this system are shown in Table 6-14 and the same data are plotted in Figure 6-14, where they are compared to data of Raal and Broukaert [1992]. As was the case for the first test system, the agreement between the present data and the literature data is very close. The excellent agreement therefore led to the conclusion that the new still could handle both completely miscible and partially miscible systems. This suggested also that all data measured using the still for heterogeneous systems would therefore be accepted as accurate. The system behaviour is complex and is characterized by a heterogeneous azeotrope of the second kind (Van Ness and Abort [1982]). This is the case when the vapour that is in equilibrium with two liquids does not lie between the compositions of the two liquids.

An interesting part of this data set is that Raal and Brouckaert [1992] could not measure vapour compositions in the homogeneous water region (for values of $x_1 > 0.97$). This failure was ascribed to the formation of an unstable emulsion in the well-stirred condensate receiver of their still, which then led to the sample compositions not being reproducible. They then computed the vapour composition from the measured liquid phase composition by using the coexistence equation. Their computed compositions are shown together with the data measured in this work in Figure 8-7 below.

A closer look at the above stated graph shows that their calculations were relatively correct. Only two points were found to be slightly off the line.

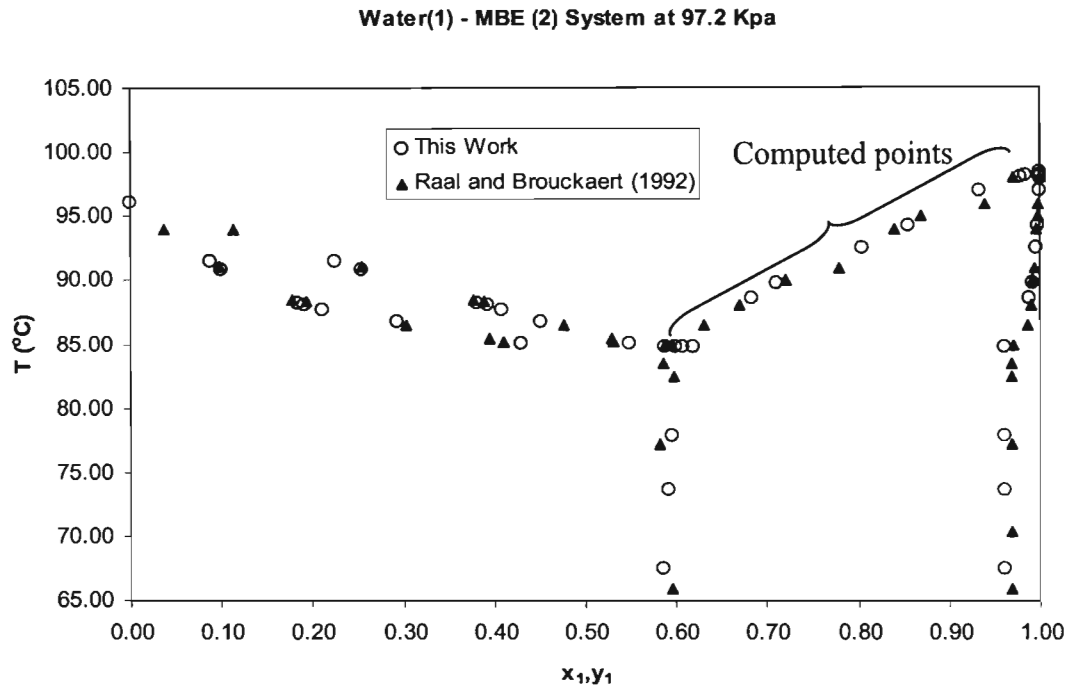

Figure 8 - 7: T-x-y data for the Water (1) + MBE (2) system at 97.2 Kpa.

Experimental activity coefficients

The calculated experimental Activity coefficients are shown in Table 6-16 and have been plotted in Figure 8-8 below. The graph also shows positive deviations from Raoults' law

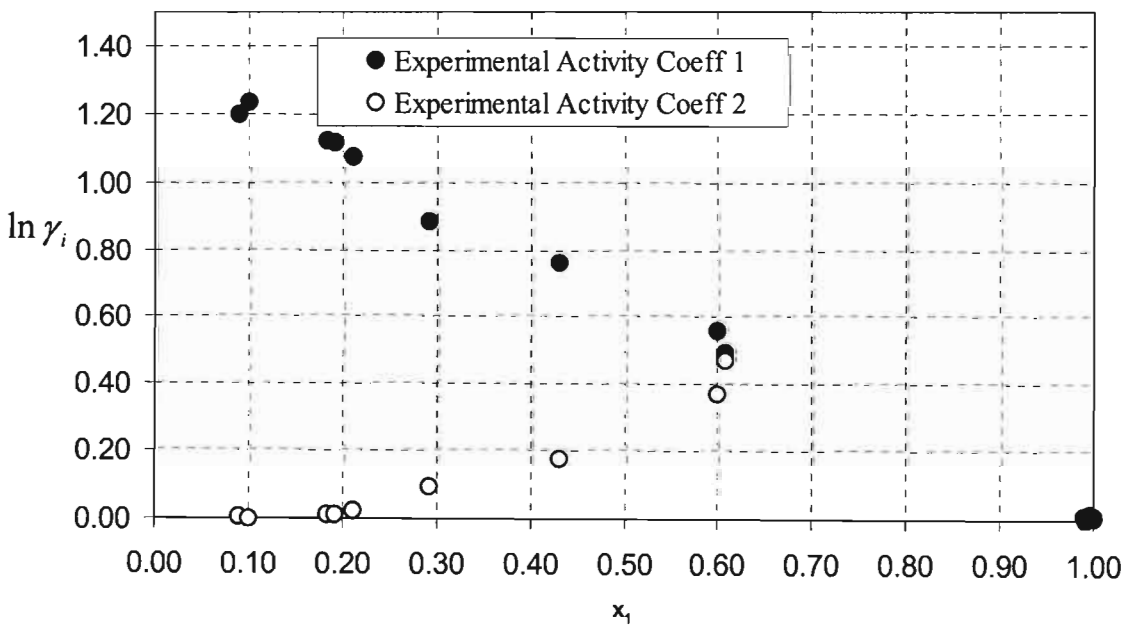

Figure 8 - 8: Experimental activity coefficients for the system: Water (1) + MBE (2) at 97.2 kPa

Data reduction

The reduction of the experimentally measured data to obtain parameters in the NRTL and TK Wilson equations has already been presented in Section 6.4. Two approaches of analysing the data were followed as was done by Raal and Broukaert [1992]. The entire data set was regressed first giving the parameters in the two model equations and then data in the homogeneous regions were regressed separately, also giving parameters in the two model equations. The model parameters for both cases are shown in Table 6-17. Fair agreement between the correlated and the experimental data was obtained for the two cases. Predicted and experimental vapour mole fractions and temperatures were in good agreement for all the cases. The predicted pressure for the first case however was found to be in error by up to 4 kPa. Raal and Broukaert [1992] obtained similar results with the pressure being in error by up to 10 kPa. The large error in their pressure values was probably due to the fact that they assumed vapour phase ideality in their calculation, an assumption that was not made in the present analysis. The vapour phase non-idealities were accounted for by fugacity coefficients evaluated from the Virial equation. Figure 8-9 compares the experimental activity coefficients to those predicted from the fitted models.

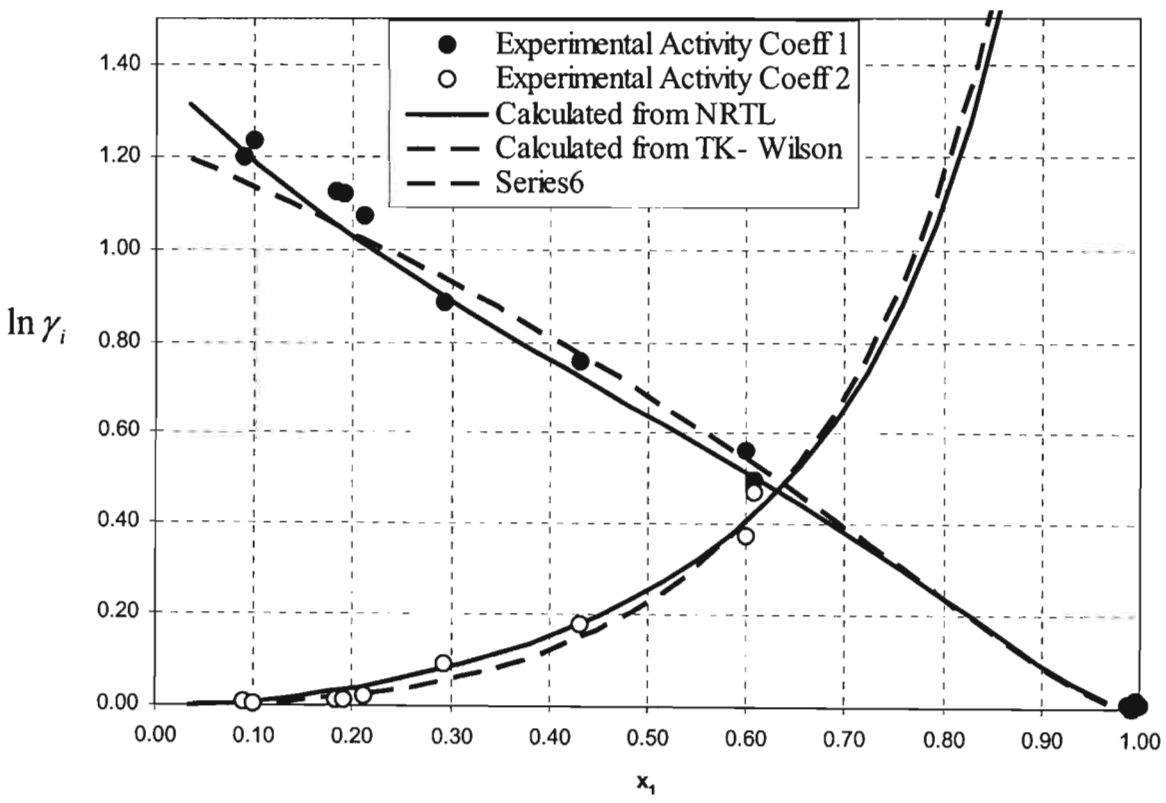

Figure 8 - 9: Comparison between experimental activity coefficients and those predicted from the model parameters for the Water (1) + MBE system at 97.2 kPa

Thermodynamic consistency testing

The area and point tests were applied to the data for this system and the results, shown in Figures 6-17 and 6-18, show that the data are consistent. The point test was applied to data in the homogenous regions. As can be seen in Figure 6-18, the absolute deviations do scatter about the zero axis - a requirement for consistency.

8.4.2 m-Cresol (1) + Water (2) system.

This, the second partially miscible system that was measured in this work, had no previous data available in the literature. Comparison to any data set therefore could not be made. The experimental data, measured at 55 kPa, are presented and analysed in great detail in Section 7.4

Pure-component properties

For both the systems' constituents, pure-component properties were obtained from the DDB.

Experimental VLLE data

These are shown in Table 7-17 and Figure 7-26. As seen in Figure 7-26, the system's behaviour is unusual with a very narrow single phase homogeneous water-rich region. Only a single point was measured in this narrow region. The behaviour is characterized by a heterogeneous azeotrope of the first kind, wherein the vapour in equilibrium with two liquids has a composition lying between those of the two liquids.

Experimental activity coefficients

Table 7-19 shows the experimental activity coefficients for this system. The same data are plotted in Figure 8-10 below.

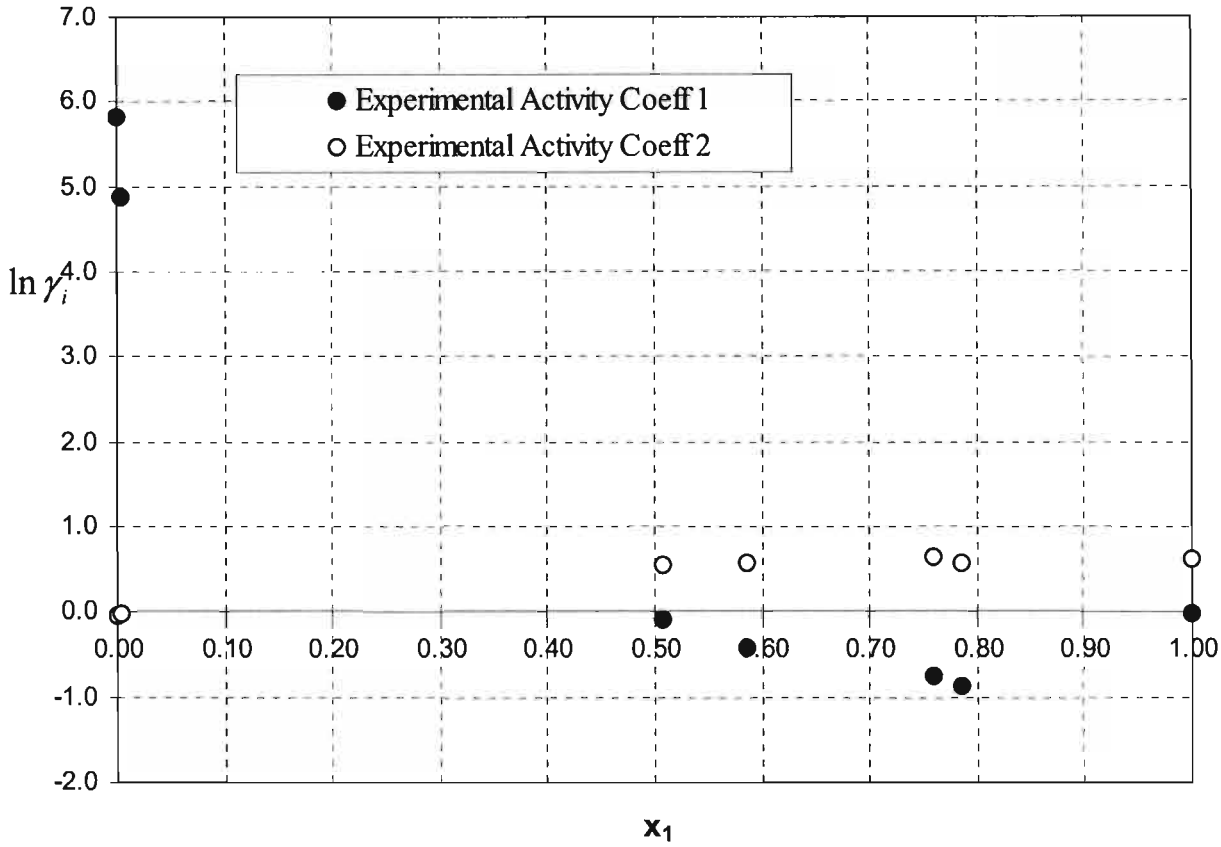

Figure 8 - 10: Experimental Activity Coefficients for the system m-Cresol (1) + Water (2) at 55 kPa

Data reduction

As was discussed in Section 7.4, this data set was regressed to give parameters in the NRTL, T-K Wilson and UNIQUAC activity coefficient models. The analysis was the same as that for the water (1) + MBE (2) system discussed above, only that for this particular case the equations could not be fitted to data in the homogeneous water rich region where only a single point was measured. Table 7-20 shows the parameters for the models and Figures 7-28, 7-29, and Figures A1-16 to A1-19 compare the experimental data to that obtained from the parameters.

The absolute average deviations in temperature and vapour compositions show that the T-K Wilson model was the best of the three. It was followed by the NRTL and once again, the UNIQUAC was the least. Figures A1-18 and A1-19 clearly show the UNIQUAC's inability to adequately describe the experimental data. This failure of the UNIQUAC model is unexpected given its more rigorous and less empirical derivation.

Figure 8-11 below compares the experimental activity coefficients to those predicted from the models.

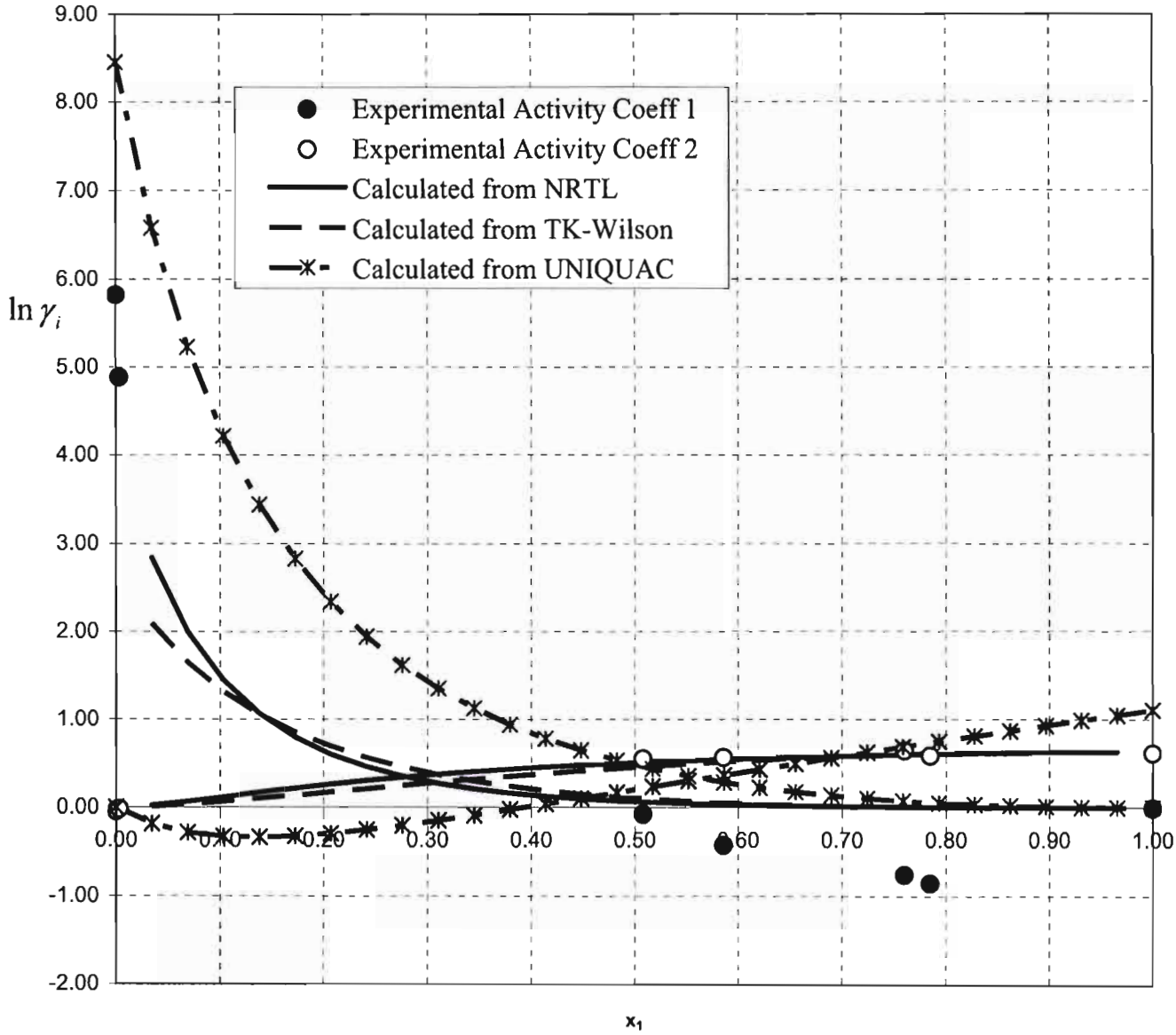

Figure 8 - 11:Comparison between experimental activity coefficients and those predicted from model parameters for the system m-Cresol (1) + Water (2) at 55 kPa

Thermodynamic consistency testing

The results for the point test, area test and the direct test were also presented and analysed in Section 7.4. Use of the UNIQUAC model gave predicted values that failed both the Point and Direct tests- a consequence of its inability to adequately describe the data. However the NRTL and the TK-Wilson models passed the tests with average absolute deviations in vapour compositions of 0.0087 and 0.0065 respectively. The data set passed the area test which is based only on the experimental activity coefficients.

8.4.3 Tolunitrile (1) + Water (2) system

The analysis of results for this system is presented in great detail in Section 7.5. As was explained in that section and under the heading experimental measurements in this chapter, VLE in the homogeneous regions could not be measured for this system. The data were therefore predicted from the LLE data which were measured from 17 °C to 83 °C.

Pure-component properties

The pure component parameters for Tolunitrile – those that were unavailable as it is the only chemical that had yet to be used, were also obtained from the DDB. The critical volume was unavailable and as explained in Section 7.5, it was computed using Lydersens' method given in Reid et al. [1988].

VLLE data

The predicted VLLE data for the system are shown in Table 7-25 and in Figures 7-38 and 7-39. The curves show a very rapid rise in pressure with liquid composition in the Tolunitrile rich region. The predicted three-phase pressure of 67.4 kPa is reached at $x_1 = 0.8468$. The pressure rise is however small in the water rich region as shown in the expanded scale of Figure 7-39.

VLLE analysis

No experimental VLE data were measured for this system and thus no experimental analysis could be made. If the analysis, however, were to be made on the predicted data, then the results would be perfect and thus thermodynamically consistent as the calculation of the data was based on correct thermodynamic equations and hence would not violate any of the laws of thermodynamics.

8.5 Ternary LLE (m-Cresol (1) + Water (2) +Naphthalene (3) system

This section wraps up this chapter and in it is presented a discussion of the results and analyses already presented in Section 7.6. Tables 7-26 and 7-28 give the LLE data for the ternary system at 80°C and 90°C respectively. The data are also plotted in Figures 7-40 and 7-41.

The two diagrams show that the system is a type 2 system. As can be seen from the LLE diagrams, the 10°C rise in temperature from 80 to 90 °C had little effect on both the size and shape of the two-phase region. Only the solubility of water in naphthalene decreased from 0.1 to 0.5 mole fraction. That for water in cresol remained almost constant having changed from 0.6712 to 0.6867.

The low solubilities of either cresol or naphthalene in water indicate that water will not be a suitable solvent for liquid-liquid extraction. This can be seen by examining the selectivties of, for example, extracting cresol from a mixture with naphthalene given by:

$$S = \frac{\left(x_1/x_3\right)_{\text{Water Rich Phase}}}{\left(x_1/x_3\right)_{\text{Organic Rich Phase}}} \tag{8-1}$$

Where x_1 refers to cresol mole fraction and x_3 refers to naphthalene mole fraction. These values have been computed for the 90°C data set and are tabulated in table 8-1 below.

Table 8 - 1: Selectivities for the mixture m-Cresol (1) + Water (2) + Naphthalene (3) at 90°C

Organic Phase			Aqueous Phase			Selectivity
x_1	x_2	x_3	x_1	x_2	x_3	
0.3133	0.6867	0.0000	0.0021	0.9880	0.0000	-
0.1864	0.1572	0.6563	0.0037	0.9890	0.0073	1.78
0.2485	0.2335	0.5180	0.0057	0.9889	0.0055	2.17
0.2879	0.2793	0.4328	0.0066	0.9880	0.0055	1.80
0.3056	0.3619	0.3326	0.0062	0.9904	0.0034	2.00
0.3125	0.3471	0.3404	0.0067	0.9894	0.0038	1.91
0.3253	0.3814	0.2933	0.0074	0.9883	0.0043	1.57

For effective separation S >> 1. As seen from the above table the selectivities are just greater than unity. This therefore confirms the above conclusion that water is not the best solvent.

Data reduction

The LLE binodal curves for the two data sets were correlated to the Hlavaty equation, beta function and to the log gamma function. As was explained in Section 7.6 and in Chapter 3, non-linear least squares regression was used to find the parameters following the method by Walas [1985]. A look at the standard deviations from Table 7 -26 clearly shows that all the models represented the data satisfactorily. For the 80°C data set, the log gamma function proved to be the best model followed by the beta function and lastly the Hlavaty correlation. For the 90°C data set, the order of the best fit remained the same as that for the 80°C. The standard deviations were 0.00699, 0.00706 and 0.00834 for the log gamma, beta and Hlavaty correlations respectively.

The tie lines were correlated using the Non-Random-Two-Liquid model and, as can be inferred from the values of the root mean squared deviations (rmsd) in Table 7 -29, good correlation of the experimental data was obtained.

Appendix to Chapter 8

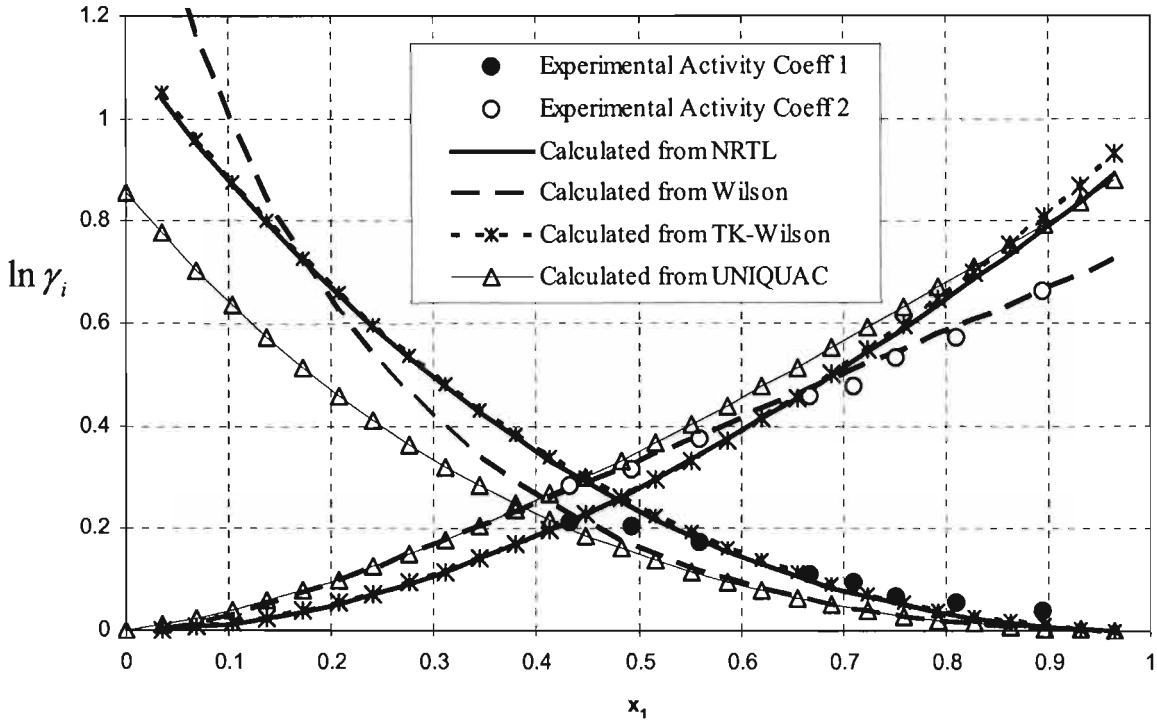

Figure 8 - 12: Comparison between experimental activity coefficients and those predicted from model parameters for the system m-Cresol (1) + Water (2) at 383.15K

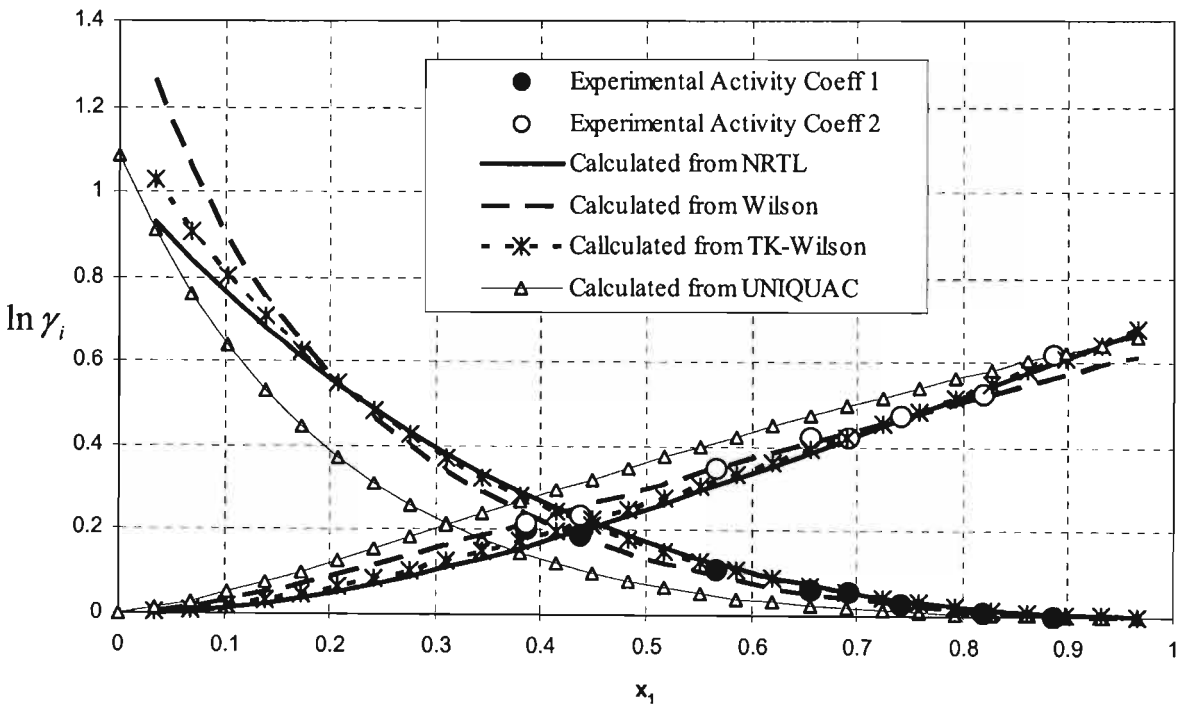

Figure 8 - 13: Comparison between experimental activity coefficients and those predicted from model parameters for the system m-Cresol (1) + Water at 393.15K

9

Chapter Nine

Conclusion and Recommendations

9.1 Conclusions

The objective of this work was to develop an apparatus together with the corresponding equipment operating procedures for measuring low pressure vapour-liquid-liquid equilibria of highly non-ideal systems. The equipment and the operating procedures that were developed were presented in Chapters 4 and 5 respectively.

The developmental work started by conducting an extensive literature review of the experimental methods that have been used previously for measuring vapour-liquid-liquid equilibria (VLLE). The research indicated that unlike in vapour-liquid equilibria (VLE), where the literature on experimental techniques to measure the data is voluminous (Malanowski [1982a]), by year 2000 there was no standard commercial instrument available for measuring the three phases in equilibrium. Researchers have therefore used modifications of conventional instruments used in the determination of VLE.

The apparatus that was used in the project is a modification of the Raal still (Raal and Muhlbauer [1998]) for homogeneous systems. The major still modification was a heated vapour take-off through a new heated valve system with sample conveyance directly to a GC. The original Raal and Muhlbauer [1998] still was based on the designs of Heertjies [1960] and Yerazunis [1964], who successfully used a packed equilibrium chamber where the liquid and vapour phases are forced downward co-currently to achieve rapid and dynamic equilibrium.

Pressure measurement in the still was effected by using a WIKA model P10 pressure transmitter connected to a WIKA model 5001 6 ½ digit pressure display. The control of the pressure was through a BUCHI model B-721 pressure controller which had a vent to the atmosphere and utilized a two-way solenoid valve connected to a vacuum pump. Overall pressure accuracy was estimated at 0.03 kPa and when the still was operated at constant pressure, the controlled pressure was within 0.01 kPa. Temperature measurement was through Pt-100 resistance temperature sensors and for isothermal runs the equilibrium temperature was controlled at fixed values manually by adjusting the pressure in the still appropriately. Raising the pressure increased the temperature and lowering the pressure had the effect of lowering the temperature. The overall accuracy of the measured temperature using this control strategy was estimated to be ± 0.02 °C. Composition measurement was through a Hewlett Packard 5890 Series II gas chromatograph which was used to obtain accurate compositions of both the equilibrium liquid and vapour samples. The GC was operated with a thermal conductivity detector (TCD).

In order to completely describe the VLLE for the systems studied, the liquid-liquid equilibrium (LLE) data for these systems were also measured. The LLE measurements were conducted in a newly-developed small jacketed glass cell (also described in more detail in Chapter 4) with temperatures maintained constant by circulating water from a bath maintained at the desired temperatures. The LLE measurements were all conducted at atmospheric pressure and thus the pressure was not measured. Temperature measurement was though a Pt 100 sensor. The controlled temperature was estimated to be accurate to 0.02 °C.

The initial testing of the still which established the operating procedures was conducted on two previously measured systems - the first which was the homogeneous cyclohexane (1) + ethanol (2) system at 40 kPa and the second the heterogeneous water (1) + 2 methyl -3 buten 2-ol (2) system at 97.2 kPa. For the homogeneous system the new vapour sampling system was tested by comparing the measured composition to that of a condensed vapour sample sent manually to the GC using a gas-tight syringe.
For the two test systems used, excellent agreement was obtained with the literature data. This led to confidence in both equipment and measuring procedures. Thus in view of the proven capabilities of the procedures and the equipment as modified for VLLE, the entire apparatus was considered suitable for other systems, both completely miscible and partially miscible.

VLE data were then measured for the very difficult m-cresol (1) + naphthalene (2) system at 55 kPa, 120°C and 110°C. VLLE were measured for the systems m-cresol (1) + water (2) and o- tolunitrile (1) + water (2) both at 55 kPa. Lastly ternary LLE data were measured for the

system m-cresol (1) + water (2) + naphthalene (3) at 80°C and at 90°C. All the measurements started by measuring the vapour pressures of the systems' components. The experimental vapour pressure data were regressed to give parameters in the Antoine and Wagner equations (Reid et al. [1988]). The Wagner equation was found to be the best overall in representing the vapour pressure data.

The experimental VLE data were regressed using both the Gamma-Phi method and the Equation of State Method, while the VLLE data were regressed using only the Gamma Phi-Method. In the Gamma-Phi method, four activity coefficient models were used to account for non-idealities in the liquid phase and these are the NRTL (Renon and Prausnitz [1968]), Wilson [1964], TK Wilson (Tsuboka and Katayama [1975]) and UNIQUAC (Abrams and Prausnitz [1975]) models. The vapour phase imperfections were described by the Virial equation with the Virial coefficients being estimated from the Pitzer and Curl [1957] correlation. In the alternative analysis three Equations of State (EOS) were used to account for non-idealities in both the liquid and vapour phases. These were the Peng and Robinson EOS [1976], the Soave Redlich-Kwong EOS [1972] and the Stryjek and Vera [1986] modified Peng and Robinson EOS. All the EOS's were used with two mixing rules-the Van der Waal one fluid mixing rules and the density independent Wong and Sandler [1992] mixing rules. The analyses were presented in Chapters 6, 7 and 8. Based on the average absolute deviations in temperature (or pressure) and vapour composition, all the models provided generally acceptable correlation of the data with only major inadequacies being found for the UNIQUAC model. Of the two mixing rules, the Wong and Sandler [1992] proved to be superior to classical mixing rules. Their use in the modeling of the VLE led to the EOS method being better that the Gamma-Phi method for the systems measured.
For the ternary LLE measurements, the binodal curves were correlated to the Hlavaty [1972] equation, the β- function (Shultz et al. [1973]) and the log-γ function (Letcher et al. [1989]). The corresponding tie line data were correlated to the NRTL model. The analyses presented in Chapters 7 and 8 showed that the three correlations and NRTL model all adequately described the LLE data.

The analysis of the experimental data included thermodynamic consistency testing of the VLE and VLLE data. For the test systems the Herington [1948] and the Point test of Van Ness et al. [1973] were used for the data, while for the new data sets, a third test, the Direct test (Van Ness [1995]) was employed. All the data sets passed the area test. With the point test, the NRTL model and the Wilson model together with its modification produced results that passed the test for all the systems. The UNIQUAC equation still fared the worst and failed the test, giving absolute average deviations in vapour compositions above the threshold

value of 0.01. The NRTL and Wilson equations also gave low consistency indices for the Direct test, and for the UNIQUAC model, because of its inability to correlate the data satisfactorily; high values of the consistency indices were obtained. In conclusion, the data sets were consistent and the Area and Point tests gave enough and reliable indication of the systems' consistency.

9.2 Recommendations

The operation of the equipment used in the project revealed to the researcher areas where further work and modifications can be done which could substantially improve both the versatility and operation of the equipment in measuring vapour-liquid-liquid equilibria. These areas are:

1. Introduction of computer control to the still in both the isobaric and isothermal modes. This would eliminate human errors and result in more precise control of the measured temperature and pressure.
2. Incorporation of a small liquid chamber on the standpipe leg of the VLLE still so that the returning condensate premixes with the liquid from the liquid receiver before mixing with the bulk of the liquid in the boiling chamber. This chamber should be mixed possibly magnetically and heated so as to raise the temperature of the contents to that of the reboiler's contents. This arrangement should help in measuring data for systems of very high relative volatilities like the tolunitrile (1) + water (2) system, for which measurements could not be made in this work.
3. The use of an Ultrasound homogeniser as by Gomis [2000] for mixing the liquid in the reboiler. This should allow operation in the two-liquid phase region which in turn will allow sampling of the two liquids in equilibrium from the same VLLE still after incorporating a small cell in the liquid receiver where the two liquids in equilibrium can be sampled as in the still by Iwakabe et al. [2001]. This will reduce the apparatus to a single piece of equipment giving both VLLE and LLE. It will also allow for easy measurement of VLLE and LLE for more than two components.
4. An investigation into the simultaneous regression and analysis of VLE and LLE data using the same model equations.

References

Abrams, D S, and Prausnitz, J M, (1975), "Statistical Thermodynamics of Liquid Mixtures: A New Expression for the Excess Gibbs Energy of Partly or Completely Miscible Systems", *American Institute of Chemical Engineers Journal*, Vol. 21 pp 116 -128.

Abbot. M. M (1986), "Low Pressure Phase Equilibria: Measurement of VLE", *Fluid Phase Equilibria*, Vol 29, p 193 -207

Baker, E M, Hubbard, O H, Huguet, J H & Michalowski, S S, (1939) " Equilibria in the Systems Ethanol – Water, Ethanol- Cellosolve, and Cellosolve – Water", *Industrial and Engineering Chemistry*, Vol 31, p 1260 – 1262.

Barker, J A, (1953), "Determination of Activity Coefficients from Total Pressure Measurements", *Australian Journal Chemistry*, Vol. 6 pp 207 – 210.

Cho, T H, Ochi, K & Kojima, K, (1984), "Isobaric vapour Liquid Equilibria for Binary systems with Limited Miscibility- Water – n-Amyl Alcohol and Water – IsoAmyl Alcohol", *Kagaku Kogaku Ronbunshu*, Vol 10, p 181

Cholinski, J, Szafranski, A and Wyrzykowska –Stankiewicz, D, (1986), "Computer Aided Second Virial Coefficient Data for Organic Individual Compounds and Binary Systems", PWN-Polish Scientific Publishers, Warsaw.

Christiansen, L J, and Fredenslund, A, (1975), "Thermodynamic Consistency Using Orthogonal Collocation or Computation of Equilibrium Vapour Compositions at High Pressures", *American Institute of Chemical Engineers Journal*, Vol. 21pp 49-57

Colburn, A P, Schoenborn, E M & Shilling David, (1943), "Equilibrium Still for partially Miscible Liquids", *Industrial and Engineering Chemistry*, Vol 35, p 1250 – 1254

Cottrell, F G (1919), "On the Determination of Boiling Points of Solutions", *Journal of American Chemical Society*, Vol. 41, p 721 – 728

Coulson, E A, Hales, J L & Herington, E F G, (1948), "Fractional Distillation. II. The use of Dilute Solutions of Thiophene in Benzene as Test Mixtures and Comparison with Mixtures of Benzene and Ethylene Dichloride", *Transactions of the Faraday Society*, Vol 44, p 636 – 644

DiElsi, D P, Patel, R B, Abbott, M M & Van Ness, H C , (1978), "Excess Thermodynamic Functions for Ternary Systems. 3: Total Pressure Data and GE for Acetone-Acetonitrile- Acetate at 50 °C", *Journal of Chemical and Engineering data*, Vol23, pp 242- 245

Dymond, J H, and Smith, E B (1980), "The Virial Coefficients of Gases and Gaseous Mixtures", Clarendon Press, Oxford

Ellis, S R M, Garbett, R D , (1960)," A new Equilibrium Still for the Study of Partially Miscible Systems", *Industrial and Engineering Chemistry*, Vol 52 , p 385 – 388

Englezos, P, Kalogerakis, N, Trebble, MA, and Bishnoi, P R, (1990 a), "Estimation of Multiple Binary Interaction Parameters in Equations of State Using VLE Data. Application to the Trebble Bishnoi Equation of State", *Fluid Phase Equilibria*, Vol .58, pp 117 – 132.

Englezos, P, Kalogerakis, N, and Bishnoi, P R, (1990b), "Simultaneous Regression of Binary VLE and VLLE Data", *Fluid Phase Equilibria*, Vol. 60, pp 1-15.

Englezos, P, Lee, J D, Susilo, R, (2005), " Liquid Liquid Equilibrium Data of water with Neohexane , Methyl cyclohexane, tert butyl Methyl ether, n- heptane and Vapour Liquid Liquid Equilibrium with methane", *Fluid Phase Equilibrium* Vol. 231. pp 20 -26

Fenske, M R, Carlson, C S & Quiggle D, (1947), " Solvent Separation of Hydocarbon Mixtures by Vapour Liquid Extraction", *Industrial Engineering Chemistry*, Vol. 39, pp 1322-1328

Flory, P J,(1942) *Journal of Physical Chemistry* Vol .10, pp 51 as in Prausnitz (1969)

Fredenslund, A, Gmehling, J, and Rasmussen, P, (1977), "Vapour Liquid Equilibrium using UNIFAC", Elsevier Scientific Publishing Company, New York.

Gess, M A, Danner, R P, and Nagvekar, M (1991), "Thermodynamic Analysis of Vapour Liquid Equilibria: Recommended Models and Standard Data base", *Design Institute for Physical Property Data, American Institute of Chemical Engineers.*

Gibbs, R E & Van Ness, H C (1972), "Vapour – Liquid Equilibria from Total Pressure Measurements. A New Apparatus", *Industrial and Engineering Chemistry-Fundamentals*, Vol 11, p 410 – 413

Gillespie, D T C, (1946), "Vapour – Liquid Equilibrium Still for Miscible Liquids". *Industrial and Engineering Chemistry, Analytical Edition*, Vol 18, p 575 – 577

Gmehling, J (2003)," Potential of Group Contribution Methods for the prediction of Phase Equilibria and the Excess Properties of Complex Mixtures, *Journal of Pure and Applied Chemistry* Vol 75, No 7, pp 875 -888.

Gomis. V, Ruiz. F, Asensi J.C, (2000) "The application of Ultrasound in the determination of Isobaric vapour- Liquid-Liquid Equilibrium Data", *Fluid Phase Equilibria*, Vol 172 , p245 – 259

Hala, E, Pick, J. Fried, V & Vilim.O (1958) " vapour Liquid Equilibrium", 1st Edition, Pergamon Press , Oxford

Hala, E, Pick, J. Fried, V & Vilim.O (1967) " vapour Liquid Equilibrium", 2nd Edition, Pergamon Press , Oxford

Hands, C.H.G, Norman, W.S, (1945) *Transactions of the Institution of Chemical Engineers* Vol 23, p76 – 88

Hayden, J G, and O'Connell, J P, (1975), "A Generalised Method for Predicting Second Virial Coefficients", *Industrial and Engineering Chemistry. Process Design and Development*, Vol. 14, pp 209 – 216.

Heertjies, P M (1960), "Determination of Vapour – Liquid – Equilibria of Binary Mixtures", *Chemical and Process Engineering Journal*, Vol 41, p 385 – 386

Herington, E F G, (1947), " A Thermodynamic Consistency Test for the Internal Consistency of Experimental Data on Volatility Ratios", *Nature , Vol .60, pp 610 -611*

Hirata, M, Konishi, H & Kato, M, (1970), "New Apparatus for Isobaric Dew and Bubble Point Method: Methanol-Water, Ethyl Acetate – Ethanol water, water- 1-Butanol, Ethyl Acetate - Water systems", *Journal of Chemical and Engineering Data*, Vol 15, pp 435 - 439

Hirata, M, Ohe, S, and Nagahama, K (1975) "Computer Aided Data Book of Vapour Liquid Equilibria:, Kodasha Limited, Elsevier Publishing Company, Tokyo.

Hlavaty, K , *Collections of the Czechoslovak Chemical Communications,* (1972), Vol 37 pp 4005, as in Letcher et al (1989).

Huggins, M L, (1942), *Journal pf Physical Chemistry* Vol .9, pp 440 as in Prausnitz (1969)

Inoue, M, Azumi, K & Suzuki, N (1975), "A new Vapour Pressure Assembly for Static vapour Liquid Equilibrium", *Industrial and Engineering Chemistry – Fundamentals*, Vol 14, p 312 – 314

Iwakabe, K & Kosuge, H, (2001)," Isobaric Vapour-Liquid – Liquid Equilibria with a Newly Developed Still", *Fluid Phase Equilibria*, Vol 192, p 171 – 186

Joseph, M A, Raal, J D & Ramjugernath, D , (2001), " Phase Equilibrium Properties of Binary Systems with Diacetyl from a computer controlled Vapour – Liquid Equilibrium still", *Fluid Phase Equilibria*, Vol 182, p 157 – 176

Joseph, M A, (2001), Master of Science in Engineering (Chemical Engineering) Thesis.

Kojima, K and Tochigi, K, (1979), "Prediction of Vapour Liquid Equilibria by the ASOG Method ", Elsevier Scientific Publishing Company, New York.

Kollar, G Y , (1952) Magyar Kem Foly, Vol 58, p 324 as in Hala et al (1958)

Lee, M J, Hu, C H, (1995), "Isothermal Vapour – Liquid Equilibria for mixtures of ethanol, acetone and diisopropyl ether", *Fluid Phase Equilibria*, Vol 109 p 83 – 98

Lee, S C (1931)," Partial Pressure Isotherms", *Journal of Physical Chemistry*, Vol 35, p 3558 – 3582

Letcher, T M, Siswana, P M, Van Der Watt, P, Radloff, S, (1989), "Phase Equilibria for (an Alkane + p-xylene + water) at 298.2 K, *Fluid Phase Equilibria*, Vol 21,pp1053 – 1060.

Liu, H, Hu, Y, and Peng, C, (2002), "Liquid Liquid Equilibria of copolymer mixtures bases on an Equation of State", *Fluid Phase Equilibria*, Vol 201, pp 19 -35.

Ljunglin, JJ, and Van Ness, H C, (1962), "Calculation of Vapour Liquid Equilibria from Vapour Pressure Data", *Chemical Engineering Science* Vol.17, pp 531 – 539.

Loehe, J, Van Ness, H C & Abbott, M M, (1983), "vapour- Liquid – Liquid Equilibrium. Total – Pressure data and G^E for water – Methyl Acetate at 50oC", *Journal of Chemical and Engineering Data*, Vol 28, p 405 – 407

Malanowski, S, (1982a, "Experimental Methods for vapour Liquid Equilibria. Part I. Circulation Methods", *Fluid Phase Equilibria*, Vol 8, p197 -219

Malanowski, S, (1982b), "Experimental Methods for Vapour Liquid Equilibria. Part II, Dew and Bubble Point Method", *Fluid Phase Equilibria*, Vol, 9, p 311-317

Malanowski, S and Anderko, A, (1992) "Modelling Phase Equilibrium: Thermodynamic Background and Practical Tools, John Wiley and Sons, Inc, New York, USA.

Marquardt, D W, (1958), "Solution of Non- Linear Chemical Engineering Models", *Chemical Engineering Progress*, Vol. 55, No. 6 pp 65 – 70.

Marquardt, D W, (1963), "An Algorithm for Least Squares Estimation of Non- Linear Parameters", *Journal of the Society for Industrial and Applied Mathematics*, Vol. 11, No. 2, pp 431 – 441.

McClellan, A L, (1963 -1974), "Tables of Experimental Dipole Moments", W. H Freeman, San Francisco.

Mixon, F C, Gumowski, B, and Carpenter, B H, (1965), "Computation of Vapour Liquid Equilibrium Data from Solution Vapour Pressure Measurements", *Industrial and Engineering Chemistry, Fundamentals*, Vol. 4, No 4 pp 455 – 459.

Newsham, D M T, Dawe, R A & Bee NG, S, (1973), "Vapour-Liquid Equilibria in mixtures of water, n-propanol and n-Butanol", *Journal of Chemical and Engineering Data*, Vol18, p 44 – 49

Null, H, R, (1980), "Phase Equilibrium in Process Design" , Robert E Krieger, New York.

Ohta, T, Todoriki, H, and Yamada, T,(2004), " Representation of Liquid Liquid Equilibria at low and High Pressures using EOS- GE Mixing rules", *Fluid Phase Equilibria* Vol. 225, pp 23 – 27.

Othmer, D F (1928) "Composition of Vapours from Boiling Binary Solutions. Improved Equilibrium still", *Industrial and Engineering Chemistry*, Vol 20, p 743 – 766

Othmer, D F (1943) "Composition of Vapours from Boiling Binary Solutions", *Industrial and Engineering Chemistry*, Vol 35, p 615 – 620

Othmer, D F (1948) "Composition of Vapours from Boiling Binary Solutions", *Industrial and Engineering Chemistry: Analytical Edition*, Vol 20, p 763

Pai, Y H, Chen, L,(1999) "Liquid – Liquid Equilibria of Two Binary Systems: Water + 1-pentanol and Water + 2-methyl – 2- butanol and Two Ternary systems: water + 1-Pentanol + 2-butyloxyethanol and Water + 2-methyl-2-butanol + 2-butyloxyethanol", *Fluid Phase Equilibria*, Vol 155, p 95

Peng, D and Robinson, D B, (1976), "A New Two constant Equation of State" *Industrial and Engineering Chemistry. Fundamentals*. Vol 15. pp 59 -64.

Perry, R H and Green, D W, (1997), " Perry's Chemical Engineers' Hand book", McGraw Hill Book Company, New York

Pitzer, K S, and Curl, R F, (1957), "Empirical Equation for the Second Virial Coefficients", *Journal of the American Chemical Society*, Vol. 79, pp 2369 – 2370

Prausnitz, J M, Anderson, T F, Grens, E A, Eckert, CA, O'Connell, J P (1967) "Computer Calculations for Multicomponent Vapour Liquid Equilibria" Prentice- Hall, Englewood Cliffs, NJ

Prausnitz, J M, (1969), "Molecular Thermodynamics of Fluid Phase Equilibria", Prentice Hall Inc. Canada

Prausnitz, J M, Anderson, T F, Grens, E A, Eckert, CA, O'Connell, J P (1980) "Computer Calculations for Multicomponent Vapour Liquid Equilibria" Prentice- Hall, Englewood Cliffs, NJ

Prausnitz, J M, and Lobien, G M, (1982), "Infinite Dilution Activity Coefficients from Differential Ebulliometry", *Industrial and Engineering Chemistry, Fundamentals*, Vol. 21, pp 109 – 113

Prausnitz, J M, Lichtenthaler, R N and De Azevedo, E G (1986) "Molecular Thermodynamics of Fluid Phase Equilibria", 2nd Edition, Prentice Hall, Englewood Cliffs, New Jersey

Raal, J D and Brouckaert, C J, (1992)," Vapour liquid and liquid liquid Equilibria in the System methl butenol - water , Fluid Phase Equilibria 74, pp 253-270.

Raal, J D and Naidoo, P (1990), "Excess Enthalpy Measurement Using A Novel Highly refined Micro flow Calorimeter and the Prediction of Vapour Liquid Liquid Equilibria from such Data", *Fluid Phase Equilibria* Vol. 57, pp 147 – 160.

Raal. J D & Muhlbauer. A L, (1998) "Phase Equilibria: Measurement and Computation", Taylor and Francis, Bristol PA

Raal, J D (2000) "Characterization of Differential Ebulliometers for Measuring Activity Coefficients", *American Institute of Chemical Engineers. Journa*l, Vol 46, p210 – 220.

Rackett, H G, (1970), "Equation of state for saturated Liquids", *Journal of Chemical and Engineering Data*, Vol. 15 pp 514-517

Redlich, O and Kwong, J N S, (1949), "On Thermodynamics of SolutionsV: An Equation of State. Fugacities of Gaseous Solutions", *Chemical Reviews* Vol. 44 pp 233 – 244.

Reid, C R, Prausnitz, J M, and Polling, B E, (1988), "The Properties of Gases and Liquids", 4th Edition, McGraw Hill Book Company, Singapore

Renon, H and Prausnitz, J M (1968), "Local Compositions in Thermodynamic Excess Functions for Liquid Mixtures", *American Institute of Chemical Engineers Journal*, Vol. 14 pp 135-144.

Rosanoff, M A, Bacon, C W. White, R H, (1914) " A rapid Laboratory Method of measuring partial vapour Pressures of Liquid Mixtures", *Journal of the American Chemical Society*, Vol 36, p 1803 – 1825

Sandler, S I, Orbey, H, and Lee, B, (1994), "Models for Thermodynamic and Phase Equilibria Calculations. Marcel Dekker, New York.

Sayegh, S G, and Vera, J H, (1980), "Model Free Methods for Vapour Liquid Equilibria Calculations. Binary Systems", *Chemical Engineering Science*, Vol. 35. pp 2247 -2256

Scatchard, G, Raymond, C L & Gilman, H H (1938), "Vapour Liquid Equilibrium. I. Apparatus for Study of Systems with Volatile Components" *Journal of the American Chemical Society*, Vol 60, p 1275 – 1287

Scatchard, G (1949), "Equilibrium in Non-Electrolyte Mixtures", *Chemical Reviews*, Vol.44, pp 7 – 35.

Schultz, D M, Crouse, C F S, (1973), *African Statistic Journal*, Vol 7, pp143

Skjold-Jorgensen, S, Rasmussen, P and Fredenslund, A, (1980), "On the Temperature Dependence of the UNIQUAC/ UNIFAC Models" *Chemical Engineering Science*, Vol. 35 pp 2389 – 2403.

Soave, G, (1972), "Equilibrium Constants from a modified Redlich-Kwong Equation of State", *Chemical Engineering Science.* Vol. 27 pp 1197 – 1203

Soave, G, (1979), "Application of an Equation of State to Vapour Liquid Equilibrium of systems containing polar compounds", *Institute of Chemical Engineers Symposium, Ser 56:* pp 1.2/1-1.2/16.

Sorensen, J M, Magnussen, T, Rasmussen, P, and Fredenslund, A, (1979a), Liquid Liquid Equilibrium Data: Their Retrieval, Correlation and Prediction, Part I: Retrieval", *Fluid Phase Equilibria*, Vol. 2 pp297 – 309

Sorensen, J M, Magnussen, T, Rasmussen, P, and Fredenslund, A, (1979b), Liquid Liquid Equilibrium Data: Their Retrieval, Correlation and Prediction, Part I1: Correlation*", Fluid Phase Equilibria*, Vol. 3. pp47 – 82

Sorensen, J M, Magnussen, T, Rasmussen, P, and Fredenslund, A, (1980), Liquid Liquid Equilibrium Data: Their Retrieval, Correlation and Prediction, Part III Correlation", *Fluid Phase Equilibria*, Vol. 4 pp 151 – 163

Smith J M, Van Ness, H C (1975) "Introduction to Chemical Engineering Thermodynamics" 3rd Edition, Mc Graw-Hill, Singapore

Smith J M, Van Ness, H C (1996) "Introduction to Chemical Engineering Thermodynamics" 5th Edition, Mc Graw-Hill, Singapore

Smith, T E & Bonner, R F (1949), "Vapour- Liquid Equilibrium Still for Partially Miscible Liquids", *Industrial Engineering Chemistry*, Vol 41 p 2867 – 2871

Smyth, C P (1955), "Dipole Moment and Molecular Structure" , *CCP5 Quarterly*, Vol. 4 pp 13 - 25

Stockhardt, J S & Hull, C M (1931) Vapour Liquid Equilibria and Boiling Point Composition Relations form Systems n- Butanol - water and Isobutanol – Water", *Industrial Engineering Chemistry*, Vol 23, p 1438 – 1440

Stryjek, R and Vera, J H, (1986), "PRSV: An Improved Peng and Robinson Equation of State for Pure Compounds and Mixtures", *The Canadian Journal of Chemical Engineering*, Vol. 64 pp 323-333.

Swietoslawski, W, (1945),"Ebulliometric Measurements", Reinhold, New York

Thornton, J D, (1951)," An Improved Type of Vapour Liquid Equilibrium Still", *Journal of Applied Chemistry*, Vol 1, p237 – 239

Trimble, H M, Potts, W, (1935), " Glycol- Water Mixtures, Vapour Pressure-Boiling Point – Composition Relations", *Industrial and Engineering Chemistry*, Vol27, p66

Tsonopoulos, C (1974), "An Empirical Correlation of the Second Virial Coefficients", *American Institute of Chemical Engineers Journal*, Vol. 20, pp 263 – 272

Tsuboka, T and Katayama, T, (1975), "Modified Wilson Equation for Vapour Liquid and Liquid Liquid Equilibria", *Journal of Chemical Engineering of Japan*, Vol.8 No. 5, pp 181 -187.

Van laar, JJ , (1910), " The Vapour Pressure of binary mixtures", *Zeitschrift feur Physik Chemie*, Vol 72. pp 723 -751.

Van Ness, H. C.; Byer, S. M.; Gibbs, R. E.; (1973); Vapor-Liquid Equilibrium: Part I An Appraisal of Data Reduction Methods, *American Institute of Chemical Engineers Journa.* Vol 19, pp 238-244.

Van Ness, H C and Abbott, M M, (1975), "Vapour Liquid Equilibrium: Part III- Data Reduction with Precise Expressions for G^E", *American Institute of Chemical Engineers Journal*, Vol 21, No. 1 pp 62 – 71

Van Ness, H C, Pedersen, F, and Rasmussen, P, (1978), "Part V: Data Reduction by maximum Likelihood", *American Institute of Chemical Engineers Journal*, Vol. 24, pp 1055 – 1063.

Van Ness, H C, and Abbott, MM, (1982), "Classical Thermodynamics of Non-Electrolyte Solutions: With Applications to Phase Equilibria", McGraw Hill, New York.

Van Ness, H C (1995), "Thermodynamics in the Treatment of Vapour Liquid Equilibrium Data" *Journal of Pure and Applied Chemistry*, Vol. 67. No 6 pp 859 – 872.

Van Zandijke, F & Verhoeye, L, (1974), "The Vapour Liquid Equilibrium of Ternary Systems with Limited Miscibility at Atmospheric Pressure", *Journal of Applied Chemistry and Biotechnology*, Vol 24, p 709 – 729

Vilim, O, Hala E, Pick, J, Fried, V, (1954), *Collections of the Czechoslovak Chemical Communications*, Vol 19, p 1330

Walas, S M (1985), " Phase Equilibrium in Chemical Engineering" Butterworth, Boston

Weast, R C (Editor) "Handbook of Chemistry and Physics, 64th Edition, (1983 -1984) CRC Press, London.

David, R L (Editor) "Handbook of Chemistry and Physics, 73rd Edition, (1992 -1994) CRC Press, London

Wilson, G M, (1964), "Vapour Liquid Equilibrium, A New Expression for the Excess Free Energy of Mixing", *Journal of American Chemical Society*, Vol. 86, pp 127 – 130.

Wong D S H, and Sandler S I, (1992), "A theoretically correct mixing rule for cubic equations of state" *American Institute of Chemical Engineers Journal*,.38, 671 -680.

Yerazunis, S, Plowright, J D & Smola, FM, (1964), "Vapour – Liquid Equilibrium Determination by a New Apparatus", *American Institute of Chemical Engineers Journal*, Vol 10, p 660 – 665

Young, S (1922), "Fractional Distillation", Macmillan and Company, London

A1

Appendix 1

Presented in this appendix are P-x-y and T-x-y graphs from Chapter 7. The graphs compare the experimental data to that predicted from the various models that were fitted to the experimental data.

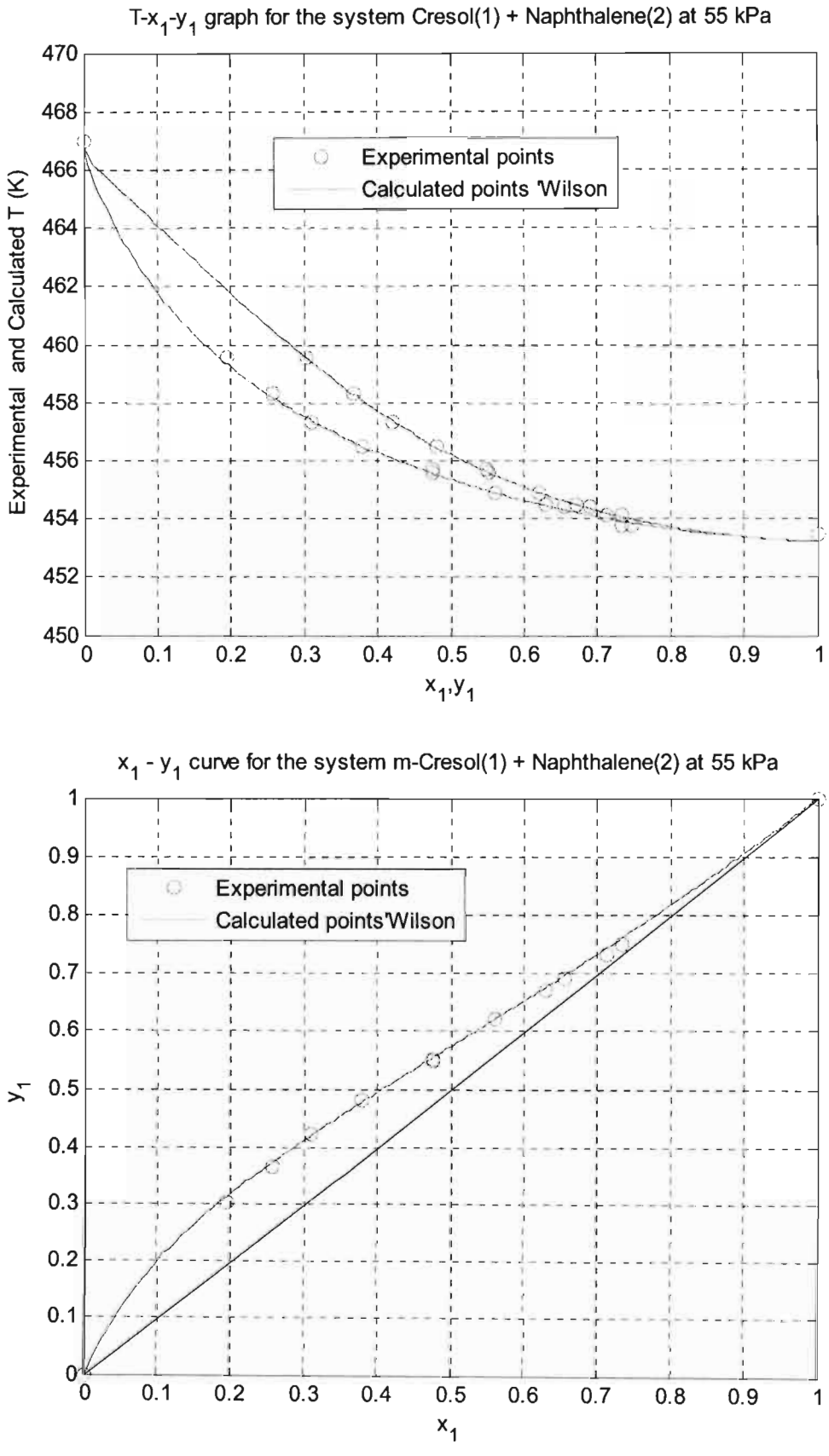

Figure A1- 1: Wilson model fitted to Experimental T-x-y data for the m-Cresol (1) + Naphthalene (2) System at 55 kPa

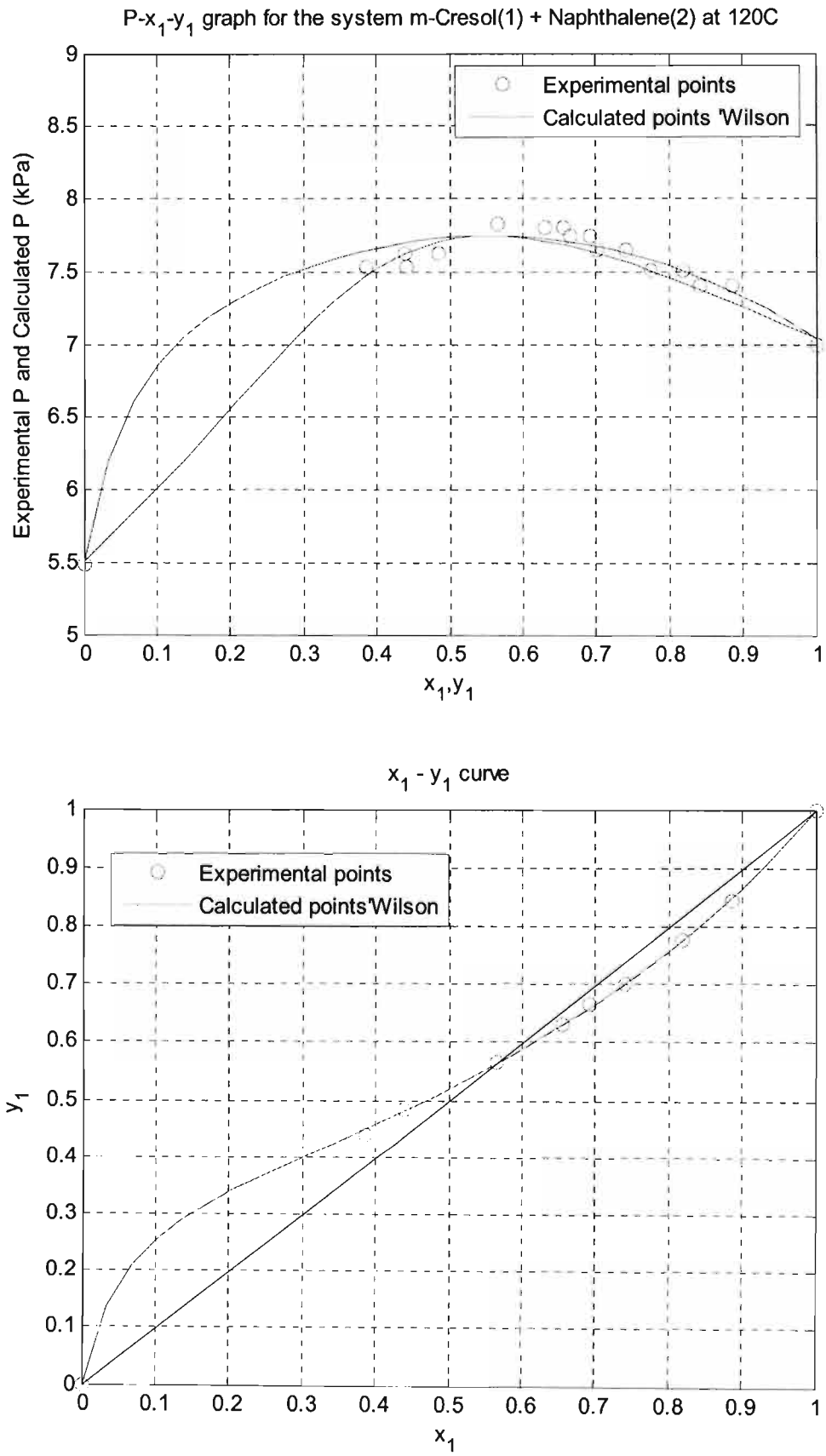

Figure A1- 2: Wilson model fitted to Experimental P-x-y data for the m-Cresol (1) + Naphthalene (2) System at 393.15 K

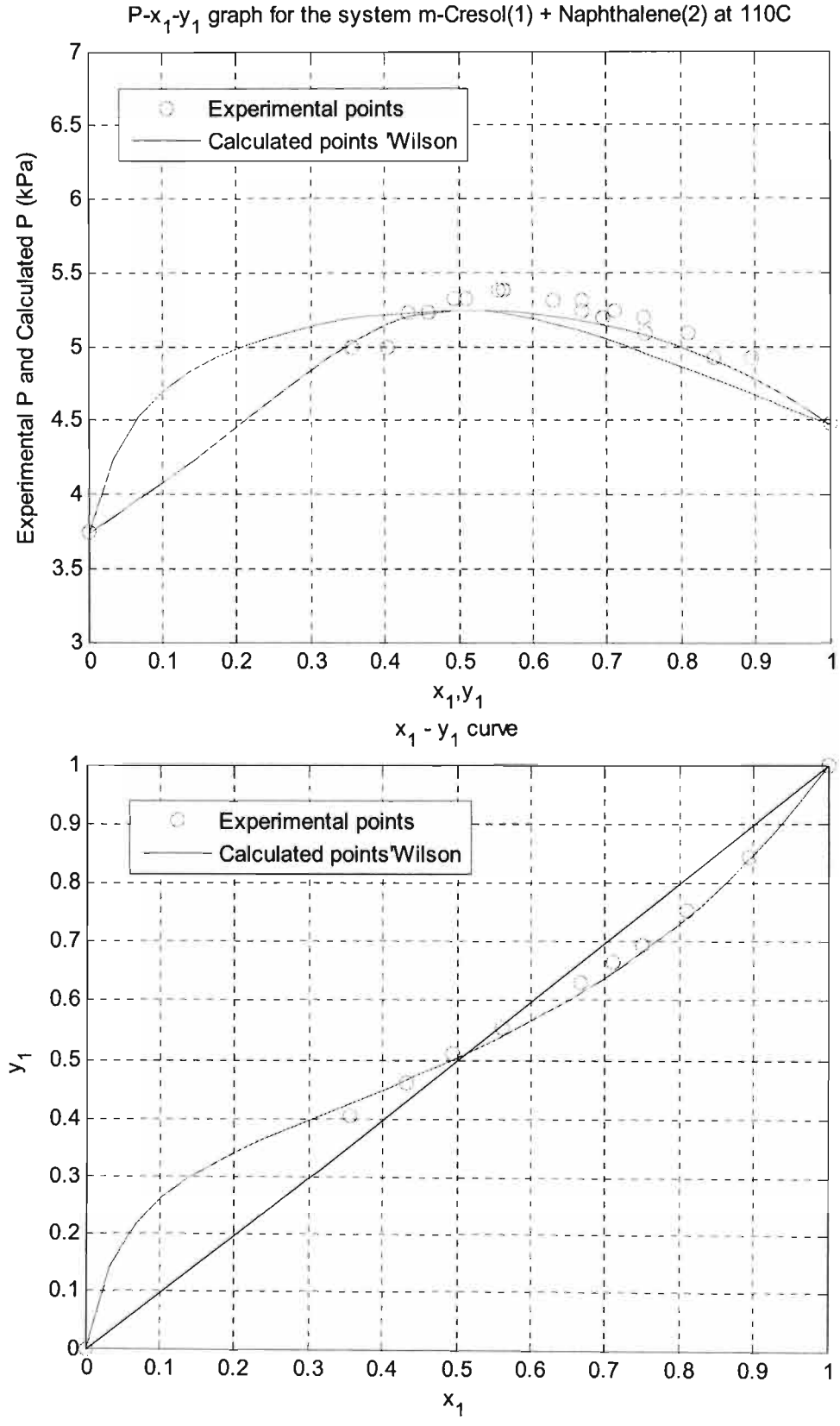

Figure A1- 3: Wilson model fitted to Experimental P-x-y data for the m-Cresol (1) + Naphthalene (2) System at 383.15 K

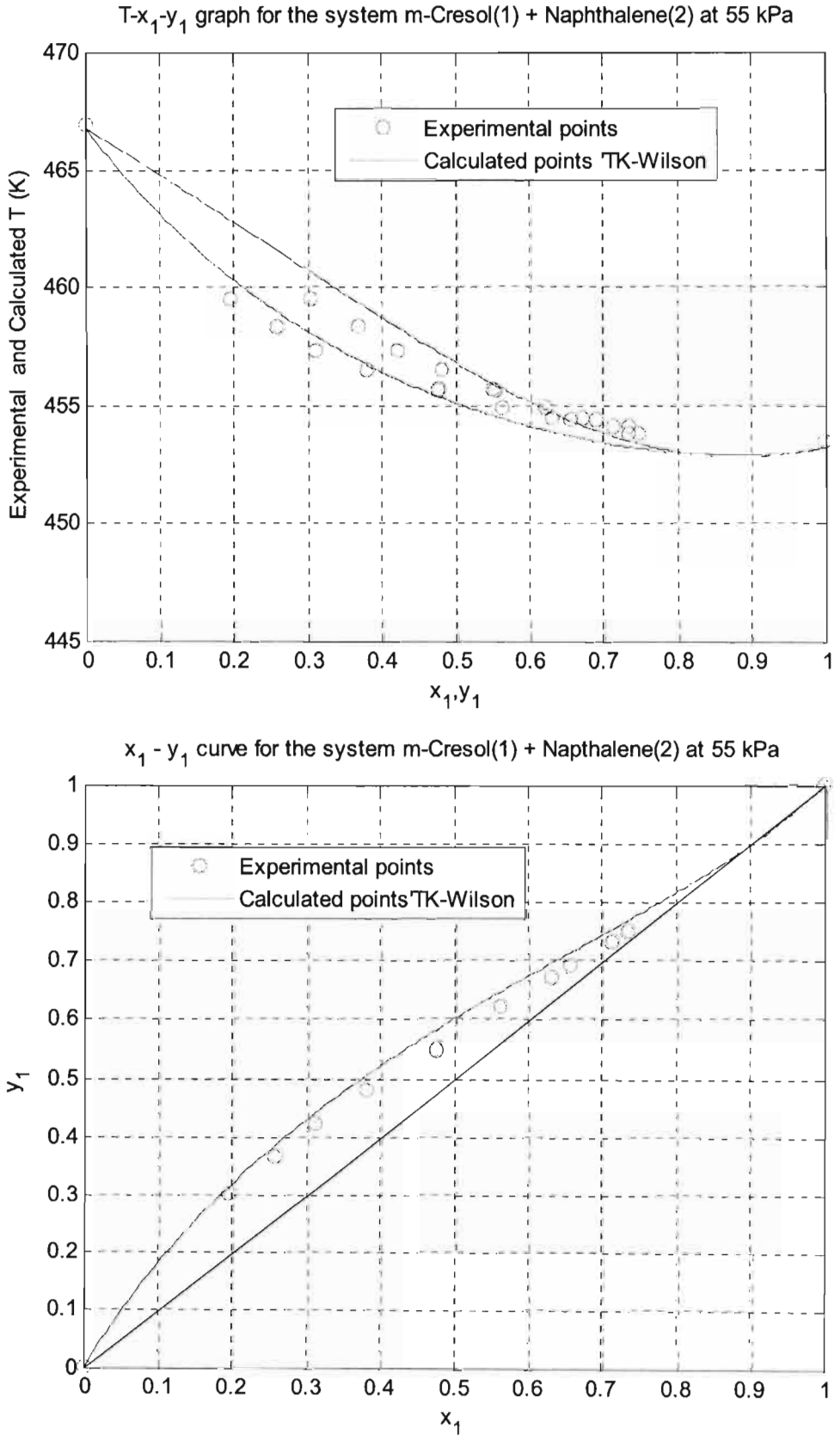

Figure A1- 4: T-K Wilson model fitted to Experimental P-x-y data for the m-Cresol (1) + Naphthalene (2) System at 55 kPa

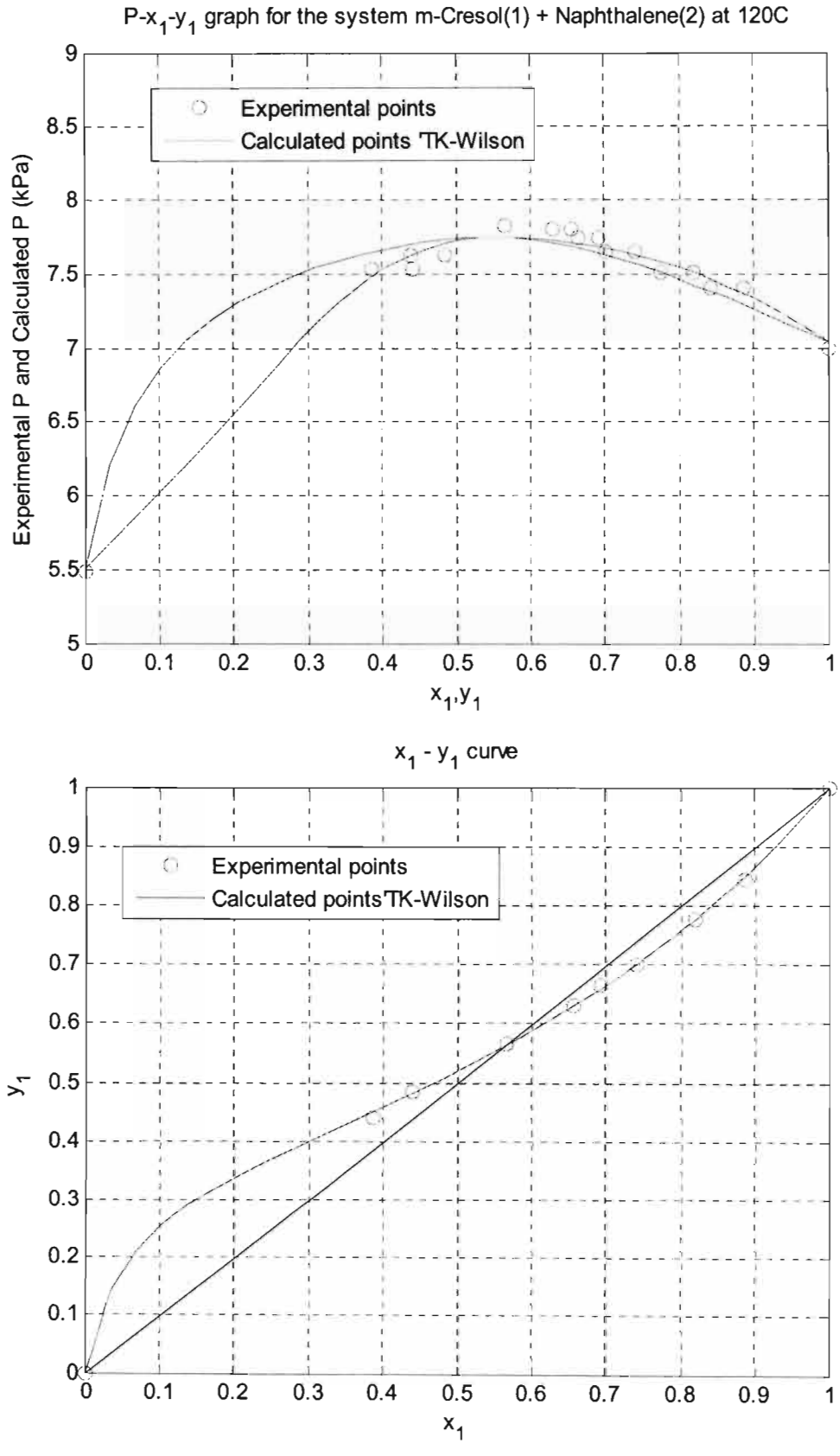

Figure A1- 5: TK-Wilson model fitted to Experimental P-x-y data for the m-Cresol (1) + Naphthalene (2) System at 393.15 K

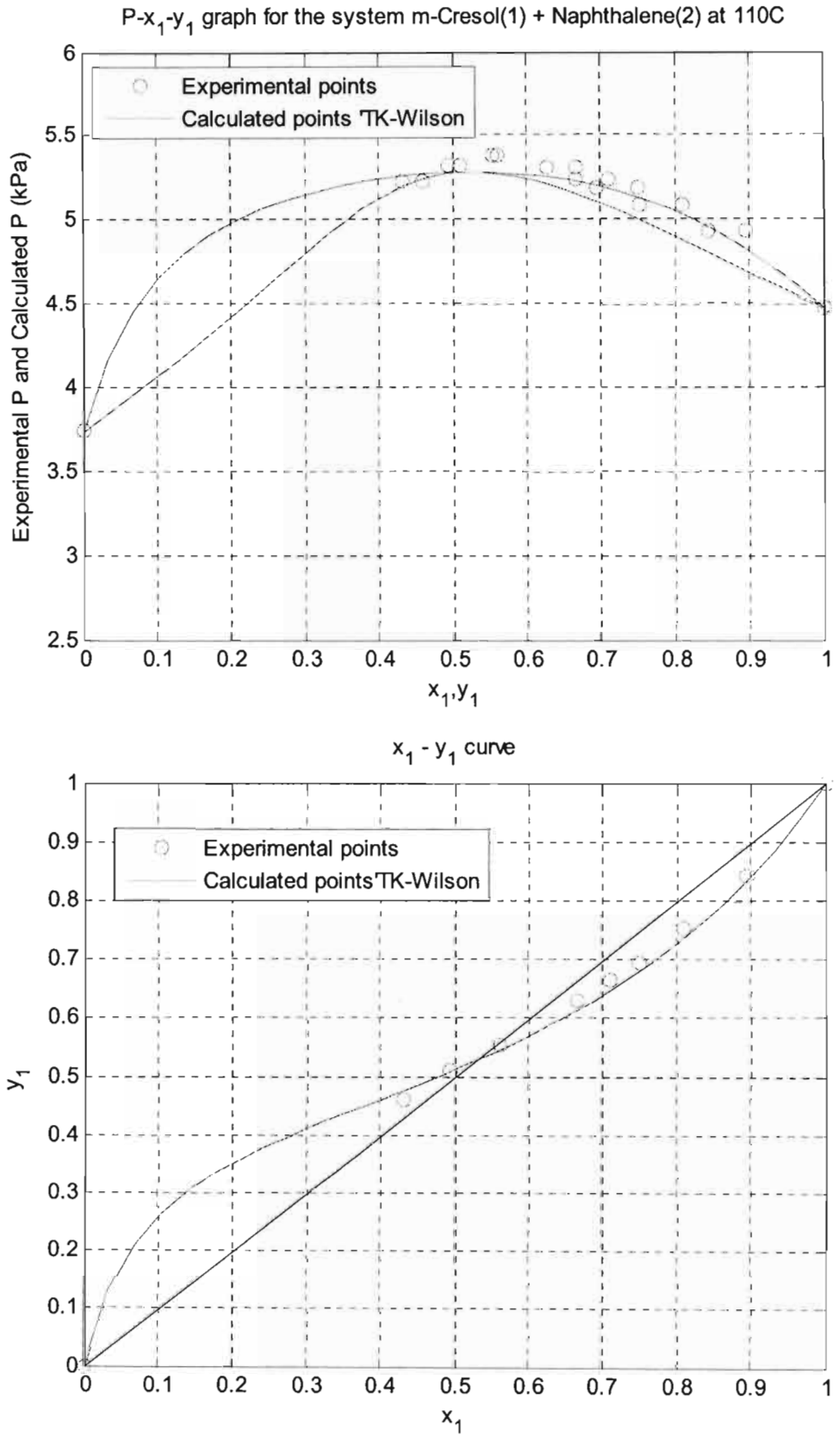

Figure A1- 6: TK-Wilson model fitted to Experimental P-x-y data for the m-Cresol (1) +Naphthalene (2) System at 383.15 K

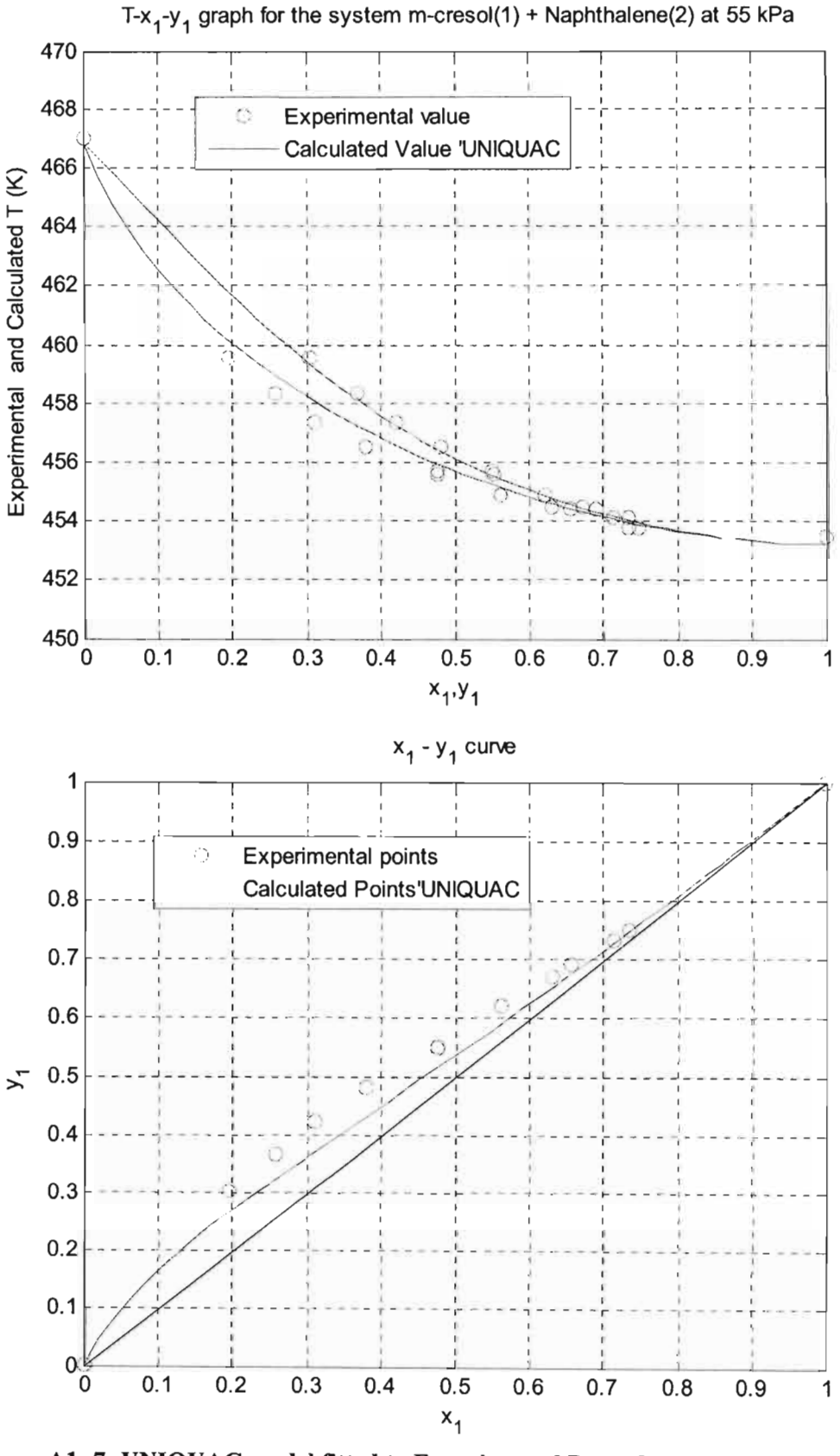

Figure A1- 7: UNIQUAC model fitted to Experimental P-x-y data for the m-Cresol (1) +Naphthalene (2) System at 55 kPa

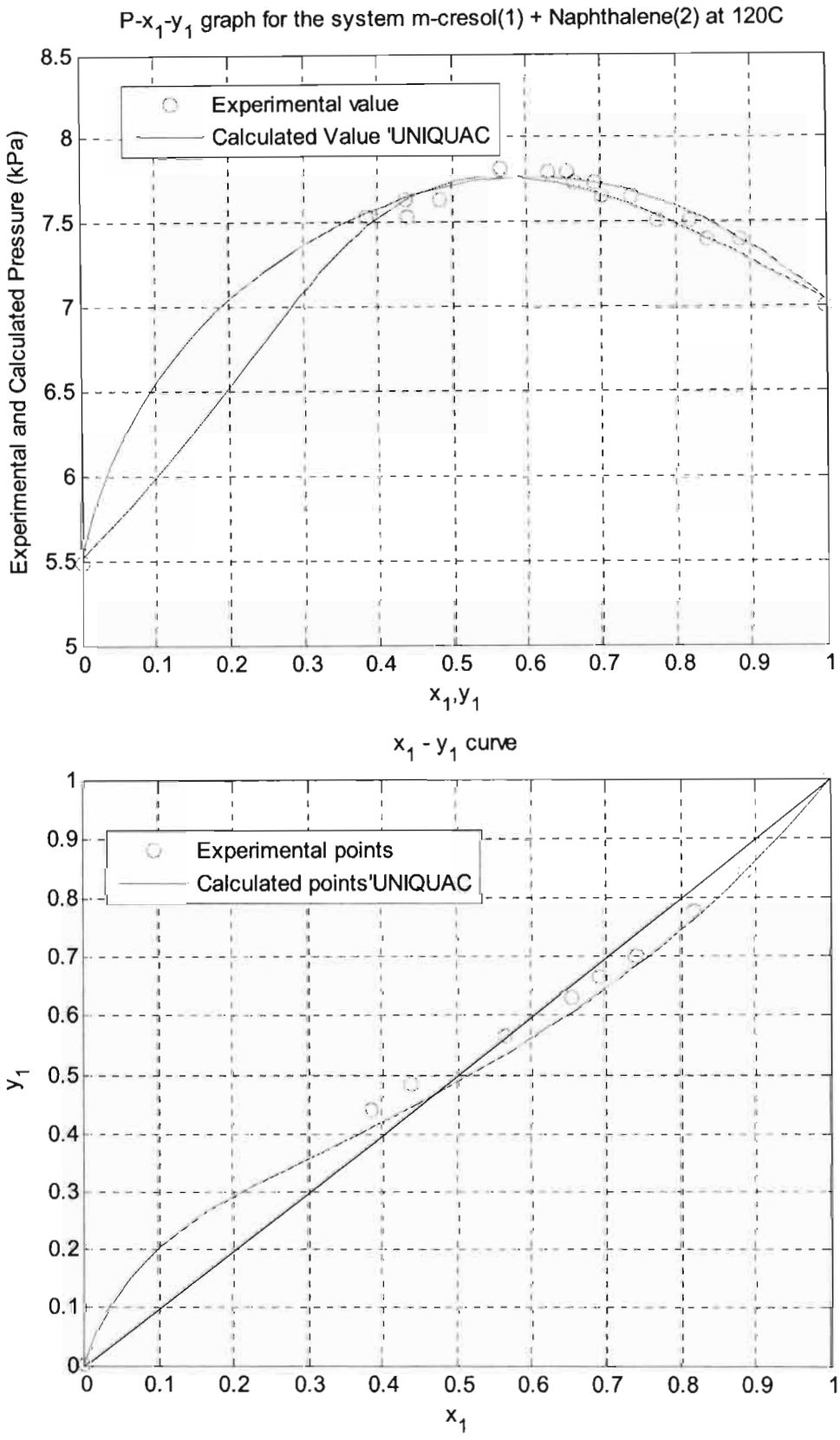

Figure A1- 8: UNIQUAC model fitted to Experimental P-x-y data for the m-Cresol (1) + Naphthalene (2) System at 393.15 K

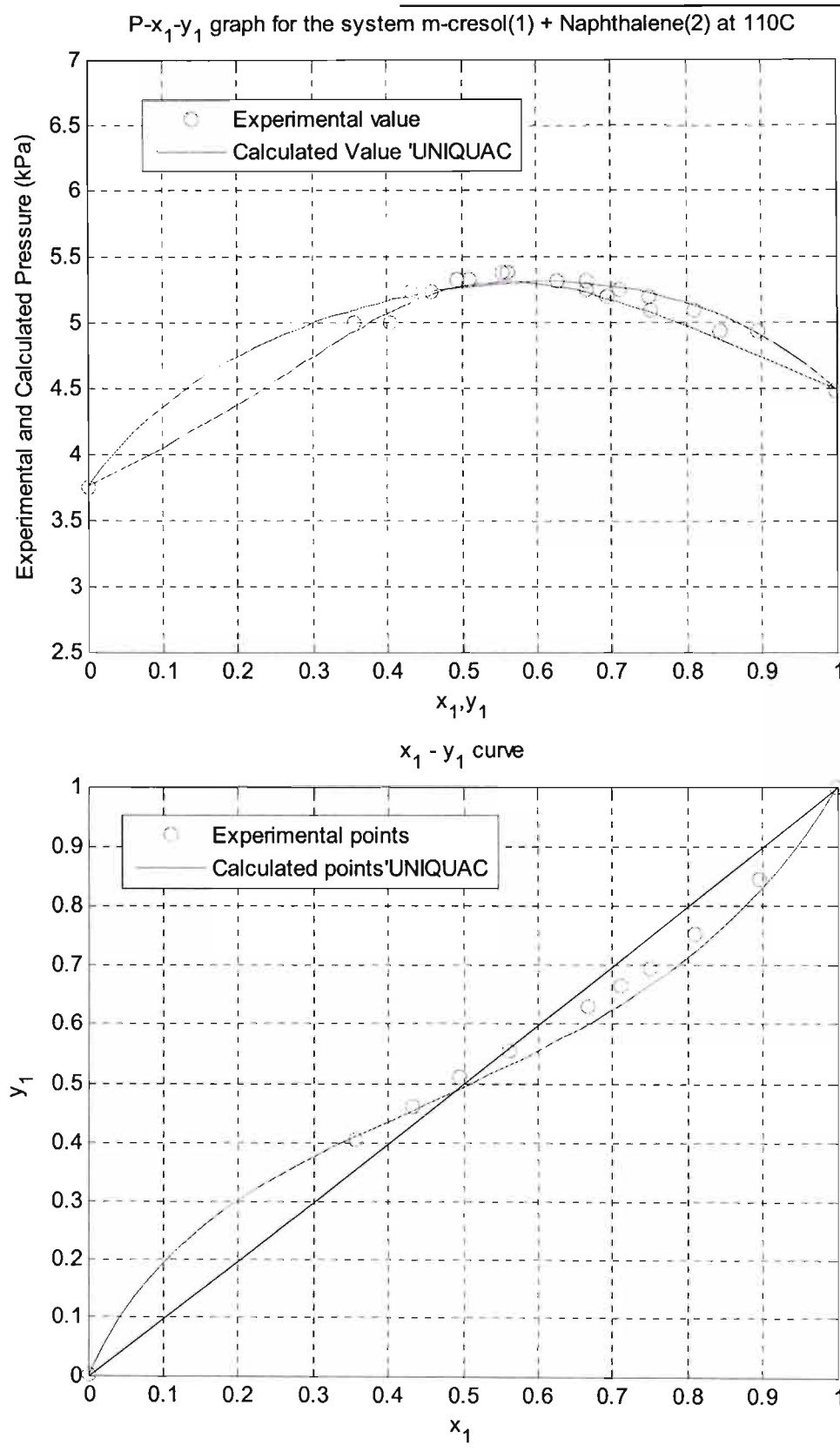

Figure A1- 9: UNIQUAC model fitted to Experimental P-x-y data for the m-Cresol (1) + Naphthalene (2) System at 393.15 K

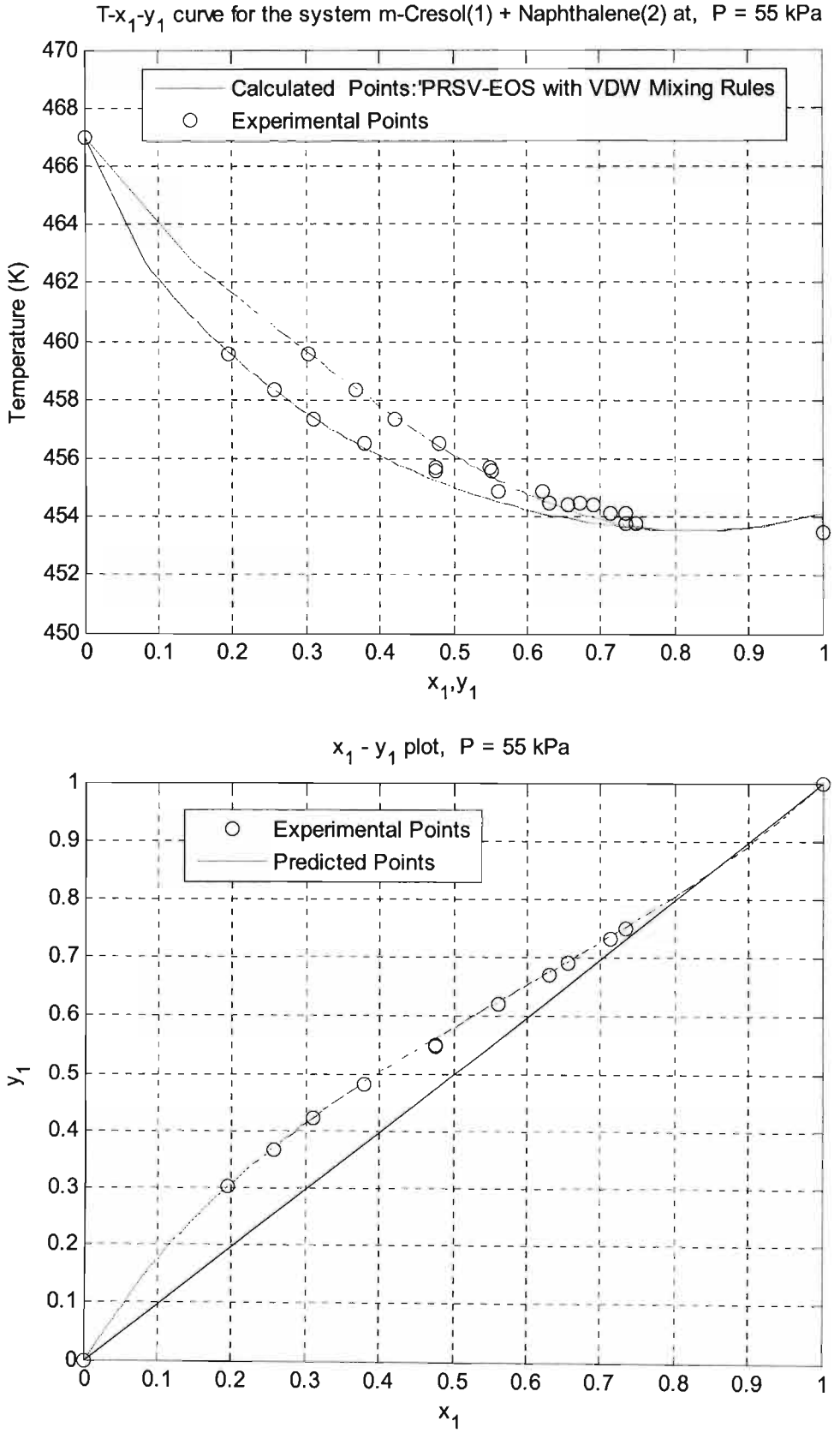

Figure A1- 10: PRSV-EOS fitted to experimental VLE data for the system m-Cresol (1) + Naphthalene (2) at 55 kPa

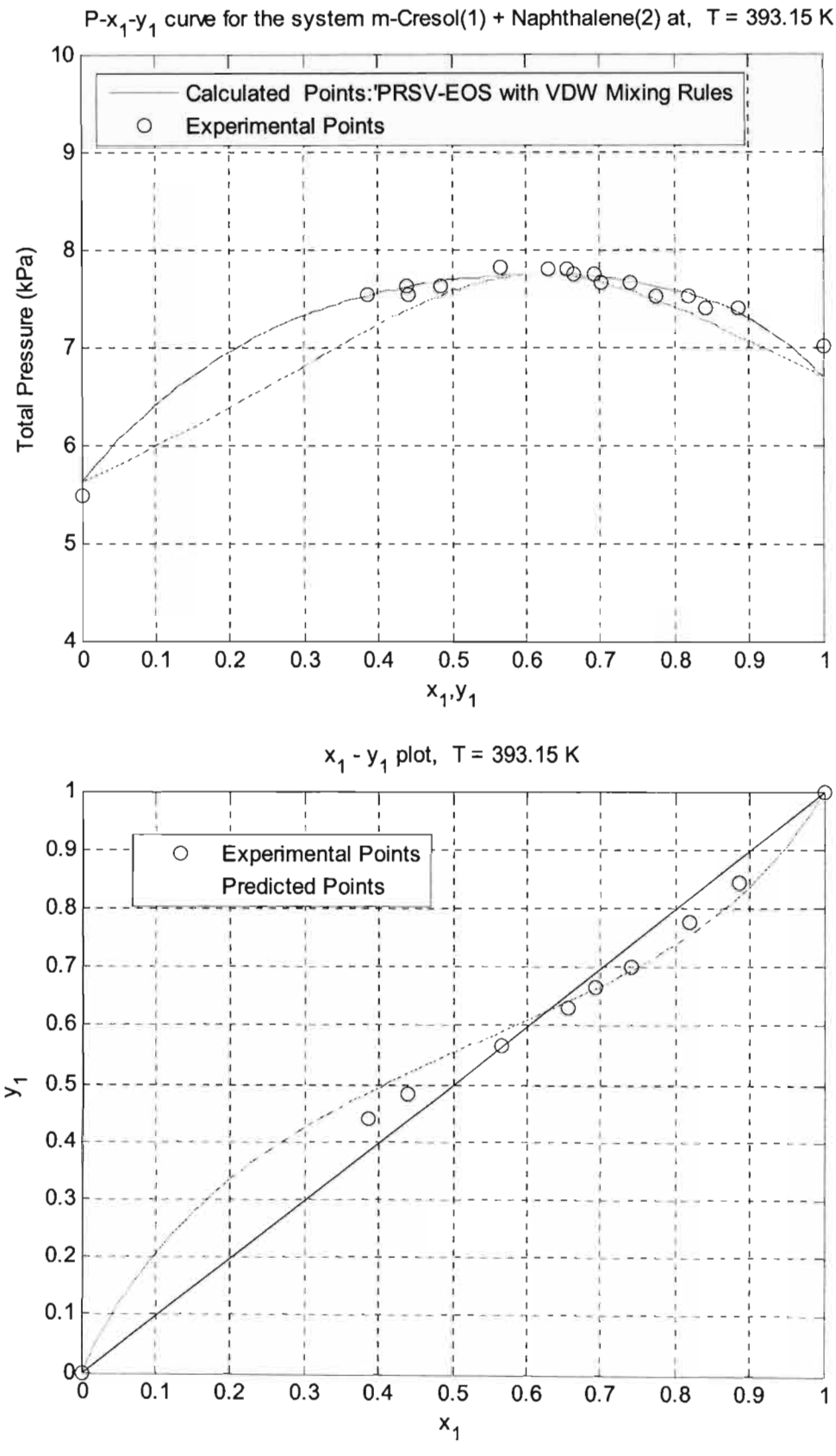

Figure A1- 11: PRSV-EOS fitted to experimental VLE data for the system m-Cresol (1) + Naphthalene (2) at 393 K

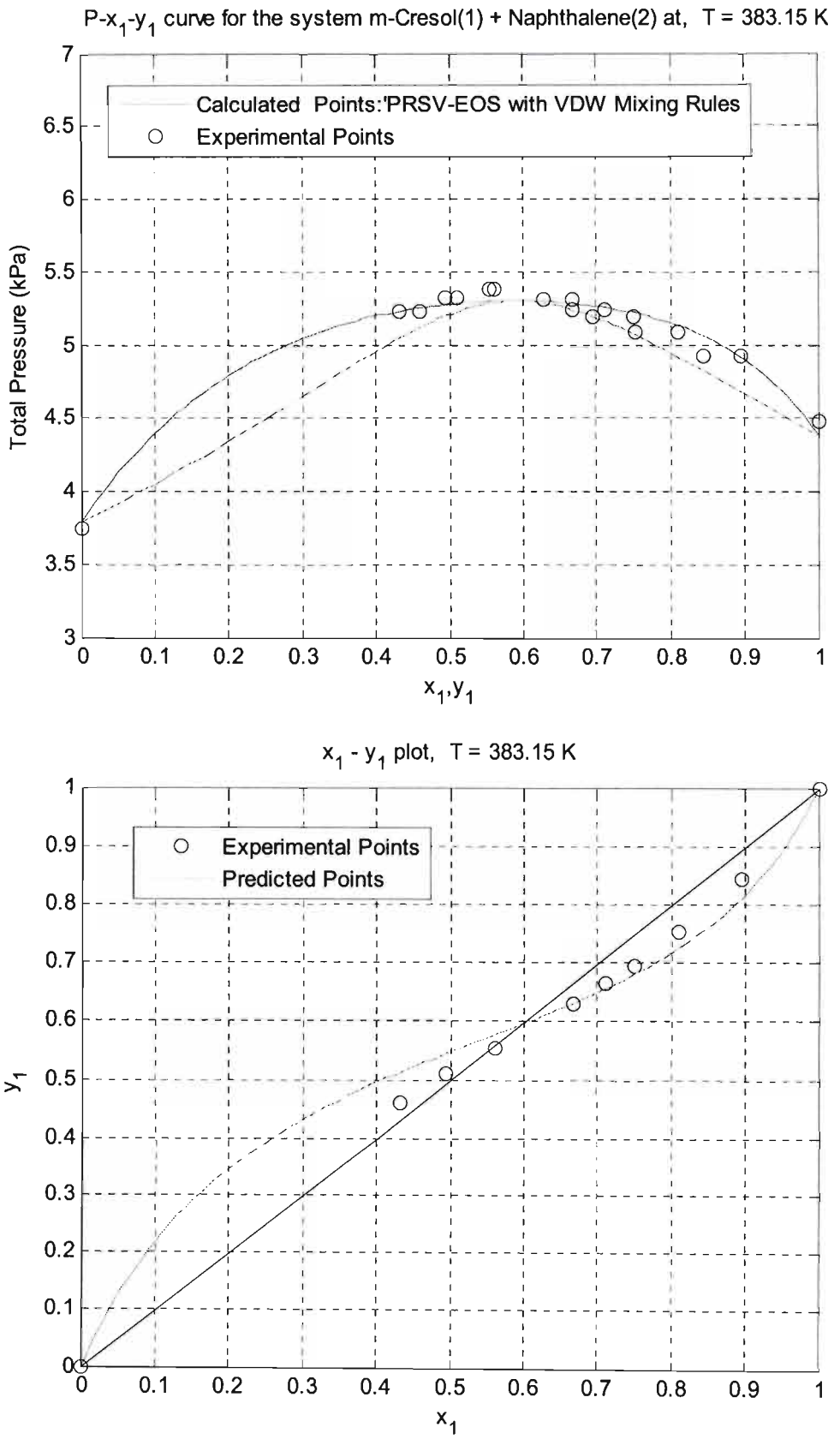

Figure A1- 12: PRSV-EOS fitted to experimental VLE data for the system m-Cresol (1) – Naphthalene (2) at 383.15 K

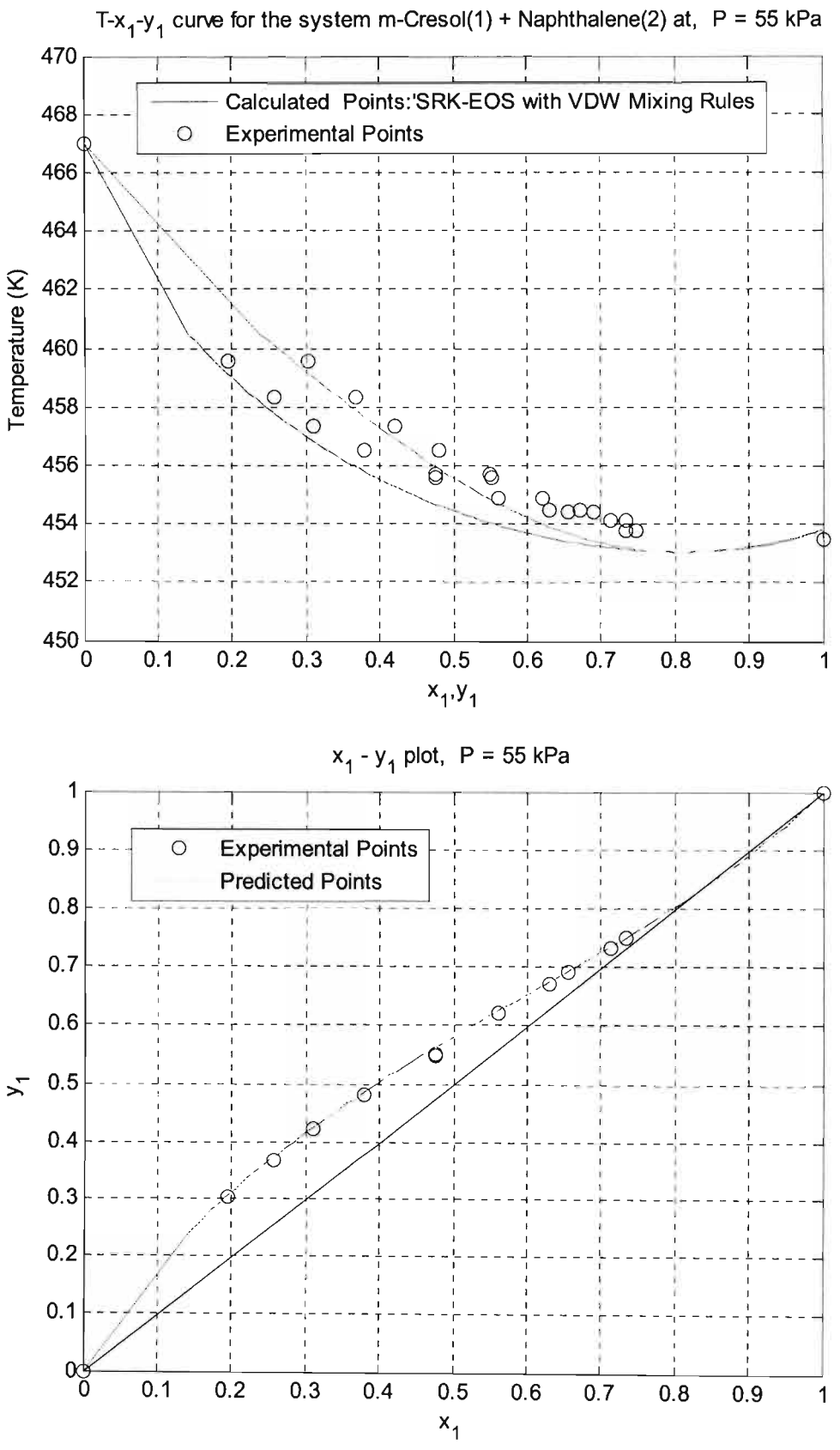

Figure A1- 13: SRK-EOS fitted to experimental VLE data for the system m-Cresol (1) + Naphthalene (2) at 55 kPa

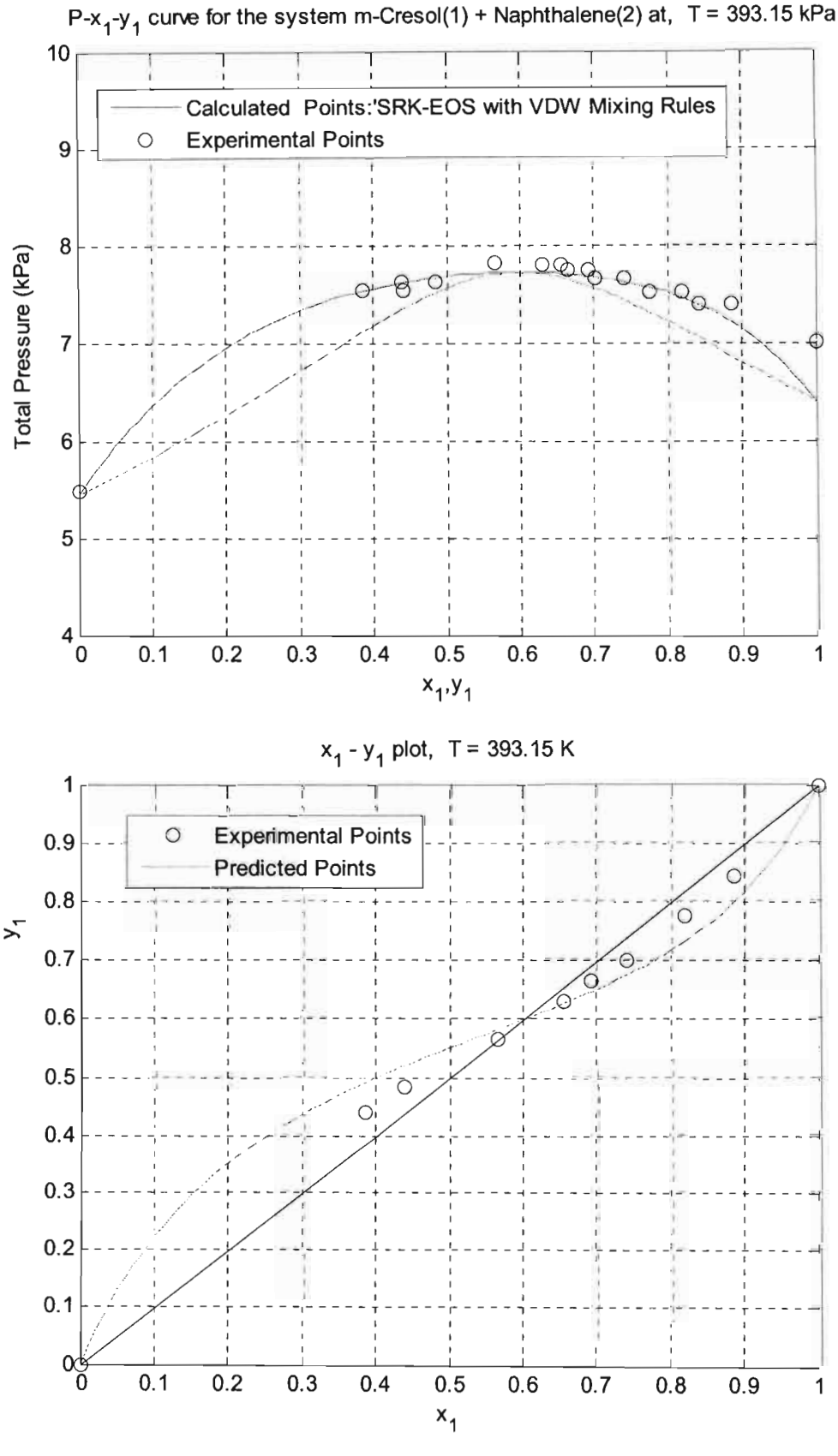

Figure A1- 14: SRK-EOS fitted to experimental VLE data for the system m-Cresol (1) + Naphthalene (2) at 393.15 K

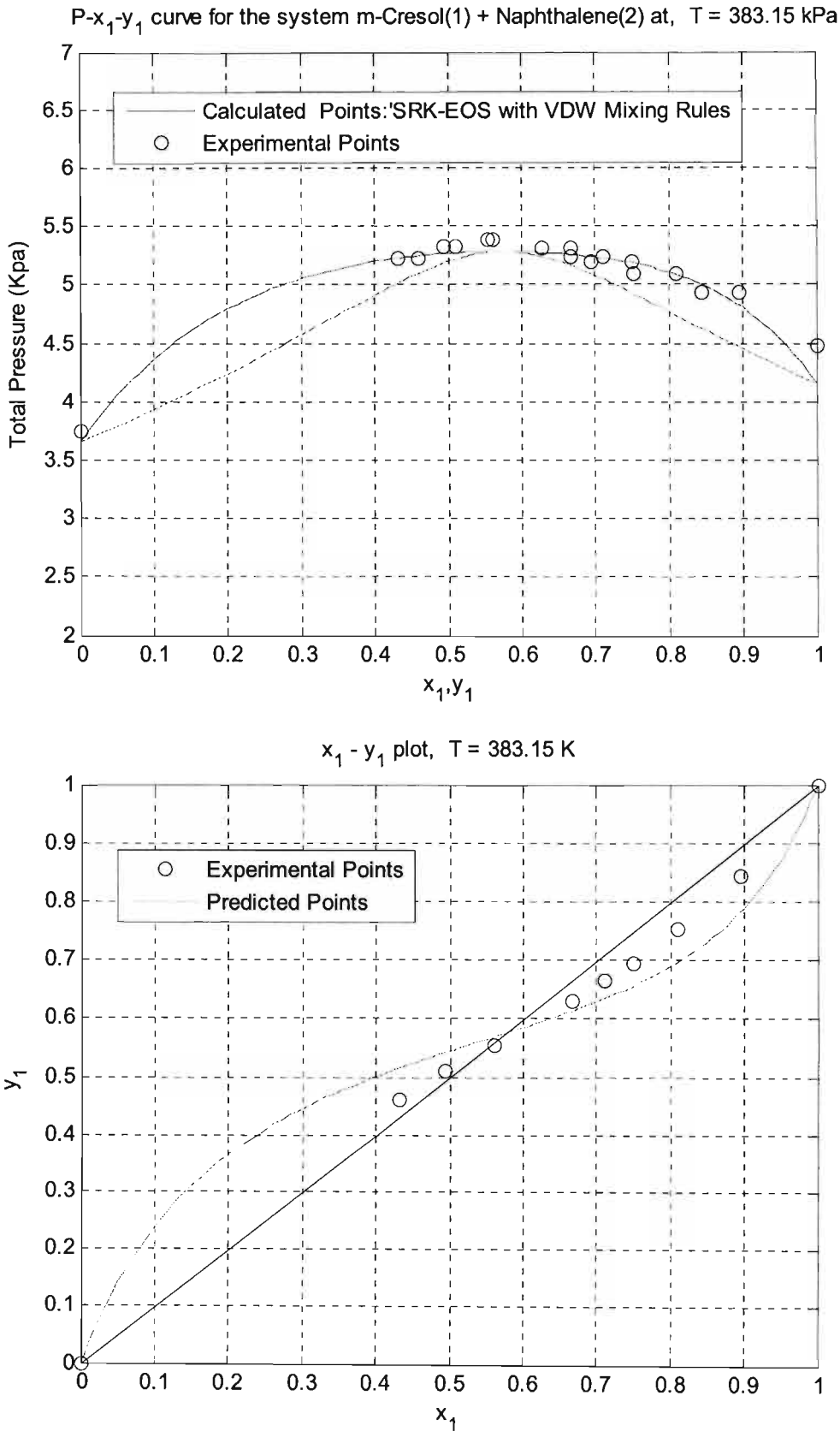

Figure A1- 15: SRK-EOS fitted to experimental VLE data for the system m-Cresol (1) + Naphthalene (2) at 383.15 K

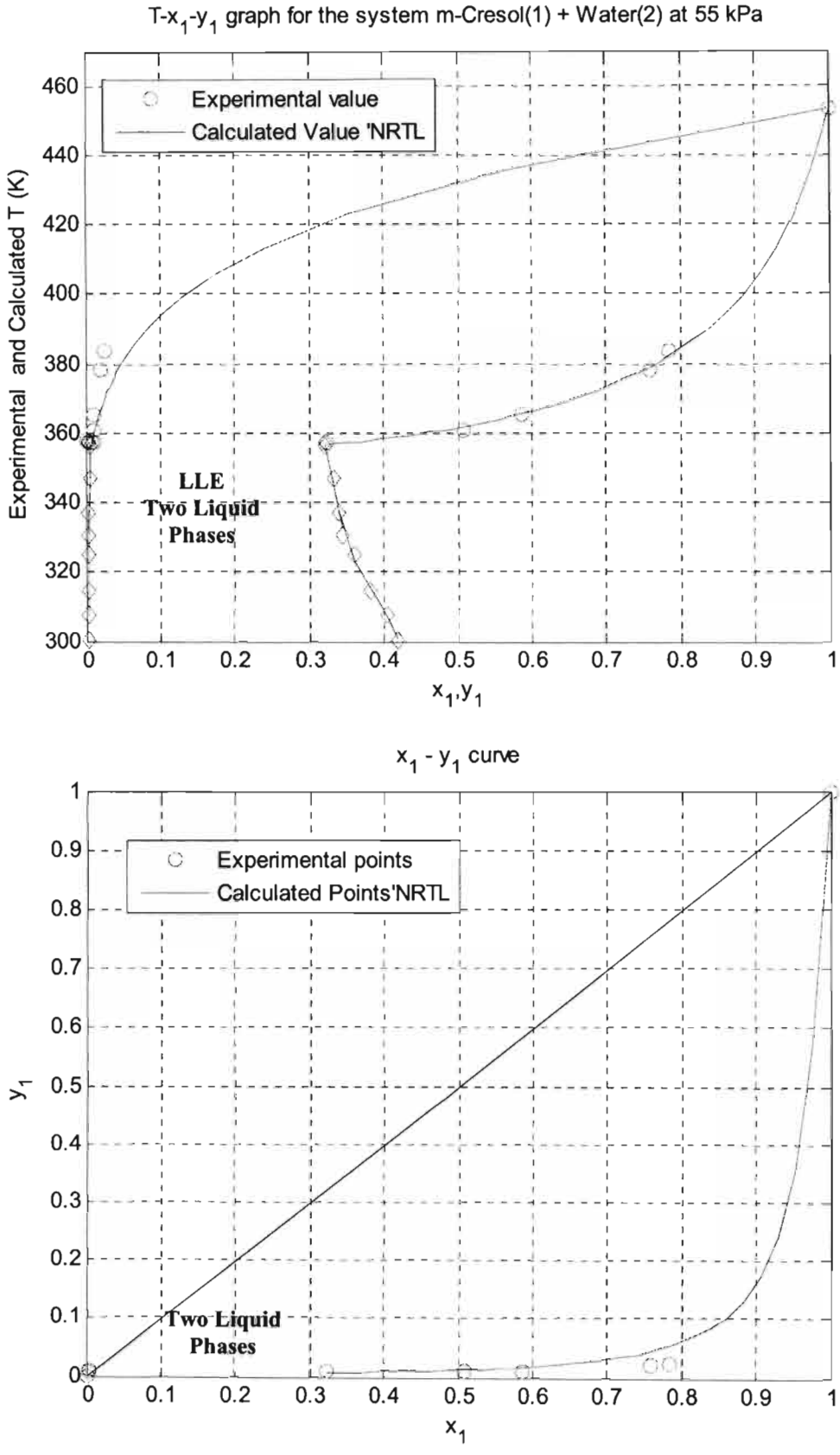

Figure A1- 16: NRTL model fitted to Entire Experimental P-x-y data for the m-Cresol (1) + Water (2) System at 55 kPa

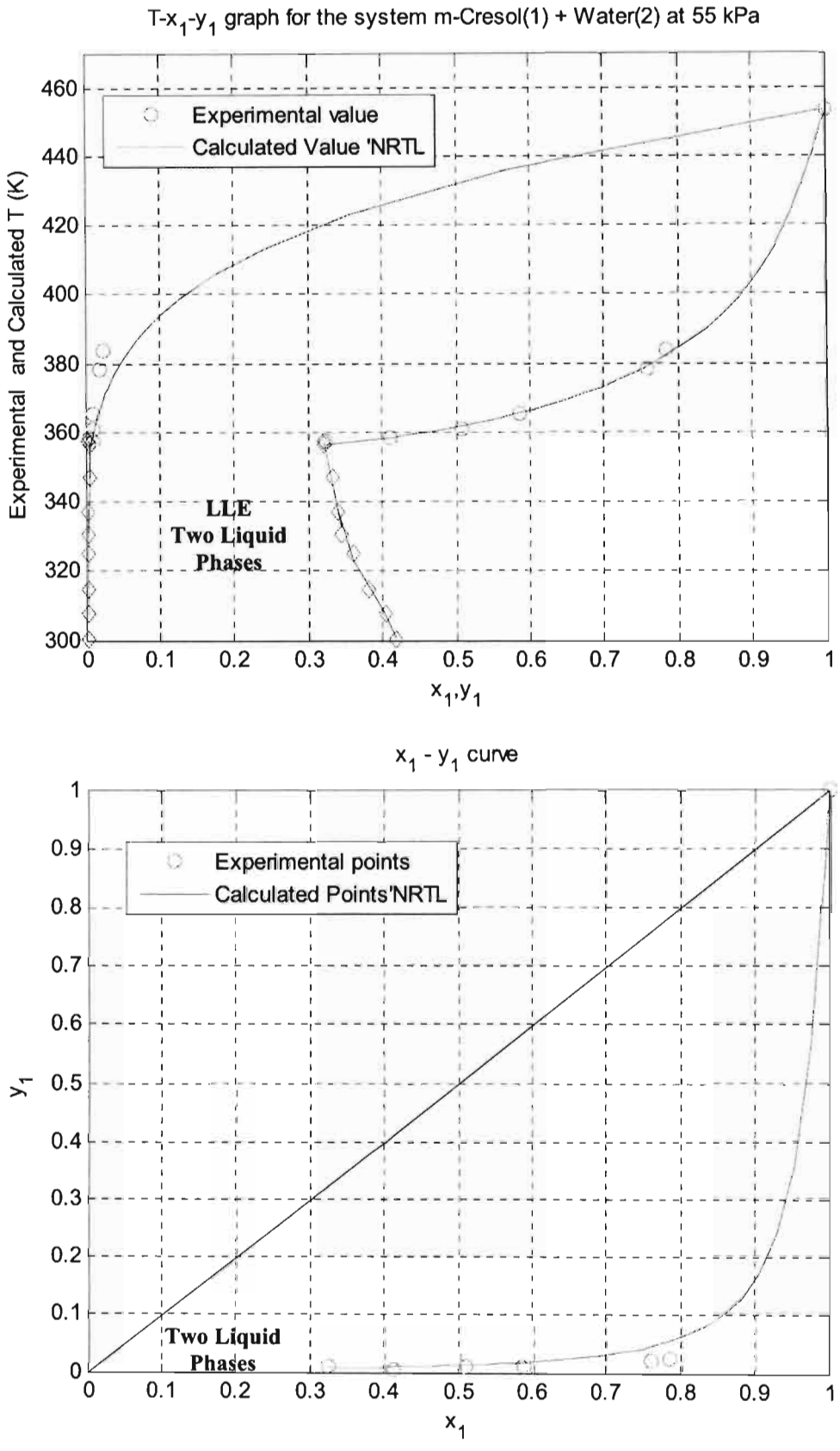

Figure A1- 17: NRTL model fitted to Experimental P-x-y data for the m-Cresol (1) + Water (2) System at 55 kPa in the homogeneous Cresol Region

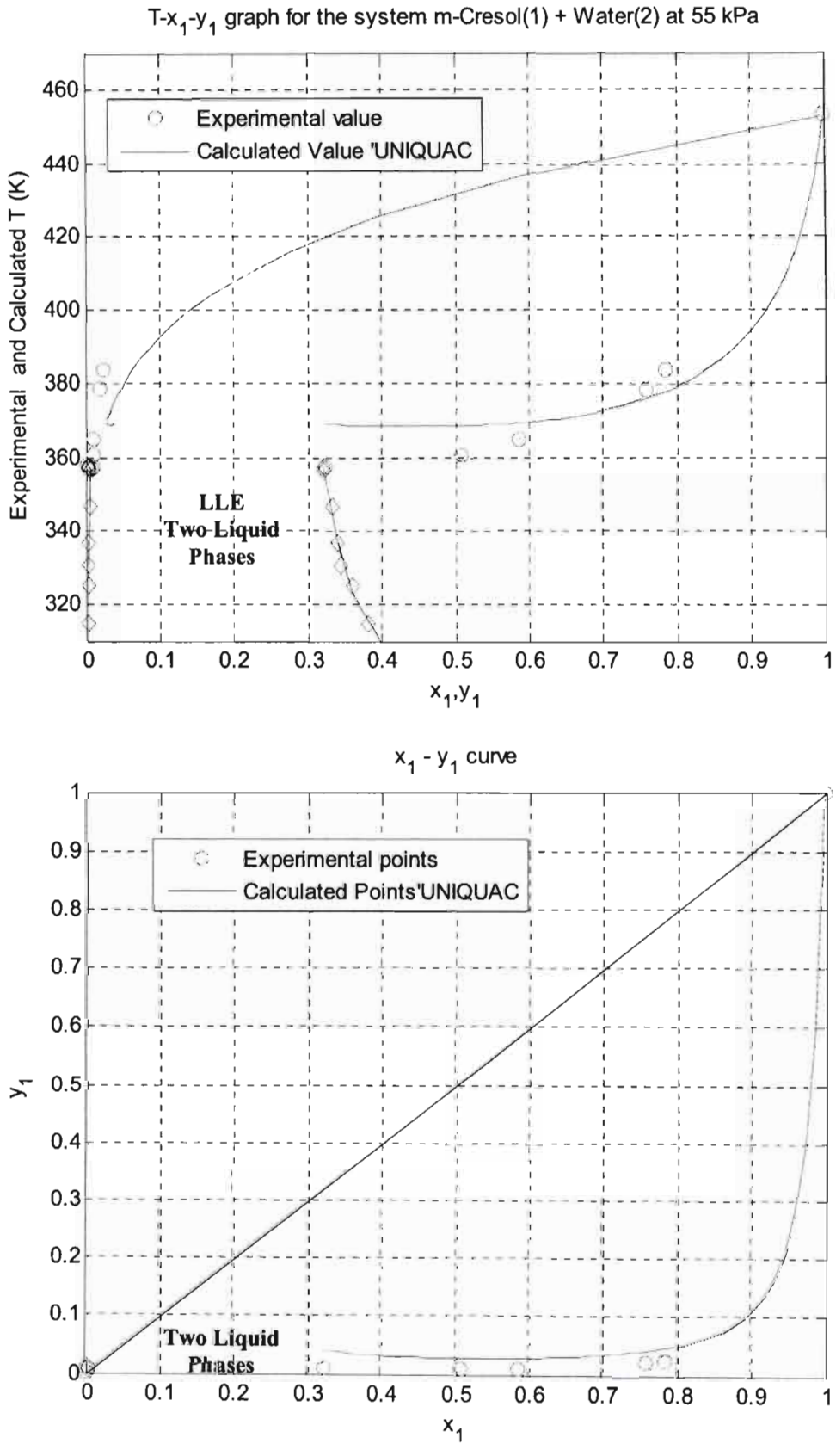

Figure A1- 18: UNIQUAC model fitted to Entire Experimental P-x-y data for the m-Cresol (1) +Water (2) System at 55 kPa

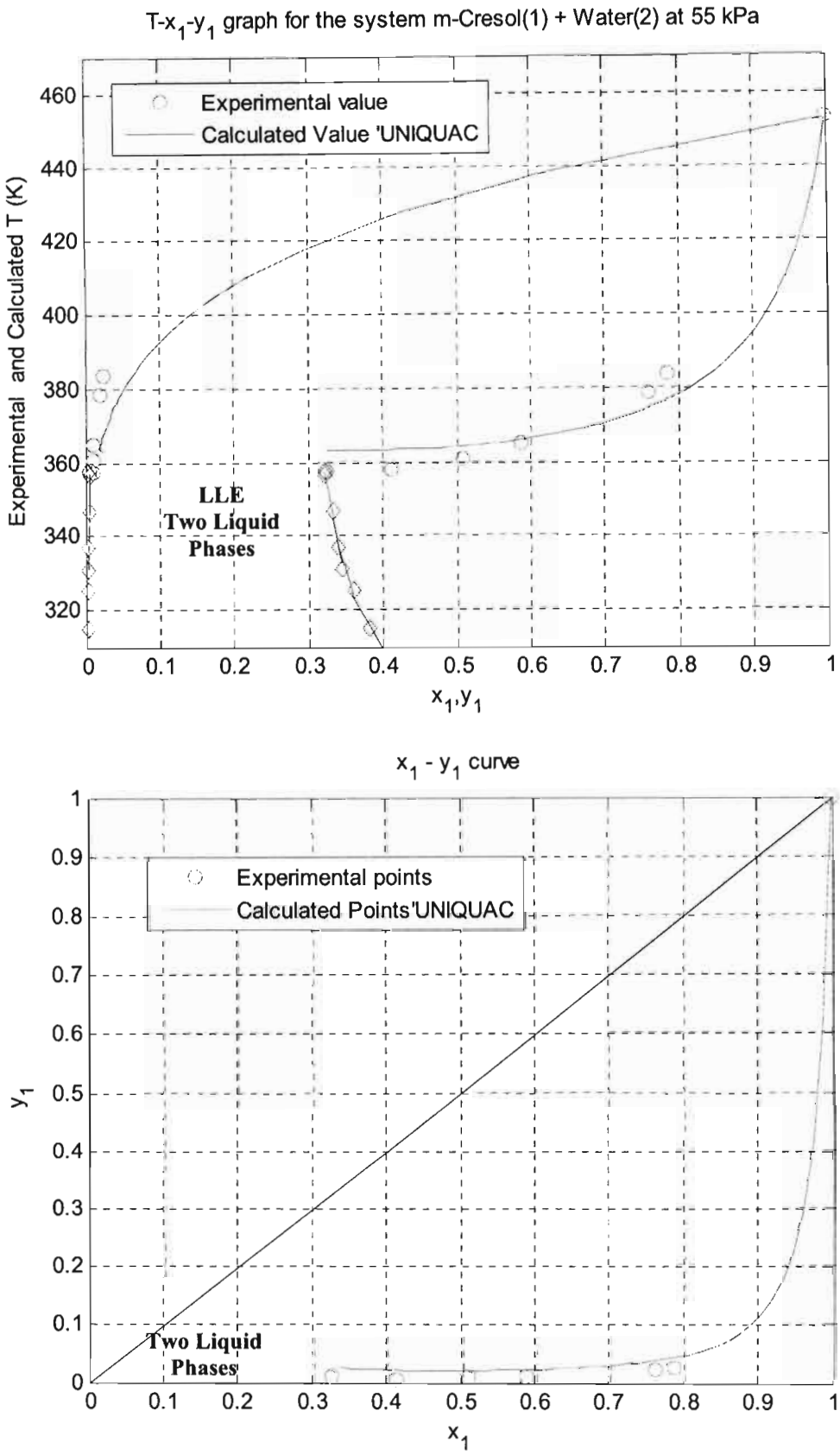

Figure A1- 19: UNIQUAC model fitted to Experimental P-x-y data for the m-Cresol (1) + Water (2) System at 55 kPa in the homogeneous Cresol Region

A2

Appendix Two

Calculation of VLE from LLE

In this appendix to section 3-10, we present equations obtained by solving equations 3 -154 and 3-155 to give parameters in the three suffix Margules and Van Laar equations (see section 3-9). Also presented are the graphs of Renon and Prausnitz for calculating the NTRL parameters from Mutual Solubility data.

The Three Suffix Margules Equations

$$\left(A_{21}-A_{12}\right)=\frac{\ln\left(\frac{x_2^{*}x_1}{x_1^{*}x_2}\right)}{1+\frac{2\left[x_1x_2\left(x_1^{*}-x_2^{*}\right)+x_1^{*}x_2^{*}\left(x_1-x_2\right)\right]}{\left(x_1+x_1^{*}\right)\left(x_2+x_2^{*}\right)}} \qquad \text{(A2-1)}$$

$$A_{12}=\ln\frac{x_1^{*}}{x_1}-2\left(A_{21}-A_{12}\right)\left[\frac{x_2^{2}x_1-(x_2^{*})^{2}x_1^{*}}{x_2^{2}-(x_2^{*})^{2}}\right] \qquad \text{(A2-2)}$$

The Van Laar Equations

$$\frac{A_{12}}{A_{21}} = \frac{\left(\frac{x_1}{x_2} + \frac{x_1^*}{x_2^*}\right)\left(\frac{\ln\left(x_1^*/x_1\right)}{\ln\left(x_2/x_2^*\right)}\right) - 2}{\frac{x_1}{x_2} + \frac{x_1^*}{x_2^*} - 2\frac{x_1 x_1^* \ln\left(x_1^*/x_1\right)}{x_2 x_2^* \ln\left(x_2^*/x_2\right)}} \qquad \text{(A2-3)}$$

$$A_{12} = \frac{\ln\left(x_1^*/x_1\right)}{\left[1+\left(A_{12}/A_{21}\right)\left(x_1/x_2\right)\right]^{-2} - \left[1+\left(A_{12}/A_{21}\right)\left(x_1^*/x_2^*\right)\right]^{-2}} \qquad \text{(A2-4)}$$

The NRTL Equation

Figures A2-1 to A2-3 show the graphs for calculating the NRTL parameters from mutual solubilities for different alpha parameneters

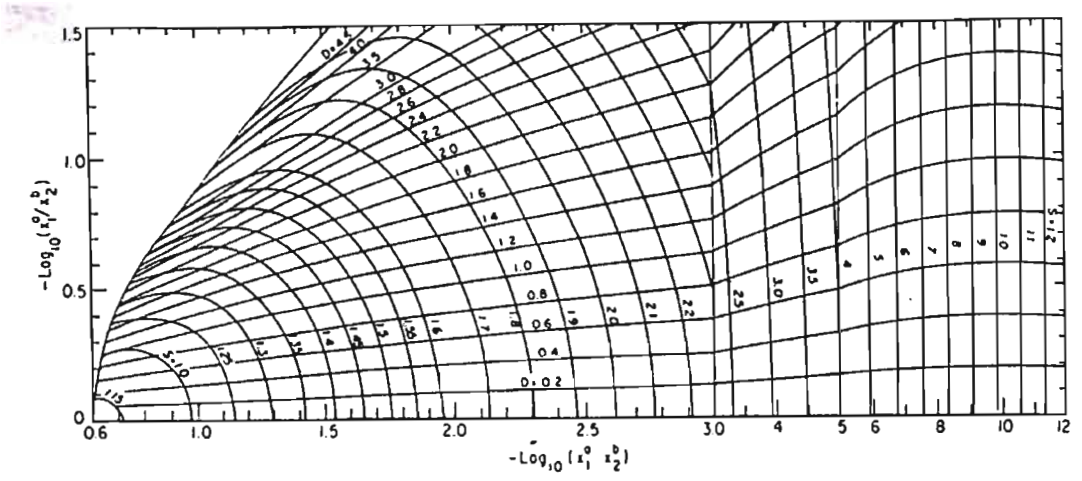

Figure A2- 1: Parameters in the NRTL equation from mutual solubilities for α_{12} = 0.2(Renon and Prausnitz [1969])

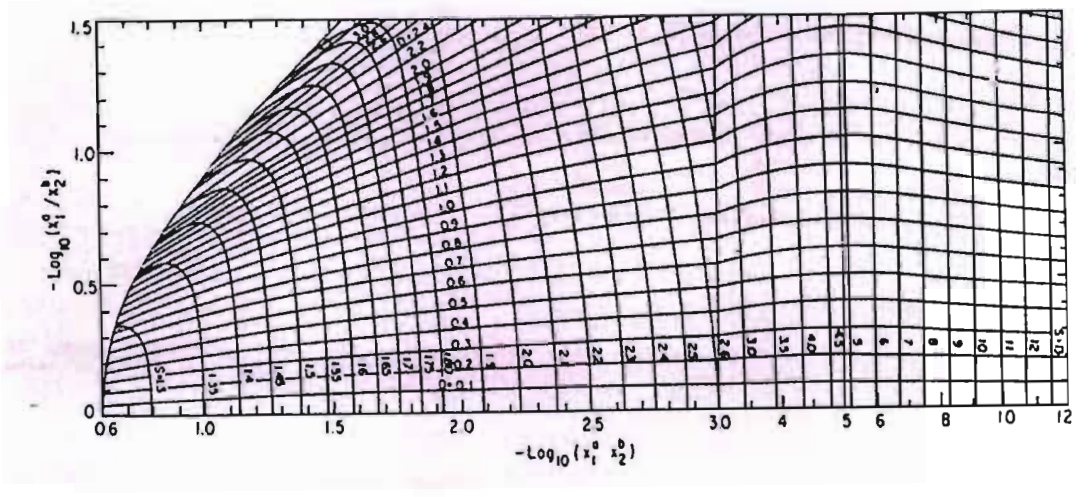

Figure A2- 2: Parameters in the NRTL equation from mutual solubilities for $\alpha_{12} = 0.3$ (Renon and Prausnitz [1969])

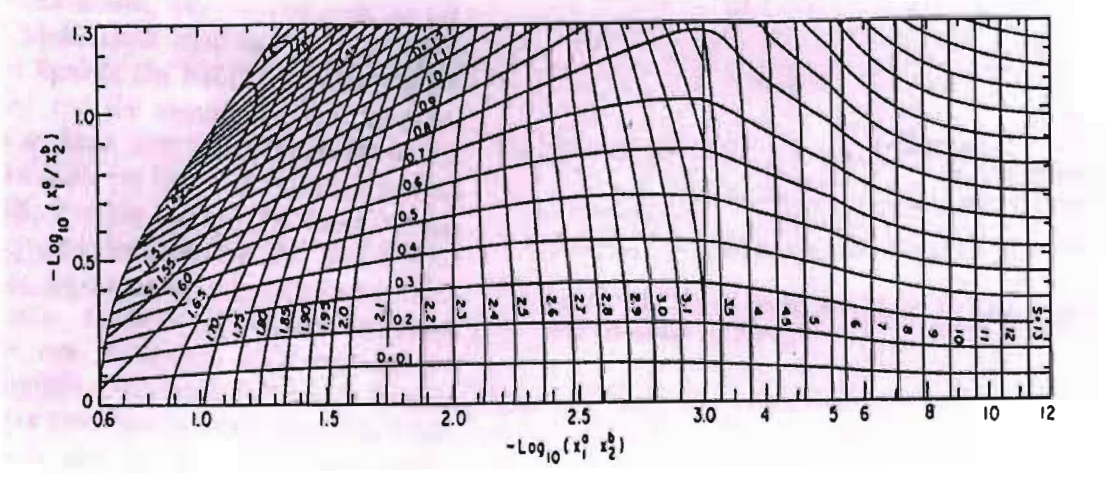

Figure A2- 3 Parameters in the NRTL equation from mutual solubilities for $\alpha_{12} = 0.4$. (Renon and Prausnitz [1969])

Appendix 3

Computer Programs

Presented in this appendix are the following programs coded in Matlab:

1. Antoine – for regressing experimental vapour pressure data to find coefficients in the Antoine equation.
2. Wagner – For regressing experimental vapour pressure data to find parameters in the Wagner equation (Reid et al [1988]).
3. Molar V – for computing the Liquid Molar Volume hat any temperature using the Racket [1970] equation
4. Virial – For computing the Virial Coefficients at any temperature using the Pitzer and Curl [1955] correlation and the mixing rules by Prausnitz et al [1986]
5. Isobaric_NRTL – For regressing experimental VLE data measured at constant pressure to give parameters in the NRTL model (Renon and Prausnitz [1968] using the Gamma – Phi method.

A3.1 Antoine

```
%-----------------------------------------------------------------------
% Regression of Antoine coefficients for Ethanol
% by fitting its vapour Pressure data to the equation
%   log(P) = A + B/(T+C)
% where T is the temperature in Kelvin.
% Programming Note: call fminsearch; needs regresantoine
%(which specifies the Objective Function)
% Authour M Ndlovu
%-----------------------------------------------------------------------

% Start afresh initialise workspace
      clear all
      close all
      clc;

% Extend data T and P to external subroutines
      global T P A B C

% Program header ------------------------------------------------------
      disp('Nonlinear regression of Antoine coefficients')
      disp('  log(P) = A+B/(T+C)')

% P- T data for ethanol

T = [77.44  74.85   68.8    65.196  61.07   56.14   50.05   46.32];
P = [99.12  89.18   69.30   59.34   49.40   39.46   29.53   24.83];

param = [-11.3318 -8793. 0921 -736.6476]; % initial guess
T = T +273.15;

param = fminsearch('regresantoine',param,... %starting from an intial
estimate of parameter find an optimum value
optimset('TolX',1e-
8,'MaxFunEvals',10000,'MaxIter',10000,'Display','Iter'))' ; %
optimization loop

% Print the coefficients ----------------------------------------------
      A = param(1);
      B = param(2);
      C = param(3);
      disp('The coefficients are:')
      disp(['  A = ', num2str(A) ])
      disp(['  B = ', num2str(B) ])
      disp(['  C = ', num2str(C) ])
      disp(['The value of sse is: ', num2str(regres8e(param)) ])

% Generate the fitted function
      Pfit = 10.^(A+B./(T+C));

      Avg_delta_P = sum(abs(P - Pfit)/(length(Pfit)));        %
Average Deltas
disp('The average values of Delta P  is')
disp(' ')
[Avg_delta_P]


% Dispaly Experimental and Calculated Values
disp( ' The experimental values are compared to the fitted values
below:')
disp ([P' Pfit' (P - Pfit)'])
```

```
plot(T, P, 'o', T, Pfit, '-')
grid
title('Vapour Pressure curve')
xlabel('Temperature (K)')
ylabel('Pressure (KPa)' )
legend(' data points',' fitted curve')

 function r = regresantoine(param)
%-------------------------------------------------------------------
% Evaluate the function (which is the objective Function) to be
minimized
% A Program by Mkhokheli Ndlovu
% ------------------------------------------------------------------

      global T P

% Use my own variables
      A = param(1);
      B = param(2);
      C = param(3);

% Calculate sse (sum of squared error)
      error = log10(P) - (A+B./(T+C));
      r = sum(error.^2);
```

A3-2 Wagner

```
%-------------------------------------------------------------------
% Regression of Wagner(Reid et al [1988] coefficients for Ethanol
% by fitting its vapour Pressure data to the equation
%   log(P/Pc) = 1/(1 - x)*(Ax + Bx^1.5 + Cx^3 + Dx^6)
% where x = (1 - T/Tc)
% Programming Note: call fminsearch; need regreswagner
%(which specifies the Objective Function)
% Authour M Ndlovu
%-------------------------------------------------------------------
% Start afresh
      clear all
      close all
      clc;
 % Extend data T, P and the critical parameters to external
subroutines
      global T P Tc Pc
 % Program header ---------------------------------------------------
      disp('Nonlinear regression of Wagner coefficients')
      disp('log(P/Pc) = 1/(1 - x)*(Ax + Bx^1.5 + Cx^3 + Dx^6)  ')
      disp( ' where x = 1 - T/Tc')

% P- T data for ethanol
T = [77.44  74.85   68.8    65.196  61.07   56.14   50.05   46.32];
P = [99.12  89.18   69.30   59.34   49.40   39.46   29.53   24.83];
Pc = 6137;
Tc = 514;
T = T + 273.15;
param = [-31.224 58.3256 -116.181 377.668]; %initial guess

        param = fminsearch('regreswagner',param,... %starting from an
intial estimate of parameter find an optimum value
```

```
              optimset('TolX',1e-
8,'MaxFunEvals',10000,'MaxIter',10000,'Display','Iter'))' ; %
optimization loop

% Print the coefficients ------------------------------------------
      A = param(1);
      B = param(2);
      C = param(3);
      D = param(4);
      disp('The coefficients are:')
      disp(['  A = ', num2str(A) ])
      disp(['  B = ', num2str(B) ])
      disp(['  C = ', num2str(C) ])
      disp(['  D = ', num2str(D) ])
      disp(['The value of sse is: ', num2str(regresreid(param)) ])

% Generate the fitted function
       a = 1 - T./Tc;
      Pfit = Pc*exp((1./(1 - a)).*(A*a + B*a.^1.5 + C*a.^3 +
D*a.^6));
 Avg_delta_P = sum(abs(P - Pfit)/(length(Pfit)));        % Average
Deltas
disp('The average values of Delta P  is')
disp(' ')
[Avg_delta_P]

% Dispaly Experimental and Calculated Values
disp( ' The experimental values are compared to the fitted values
below:')
disp ([P' Pfit' (P - Pfit)'])
plot(T, P, 'o', T, Pfit, '-')
grid
xlabel('Temperature (K)')
ylabel('Pressure (KPa)' )
gtext('o : data points, --: fitted curve')

      function r= regreswagner(param)
%-----------------------------------------------------------------
% Evaluate the function (which is the objective Function) to be
minimized
% A Program by Mkhokheli Ndlovu
% ----------------------------------------------------------------
global T P Tc Pc
 % Use my own variables
      A = param(1);
      B = param(2);
      C = param(3);
      D = param(4);

% Calculate sse (sum of squared error)
    x = 1 - T ./ Tc;
      error = log(P / Pc) -(1 ./ (1 - x)) .* (A * x + B * x .^ 1.5 +
C * x .^ 3 + D * x .^ 6);
      r = sum(error .^ 2);
_
```

A3-3 Molar V

```
% function to calculate the molar volume using the Racket Equation
function r = molarV(a)
 % Critical Properties; Source: KDB Data for Cyclohexale(1) -
Ethanol(2)

 Vc = [308.00   168.00]; % cm3/mol
Zc = [0.27  0.24];
Tc = [553.80    514.00]; % K
omega = [0.21   0.64];
Pc = [4080.00   6137.00]; % kpa

%use my own variables
T = a;
Tr = T ./Tc;
vol = Vc .*( Zc .^((1 - Tr) .^ 0.2857));
r = vol/1.0e6; % m^3
```

A3-4 Virial

```
%-------------------------------------------------------------------
% function to calculate the virial coefficients from a given T
% using the Pitzer - Curl correlation and the Mixing rules
% proposed by Prausnitz etal (1986): Molecular Thermodynamics of
Fluid Phase
% Equilibria. 2nd Edition, Prentice Hall.
% Authour M Ndlovu
%-------------------------------------------------------------------
function r = Virial(a)

% Critical Properties; Source: Korea thermophysical Property Data
bank Data for Cyclohexale(1) - Ethanol(2)

 Vc = [308.00   168.00]; % cm3/mol
Zc = [0.27  0.24];
Tc = [553.80    514.00]; % K
omega = [0.21   0.64];
Pc = [4080.00   6137.00]; % kpa
R = 8.314; %Molar gas constant

% Use my own variables
T = a;
Pcnew = Pc*1000; % converting Pc to Pa
omegaij = sum(omega)/2;
Zcij = sum(Zc)/2;
Vcij =  (sum (Vc .^ (1/3))/2)^3;
Tcij = sqrt(Tc(1)* Tc(2));
Pcij = (82.057 * 100 * 1.01325 *1000* Zcij .* Tcij ) ./ Vcij;
 TcNew = [ Tc Tcij];
PcNew = [ Pcnew Pcij];
omegaNew = [omega omegaij];
Tr = T ./ TcNew;
Bo = 0.083 - 0.422 ./ (Tr.^ 1.6);
B1 = 0.139 - 0.172 ./ (Tr .^ 4.2);

r = (R * TcNew .* (Bo + omegaNew .* B1)) ./ PcNew;
```

A3-5 Isobaric NRTL

```
%-------------------------------------------------------------------
% A program to determine the  coefficients in Renon' s NRTL equation
from
% measured T-x-y data using the Nelder-Mead simplex method'
%-------------------------------------------------------------------

clear all
close all
clc;
global P  R Tsat x1 x2 param Texp y1cal ln_gammai_1 ln_gammai_2 A1_2
A2_1 alpha1_2 Texp....
    y1exp Tcal y2cal AA BB CC Tb Tp Vc Tc Pc Zc omega phi
ln_gratioexp ln_gratiocal ....
    xalpha Talpha Tnwea xbeta Tbeta Tewb
%Program Header
disp('     A program to determine the NRTL coefficients from ')
disp('measured T-x-y data using the Nelder-Mead simplex method')
disp('_____________________by Mkhokheli
Ndlovu_____________________ ')
disp(' ')


t0 = clock;% start the clock
cresol_55kpa; % call the script data_input to input experimental
data.
x2 = 1-x1;% composition for component 2

%initial values of phi_1 and phi_2- the fugacity coefficients
    phi = [0.75 0.75];
% set new optimisation parameters
mk = optimset('MaxFunEvals',500,'MaxIter',500);

% Call a routine (fminsearch) to find the parameters % --------------

      [param,FVAL,EXITFLAG,OUTPUT] = fminsearch('regressPnrtl2',
param, mk);

      % Print the coefficients ----------------------------------
     A1_2 = param(1);
     A2_1 = param(2);
     alpha1_2 = param(3);
     AvgT = sum(Texp)/length(Texp);

     g12_g11 =  A2_1 * R * AvgT;
     g12_g22 =  A1_2 * R * AvgT;

     disp('The  fitted coefficients are:')
     disp('   ')
      disp([' A12 = ', num2str(A1_2) ])
      disp([' A21 = ', num2str(A2_1) ])
      disp([' apha12 = ', num2str(alpha1_2)])
      disp( '  ')
      disp('or')
      disp('  ')
      disp(['g12_g11 in J/mol:  ', num2str(g12_g11)])
```

```
      disp(['g12_g22 in J/mol:  ', num2str(g12_g22)])
      disp(['  apha12 = ', num2str(alpha1_2)])
      disp('  ')
%_____________________________________________________________________
%compute vapour composition, Pressure and ln(gammai) using optimised
parameters at the average
%Temperature

Psatopt = psat(AvgT);
gammaopt = [];

for h = 1:length(x1)
   x1sm = [x1(h) (1- x1(h))];
   g = active(A1_2, A2_1, alpha1_2,x1sm,AvgT);
   gammaopt(:,h) = g;
   y = (x1sm .*g .*Psatopt)/P;
   yopt(:,h) = y;
end
Popt = Psatopt(1) * gammaopt(1,:) .* x1 +  Psatopt(2) * gammaopt(2,:)
.* (1-x1); %P = sum(x1*gammai*Pisat)

%_____________________________________________________________________

  % compute experimental activity coefficeints
  gammaexp = [];



for c = 1:length(x1);
      x1expsm = [x1(c) (1-x1(c))];
      Texpsm = Texp(c);
      Psatexpsm = psat(Texpsm);
      yexpsm = [y1exp(c) (1-y1exp(c))];
      phiexpsm = phical(Texpsm,yexpsm,Psatexpsm);
      gammaexpsm =  (P* yexpsm .* phiexpsm) ./ (x1expsm .*
Psatexpsm);
      gammaexp(:,c) = gammaexpsm;
end

for k = 1: length(x1)% catering for the points x1 = 1 and x1 = 0

    if x1(k) == 0
     gammaexp(1,k) = exp(A2_1 + A1_2 * exp(-alpha1_2 * A1_2));
    else if x1(k) == 1
          gammaexp(2,k) = exp(A1_2 + A2_1 * exp(-alpha1_2 * A2_1));
        end
    end
end

%computing Predicted Presure using measured Temperatures
gammapred = [];
Ppredicted = [];
 for  j = 1 : length(x1)
     x1predsm =[x1(j)  (1-x1(j))];
     Tpredsm = Texp(j);
     Psatpredsm = psat(Tpredsm);
     ypredsm = [y1cal(j) (1-y1cal(j))];
     phipredsm = phical(Tpredsm,ypredsm,Psatpredsm);
   gpred = active(A1_2, A2_1, alpha1_2,x1predsm,Tpredsm);
   gammapred(:,j) = gpred;
```

```
   Ppredicted(j) = sum( (x1predsm .* gpred .* Psatpredsm) ./
phipredsm);
 end
 disp(' ')
 disp(' Below is a table showing the values Predicted Pressure gam1
and gam2')
 disp( ' ')
 [ Ppredicted' gammapred' ]

disp('The experimental and calculated vapour compositions are
compared below')
disp(' ')
disp(' The table shows the values: ')
disp(' x1exp  y1exp    y1cal    (Delta y1)    Texp     Tcal     Delta
T    gam1_exp   gam2_exp ')
disp('  ')

[ x1' y1exp'  y1cal'   (y1exp - y1cal)'    (Texp)'     (Tcal)'
(Texp - Tcal)'  gammaexp(1,:)'  gammaexp(2,:)' ]

t1 = etime(clock,t0); % stop clock
disp(['The  elapsed time in seconds is:  ' ,num2str(t1)])

delta_T = ((Texp - Tcal));      % Deviations
delta_y1 = (y1exp - y1cal);

Avg_delta_T = sum(abs(delta_T))/length(Texp);        % Average Deltas
Avg_delta_y1 = sum(abs(delta_y1))/length(y1exp);

disp('The average values of  absolute Delta T and Delta y1 are:')
disp(' ')
[Avg_delta_T Avg_delta_y1]

%_____________________________________________________________________
%compute the coefficients in the Redlich Kister expansion:
% ln(gm1/gm2) = a + b(x2 - x1) + c(6x1x2 - 1) + d(x1 - x2)(8x1x2 - 1)
coeff = [0.5  5  5  0.5];
ln_gratioexp = log(gammaexp(1,:))-log(gammaexp(2,:));
[coeff,FVAL,EXITFLAG,OUTPUT] = fminsearch('regKister',coeff, mk);
%Print coefficients
a = coeff(1); b = coeff(2);c = coeff(3); d = coeff(4);

disp(' ')
disp(' The Redlich Kister coefficients are: ')
disp(' ')
[ a b c d]
%find the area under the curve ln_gratioexp vs x1



% Find the area by intergrating the the Redlich Kister Expansion
xs1 = linspace(0,1,1000);
xs2 = 1-xs1;
kister = a + b*(xs2 - xs1) + c*(6*xs1.*xs2 - 1) + d*(xs1 -
xs2).*(8*xs1.*xs2-1);
Areaunder = area(xs1,kister);
disp([' The area under the ln(gamma1/gamma2) vs x1 curve is',
num2str(Areaunder) ])
Area_above_axis = abs(area(xs1,(kister > 0).*kister));
Area_below_axis = abs(area(xs1,(kister < 0).*kister));
disp(' ')
```

```
disp([' The area above the x1 axis is: ', num2str(Area_above_axis)])
disp([' The area under the x1 axis is: ', num2str(Area_below_axis)])
%_____________________________________________________________________

% Direct Test of Vaness ( Compare dln(gamma1/gamma2) residuals)
ln_gratiocal = log(gammapred(2,:)) - log(gammapred(1,:));
gammaresidual = ln_gratioexp - ln_gratiocal;
figure(6)
plot(x1,gammaresidual,'ro')
title('Direct Test applied to the system M-Cresol (1) - Water(2) at
55Kpa')
ylabel('Activity Coefficient Residual')
xlabel('x_1')
hold on
plot([0 1],[0 0],'b')
grid on

RMSgammaratio = sqrt(sum(gammaresidual.^2)/length(x1));
disp(' ')
disp(['The RMS Value of dln(gamma1/gamma2) =
',num2str(RMSgammaratio)])
disp( ' ')
%_____________________________________________________________________


%Plot Deviations
figure(1);
subplot(221)
plot(x1,delta_T(:),'r.')
grid on
xlabel('x1')
ylabel('Delta T')
legend('DeltaT')

subplot(222)
plot(x1,delta_y1(:),'k.')
grid on
xlabel('x1')
ylabel('Delta y1')
legend('Delta y1')

subplot(223)
plot(x1,Texp,'r+',x1,Tcal,'ko'), grid on
ylabel(' Exp T and Calc T')
xlabel('x1')
legend('Texp','Tcal')

subplot(224)
plot(x1,y1exp,'dk',x1,y1cal,'bo'), grid on
ylabel(' Exp y and Calc y')
xlabel('x1')
legend('y1exp','y1cal')

figure(2)
plot(x1,log(gammapred(1,:)),'k.',x1,log(gammaexp(1,:)),'rd')
hold on
plot(x1,log(gammapred(2,:)),'r.',x1,log(gammaexp(2,:)),'b*')
grid on
xlabel('x1opt')
ylabel('ln gamma')
```

```
legend('ln gamma1 opt','ln gamma1 exp','ln gamma 2 opt','ln gamma2
exp')

figure(3)
plot(x1,ln_gratioexp,'bo',xs1,kister,'r-')
grid on
xlabel('x1')
ylabel(' ln [(gamma1)/gamma(2)] ')
title('Herington''s Area Test')
legend('Experimental Value', 'Redlich-Kister expansion')

figure(4)
plot(x1,Texp,'ro',x1,Tcal,'b*', y1exp,Texp,'ro',y1cal,Tcal,'b*'),
grid on
axis([ 0 1 450 470])
ylabel(' Experimental  and Calculated T (K)')
xlabel('x_1,y_1')
legend('Experimental value','Calculated Value ''NRTL')
title('T-x_1-y_1 graph for the system: MCresol(1) -  Water(2) at 55
Kpa')


figure(5)
plot(x1,y1exp,'ro',x1,y1cal,'b*'), grid on
xlabel('x_1')
ylabel('y_1')
title('x_1 - y_1 curve for the system: M-Cresol(1) - Water(2) at 55
Kpa')
hold on
plot([0 1],[0 1],'k')
legend('Experimental Value', 'Calculated Value ''NRTL')

%_____________________________________________________________________
```

Script named cresol_55kpa

```
% m -Cresol (1) - Naphthalene(2) at 55KPa Experimental data to be
analysed

Texp = [ 453.49 453.79574   454.09802   454.4003    454.50106
454.9041    455.60942   455.71018   456.51626   457.32234   458.32994
459.53906 467];
y1exp =[1 0.748567408   0.733838112 0.690992662 0.671950341
0.621326676 0.551644419 0.549002811 0.481231134 0.421307945
0.367668961 0.303885696 0];
x1  = [ 1 0.734720911   0.71385865  0.655911751 0.630148327
0.561678175 0.475087248 0.474770904 0.378588627 0.309864483
0.25736505  0.195310233 0];



P = 55  ;  %Kpa
R = 8.3144; % molar gas constant in SI units
param = [0.1 0.1  0.5];% initial guess of NRTL parameters

% Antoine equation parameters Log P = A + B/(T + C)P in Kpa, T in
Kelvin
AA = [6.1119 7.39];
BB = [-1478.9614 -2761.2501];
CC = [-114.9079 21.9129 ];
```

```
%_____________________________

% Critical Properties; Source: Korea thermophysical Property Data
bank
Vc = [310.00    410]; % cm3/mol
Zc = [0.240879  0.267065];
Tc = [705.80    748.3999]; % K
omega = [0.464  0.302];
Pc = [4559.625  4053]; % kpa


%_____________________________________________________________

function r = regressPnrtl2(param)
%-------------------------------------------------------------------
---
% Evaluate the function (which is r) to be minimized
% Objective function = sum((Texp - Tcal)/Texp )^2 + sum((yexp -
ycal)/yexp )^2
% ------------------------------------------------------------------
---
global  x1 x2 P  Ps Texp Tsat y1exp  y1cal gamma2 Tcal phi

 % Use my own variables
      A1_2 = param(1);
      A2_1 = param(2);
      alpha1_2 = param(3);

error=0.000001;                          % tolerance for compositions
determined
checkTy = 0;                                      % composition check
Tsat = temperature(P) ;                             % saturated
temperature K

xsimul = x1;

for i = 1:length(xsimul)
xi = [xsimul(i) 1-xsimul(i)];                                      % liq.
composition
Tinitial = sum(Tsat(1)*xi(1) + Tsat(2)*xi(2));      % initial Temp
guess for calculation
Tb = Tinitial;

counter = 0;
while 1;

    gamma2 = active(A1_2, A2_1, alpha1_2,xi,Tb); % calculating the
activity coefficient
    relativevolatility  = volatility(Tb) ;             % by Daltons
Law
    P1sat = P / sum((xi.*gamma2.*relativevolatility)./phi);  %
sat.press component 1 using modified raoult's law
    Tbnew = temperature1(P1sat);                          % storage
vector, of temperature
    Ps = psat(Tbnew) ;                                    % kPa
    yi = (xi.*gamma2.*Ps)/P;
    checkTy = sum(yi);
    yinormalised = yi / checkTy ;                         %
normalisation of vapour composition
    phi = phical(Tb,yinormalised,Ps);
    checkTy2 = sum(yinormalised);
```

```
    if abs(Tbnew-Tb)<=error & abs(checkTy2-1)<=error
        break;
    end;                                                    % end if
    Tb = Tbnew;

end;                                                        % end while
 Tcal(i) = Tb ;
 y1cal(i) = yi(1);
 Texp1(i) = Texp(i);
 y1exp1(i) = y1exp(i);
end%end for

Terror = ((Texp1 - Tcal).^2 )./ (Texp1).^2;
%Yerror = ((y1exp1 - y1cal).^2)./ (y1exp1).^2;

r = sum(Terror )%+ Yerror)


%-------------------------------------------------------------------
%A function to evaluate the activity coefficients using the NRTL
equation
% given xi and T
% -------------------------------------------------------------------

function  [r] = active(r, s, t,u,v)

%use my own variables
A1_2 = r;
A2_1 = s;
alpha1_2 = t;
xi = u;
T = v;


G1_2 = exp(-alpha1_2 * A1_2);
G2_1 = exp(-alpha1_2 * A2_1);


      act(1) = exp(xi(2) * xi(2) *(A2_1 * (G2_1/(xi(1) + xi(2) *
G2_1))^2 + A1_2 * G1_2/(xi(2) + xi(1) * G1_2)^2));
      act(2) = exp(xi(1) * xi(1) * (A1_2 * (G1_2/(xi(2) + xi(1) *
G1_2))^2 + A2_1 * G2_1/(xi(1) + xi(2) * G2_1)^2));

r =  act;




% calculation of relative volatilies from vapour pressures
function [revol] = volatility(s)
global A B C
T = s;
pressure = psat(T);

revol(1) = pressure(1) / pressure(1);
revol(2) = pressure(2) / pressure(1);
```

```
% function to calculate the virial coefficients from a given T
% using the Pitzer - Curl correlation and the Mixing rules
% proposed by Prausnitz etal (1986): Molecular Thermodynamics of
Fluid Phase
% Equilibria. 2nd Edition, Prentice Hall.

function r = Virial(a)
global Vc Pc Tc Zc R omega

% Use my own variables
T = a;
Pcnew = Pc*1000; % converting Pc to Pa

%Zc = Pcnew .* Vc ./ (R * Tc);

omegaij = sum(omega)/2;
Zcij = sum(Zc)/2;
Vcij =  (sum (Vc .^ (1/3))/2)^3;
Tcij = sqrt(Tc(1)* Tc(2));
Pcij = (82.057 * 100 * 1.01325 *1000* Zcij .* Tcij ) ./ Vcij;

TcNew = [ Tc Tcij];
PcNew = [ Pcnew Pcij];
omegaNew = [omega omegaij];
Tr = T ./ TcNew;
Bo = 0.083 - 0.422 ./ (Tr.^ 1.6);
B1 = 0.139 - 0.172 ./ (Tr .^ 4.2);


r = (R * TcNew .* (Bo + omegaNew .* B1)) ./ PcNew;

%function to determine the saturated temperature for component 1 from
the
%antoine equation

function [temperature] = temperature1(P1sat)
global AA BB CC

temperature = (BB(1) / (log10(P1sat) - AA(1))) - CC(1);




%function that returns the temperature(K) based on pressure(kPa) from
the
%Antoine equation

function [temp]=temperature(w)
global AA BB CC
P = w;
temp =( BB ./ (log10(P) - AA)) - CC;

% function to be minimised when regressing the activity cofficient
ratio of
% obtain parameteters in the Redlich Kister expansion
% ln(gm1/gm2) = a + b(x2 - x1) + c(6x1x2 - 1) + d(x1 - x2)(8x1x2 - 1)

function  r1 = regKister(coeff)
```

```
global x1 ln_gratioexp ln_gratiocal

%use own variables
x2 = 1-x1;
a = coeff(1);
b = coeff(2);
c = coeff(3);
d = coeff(4);

for z = 1:length(x1)
   ln_gratiocal(z)  = a + b*(x2(z) - x1(z)) + c*(6*x1(z)*x2(z) - 1) +
d*(x1(z) - x2(z))*(8*x1(z)*x2(z)-1);
end

gerror = ln_gratioexp - ln_gratiocal;

r1 = sum((gerror).^2);

% a function to calculate saturated vapour pressures from the Antoine
% Equation

function [press] = psat(Tp)
global AA BB CC
press = 10.^(AA + BB ./ (Tp +  CC));



%-------------------------------------------------------------------
% A  function tom evaluate the correction factor
% Phi = exp((Vii - Bii)(P - Pisat) + Pyi^2 dij)/RT
%-------------------------------------------------------------------

function  [r] = phi(a,b,c)

global  P R

Pnow = P*1000; % convert Pressure to Kpa
Ps = c;
Psnow = Ps * 1000;
%use my own variables
Temp1  = a;
y1calc = b(1);
y2calc = b(2);

B = Virial(Temp1);% call  a function to calculate the Virial
coefficients
B11 = B(1);
B22 = B(2);
B12 = B(3);
del_12 = 2 * B12 - B11 - B22;

V = molarV(Temp1); % call a function to evaluate the liquid molar
volume
Vi_1 = V(1);
Vi_2 = V(2);
% evaluate the vapour fugacity coefficients
ln_phi_1 = ((B11 - Vi_1) * (Pnow - Psnow(1)) + Pnow * y2calc * y2calc
* del_12) / (R * Temp1 );
ln_phi_2 = ((B22 - Vi_2) * (Pnow - Psnow(2)) + Pnow* y1calc * y1calc
* del_12) / (R * Temp1 );
```

```
r(1) = exp(ln_phi_1);
r(2) = exp(ln_phi_2);



% function to calculate the molar volume using the Racket Equation
function r = molarV(a)
global Tc Vc Pc R Zc

%use my own variables

T = a;
%Pc_new = Pc * 1000;
%Zc = Pc_new .* Vc ./ (R * Tc);
Tr = T ./Tc;
vol = Vc .*( Zc .^((1 - Tr) .^ 0.2857));
r = vol/1.0e6;

% function to evaluate an integral numerically
% F = sum(Fiav * delta xi)

function r2 = area(m,q)

%use own variables

x1 = m;
f = q;
for i = 1:(length(x1)-1);

    fav(i) =0.5*( f(i) + f(i+1));
    delx(i) = x1(i+1)- x1(i);
end
r2 = sum(fav.*delx);
```

Appendix 4

Gas Chromatograph Operating Conditions

Below is a table showing the GC operating conditions for the new systems that were measured in this work.

Operating Condition	System	
	M-Cresol – Naphthalene and M-Cresol - Water -Naphthalene	**M-Cresol – Water And Tolunitrile- Water**
Gas Flowrate	30	30
Oven Temperature Profile		
Initial Temperature(°C)	240	220
Hold Time (min)	-	-
Temperature Ramp (°C/min)	-	-
Final Temperature (°C)	-	-
Hold Time (min)	-	-
Deterctor Profile		
Deterctor Type	**TCD**	**TCD**
Temperature (°C)		240
Attenuation	1	1
Range	-	-
Injector Profile		
Temperature	260	240

Table A4- 1: Operating Conditions of the Hewlett-Packard 5890 Series II Gas Chromatograph.